DESIGN AND PERFORMANCE TESTING OF A NOVEL 3-FLUID LIQUID-TO-AIR MEMBRANE ENERGY EXCHANGER

A Thesis Submitted to the College of

Graduate Studies and Research

In Partial Fulfillment of the Requirements

For the Degree of Doctor of Philosophy

In the Department of Mechanical Engineering

University of Saskatchewan

Saskatoon

By

Mohamed Abdel-Salam

PERMISSION TO USE

In presenting this thesis in partial fulfillment of the requirements for a Postgraduate degree from the University of Saskatchewan, I agree that the Libraries of this University may make it freely available for inspection. I further agree that permission for copying of this thesis in any manner, in whole or in part, for scholarly purposes may be granted by the professors who supervised my thesis work or, in their absence, by the Head of the Department or the Dean of the College in which my thesis work was done. It is understood that any copying, publication, or use of this thesis or parts thereof for financial gain shall not be allowed without my written permission. It is also understood that due recognition shall be given to me and to the University of Saskatchewan in any scholarly use which may be made of any material in my thesis.

Requests for permission to copy or to make other uses of materials in this thesis in whole or in part should be addressed to:

Head of the Department of Mechanical Engineering
57 Campus Drive
University of Saskatchewan
Saskatoon, Saskatchewan S7N 5A9 Canada

OR

Dean
College of Graduate Studies and Research
University of Saskatchewan
107 Administration Place
Saskatoon, Saskatchewan S7N 5A2 Canada

ABSTRACT

Liquid-to-air membrane energy exchangers (LAMEEs) allow simultaneous heat and moisture transfer between air and desiccant solution streams that are separated by semi-permeable membranes. Moisture transfer between the air and desiccant solution is accompanied by the release/absorption of phase change energy which increases/decreases the temperature of the desiccant solution as it flows through the exchanger. The resulting change in the desiccant solution temperature decreases the driving potential for heat and moisture transfer (i.e. the differences between the air and desiccant solution temperatures and vapor pressures), which decreases the rates of heat and moisture transfer between the air and desiccant solution inside the exchanger. To overcome this problem, a novel 3-fluid LAMEE prototype is designed, built and tested. The 3-fluid LAMEE is composed of several adjacent parallel air and solution channels separated by semi-permeable membranes with refrigerant tubes within each solution channel. The aim of these refrigerant tubes is to reduce the change in the desiccant solution temperature inside the exchanger to guarantee high differences between the air and desiccant solution temperatures and vapor pressures along the entire length of the exchanger.

This thesis has three main objectives. The first objective is to determine the practical nominal air and solution channel widths for flat-plate LAMEEs, and the effects of flow maldistribution caused by membrane deflections on the performance of flat-plate LAMEEs. The results in this thesis show that the practical air and solution channel widths for flat-plate LAMEEs are 5-6 mm and 1-2 mm, respectively. The second objective is to test and compare the rates of heat and moisture transfer between the air and desiccant solution in 3-fluid and 2-fluid LAMEEs under several operating conditions. Results show that the 3-fluid LAMEE can achieve the same heat and moisture transfer rates between the air and desiccant solution as a 2-fluid LAMEE at lower desiccant solution mass

flow rates and with smaller membrane surface areas. Therefore the size of LAMEEs can be significantly decreased if refrigerant tubes are installed inside the solution channels. The third objective is to present performance definitions for evaluating the overall performance of 3-fluid LAMEEs. Unlike the traditional energy exchanger effectiveness equations, results show that the overall performance definitions can be used to evaluate the overall sensible and latent effectivenesses of 3-fluid LAMEEs and are less sensitive to the inlet refrigerant temperature.

ACKNOWLEDGEMENTS

First and foremost, I would like to express my deep thanks to my supervisors Professor Carey Simonson and Professor Emeritus Robert Besant for their guidance, inspiration, encouragement and consistent support throughout my Ph.D. studies.

I would like to thank my advisory committee members Professors David Sumner, David Torvi, and Lope Tabil for their valuable comments and suggestions throughout my Ph.D. studies.

Special thanks go to my brother Dr. Ahmed Abdel-Salam for his support, useful suggestions and the fruitful discussions throughout my Ph.D. studies. I would also like to thank my colleagues Dr. Gaoming Ge, Dr. Melanie Fauchoux, Mr. Farhad Fathieh, and Mr. Mohammad Rafatinasr for their unconditional support throughout my Ph.D. studies.

Financial support by Natural Sciences and Engineering Research Council of Canada (NSERC), Department of Mechanical Engineering at the University of Saskatchewan, American Society of Heating, Refrigerating, and Air-Conditioning Engineers (ASHRAE) Grant-In-Aid Award, ASHRAE Honorarium Award, Saskatchewan Government's Innovation and Opportunity Scholarship, George Carter Scholarship, George Ira Hanson Post-Graduate Award in Energy Research, Frederick Wheeler and W.H.T. Spary Graduate Scholarship, and Russell Haid Memorial Award is highly appreciated.

DEDICATION

I dedicate this thesis to my parents, my wife, and my brother.

Thank you very much for your love, encouragement and support throughout my life.

TABLE OF CONTENTS

PAGE

LIST OF FIGURES

LIST OF TABLES

NOMENCLATURE

ACRONYMS

AHRI	Air-Conditioning, Heating and Refrigeration Institute
COP	Coefficient of Performance
EPS	Enthalpy Pump System
HVAC	Heating, Ventilating, and Air-Conditioning
LAMEE	Liquid-to-Air Membrane Energy Exchanger
LDMAC	Liquid Desiccant Membrane Air-Conditioning
RAMEE	Run-Around Membrane Energy Exchanger
RH	Relative Humidity
SCC	Sensible Cooling Capacity
VDR	Vapor Diffusion Resistance

SYMBOLS

A	surface area (m^2)
B	bias uncertainty
C	heat capacity rate (W/K); concentration ($kg_{LiCl}/kg_{solution}$)
Cr	ratio between minimum and maximum heat capacity rates
Cr^*	ratio between desiccant solution and air heat capacity rates
c_p	specific heat capacity (J/(kg·K))
D	diameter (m), mass diffusivity (m^2/s); diameter of the cylindrical bars of the air channel insert (mm)
D_h	hydraulic diameter (m)
D_o	mean hydraulic diameter of all the pore channels in an energy wheel (m); mean hydraulic diameter of all air channels in a flat-plate LAMEE (m)
E	modulus of elasticity (Pa)
f_D	Darcy friction factor
h	convective heat transfer coefficient ($W/(m^2 \cdot K)$); membrane deflection (m)

h_m	convective mass transfer coefficient (kg/(m^2·s))
H	spacing between the cylindrical bars (mm); enthalpy (J/kg)
H^*	operating condition factor
H_{ex}	LAMEE's height (m)
ΔH	difference in total enthalpy per mass of dry air (J/kg$_{air}$)
J	mass flux (kg/(m^2·s))
k	coefficient of thermal conductivity (W/(m·K))
k_m	membrane water vapor permeability (kg/(m·s))
L	length (m)
Le	Lewis number
$\dot{m}$	mass flow rate (kg/s)
$\dot{m}_{rr}$	moisture removal rate (g$_v$/s)
N_{air}	number of air channels
N_{mem}	number of semi-permeable membranes
N_{sol}	number of solution channels
NTU	number of heat transfer units
NTU_m	number of mass transfer units
Nu	Nusselt number
P	pressure (Pa)
ΔP	pressure drop across the LAMEE (Pa); pressure drop across an energy wheel with non-uniform pores (Pa)
ΔP_o	pressure drop across an energy wheel with uniform pores (Pa)
Pe	Péclet number
Pr	Prandtl number
r	radius (m)
R_m	membrane mass resistance (s/m)
Re	Reynolds number
S	precision error
Sh	Sherwood number

t	membrane thickness (m)
t^*	student-t distribution constant
T	temperature (°C)
T^*	temperature ratio
u	velocity (m/s)
U	overall heat transfer coefficient (W/(m^2·K))
U_m	overall mass transfer coefficient (kg/(m^2·s))
$U_{95\%}$	overall uncertainty at the 95% confidence level
W	humidity ratio (kg_v/kg_{air})
$W_{sol,in\ @C_{sol,in}\ \&\ T_{ref,in}}$	equivalent inlet desiccant solution humidity ratio calculated at inlet desiccant solution concentration and inlet refrigerant temperature (g/kg).

GREEK SYMBOLS

α	thermal diffusivity (m^2/s)
δ	thickness (m); channel width (m)
ε	effectiveness
ν	Poisson's ratio
σ	standard deviation of hydraulic diameters of all pore channels in an energy wheel (m); standard deviation of hydraulic diameters of all air channels in a flat-plate LAMEE (m)
$\partial\varepsilon_m$	dimensionless ratio of effectiveness change as a function of mass flow rate

SUBSCRIPTS

air	air
c	cold fluid
ex	exchanger
h	hot fluid
i	inner; intermediate fluid
in	inlet

lat	latent
max	maximum
mem	membrane
min	minimum
o	outer
out	outlet
ref	refrigerant
s	desiccant salt
sen	sensible
sol	solution
tot	total
tube	refrigeration tubes
v	vapor
w	water

CHEMICAL SYMBOLS

$CaCl_2$	calcium chloride
CO_2	carbon dioxide
LiBr	lithium bromide
LiCl	lithium chloride
$MgCl_2$	magnesium chloride

CHAPTER 1

INTRODUCTION

1.1 OVERVIEW OF CHAPTER 1

The purpose of this chapter is to briefly present liquid desiccant HVAC technologies, types and applications of LAMEEs, and the hypothesis, objectives, and structure of this Ph.D. thesis. This chapter contains brief excerpts from the following published review papers.

Abdel-Salam M.R.H., Ge G., Fauchoux M., Besant R., Simonson C., 2014. State-of-the-art in liquid-to-air membrane energy exchangers (LAMEEs): A comprehensive review, Renewable and Sustainable Energy Reviews, ***39****, 700-728.*

Abdel-Salam M.R.H., Fauchoux M., Ge G., Besant R., Simonson C., 2014. Expected energy and economic benefits, and environmental impacts for liquid-to-air membrane energy exchangers (LAMEEs) in HVAC systems: A review, Applied Energy, ***127****, 202-218.*

Dr. Gaoming Ge, Dr. Melanie Fauchoux, and Ph.D. supervisors (Professors Besant and Simonson) are co-authors of these two papers. Dr. Ge is a Postdoctoral fellow and Dr. Fauchoux is a Departmental Assistant in the Department of Mechanical Engineering at the University of Saskatchewan. Dr. Ge and Dr. Fauchoux contributed to these two papers by critically reviewing them and giving comments and advice which enhanced the quality of the papers. My contributions to these two papers are: (a) conducting the literature reviews, (b) writing the papers, and (c) responding to the reviewer's comments.

1.2 INTRODUCTION

Between 2000 and 2011, global energy consumption increased by 32% (British Petroleum (2009, 2012)) and the building sector is responsible for 40% of this total (Kolokotsa et al. (2011); Wyon (2004)). In recent years, much research has been conducted to reduce cooling and heating energy consumption in buildings (Kusiak et al. (2010); Schulze and Eicker (2013); Chua et al. (2013); Haniff et al. (2013); Wang et al. (2013); Budaiwi and Abdou (2013)). Heating, ventilation, and air-conditioning (HVAC) systems are responsible for a substantial portion of the total energy consumed in buildings; for instance, space cooling consumes 70% of the building total energy consumption in the Middle East region (El-Dessouky et al. (2004)) and 58% of the total energy consumption in Canadian buildings is consumed by HVAC systems (NRCan (2014)).

Since people spend more than 90% of their time in buildings (Spengler and Sexton (1983)), it is important to provide good and healthy indoor environment for occupants. Depending on the climate (cold, hot, humid, etc.) and building type (hospital, school, residence, etc.), conditioning outdoor ventilation air can account for up to 30-60% of the total energy consumption in buildings (Awbi et al. (1998)). Wyon et al. (2004) found that poor indoor air quality may reduce the performance of the occupants in an office by up to 6-9%. Therefore, if ventilation rates are reduced below acceptable standards to save energy, occupant productivity losses are likely.

In vapor compression HVAC technologies, the moisture content of the indoor air is reduced by cooling the supply air to a temperature lower than its dew point temperature; thereafter the supply air is reheated to a comfortable supply air temperature. In this process, a significant amount of energy is consumed to condense the water vapor out of the air and then reheat the air. Moreover, liquid water in the cooling coil may lead to mold growth or the re-evaporation of water into the airstream, which may reduce the indoor air quality and increase the supply air humidity.

Over the past two decades, research has shown that using liquid desiccant HVAC systems in buildings can achieve high energy savings compared to conventional vapor compression HVAC systems (Abdel-Salam et al. (2014c)). The core component of liquid desiccant HVAC systems is a liquid desiccant energy exchanger, which is used to simultaneously transfer heat and moisture between the supply air and desiccant solution streams. Different types of liquid desiccant energy exchangers used in liquid desiccant HVAC systems are described in the following sections.

1.3 DIRECT-CONTACT LIQUID DESICCANT ENERGY EXCHANGERS

In the last two decades, direct-contact liquid desiccant air-conditioning systems, where the supply air is dehumidified through direct contact with a liquid desiccant solution, have been studied (Radhwan et al. (1993); Daou et al. (2006); Mei and Dai (2008); Wang et al. (2013); Enteria et al. (2013)). Direct-contact liquid desiccant systems investigated have included designs with two packed beds; one bed dehumidifies the airflow and the other bed regenerates the desiccant solution. In the dehumidifier, a cooled desiccant solution is sprayed over the packed bed which comes in direct contact with the hot-humid supply air. The supply air is cooled and dehumidified in the dehumidifier and the desiccant solution is heated and humidified. After the dehumidifier, the air is supplied to the HVAC unit whereas the diluted desiccant solution is heated and pumped to the regenerator, where it comes in direct contact with the exhaust air from the building, which cools and dries the solution. Further cooling of the solution may be required in an auxiliary heat exchanger (Radhwan et al. (1993); Daou et al. (2006); Mei and Dai (2008); Wang et al. (2013); Enteria et al. (2013)).

Despite the fact that direct-contact liquid desiccant systems may show significant energy savings when integrated in HVAC systems, there are several problems associated with these systems. (1) A high pressure drop on the airside increases the operating costs of fans and decreases the coefficient

of performance (COP) of the HVAC system. (2) Carryover of liquid desiccant aerosols where some droplets of the desiccant solution are carried downstream by the supply airflow, thus reducing indoor air quality, causing health problems for occupants, and corroding the ducting system.

1.4 LIQUID-TO-AIR MEMBRANE ENERGY EXCHANGERS (LAMEEs)

Liquid-to-air membrane energy exchangers (LAMEEs), where the air and desiccant solution are separated by a micro-porous membrane, have much lower pressure drop on the airside than that in the direct-contact liquid desiccant packed beds, and can eliminate the carryover problem associated with direct-contact liquid desiccant air-conditioning systems. In addition, for well-designed exchangers without significant air and liquid flow maldistributions, the effectiveness of each exchanger can be increased to more than 80%. The elimination of the carryover of desiccant droplets in LAMEEs means not only a reduction in the operating costs, but also the transient response delay times are reduced because smaller masses of liquid desiccant solution are required within each exchanger (Conde and Weber (2006)).

LAMEEs can be used as active air dehumidifiers and desiccant solution regenerators in liquid desiccant dehumidification systems. As well, two or more LAMEEs can be combined to constitute a run-around membrane energy exchanger (RAMEE) system for passive energy recovery from the exhaust air to precondition the supply air in HVAC systems. By rerouting the liquid desiccant flow with valves and pumps in the liquid flow loops, several HVAC system configurations can be achieved using the same set of exchangers (i.e. the passive operating condition may be used for one set of inlet air conditions and external auxiliary energy inputs make it an active HVAC system for other inlet air conditions).

1.5 LAMEE TYPES

1.5.1 Flat-Plate LAMEE

A flat-plate LAMEE has a structure similar to a parallel-plate heat exchanger, only the stiff metal or plastic plates are replaced by flexible micro-porous membranes. Figure 1.1 shows a schematic of a flat-plate LAMEE. The micro-porous membranes separate the desiccant solution and air streams, and allow simultaneous heat and moisture transfer between the two streams. A flat-plate LAMEE may have a cross-flow, counter-flow, or counter-cross-flow configuration. It can be employed as a dehumidifier or a regenerator in the liquid desiccant air conditioning systems. When a LAMEE is used for air cooling and dehumidifying, the heat and moisture are transferred from the hot-humid air to the desiccant solution, whereas the heat and moisture are transferred from the desiccant solution to the air when the LAMEE is employed as a solution regenerator.

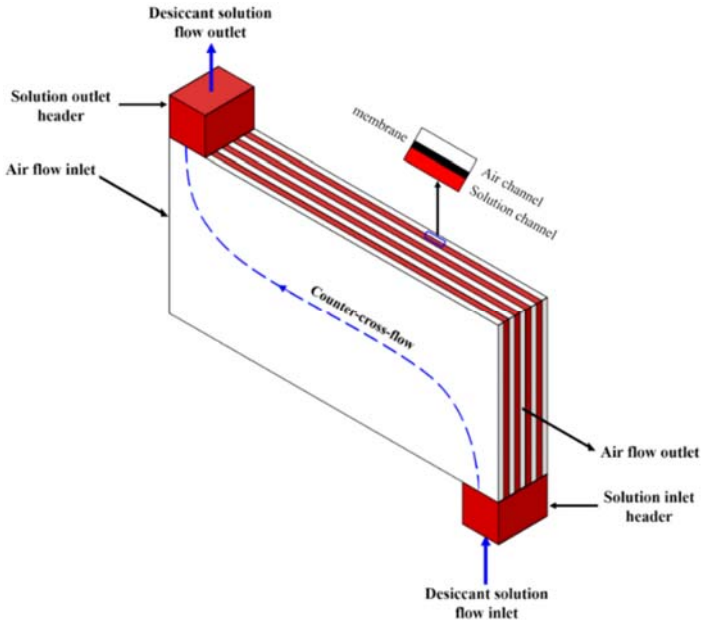

FIGURE 1.1. Schematic diagram of a counter-cross flat-plate LAMEE.

1.5.2 Hollow-Fiber LAMEE

Figure 1.2 shows a typical configuration of a hollow-fiber LAMEE. Its structure is similar to a

shell-and-tube heat exchanger but the metal tubes are replaced with hollow fiber semi-permeable membranes that allow simultaneous heat and moisture transfer between the working fluids. The air and liquid flow configurations inside the hollow-fiber LAMEE can be counter-flow or cross-flow, where the liquid flows inside the hollow fibers and the air flows around the fibers. Hollow fibers can be either staggered or aligned with the flow (Zhang (2011); Zhang et al. (2012a); Zhang et al. (2012b)).

(a)

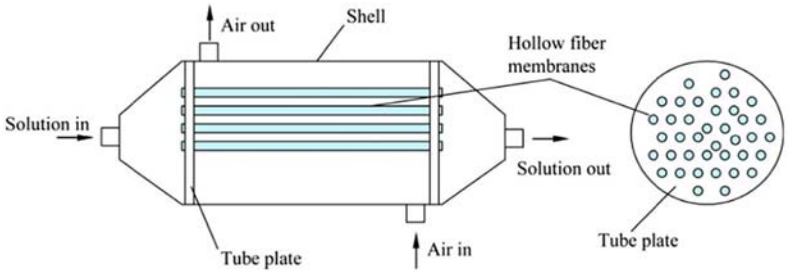

(b)

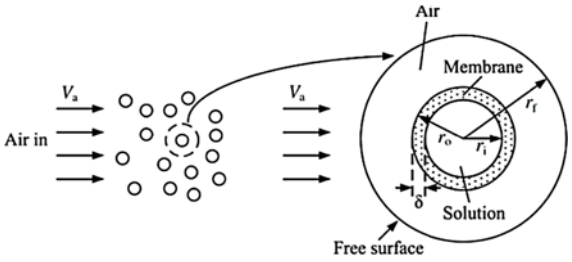

FIGURE 1.2. (a) Structure of a hollow-fiber LAMEE (Zhang (2011)) (b) a detailed schematic of a single hollow fiber (Zhang et al. (2012a)).

1.6 LAMEE APPLICATIONS

1.6.1 LAMEE-Based Hybrid Liquid Desiccant Air-Conditioner

Figure 1.3 shows a schematic diagram of a LAMEE-based hybrid liquid desiccant air-conditioner. A LAMEE-based hybrid air-conditioner is composed of a conventional air-conditioning system integrated with a LAMEE-based dehumidification system, where two flat-plate or hollow-fiber LAMEEs are used as an active dehumidifier and regenerator. The novel hybrid air-conditioner has

the ability to eliminate the problem of desiccant solution droplet carryover and maintains the advantages of conventional direct-contact liquid desiccant dehumidification systems. The hybrid air-conditioner can be utilized either in buildings or automobiles. Over the past decade, research (Abdel-Salam et al. (2013, 2014a); Abdel-Salam and Simonson (2014a, 2014b); Zhang and Zhang (2014); Bergero and Chiari (2010, 2011); Vestrelli (2006)) has been conducted to improve the performance of the LAMEE-based hybrid air-conditioner.

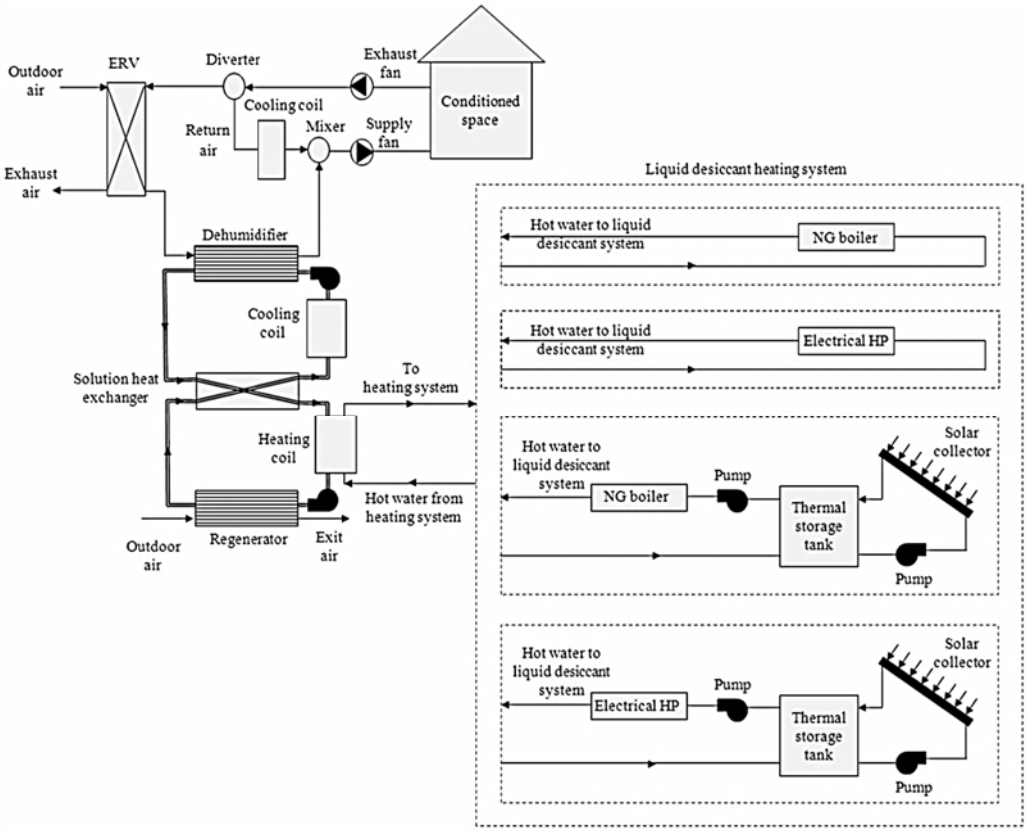

FIGURE 1.3. Schematic diagram of the hybrid membrane liquid desiccant air-conditioning systems (Abdel-Salam et al. (2014a)).

1.6.2 Run-Around Membrane Energy Exchangers (RAMEEs)

A RAMEE system is typically composed of two flat-plate LAMEEs coupled within a liquid desiccant solution loop. One of the LAMEEs is located in the supply air stream and is referred to

as the supply LAMEE, while the other LAMEE is located in the exhaust air stream and is referred to as the exhaust LAMEE. Figure 1.4 shows a schematic diagram of a RAMEE installation in a building. During summer seasons, heat and moisture are transferred from the hot-humid outdoor air into the desiccant solution in the supply LAMEE. The outdoor air is cooled and dehumidified and the desiccant solution becomes diluted. At steady-state conditions for the loop, the exhaust air from the conditioned space passes through the exhaust LAMEE to regenerate the diluted desiccant solution while the exhaust air is discharged to the outside at a higher temperature and humidity content than its inlet conditions. The same process may occur during winter but the direction of heat and mass transfer is reversed; however, when the outside air is very dry in the winter, it is necessary to continuously add water to the loop to prevent the crystallization of the desiccant solution and maintain steady-state operating conditions. RAMEEs can be installed in existing or new buildings because they do not require the supply and exhaust air streams to be adjacent. Moreover, RAMEEs reduce the capital costs of the HVAC heating/cooling equipment and reduce the operating costs by reducing the heating and cooling energy consumption of the HVAC system (Fan et al. (2005); Fan et al. (2006); Seyed (2008); Vali (2009); Afshin (2010); Mahmud et al. (2010); Hemingson et al. (2011a); Ge et al. (2013a)).

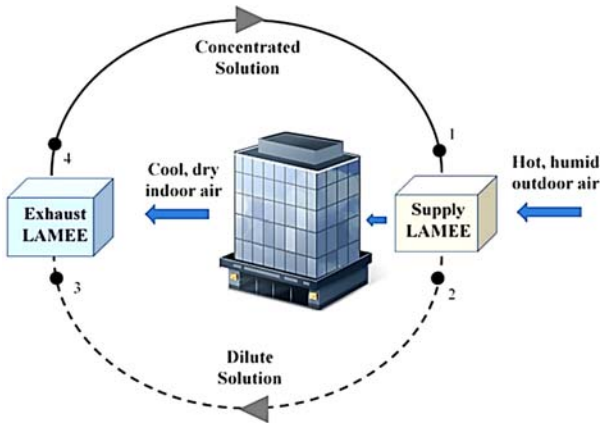

FIGURE 1.4. Schematic diagram of a RAMEE installed in a building during summer operating conditions (Afshin (2010)).

1.7 RESEARCH HYPOTHESIS AND OBJECTIVES

In 2-fluid LAMEEs, moisture transfer between the air and desiccant solution is accompanied with the release/absorption of phase change energy which changes the temperature of the desiccant solution and reduces the differences between the air and desiccant solution temperatures and vapor pressures inside the exchanger. Therefore, the change in the temperature of the desiccant solution reduces the rates of heat and moisture transfer between the air and desiccant solution inside the exchanger.

Adding a third fluid within the desiccant solution may reduce the variations in the temperature and vapor pressure of the desiccant solution inside the exchanger during heat and moisture transfer between the air and desiccant solution, which may improve the LAMEE performance. A novel 3-fluid LAMEE is proposed in this thesis. The 3-fluid LAMEE will have refrigerant tubes installed inside the solution channels to control the temperature of the desiccant solution along the entire length of the exchanger during the process of heat and moisture transfer between the air and desiccant solution. The main hypothesis of this thesis is that adding a third fluid to control the desiccant solution temperature inside the 3-fluid LAMEE may improve the rates of heat and moisture transfer between the air and desiccant solution compared to 2-fluid LAMEEs.

The main goal of this thesis is to develop a novel flat-plate liquid desiccant membrane energy exchanger (3-fluid LAMEE) and to test and compare the performance of the 3-fluid and 2-fluid LAMEEs. Three objectives are set to fulfill the main goal as summarized in Figure 1.5.

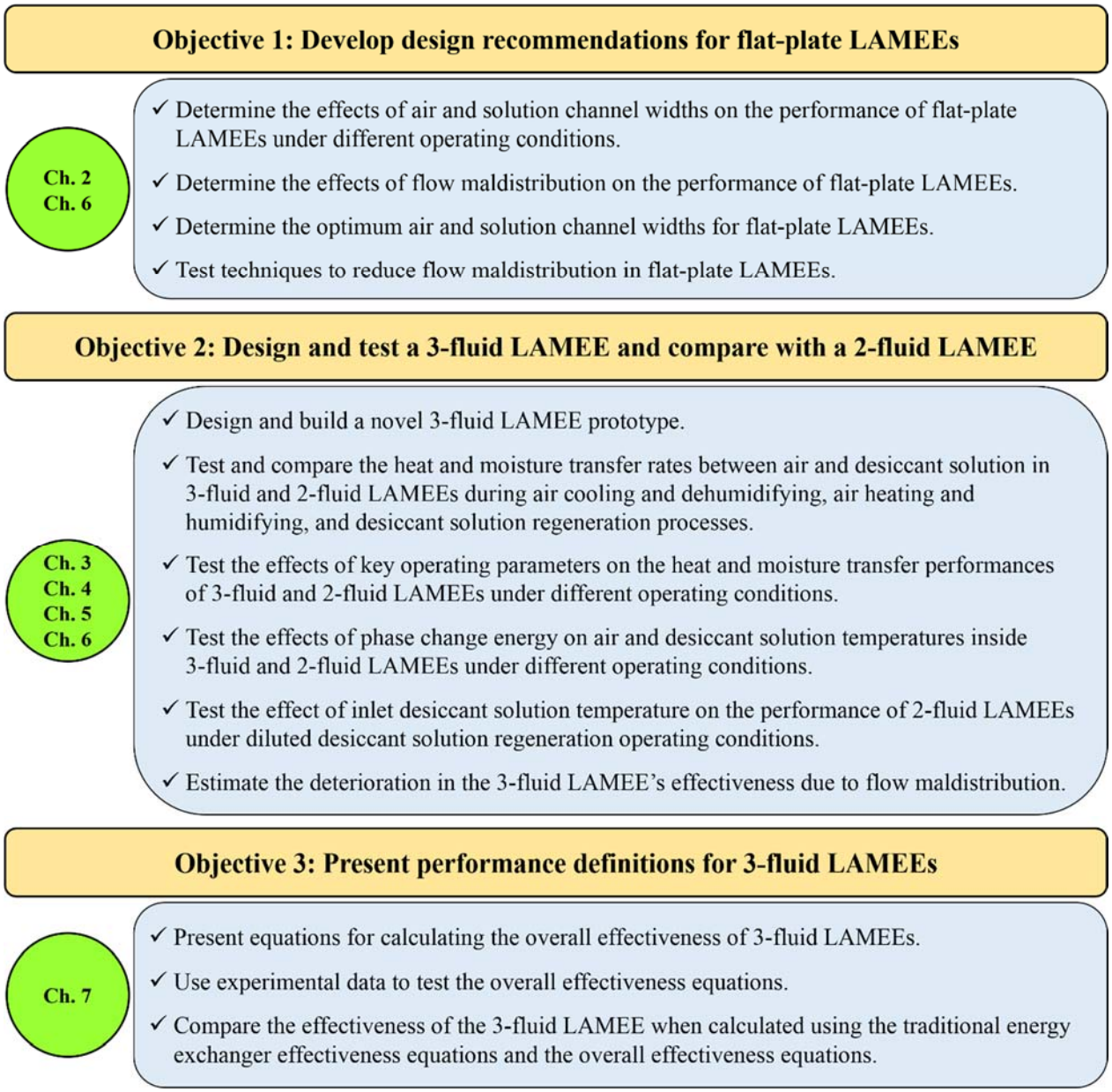

FIGURE 1.5. Objectives and content of this Ph.D. thesis.

1.8 THESIS STRUCTURE

As shown in Figure 1.5, this thesis is composed of eight chapters. Each chapter, except Chapter 8, contains a research paper that addresses part of the objectives of the thesis. The first objective (to develop design recommendations for flat-plate LAMEEs) is addressed in Chapters 2 and 6. In Chapter 2, two key design parameters ((a) thickness of the air and solution channels and (b) air

flow maldistribution) will be studied numerically. These studies will provide guidelines for LAMEE designers and will be used to design the 3-fluid LAMEE used to meet the second objective of this thesis. Chapter 6 is connected to the design recommendations objective because it will present the feasibility of using membrane pre-tension to reduce flow maldistribution caused by membrane deflections in flat-plate LAMEEs.

The second objective of this thesis is to design, fabricate and test a novel 3-fluid LAMEE and compare its performance with conventional 2-fluid LAMEEs. This objective will be addressed in Chapters 3, 4, 5, and 6. Chapter 3 presents the design of the 3-fluid LAMEE based on the results of the numerical studies presented in Chapter 2. The design and fabrication of the 3-fluid LAMEE and the experimental setup are described in Chapter 3. The heat and moisture transfer rates between the air and desiccant solution in the 3-fluid LAMEE and a 2-fluid LAMEE will be tested and compared during: (a) air cooling and dehumidifying in Chapters 3 and 4, (b) desiccant solution regeneration in Chapter 5, and (c) air heating and humidifying in Chapter 6. In all four chapters (Chapter 3-6), the sensitivity of the heat and moisture transfer rates to key operating parameters will be investigated. To quantify the importance of the phase change energy on LAMEE performance, the effects of phase change energy on the temperature of the desiccant solution and air will be tested during air cooling and dehumidifying process in Chapter 4 and during air heating and humidifying process in Chapter 6.

The third objective of this thesis is to present performance definitions for 3-fluid LAMEEs. In Chapter 7, performance definitions for calculating the overall effectiveness of 3-fluid LAMEEs will be presented and tested using the experimental data presented in Chapter 3. The effectiveness of the 3-fluid LAMEE will be calculated using the overall definitions and compared with the traditional energy exchanger effectiveness equations presented in Chapter 3.

Chapter 8 provides a summary of the research presented in the thesis and identifies the important conclusions and contributions of the thesis and suggests topics for future research. The copyright permissions for manuscripts used in this thesis are presented in Appendix A.

1.9 LIST OF PUBLICATIONS

1.9.1 Papers in Refereed Journals

The following papers are included in the following chapters in this thesis.

Chapter 1: Abdel-Salam M.R.H., Ge G., Fauchoux M., Besant R.W., Simonson C.J., 2014. State-of-the-art in liquid-to-air membrane energy exchangers (LAMEEs): a comprehensive review. *Renewable and Sustainable Energy Reviews*, **39**, 700-728.

Chapter 1: Abdel-Salam M.R.H., Fauchoux M., Ge G., Besant R.W., Simonson C.J., 2014. Expected energy and economics benefits, and environmental impacts for liquid-to-air membrane energy exchangers (LAMEEs) in HVAC systems: a review. *Applied Energy*, **127**, 202-218.

Chapter 2: Abdel-Salam M.R.H., Besant R.W., Simonson C.J., 2015. Sensitivity of the performance of a flat-plate liquid-to-air membrane energy exchanger (LAMEE) to the air and solution channel widths and flow maldistribution. *International Journal of Heat and Mass Transfer*, **84**, 1082-1100.

Chapter 3: Abdel-Salam M.R.H., Besant R.W., Simonson C.J., 2016. Design and testing of a novel 3-fluid liquid-to-air membrane energy exchanger (3-Fluid LAMEE). *International Journal of Heat and Mass Transfer*, **92**, 312-329.

Chapter 4: Abdel-Salam M.R.H., Ge G., Besant R.W., Simonson C.J., 2016. Experimental study of effects of phase-change energy and operating parameters on performances of two-fluid and three-fluid liquid-to-air membrane energy exchangers. *ASHRAE Transactions*, **122(1)**, 134-145.

Chapter 5: Abdel-Salam M.R.H., Besant R.W., Simonson C.J., 2016. Performance testing of a novel 3-fluid liquid-to-air membrane energy exchanger (3-fluid LAMEE) under desiccant solution regeneration operating conditions. *International Journal of Heat and Mass Transfer*, **95**, 773-786.

Chapter 6: Abdel-Salam M.R.H., Besant R.W., Simonson C.J., 2016. Performance testing of 2-fluid and 3-fluid liquid-to-air membrane energy exchangers for HVAC applications in cold-dry climates. *International Journal of Heat and Mass Transfer*, Submitted.

Chapter 7: Abdel-Salam M.R.H., Besant R.W., Simonson C.J., 2016. Performance definitions for 3-fluid heat and moisture exchangers. *Transactions of the ASME: Journal of Heat Transfer*, Submitted.

1.9.2 Papers in Conference Proceedings

The following conference paper was published but is not included as part of the thesis.

Abdel-Salam M.R.H., Besant R.W., Simonson C.J., 2015. Performance testing of a novel 3-fluid liquid-to-air membrane energy exchanger (3-fluid LAMEE) for HVAC applications. Proceedings of the 28th International Conference on Efficiency, Cost, Optimization, Simulation and Environmental Impact of Energy Systems, June 30-July 3, Pau, France, 11 pages.

1.10 PATENTS

The following provisional patent was submitted to the US Patent Office based on the research from this thesis.

Simonson C.J., Abdel-Salam M.R.H., Besant R.W., 3-fluid liquid-to-air membrane conditioning module, US provisional patent application number 62/185406, filed on June 26, 2015.

CHAPTER 2

DESIGN OF FLAT-PLATE LAMEES

2.1 OVERVIEW OF CHAPTER 2

Several flat-plate LAMEEs have been designed and tested over the past two decades; however, to the best of my knowledge, no studies have been conducted that provide design guidelines on channel spacing and flow maldistribution in flat-plate LAMEEs. This chapter addresses the first objective of this thesis (i.e. to develop design recommendations for flat-plate LAMEEs). A numerical model is used to study the effects of air and solution channel widths on the performance of flat-plate LAMEEs. The effects of flow maldistribution on the performance of flat-plate LAMEEs are numerically studied, and practical air and solution channel widths for flat-plate LAMEEs are determined. The results of the numerical studies presented in this chapter will guide the design of the novel 3-fluid LAMEE presented in Chapter 3 and tested in Chapters 3-7 of this thesis.

The manuscript presented in this chapter is published in the International Journal of Heat and Mass Transfer.

Sensitivity of the Performance of a Flat-Plate Liquid-To-Air Membrane Energy Exchanger (LAMEE) to the Air and Solution Channel Widths and Flow Maldistribution

(International Journal of Heat and Mass Transfer, 2015, Volume 84)

Mohamed R. H. Abdel-Salam, Robert W. Besant, Carey J. Simonson

2.2 ABSTRACT

Liquid-to-air membrane energy exchangers (LAMEEs) are novel energy exchangers which use semi-permeable membranes to separate air and desiccant solution streams. The semi-permeable membrane allows simultaneous heat and water vapor transfer between the air and the desiccant solution streams. These exchangers, which include bonded elastic membranes, are prone to significant variations in the flow channel widths, which causes flow maldistribution and lead to reduced performance. In this chapter, a numerical model is used to show the sensitivity of the steady-state performance of a flat-plate LAMEE to the air and solution channel widths, when operated as a supply air dehumidifier and a diluted desiccant solution regenerator. Simulation results show that, without air flow channel width variations, the effectiveness of both the dehumidifier and the regenerator can always be increased toward 1.0 by reducing the air and solution channel widths. To account for variations in the air channel widths, which occur due to construction tolerances and pressure differences across the membrane, equations are used to investigate the influence of random variations in the air channel widths on the performance (i.e. effectiveness and air pressure drop) of the flat-plate LAMEE. The main contribution of this chapter is that it shows that there exists an optimal air channel width for flat-plate LAMEEs with flow maldistribution due to random variations in the air channel width. Decreasing the air channel width below this optimal value will result in a decrease in effectiveness. Based on the results presented in this chapter, it is found that the recommended practical air channel width for flat-plate LAMEEs

is in the range of 5-6 mm and the practical solution channel width is 1-2 mm.

2.3 INTRODUCTION

Buildings are responsible for about 40% of the global energy consumption (Wyon (2004); Omer (2008); Kolokotsa et al. (2011)). Heating, ventilation, and air-conditioning (HVAC) systems consume a substantial portion of this total. For instance, HVAC systems were responsible for 58% of the total energy consumed by Canadian buildings in 2011 (NRCan (2014)). Over the last decade, the integration of liquid desiccant technologies into HVAC systems became of interest for research groups due to the promising energy savings that can be achieved by liquid desiccant HVAC systems, as compared to conventional HVAC systems. Laboratory tests have shown that direct-contact liquid desiccant conditioners can have a good effectiveness when they are well designed, constructed and operated (Liu et al. (2007); Martin and Goswami (2000); Elsayed et al. (1993)). Although these exchangers have showed promising performance and energy savings, the carryover of desiccant solution aerosols into the supply airstream is a concern when using direct-contact exchangers, because it may lead to the degradation of indoor air quality and the corrosion of the downstream air ducting.

The desiccant carryover problem can be eliminated by using a liquid-to-air membrane energy exchanger (LAMEE). The LAMEE is a novel energy exchanger, in which air and desiccant solution streams are separated using semi-permeable membranes. These membranes allow simultaneous heat and moisture transfer between the air and desiccant solution streams, but do not allow the transfer of any liquid droplets, and thus eliminate the desiccant carryover problem. LAMEEs can be used for several types of applications in HVAC systems. For instance, two LAMEEs can be used as an air dehumidifier and a diluted desiccant solution regenerator in a membrane liquid desiccant air-conditioning system (Zhang and Zhang (2014); Abdel-Salam and

Simonson (2014a, 2014b); Abdel-Salam et al. (2013, 2014a); Bergero and Chiari (2011)), or in a run-around membrane energy exchanger (RAMEE) system (Erb et al. (2009); Mahmud et al. (2010); Hemingson et al. (2011a); Akbari et al. (2012); Patel et al. (2014)) for passive energy recovery in buildings.

2.4 LITERATURE REVIEW

Comprehensive reviews of the fundamentals of different types of LAMEEs (e.g. flat-plate and hollow-fiber) and their applications are presented in Abdel-Salam et al. (2014b, 2014c) (excerpts from these two papers are presented in Chapter 1) and Ge et al. (2013a). Over the past decade, several research studies were conducted on the steady-state performance of a flat-plate LAMEE when used as a supply air dehumidifier (Isetti et al. (1997); Zhang (2011); Ge et al. (2013b, 2014a); Moghaddam et al. (2013a, 2013b 2013c); Namvar et al. (2012)). Isetti et al. (1997) theoretically studied the influences of different design and operating parameters on the rate of moisture transfer through the semi-permeable membrane of a LAMEE. An analytical model for a semi-permeable hollow-fiber LAMEE was developed by Zhang (2011), and then modified for a flat-plate LAMEE by Ge et al. (2013b). Moghaddam et al. (2013a) experimentally studied the influence of different desiccant solution concentrations on the LAMEE's performance and showed an enhancement in the LAMEE's performance due to the increase of the desiccant solution concentration.

The influences of several design and operating parameters on the LAMEE's performance when used for air dehumidification were investigated by Ge et al. (2014a), and it was found that the moisture flux ratio (i.e. the ratio between the actual moisture transfer rate across the membrane and the moisture transfer capacity of the membrane (Ge et al. (2014a))) decreased with the increase in the number of heat transfer units (*NTU*). Moghaddam et al. (2013b) found that installing an insert in the air channels of the LAMEE enhanced the convective heat transfer coefficient of the

airside by up to 150%. Namvar et al. (2012) found that the LAMEE's sensible, latent, and total effectivenesses increased with the increase of either *NTU* or solution-to-air heat capacity ratio (*Cr**) until a certain point, and thereafter no significant enhancements occurred. Moghaddam et al. (2013c) found that the latent effectiveness of the LAMEE under air cooling and dehumidifying operating conditions (i.e. summer operating conditions) was higher than that under air heating and humidifying operating conditions (i.e. winter operating conditions).

Fewer studies were reported in the literature on the steady-state performance of the flat-plate LAMEE when used as a diluted desiccant solution regenerator. Ge et al. (2014a) experimentally studied the influences of several design and operating parameters on the performance of the regenerator. They found that the moisture flux ratio increased with the increase of either *Cr** or the desiccant solution inlet temperature. Moghaddam et al. (2013d) experimentally investigated the influences of the desiccant solution inlet temperature on the effectiveness and the moisture removal rate of the regenerator. The results showed that increasing the desiccant solution inlet temperature resulted in a decrease in the effectiveness and an increase in the moisture removal rate. During regeneration of the diluted desiccant solution, the main objective is to increase the concentration of the diluted desiccant solution by transferring water vapor from the desiccant solution to the regeneration air. The effectiveness of a regenerator is usually evaluated based on the airside temperature and humidity ratio. Moghaddam et al. (2014) presented new correlations to calculate the solution side effectiveness of a LAMEE, and conducted a study on the differences between evaluating the effectiveness of a regenerator based on the temperature and humidity ratio of the airside versus the temperature and humidity ratio of the solution side.

The term "*Compact*" in the field of heat/energy exchangers refers to a high area density, which is the ratio between the exchanger surface area for heat/mass transfer and the total volume of the

exchanger. Compact exchangers have an area density ≥ 700 m^2/m^3 if the working fluids are gases and ≥ 300 m^2/m^3 if the working fluids are liquid or two-phase (Reay (2002)). Mehendale et al. (2000) stated that the hydraulic diameter (D_h) of channels of compact heat exchangers constructed using welded metal methods ranges between 1 mm and 6 mm. Compared with conventional heat/energy exchangers, compact exchangers can have higher effectiveness, smaller volume, lighter weight, lower costs, and higher safety (Reay (2002)). Therefore, compact heat/energy exchangers are attractive in various applications (e.g. electronics cooling, automotive industry, power plants, chemical plants, petroleum industry, HVAC systems, solar thermal systems, food industry, etc.). One of the most effective techniques for increasing the compactness of a flat-plate LAMEE is to decrease the widths of the air and/or solution channels. Narrow exchanger flow channels, however, are not without disadvantages and risks. Narrow channels usually imply high pressure drop in the airside of the exchanger, which increases the operating costs of the system (i.e. energy consumption of fans).

2.5 MOTIVATION OF THE CURRENT STUDY

One cannot find the best design channel width for flat-plate LAMEEs without considering all the factors that impact design and performance. As discussed, narrow channel widths may boost the performance of a flat-plate LAMEE. However, attention must be paid to the variation in channel width, from one channel to the next. Small variations may occur due to manufacturing tolerances, as well as due to elastic and plastic deformations of the flow channels during operation. Flow maldistribution through a channel can be significant when the variation in channel width exceeds 5% of the nominal channel width (Shang and Besant (2005)). Narrow channels also require more spacer supports within the airflow channels when elastic membranes are used, and require minimizing the membrane deflections due to pressure differences across the membrane. For

exchangers with multiple flow channels, variations in flow velocity from one channel to another can also occur and the resulting maldistribution must be accounted for and minimized in the design. As well, narrow channels create more difficulties when it comes to filtering and cleaning the airflow channel surfaces. Finding the best channel width is a complex design problem. In this study, flow channel variations will be accounted for in the results by selecting an assumed magnitude of variation and correcting the effectiveness for this width and the other widths selected for study.

Table 2.1 lists several flat-plate LAMEE prototypes which have been designed, constructed, and tested over the past decade. Although each prototype was designed with different air and solution channel widths, no studies have been conducted to evaluate the performance impacts of air and solution channel widths of the flat-plate LAMEEs. The only information available in the literature about the influences of different air and solution channel widths on the performance of membrane energy exchangers is provided by Fan (2005); however, this brief study focused on the performance of a RAMEE system, which is composed of two flat-plate LAMEEs coupled in a closed pumped desiccant solution loop. The theoretical study conducted by Fan (2005) showed that decreasing the width of the solution channels from 2 mm to 0.4 mm had almost no influence on the sensible, latent, and total effectivenesses of the system, while decreasing the width of the air channels from 7 mm to 2 mm may have the potential to increase the sensible, latent, and total effectivenesses by 7%, 9%, and 8%, respectively. Thus, the objective of this chapter is to investigate the influences of the nominal air and solution channel widths and flow maldistribution on the steady-state performance of a flat-plate LAMEE.

TABLE 2.1. Nominal air and solution channel widths of several flat-plate LAMEE prototypes tested by several researchers.

Flat-Plate LAMEE prototype	Air channel width (mm)	Solution channel width (mm)
Bergero and Chiari (2011)	2.5	1.2
Bergero and Chiari (2004)	3	2
Mahmud et al. (2010)	3.18	1.5
Erb et al. (2009)	4.76	1.7
Moghaddam et al. (2013a)	5	1.6
Ge et al. (2014)	5	2.4
Beriault (2011); Namvar et al. (2012)	6.35	3.17

2.6 THE FLAT-PLATE LAMEE

2.6.1 Design

Figure 2.1 shows a schematic of a flat-plate LAMEE comprised of several adjacent air and solution channels separated by semi-permeable membranes. The semi-permeable membrane transfers heat and water vapor between the air and desiccant solution streams and prevents liquid desiccant solution from passing through it, as long as the pressure difference between the air and desiccant solution streams is less than the membrane's liquid penetration pressure. The temperature and water vapor pressure differences between the air and desiccant solution streams are the driving forces for the heat and water vapor transfer. A flat-plate LAMEE can be used for air cooling and dehumidifying or diluted desiccant solution regeneration, depending on the inlet air and desiccant solution conditions. In the air cooling and dehumidification processes, heat and water vapor are transferred from the hot-humid airflow to the desiccant solution stream, causing the desiccant solution to become diluted. Afterwards, the desiccant solution regenerator is used to reconcentrate the diluted desiccant solution, where the heat and water vapor are transferred from the diluted desiccant solution stream to the regeneration airflow.

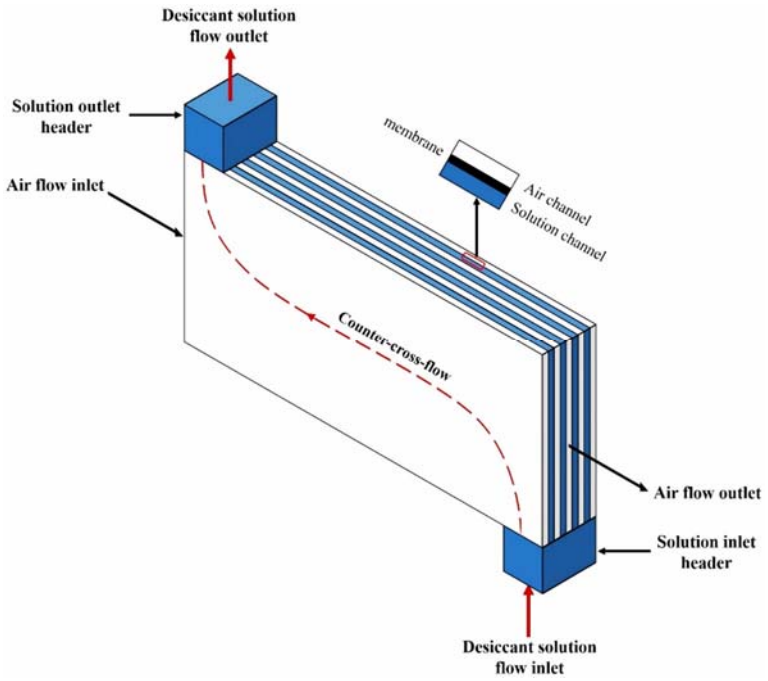

FIGURE 2.1. Schematic of a counter-cross flat-plate LAMEE (Abdel-Salam et al. (2014c)).

An exchanger with a counter-flow configuration has a higher effectiveness than one with a cross-flow or parallel-flow configuration (ASHRAE (2004)). However, it is difficult to construct a flat-plate LAMEE with adjacent inlets/outlets for the supply air and desiccant solution streams. Therefore, a counter-cross-flow configuration was proposed by Vali (2009) and Vali et al. (2009). In this exchanger, no internal guides were used to force the desiccant solution to be in counter flow with the airflow. Subsequently, it was found that internal solution flow guides would insure that more than 90% of the exchanger surface was counter-flow (Moghaddam et al. (2013e)). Figure 2.2 shows a schematic of a solution channel where internal guides are used to create a counter-cross-flow configuration in a flat-plate LAMEE reported by Moghaddam et al. (2013e). The air and desiccant solution streams have a counter-flow configuration along more than 90% of the LAMEE's length, and a cross-flow configuration only in the inlet and outlet regions (i.e. solution inlet/outlet headers). The ratio between the length of inlet/outlet solution header and the total length of the LAMEE is referred to as the entrance ratio (Vali (2009)).

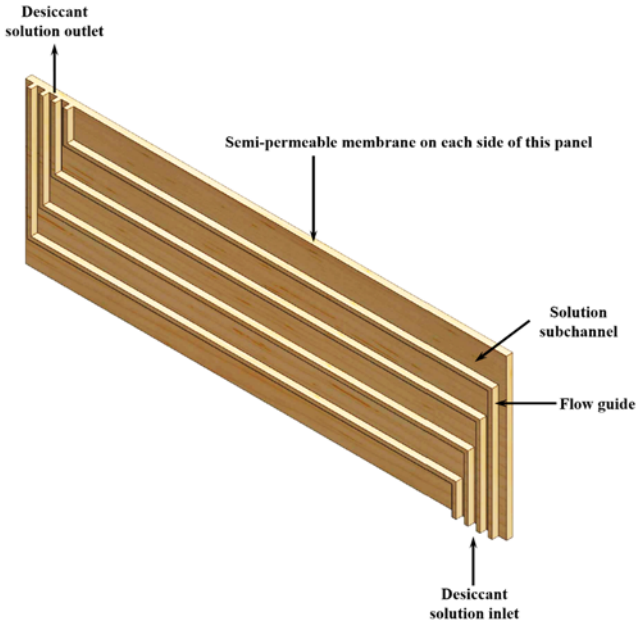

FIGURE 2.2. Schematic of a solution channel with internal guides to create a counter-cross-flow configuration in a flat-plate LAMEE.

The design of LAMEEs depends on multiple design parameters including the channel width, the exchanger length and height, the surface area for heat/mass transfer, the flow configuration between the working fluids, the membrane thermo-physical properties, and the heat and moisture transfer capacity rates of the fluids. In addition, the operating conditions (air cooling and dehumidifying, air heating and humidifying, diluted solution regeneration) affect the performance (Kamali et al. (2016)). A multi-objective algorithm can be used to optimize the design of the LAMEE for a specific operating condition or a range of operating conditions based on effectiveness, airside pressure drop, compactness and capital/maintenance costs.

In this Chapter, the only design recommendations that will be developed are the air and solution channel widths for flat-plate LAMEEs. A numerical study will be performed to determine the effects of the air and solution channel widths on the heat and moisture transfer rates in LAMEEs. Other design and operating parameters (the exchanger length and height, the surface area of heat/mass transfer, the membrane thermo-physical properties, the air and solution flow

configurations, air and solution mass flow rates, inlet air and solution temperatures, inlet air humidity ratio, and inlet solution concentration) are kept constant and the sensitivity of the LAMEE performance to the variations in the air and solution channel widths will be investigated.

2.6.2 Performance Evaluation of Flat-Plate LAMEEs

Effectiveness is the most important performance factor for energy exchangers (ASHRAE Standard 84 (2008)). Sensible, latent, and total effectivenesses of a flat-plate LAMEE are defined as the ratios between the actual and maximum sensible energy, latent energy, and total energy transfer rates, respectively, into/from the airflow as it passes through the LAMEE. For solution-to-air exchangers with a heat capacity ratio greater than unity ($Cr^* \geq 1$), sensible, latent, and total effectivenesses are calculated from Equations (2.1) to (2.3) (Simonson and Besant (1999)).

$$\varepsilon_{\text{sen}} = \frac{T_{\text{air,in}} - T_{\text{air,out}}}{T_{\text{air,in}} - T_{\text{sol,in}}} \tag{2.1}$$

$$\varepsilon_{\text{lat}} = \frac{W_{\text{air,in}} - W_{\text{air,out}}}{W_{\text{air,in}} - W_{\text{sol,in}}} \tag{2.2}$$

$$\varepsilon_{\text{tot}} = \frac{\varepsilon_{\text{sen}} + H^* \varepsilon_{\text{lat}}}{1 + H^*} \tag{2.3}$$

where ε is the effectiveness, T is the temperature (ºC), W is the humidity ratio (kg/kg), and H^* is the operating factor which is calculated from equation (2.4) (Simonson and Besant (1999)). Subscripts *sen*, *lat*, and *tot* refer to sensible, latent, and total, respectively, while subscripts *air*, *sol*, *in*, and *out* refer to air, solution, inlet, and outlet, respectively.

$$H^* \approx 2500 \, \frac{W_{\text{air,in}} - W_{\text{sol,in}}}{T_{\text{air,in}} - T_{\text{sol,in}}} \tag{2.4}$$

Moisture removal rate ($\dot{m}_{\text{rr}}$) is another important parameter that is used to evaluate the

performance of flat-plate LAMEEs. The moisture removal rate is defined as the mass flow rate of water vapor between the air and desiccant solution streams across the semi-permeable membrane, and is calculated from equation (2.5). This term comes into play for desiccant solution regeneration or drying processes because crystallization problems can occur within a porous membrane when the moisture removal rate is high and the desiccant solution is near crystallization conditions.

$$\dot{m}_{\mathrm{rr}} = \dot{m}_{\mathrm{air}} \left| W_{\mathrm{air,in}} - W_{\mathrm{air,out}} \right| \tag{2.5}$$

where $\dot{m}_{\mathrm{air}}$ is the mass flow rate of air (kg/s).

The sensible, latent, and total effectivenesses, and moisture removal rate of a flat-plate LAMEE significantly depend on three dimensionless numbers: *Cr*, NTU*, and the number of mass transfer units (NTU_{m}). *Cr*, NTU*, and NTU_{m} are calculated from equations (2.6) to (2.10).

$$C_r^* = \frac{C_{\mathrm{sol}}}{C_{\mathrm{air}}} = \frac{\dot{m}_{\mathrm{sol}}\, c_{\mathrm{p,sol}}}{\dot{m}_{\mathrm{air}}\, c_{\mathrm{p,air}}} \tag{2.6}$$

where *Cr** is the heat capacity ratio, *C* is the heat capacity rate (W/K), $\dot{m}_{\mathrm{sol}}$ is the mass flow rate of desiccant solution (kg/s), and c_{p} is the specific heat capacity (J/(kg·K)).

$$NTU = \frac{UA}{C_{\mathrm{min}}} \tag{2.7}$$

$$U = \left[\frac{1}{h_{\mathrm{air}}} + \frac{\delta_{\mathrm{mem}}}{k_{\mathrm{mem}}} + \frac{1}{h_{\mathrm{sol}}} \right]^{-1} \tag{2.8}$$

where *U* is the overall heat transfer coefficient (W/(m^2·K)), *A* is the membrane surface area (m^2), C_{min} is the minimum heat capacity rate of air and desiccant solution flows (W/K), *h* is the convective heat transfer coefficient (W/(m^2·K)), δ_{mem} is the membrane thickness (m), and k_{mem} is the thermal conductivity of the membrane (W/(m·K)).

$$NTU_{\mathrm{m}} = \frac{U_{\mathrm{m}} A}{\dot{m}_{\min}} \tag{2.9}$$

$$U_{\mathrm{m}} = \left[\frac{1}{h_{\mathrm{m,air}}} + \frac{\delta_{\mathrm{mem}}}{k_{\mathrm{m}}} + \frac{1}{h_{\mathrm{m,sol}}} \right]^{-1} \tag{2.10}$$

where U_{m} is the overall mass transfer coefficient (kg/(m^2·s)), $\dot{m}_{\min}$ is the minimum mass flow rate of air and desiccant solution flows (kg/s), h_{m} is the convective mass transfer coefficient (kg/(m^2·s)), and k_{m} is the water vapor permeability of the membrane (kg/(m·s)).

The convective heat and mass transfer coefficients of the air and desiccant solution are calculated from equations (2.11) and (2.12).

$$Nu = \frac{h D_{\mathrm{h}}}{k} \tag{2.11}$$

$$Sh = \frac{h_{\mathrm{m}} D_{\mathrm{h}}}{D} \tag{2.12}$$

where Nu is Nusselt number, D_{h} is the hydraulic diameter (m), k is the coefficient of thermal conductivity (W/(m·K)), Sh is Sherwood number, h_{m} is the convective mass transfer coefficient (m/s), and D is the mass diffusivity (m^2/s).

Nusselt number is assumed to be 8.24 for a fully developed laminar flow between two infinite rectangular parallel plates with a constant heat flux (Incropera and Dewitt (2002); Kays and Crawford (1990); Nellis and Klein (2009); Çengel (2006)). Sh and h_{m} can be calculated using the *Chilton-Colburn analogy* (Colburn (1933); Chilton and Colburn (1934)) as follows (Çengel (2006); Welty et al. (2001)).

$$Nu = Sh \cdot Le^{1/3} \tag{2.13}$$

$$Le = \frac{\alpha}{D} \tag{2.14}$$

$$h_{\mathrm{m}} = \frac{h}{c_{\mathrm{p}}}\, Le^{-2/3} \tag{2.15}$$

where *Le* is Lewis number, and α is the thermal diffusivity (m^2/s).

2.7 NUMERICAL STUDY

2.7.1 Numerical Model

A numerical study is performed to investigate the influences of the air and solution channel widths on the sensible, latent, and total effectivenesses, the moisture removal rate, and the airside pressure drop of a flat-plate LAMEE when used for both air cooling and dehumidifying and diluted desiccant solution regeneration. The numerical study is performed using a simulation program called "Enthalpy Pump System (EPS)". The EPS program was developed and validated at the University of Saskatchewan, and, after many test comparisons, it was found to be reliable to evaluate the performance of flat-plate LAMEEs (Fan (2005); Fan et al. (2006); Seyed (2008); Seyed et al. (2009); Vali (2009); Vali et al. (2009); Hemingson (2010)). The EPS program can be used to simulate the steady-state and the transient performances of a flat-plate LAMEE with different flow configurations (i.e. counter-flow, cross-flow, counter-cross-flow) when used for air cooling and dehumidifying, air cooling and humidifying, air heating and dehumidifying, air heating and humidifying, and diluted desiccant solution regeneration.

The EPS model uses the finite difference method to discretize the heat and moisture transfer governing equations presented in Appendix B. The Gauss-Seidel method is used to solve the coupled algebraic equations. The numerical study is performed with 200 X 200 spatial nodes. The numerical model was developed based on the following assumptions (Fan (2005); Fan et al. (2006); Seyed (2008); Seyed et al. (2009); Vali (2009); Vali et al. (2009); Hemingson (2010)).

1. The air and desiccant solution are fully developed laminar flows in each flat plate flow channel.
2. There are only negligible heat losses to the surroundings because the LAMEE is well insulated.
3. The heat conduction and mass diffusion in the axial direction are negligible for both air and desiccant solution flows ($Pe > 20$) (Luo and Roetzel (1998)).
4. The direction of heat and water vapor flux between the air and desiccant solution is normal to the semi-permeable membrane.
5. The properties of the semi-permeable membrane are constant.
6. Only water vapor and heat are transferred across the semi-permeable membrane.
7. The influences of flow maldistribution in air and desiccant solution channels are neglected in the numerical model (however, because of their importance for liquid-to-air membrane energy exchangers, they will be considered separately in this chapter).
8. Energy of phase change for water is only added/removed to/from the desiccant solution.
9. No frosting or condensation of water occurs external to the membrane pores.
10. Crystallization of the desiccant salt within the membrane pores is assumed to be negligible.

2.7.2 LAMEE Specifications and Operating Conditions

The specifications of the flat-plate LAMEE used in the current study are given in Table 2.2. The LAMEE has a counter-cross-flow configuration (see Figure 2.1). The air and desiccant solution streams are separated by a GE semi-permeable membrane. Lithium chloride (LiCl) has a low surface vapor pressure (Mei and Dai (2008)) and low risk of crystallization (Afshin (2010)); therefore, it is used in this study. Table 2.3 shows the operating conditions for the dehumidifier and the regenerator. The outdoor air conditions for the dehumidifier were chosen according to AHRI Standard 1060 (AHRI Standard 1060 (2005)) summer conditions. Although the effectiveness of the flat-plate LAMEE increases at higher Cr^* values (Namvar et al. (2012)), it

should be noted that flow maldistribution due to membrane deflections increases as Cr^* increases. Therefore, a Cr^* of 5 is chosen for both the dehumidifier and the regenerator in the current study.

TABLE 2.2. Specifications of the flat-plate LAMEE for the numerical model.

	Parameter	Value	Unit
Exchanger	flow configuration	counter-cross	-
	length	490	mm
	height	100	mm
	exchanger aspect ratio (height/length) (Vali (2009))	0.2	-
	exchanger solution entrance ratio (Vali (2009))	0.04	-
	number of air channels	21	-
	number of solution channels	20	-
	air channel width (δ_{air})*	1-6	mm
	solution channel width (δ_{sol})**	1-4	mm
Membrane (Moghaddam et al. (2014))	membrane type	GE	-
	δ_{mem}	0.265	mm
	R_m	24	s/m
	k_{mem}	0.065	W/(m·K)

* *varies from 1 to 6 mm by 0.5 mm increment;* ** *varies from 1 to 4 mm by 1 mm increment*

TABLE 2.3. Operating conditions for the dehumidifier and the regenerator.

Parameter	Dehumidifier		Regenerator	
	Value	Unit	Value	Unit
$T_{air,in}$	35	°C	28	°C
$W_{air,in}$	17.5	g_v/kg_{air}	13	g_v/kg_{air}
$T_{sol,in}$	24	°C	44	°C
$C_{sol,in}$	32	%	31.7	%
H^*	2.3	-	1.6	-
$\dot{m}_{air}$	1.95	g/s	1.95	g/s
$\dot{m}_{sol}$	3.43	g/s	3.46	g/s
Cr^*	5	-	5	-

2.8 RESULTS AND DISCUSSION

2.8.1 The Dehumidifier

Figure 2.3 (a) shows the variation of *NTU* with air channel width (δ_{air}) for four solution channel widths (δ_{sol}), when the LAMEE is used for air cooling and dehumidifying. It is found that *NTU* increases with the decrease of either δ_{air} or δ_{sol}, but is more heavily influenced by δ_{air} than δ_{sol}. For instance, at δ_{sol} = 1 mm, *NTU* increases by 336% with the decrease of δ_{air} from 6 mm to 1 mm, whereas, *NTU* increases only by 10% with the decrease of δ_{sol} from 4 mm to 1 mm at δ_{air} = 1 mm. Moreover, the influence of δ_{air} on *NTU* becomes more significant at lower values of δ_{air}. For instance, at δ_{sol} = 1 mm, *NTU* increases by 67% and 17% with the decrease of δ_{air} from 2 mm to 1 mm and from 6 mm to 5 mm, respectively. At δ_{air} values greater than 1.5 mm, δ_{sol} has almost no influence on *NTU*.

Figure 2.3 (b) shows the variations in the outlet air and desiccant solution temperatures with δ_{air} and δ_{sol}, and Figure 2.3 (c) shows the variations in the outlet air and desiccant solution humidity ratios with δ_{air} and δ_{sol}, when the LAMEE is used for air cooling and dehumidifying. It is found that the increase in *NTU* with the reduction of either δ_{air} or δ_{sol} results in lower outlet air temperatures and humidity ratios. Again, the results are more influenced by δ_{air} than δ_{sol}. For instance, at δ_{sol} = 1 mm, the reduction of δ_{air} from 6 mm to 1 mm results in decreases of 14% and 19% in the outlet air temperature and humidity ratio, respectively. While at δ_{air} = 1 mm, the reduction of δ_{sol} from 4 mm to 1 mm results in decreases of 0.8% and 7% in the outlet air temperature and humidity ratio, respectively.

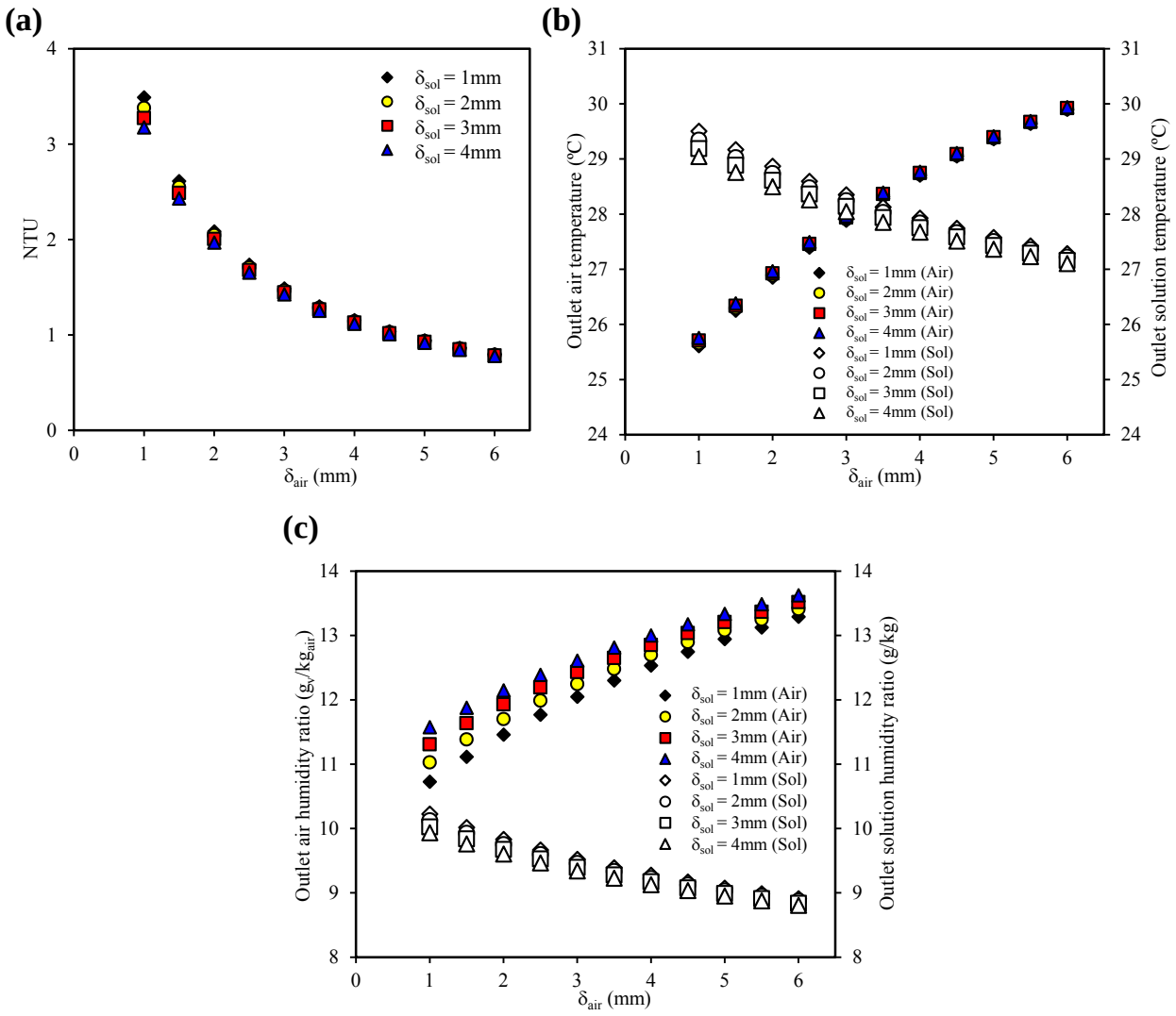

FIGURE 2.3. Variations of (a) *NTU* (b) outlet air and desiccant solution temperatures (c) outlet air and desiccant solution humidity ratios with widths of air and solution channels of the dehumidifier ($T_{air,in}$ = 35°C, $W_{air,in}$ = 17.5 g_v/kg_{air}, $T_{sol,in}$ = 24°C, $C_{sol,in}$ = 32%).

In addition, Figures 2.3 (b) and 2.3 (c) show that the changes in the outlet desiccant solution temperature and humidity ratio are less significant than the changes in the outlet air temperature and humidity ratio. For instance, at δ_{sol} = 1 mm, the reduction of δ_{air} from 6 mm to 1 mm results in an 8% increase in the outlet desiccant solution temperature compared to a 14% decrease in the outlet air temperature. More details about the effects of δ_{air} and δ_{sol} on the sensible, latent and total effectivenesses, and moisture removal rate of the dehumidifier are presented in the next sections.

2.8.1.1 Sensible Effectiveness

Figure 2.4 shows the variations in the sensible effectiveness of the dehumidifier with changing δ_{air} and δ_{sol}. The sensible effectiveness increases significantly with the decrease of δ_{air}. For instance, the sensible effectiveness increases from 46% to 85% as δ_{air} decreases from 6 mm to 1 mm. The sensible effectiveness is more sensitive to the variations in δ_{air} at lower values of δ_{air}. The improvement in the sensible effectiveness can be explained as follows. For a fully developed laminar flow, Nusselt number is constant and independent of Reynolds number (Re) (Nellis and Klein (2009)). Since the airflow is both fully developed and laminar ($Re_{air} < 2300$), this means that the convective heat transfer coefficient increases inversely with δ_{air} according to equation (2.11). As a result, the overall heat transfer coefficient increases which leads to the increase of NTU (see Figure 2.3 (a)), and consequently the sensible effectiveness increases (see equations (2.7) and (2.8)).

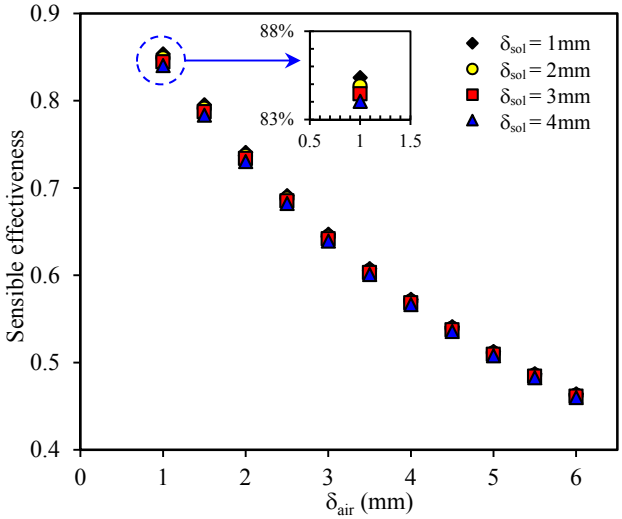

FIGURE 2.4. Influences of air and solution channel widths on the sensible effectiveness of the dehumidifier ($T_{air,in}$ = 35°C, $W_{air,in}$ = 17.5 g_v/kg_{air}, $T_{sol,in}$ = 24°C, $C_{sol,in}$ = 32%).

On the other hand, it is found that δ_{sol} has a negligible influence on the sensible effectiveness

compared to δ_{air}. As can be seen from Figure 2.4, the maximum improvement encountered in the sensible effectiveness with the decrease of δ_{sol} from 4 mm to 1 mm is less than 2% over the entire range of δ_{air} studied. This is attributed to the fact that the solution side of the flat-plate LAMEE has a much higher convective heat transfer coefficient (~4,500 W/(m^2·K)) than the airside (~220 W/(m^2·K)). As well, the thickness of the semi-permeable membrane is very small (0.265 mm). Therefore, it is concluded that the heat transfer resistance of the airside dominates the total heat transfer resistance within flat-plate LAMEEs, and the solution side accounts for only a very small fraction (see equation (2.8)). It is worth mentioning that this is in accordance with previous results reported by Zhang and Huang (2011), which state that the airside resistance represented more than 98% of the total heat transfer resistance in a hollow-fiber LAMEE.

2.8.1.2 Latent Effectiveness

The variations in the latent effectiveness of the dehumidifier with changing δ_{air} and δ_{sol} are illustrated in Figure 2.5. It is found that the latent effectiveness increases inversely with either δ_{air} or δ_{sol}, with a larger increase due to changes in δ_{air}. The latent effectiveness increases by up to 25% as δ_{air} decreases from 6 mm to 1 mm, and it increases by up to 8% with the reduction of δ_{sol} from 4 mm to 1 mm. The enhancement in the latent effectiveness with the reduction of either δ_{air} or δ_{sol} can be explained as follows. Since the convective heat transfer coefficient increases with the reduction of the channel width, as previously mentioned in Section 2.8.1.1, the convective mass transfer coefficient will increase according to the *Chilton-Colburn analogy* (Colburn (1933); Chilton and Colburn (1934)) (i.e. equation 2.15). The higher the convective mass transfer coefficient the higher the overall mass transfer coefficient (see equation (2.10)), and consequently, the higher the number of mass transfer units (NTU_m) (see equation (2.9)), which leads to the increase in the latent effectiveness.

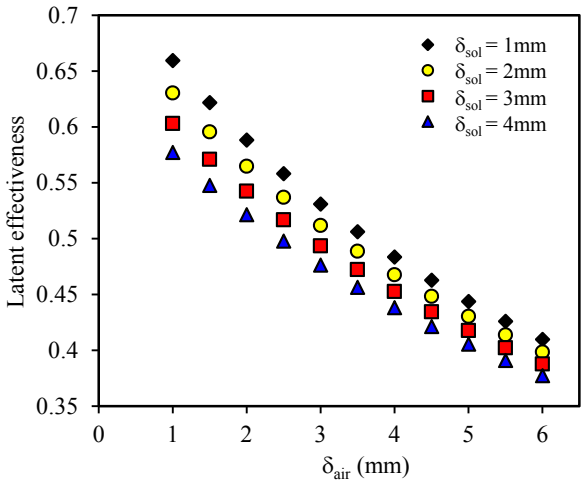

FIGURE 2.5. Influences of air and solution channel widths on the latent effectiveness of the dehumidifier ($T_{air,in}$ = 35°C, $W_{air,in}$ = 17.5 g_v/kg_{air}, $T_{sol,in}$ = 24°C, $C_{sol,in}$ = 32%).

According to the results presented in the previous sections, it is found that the latent effectiveness is lower than the sensible effectiveness of the dehumidifier. This is attributed to the fact that the heat transfer resistance of the membrane is negligible compared to its mass transfer resistance. The resistance to water vapor diffusion through pores of a semi-permeable membrane is referred to as vapor diffusion resistance (VDR) (Larson (2006)). Table 2.4 shows the VDR values for several commercial semi-permeable membranes. The VDR of the membrane used in the studied flat-plate LAMEE is 24 s/m.

Figure 2.6 displays the variation in the latent effectiveness of the dehumidifier with the VDR of the membrane. At δ_{air} = 2 mm and δ_{sol} = 2 mm, the latent effectiveness increases from 10% to 67% as the VDR decreases from 400 s/m to 10 s/m. It can be concluded that the vapor diffusion resistance of the membrane is the key parameter to enhance the latent effectiveness of flat-plate LAMEEs. It is worth mentioning that this agrees with the results reported by Zhang and Huang (2011) which state that the membrane was responsible for more than 83% of the total mass transfer resistance in a hollow-fiber LAMEE. Moreover, the influence of δ_{air} on the latent

effectiveness is found to be less significant than its influence on the sensible effectiveness of the dehumidifier. This is because, as previously mentioned in Section 2.8.1.1, the airside resistance represents the majority of the total heat transfer resistance in flat-plate LAMEEs.

TABLE 2.4. VDR for several commercial membranes (Beriault (2011)).

Membrane	VDR (s/m)
GE (Moghaddam et al. (2014))	24
Porex® X-4904	40
Porex® PM3V	57
Porex® PM6M	84
AY Tech Laminant	97
Porex® X-7744	102
Propore™	158
Tyvek®1059B	215
Tyvek®1025B	245
Japanese Tyvek®	329
Aptra™ RKW	385

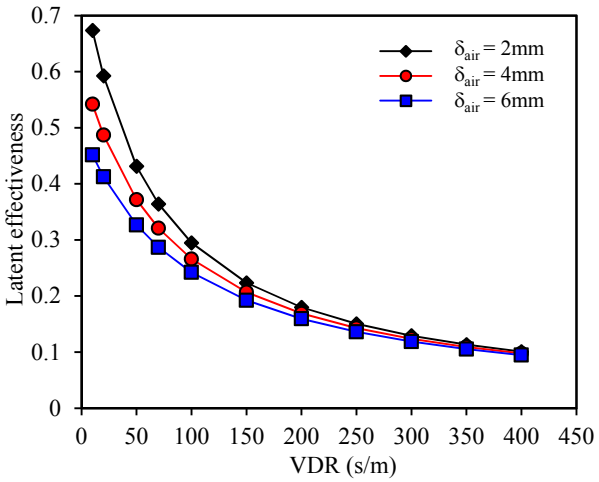

FIGURE 2.6. Variation in latent effectiveness with VDR of the membrane for different δ_{air} values and δ_{sol} = 2 mm ($T_{air,in}$ = 35°C, $W_{air,in}$ = 17.5 g_v/kg_{air}, $T_{sol,in}$ = 24°C, $C_{sol,in}$ = 32%).

2.8.1.3 Total Effectiveness

Figure 2.7 displays the variations in the total effectiveness of the dehumidifier with changing δ_{air} and δ_{sol}. The total effectiveness increases inversely with either δ_{air} or δ_{sol}, where it increases by up to 29% as δ_{air} decreases from 6 mm to 1 mm, and it increases by up to 6% when δ_{sol} is reduced from 4 mm to 1 mm. This is expected because the total effectiveness of the LAMEE is dependent on its sensible and latent effectivenesses (see equation (2.3)). Since the reduction of either δ_{air} or δ_{sol} leads to the increase in the sensible and latent effectivenesses, consequently the total effectiveness increases. It is worth mentioning that in equation (2.3), the latent effectiveness is multiplied by the operating factor (H^*), which is higher than unity (see Table 2.3)); therefore, the change in the latent effectiveness has a higher influence on the total effectiveness than the change in the sensible effectiveness. Accordingly, the influences of both δ_{air} and δ_{sol} on the total effectiveness are very similar to their influences on the latent effectiveness.

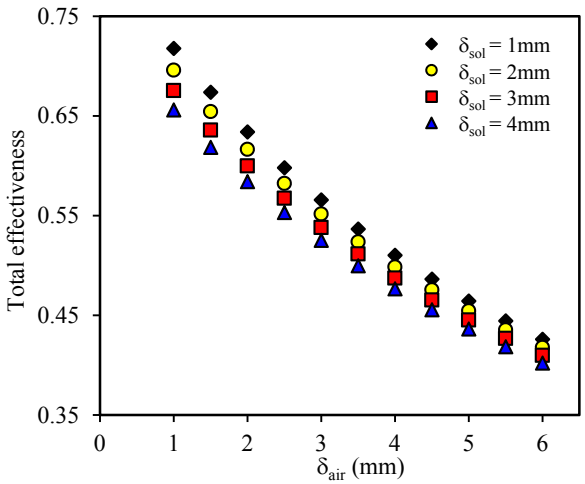

FIGURE 2.7. Influences of air and solution channel widths on the total effectiveness of the dehumidifier ($T_{air,in}$ = 35°C, $W_{air,in}$ = 17.5 g_v/kg_{air}, $T_{sol,in}$ = 24°C, $C_{sol,in}$ = 32%).

2.8.1.4 Moisture Removal Rate

The moisture removal rate ($\dot{m}_{rr}$) is the mass flow rate of water vapor between the air and desiccant solution streams across the semi-permeable membrane. The influences of δ_{air} and δ_{sol} on $\dot{m}_{rr}$ are illustrated in Figure 2.8. The $\dot{m}_{rr}$ increases by up to 61% when δ_{air} decreases from 6 mm to 1 mm, and it increases by up to 14% with the reduction of δ_{sol} from 4 mm to 1 mm. Figure 2.3 (c) shows that the change in the air humidity ratio across the dehumidifier increases with the decrease of either δ_{air} or δ_{sol}. Since $\dot{m}_{rr}$ increases with an increase in the change of air humidity ratio across the dehumidifier (see equation (2.5)), $\dot{m}_{rr}$ increases inversely with either δ_{air} or δ_{sol}. This is attributed to the increase in the convective mass transfer coefficients of the air and desiccant solution streams with the reduction of δ_{air} and δ_{sol}, respectively. It can be concluded that δ_{air} has a strong influence on the $\dot{m}_{rr}$; however, as previously mentioned in Section 2.8.1.2, the vapor diffusion resistance of the membrane has an important influence for achieving significant enhancements in the latent effectiveness of the dehumidifier and therefore its $\dot{m}_{rr}$. Figure 2.9 shows the variation in $\dot{m}_{rr}$ with changing the VDR of the membrane. The $\dot{m}_{rr}$ increases significantly as the VDR decreases, especially for VDR values less than 150 s/m. It can be concluded that the VDR of the membrane has a strong influence on the moisture removal rate in the dehumidifier.

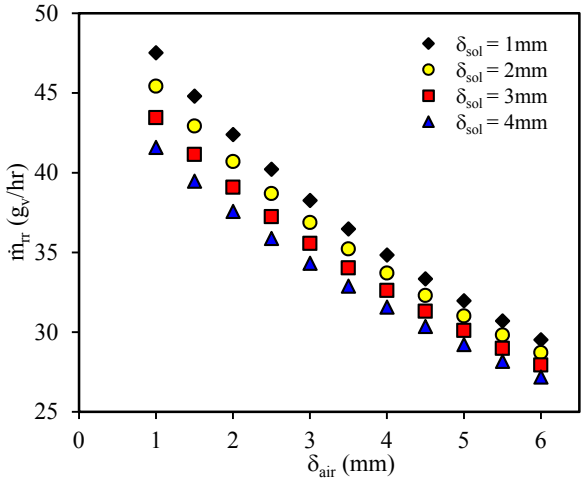

FIGURE 2.8. Influences of air and solution channel widths on the moisture removal rate in the dehumidifier ($T_{air,in}$ = 35°C, $W_{air,in}$ = 17.5 g_v/kg_{air}, $T_{sol,in}$ = 24°C, $C_{sol,in}$ = 32%).

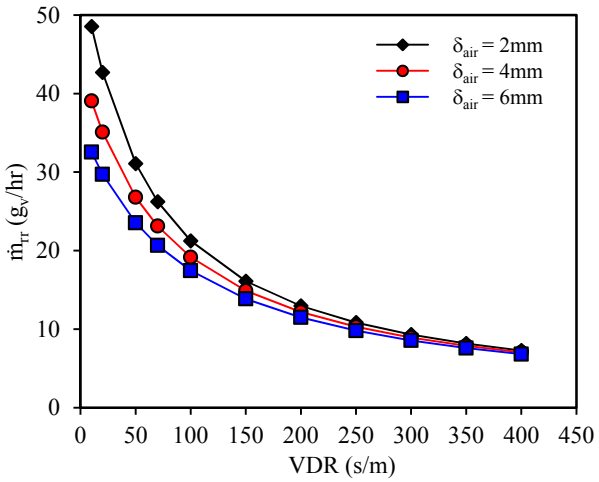

FIGURE 2.9. Variation of moisture removal rate with VDR of the membrane for different δ_{air} values and δ_{sol} = 2 mm ($T_{air,in}$ = 35°C, $W_{air,in}$ = 17.5 g_v/kg_{air}, $T_{sol,in}$ = 24°C, $C_{sol,in}$ = 32%).

2.8.2 The Regenerator

Figure 2.10 (a) shows the variations of *NTU* with δ_{air} and δ_{sol}, when the LAMEE is used for diluted desiccant solution regeneration. *NTU* increases inversely with either δ_{air} or δ_{sol}, where δ_{air} has a more significant influence on *NTU* than δ_{sol}. For instance, at δ_{sol} = 1 mm, *NTU* increases by 335% with the reduction of δ_{air} from 6 mm to 1 mm; whereas at δ_{air} = 1 mm, *NTU* increases only by 9%

with the reduction of δ_{sol} from 4 mm to 1 mm.

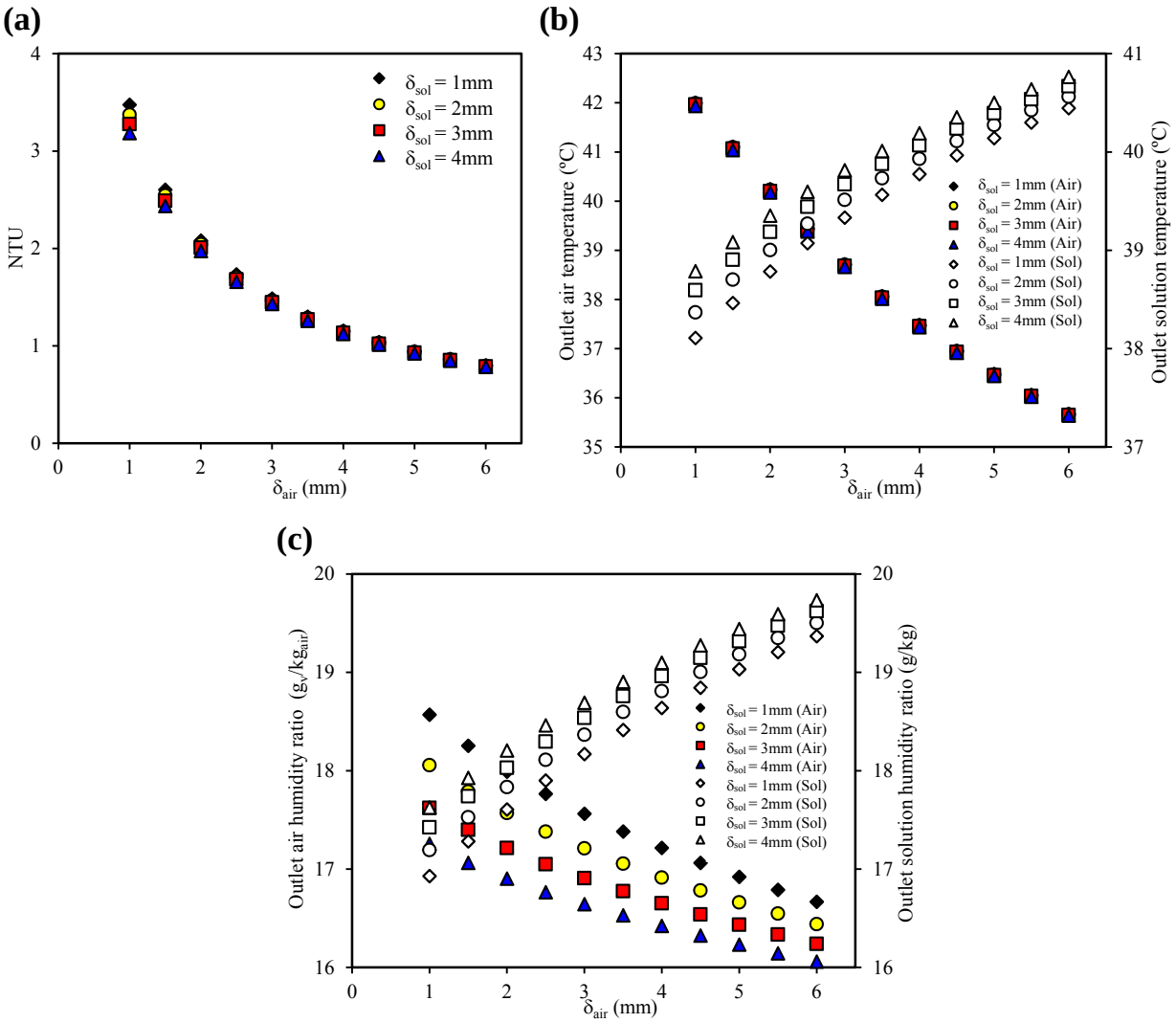

FIGURE 2.10. Variations of (a) *NTU* (b) outlet air and desiccant solution temperatures (c) outlet air and desiccant solution humidity ratios with widths of air and solution channels of the regenerator ($T_{air,in}$ = 28°C, $W_{air,in}$ = 13 g_v/kg_{air}, $T_{sol,in}$ = 44°C, $C_{sol,in}$ = 31.7%).

Figure 2.10 (b) displays the variations in the outlet air and desiccant solution temperatures with δ_{air} and δ_{sol}, while the variations in the outlet air and desiccant solution humidity ratios with δ_{air} and δ_{sol} are presented in Figure 2.10 (c). As was mentioned in Sections 2.8.1.1 and 2.8.1.2, the sensible and latent effectivenesses of the flat-plate LAMEE increase as *NTU* increases, thus the outlet desiccant solution temperature and humidity ratio in the regenerator decrease with the decrease of either δ_{air} or δ_{sol} (i.e. high *NTU* values). For instance, at δ_{sol} = 1 mm, the outlet solution temperature decreases by 6% and the outlet solution humidity ratio decreases by 13% with the decrease of δ_{air} from 6 mm to 1 mm. On the other hand, δ_{sol} has less influences on the outlet solution temperature and humidity ratio, where at δ_{air} = 1 mm, the outlet solution temperature and humidity ratio decrease only by 2% and 4%, respectively, with the decrease of δ_{sol} from 4 mm to 1 mm.

Figure 2.11 (a) displays the influences of δ_{air} and δ_{sol} on the sensible effectiveness of the regenerator. It is found that δ_{air} has a strong influence on the sensible effectiveness; for instance, the sensible effectiveness increases from 48% to 88% as δ_{air} decreases from 6 mm to 1 mm. As mentioned in Section 2.8.1.1, Nusselt number is constant and independent of Reynolds number for a fully developed laminar flow (Nellis and Klein (2009)). Accordingly, decreasing δ_{air} increases the convective heat transfer coefficient of the airside, thus the overall heat transfer coefficient, *NTU*, and sensible effectiveness increase. Decreasing δ_{sol} from 4 mm to 1 mm is found to improve the sensible effectiveness by less than 1%; therefore, it can be concluded that δ_{sol} has a negligible influence on the sensible effectiveness of the regenerator.

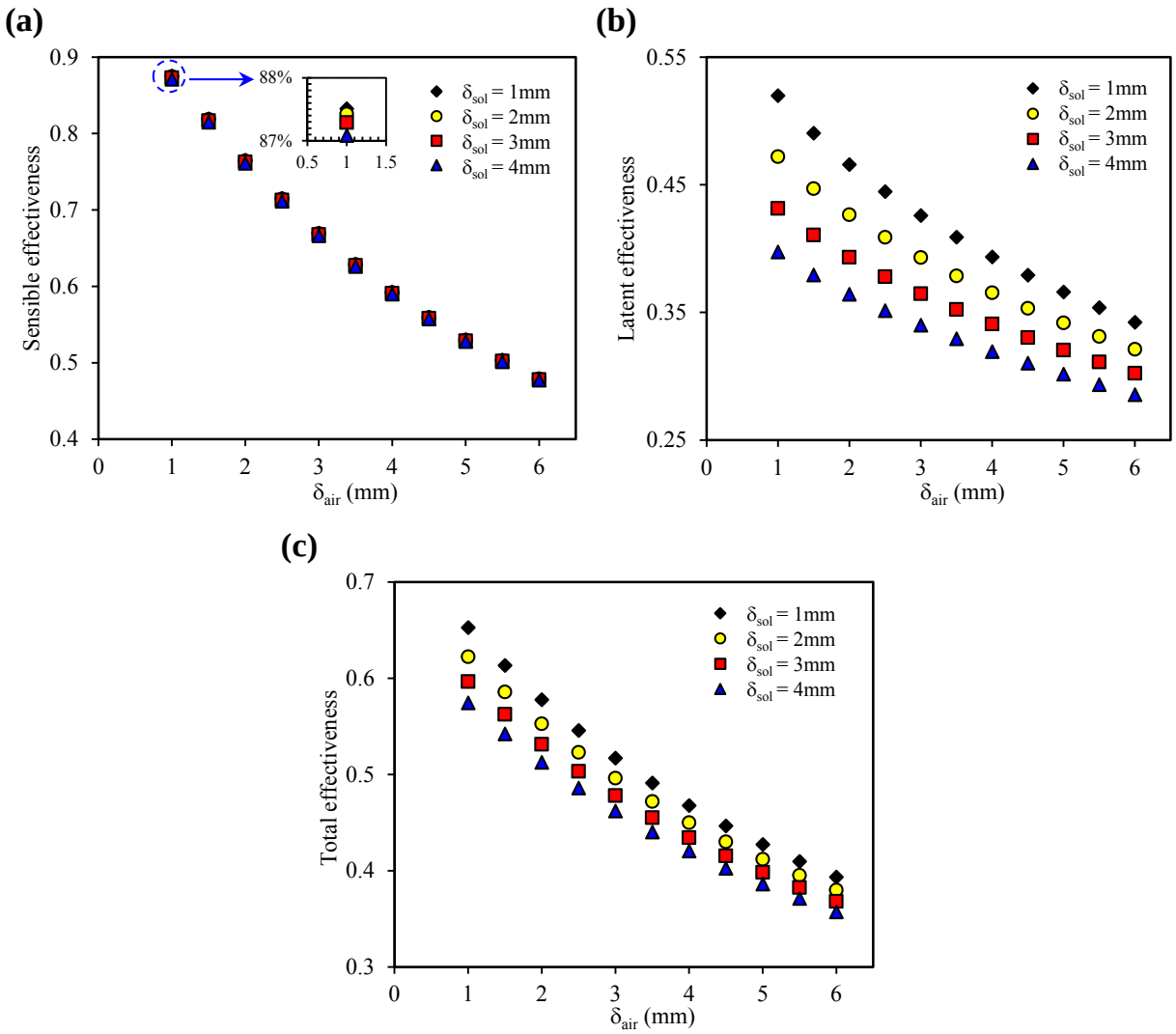

FIGURE 2.11. Influences of air and solution channel widths on the (a) sensible effectiveness (b) latent effectiveness (c) total effectiveness of the regenerator ($T_{air,in}$ = 28°C, $W_{air,in}$ = 13 g_v/kg_{air}, $T_{sol,in}$ = 44°C, $C_{sol,in}$ = 31.7%).

The variations in the latent effectiveness of the regenerator versus δ_{air} and δ_{sol} are presented in Figure 2.11 (b). The latent effectiveness increases with the decrease of either δ_{air} or δ_{sol}. For instance, at δ_{sol} = 1 mm, the latent effectiveness increases from 34% to 52% with the reduction of δ_{air} from 6 mm to 1 mm, whereas at δ_{air} = 1 mm, the latent effectiveness increases from 40% to 52% as δ_{sol} decreases from 4 mm to 1 mm. At the same δ_{air} and δ_{sol}, the latent effectiveness of the regenerator is lower than the latent effectiveness of the dehumidifier. For instance, at δ_{air} = 1 mm

and δ_{sol} = 1 mm, the latent effectivenesses of the dehumidifier and the regenerator are 66% and 52%, respectively. One reason may be that the difference between the inlet temperatures of air and desiccant solution streams in the regenerator is higher than in the dehumidifier, thus the potential for heat and water vapor transfer in the regenerator is higher than the dehumidifier. Consequently, more heat of phase change is released into the desiccant solution side in the regenerator, which degrades the potential for heat and water vapor transfer between the air and desiccant solution streams. Another reason may be that the slope of LiCl on the psychrometric chart for the dehumidifier operating conditions is lower than the regenerator.

Figure 2.11 (c) illustrates the influences of δ_{air} and δ_{sol} on the total effectiveness of the regenerator. The total effectiveness of the regenerator increases inversely with either δ_{air} or δ_{sol}. As mentioned in Section 2.8.1.3, the total effectiveness of a LAMEE is dependent on its sensible and latent effectivenesses, thus increasing the sensible and latent effectivenesses with the decrease of either δ_{air} or δ_{sol}, increases the total effectiveness of the regenerator. As well, it is found that the variations in the total effectiveness of the regenerator versus δ_{air} and δ_{sol} have a trend similar to the variations in the total effectiveness of the dehumidifier versus δ_{air} and δ_{sol}. For instance, at δ_{sol} = 1 mm, the total effectivenesses of the regenerator and the dehumidifier increase by 26% and 29%, respectively, as δ_{air} decreases from 6 mm to 1 mm, whereas, at δ_{air} = 1 mm, decreasing δ_{sol} from 4 mm to 1 mm increases the total effectiveness of the regenerator and the dehumidifier by 8% and 6%, respectively.

The main objective of a desiccant solution regenerator is to increase the concentration of the diluted desiccant solution by removing water vapor from it. Therefore, higher values of $\dot{m}_{rr}$ indicate higher performance of a regenerator. The variations in $\dot{m}_{rr}$ versus δ_{air} and δ_{sol} of the

regenerator are presented in Figure 2.12. It is found that the $\dot{m}_{rr}$ increases with the decrease of either δ_{air} or δ_{sol}. For instance, the $\dot{m}_{rr}$ increases by up to 52% and 31% with the decrease of δ_{air} from 6 mm to 1 mm and δ_{sol} from 4 mm to 1 mm, respectively. Moghaddam et al. (2013d) found that increasing the potential for heat and water vapor transfer in the regenerator by increasing the inlet desiccant solution temperature, increases $\dot{m}_{rr}$ but decreases the effectiveness. Accordingly, designing a regenerator with smaller δ_{air} and δ_{sol} is an effective technique to enhance both the effectiveness and $\dot{m}_{rr}$.

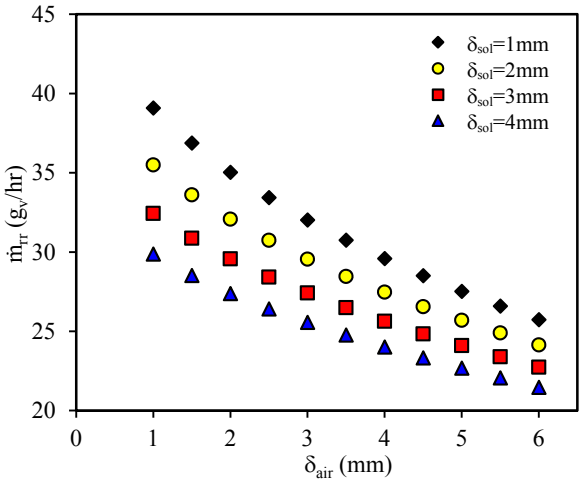

FIGURE 2.12. Influences of air and solution channel widths on the moisture removal rate in the regenerator ($T_{air,in}$ = 28°C, $W_{air,in}$ = 13 g_v/kg_{air}, $T_{sol,in}$ = 44°C, $C_{sol,in}$ = 31.7%).

2.8.3 Comparison between the Influences of Air and Solution Channel Widths on the Effectivenesses of the Dehumidifier and Regenerator

Figure 2.13 shows a comparison between the absolute enhancements in the sensible, latent, and total effectivenesses of the studied flat-plate LAMEE, when used for air cooling and dehumidifying and diluted desiccant solution regeneration. Air channel width of 6 mm is selected as the reference case for the percent changes in the sensible, latent, and total effectivenesses of the dehumidifier and the regenerator displayed in Figure 2.13. The enhancements in the sensible

effectivenesses of the dehumidifier and the regenerator are almost the same; however, the enhancements in the latent effectiveness of the dehumidifier is higher than the regenerator, especially at small values of δ_{air}. This is likely because, at the same δ_{air} and δ_{sol}, the latent effectiveness of the regenerator is lower than the latent effectiveness of the dehumidifier, thus the absolute enhancements in the latent effectiveness of the regenerator are lower than the dehumidifier. In conclusion, the sensible, latent, and total effectivenesses of both the dehumidifier and the regenerator, when operated with constant air and solution channel widths and without flow maldistribution, increase as δ_{air} or δ_{sol} decreases.

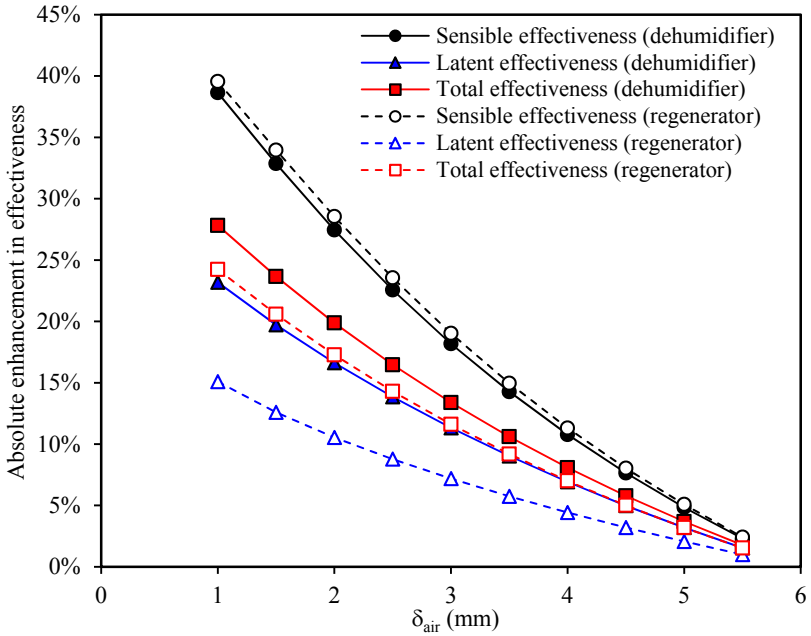

FIGURE 2.13. Comparison between the absolute enhancements in the sensible, latent, and total effectivenesses of the dehumidifier and the regenerator for different δ_{air} values (at δ_{sol} = 2 mm).

2.8.4 Pressure Drop

The economic performance of a LAMEE significantly depends on the airside pressure drop. Higher air pressure drops mean higher power requirements for fans, and thus higher operating costs. Using an hourly simulation for a building, Rasouli et al. (2014) found that the payback

period of a RAMEE system (i.e. composed of two identical flat-plate LAMEEs coupled by a pumped closed liquid desiccant loop) installed in a building in Miami and Phoenix, USA, increased when the air pressure drop across each LAMEE increased (see Figure 2.14).

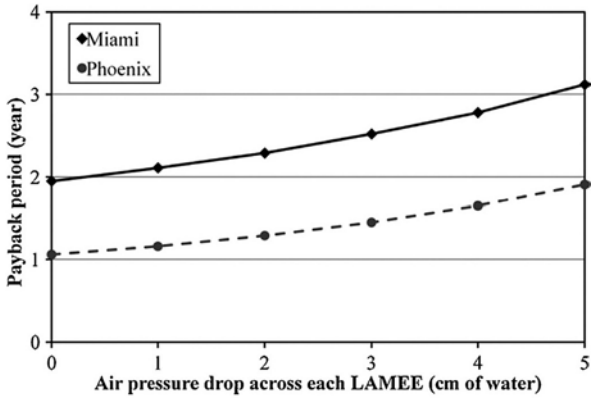

FIGURE 2.14. Variation of the payback period of a RAMEE system when installed in a building in Miami and Phoenix versus the air pressure drop across each LAMEE (Rasouli et al. (2014)).

As well, fluid accelerations, elevation changes, and inlet/exit manifolds pressure drops normally account for less than 4% of the total pressure drop in flat-plate heat exchangers (Khan et al. (2012)). Since the liquid flow pressure drop is usually small, only the air flow channel frictional pressure drop needs to be calculated for the preliminary design of a flat-plate LAMEE. Using the *Darcy-Weisbach* equation (equation (2.16)) (White (1998)), the pressure drop for fully developed flow in a duct is given by:

$$\Delta P = f_D \cdot \frac{L_{\text{ex}}}{D_{\text{h}}} \cdot \frac{\rho_{\text{air}} \cdot u_{\text{air}}^2}{2} \tag{2.16}$$

where ΔP is the frictional pressure drop in the airstream across the LAMEE (Pa), f_D is the Darcy friction factor, L_{ex} is the LAMEE length (m), D_{h} is the air channel hydraulic diameter (m), ρ_{air} is the air density (kg/m^3), and u_{air} is the average air bulk velocity through the exchanger channel (m/s).

It is clear from equation (2.16) that the pressure drop for the airside across a heat/energy exchanger strongly depends on the design parameters (i.e. exchanger length and hydraulic diameter of air channels) and operating conditions (i.e. velocity of the airflow). The pressure drop increases inversely with δ_{air}. For example, the pressure drop is 255 Pa at $\delta_{air} = 2$ mm, and, with the same mass flow rate in each channel, the pressure drop is around 2,000 Pa for $\delta_{air} = 1$ mm. Accordingly, it can be concluded that, if the air pressure drop for a flat-plate LAMEE is not to be excessive, δ_{air} should be ≥ 2 mm in order to keep the pressure drop in the airside within an acceptable range.

2.8.5 Influences of Variations in Channel Width on the Dehumidifier Performance

Manufacturing tolerances in channel spacing and inlet/outlet headers will alter the performance (i.e. effectiveness and pressure drop) of heat/energy exchangers (Shang and Besant (2005); Nielsen et al. (2013)). Nielsen et al. (2013) found that the degradation in the performance of a parallel-plate heat exchanger due to the non-uniformity of the widths of channels and plates depends on the design parameters and operating conditions (i.e. thermal conductivity of the exchanger material, Reynolds number, and standard deviation of the variations). Their results showed that depending on Reynolds number and thermal conductivity of the exchanger material, the non-uniformity of the channels and plates of a parallel-plate heat exchanger may significantly degrade its performance even at low standard deviations of variations of 5%-10%.

Therefore, the critical design problem for flat-plate exchangers is:

(1) How should they be designed to make flow maldistribution effects small, especially as they reduce the exchanger effectiveness? And,

(2) When elastic membrane exchangers are used, what are the most important design considerations?

Variations in the air and solution channel widths of a flat-plate LAMEE depend on the manufacturing tolerances in the frames of the channels, the variations in the membranes thickness and elastic properties, the pre-stretching tension within the membranes at the time of the exchanger construction, the gluing process where the membranes are bonded to the frames of the channels, and the pressure differences across each membrane during operation. Thus, flat-plate LAMEEs may experience larger variations in the widths of the air and solution channels than other types of heat/energy exchangers. Hemingson et al. (2011b) showed that the channel width variations may be large in membrane energy exchangers. They found that flow maldistribution caused by membrane deflections can reduce the effectiveness of a RAMEE system by up to 29%.

Figure 2.15 shows a cross section of a flat-plate membrane for a series of increasing liquid pressures, and Figure 2.16 shows measured values for membrane deflections as a function of liquid pressure (Kamali (2014)). These figures show that, as the liquid pressure increases, the elastic deformation of the membrane increases. Figure 2.16 also shows that the initial increase in liquid pressure (i.e. 0-0.5 psig) results in a large step change in membrane deflection, after which, the changes in membrane deflections with increasing liquid pressure are much smaller and suggest a non-linear step change relationship for membrane deformation versus liquid pressure (see (Larson (2006); Larson et al. (2007); Kamali (2014)) for more details). The large step in membrane deflection and the total membrane deflections can be reduced by pre-tensioning the membrane prior to clamping or gluing the membrane to the liquid flow channel (Larson et al. (2007)). As well, the total membrane deflections can be reduced by attaching a support grid to the membrane. For example, Ge et al. (2014b) found that using a support grid reduced the membrane deflections from 4.6 mm to 2 mm at a pressure of 13,800 Pa (see Figure 2.17). However, attaching a support grid to the membrane results in a partial blockage of

the membrane surface area which reduces the rate of heat and water vapor transfer across the membrane.

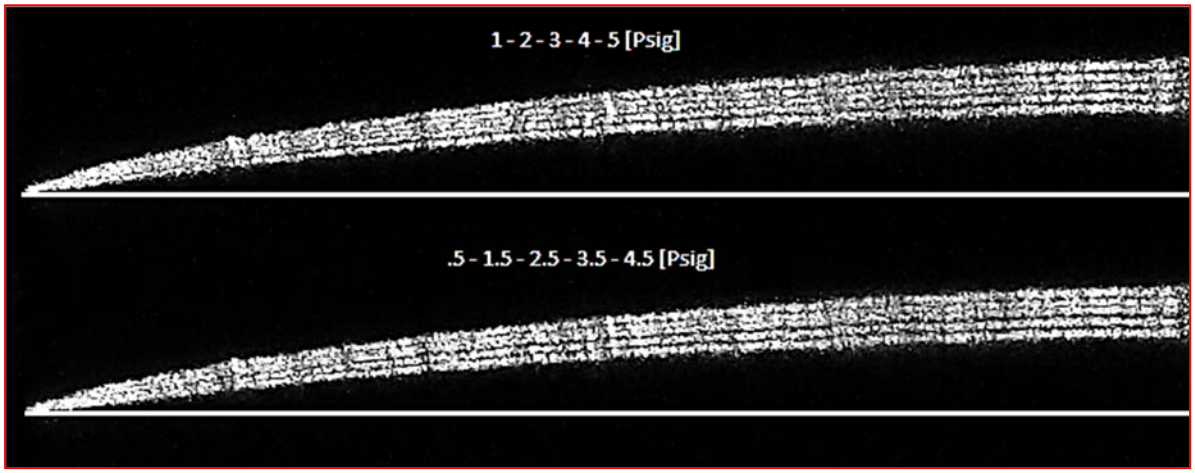

FIGURE 2.15. Photograph of membrane deflections versus flow channel length (0 to the center-line) for several different liquid pressures (Kamali (2014)).

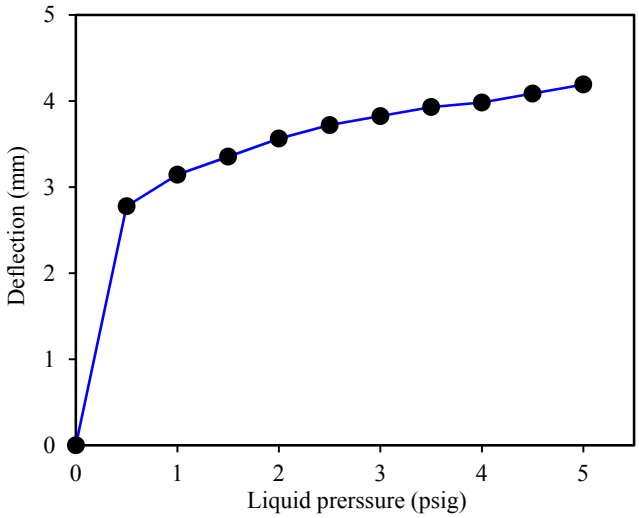

FIGURE 2.16. Membrane center-line deflection versus liquid pressure applied on the membrane (Kamali (2014)).

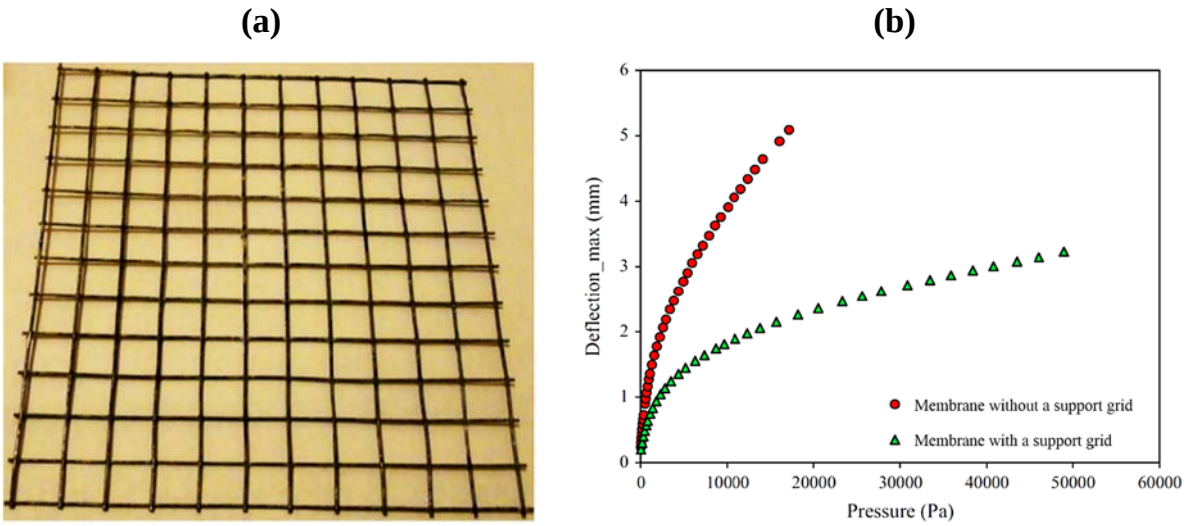

FIGURE 2.17. (a) Photograph of a support grid (b) membrane center-line deflection versus liquid pressure applied on the membrane with and without a support grid (Ge et al. (2014b)).

These figures imply that not only will elastic membrane deflections be significant, but they will also change with membrane property variations, pre-tensioning variations of the membrane during exchanger construction, attaching a support grid to the membrane, and operating conditions (i.e. spatial and temporal pressure and temperature changes). Each of these cause flow channel hydraulic diameter variations. These variations imply another two problems; (1) How to define the correct air flow channel width when deflections are present, and (2) What will be the relative size of the flow channel width changes when liquid pressures change. As well, variations in air flow channel bulging from channel-to-channel (i.e. due to membrane property variations and construction and gluing variations) will cause maldistribution in the air flows as well as the liquid desiccant solution flow. These complex design problems require a theoretical method of attack to show the relationship between variations in the air flow channel hydraulic diameter and the reduction in the exchanger effectiveness and air pressure drop.

For typical air flow rates and for fixed parallel flow channels, Shang and Besant (2004) showed theoretically that both the effectiveness and pressure drop decrease as the flow channel width

variations increase for an energy wheel. For a particular energy wheel design and for a given mass flow rate and mean hydraulic diameter for the flow channels, the maximum effectiveness and pressure drop will occur only when the channel width variations are negligible. Using this theory for a large number of flow channels and measuring flow channel hydraulic diameter variations for a parallel exchanger surface desiccant-coated manufactured energy wheel, and using data for variations in surface spacing, they estimated a reduction of the effectiveness and pressure drop of 13% and 14%, respectively. They developed equations (i.e. equations (2.17) and (2.18)) to calculate the reduction in the effectiveness and pressure drop of an energy wheel due to variations in channel width. These equations, which indicate that flow maldistribution is caused only by increasing the ratio of standard deviation of flow channel hydraulic diameter divided by the mean hydraulic diameter for the exchanger, σ/D_o, are shown graphically in Figures 2.18 (a) and 2.18 (b) for heat and energy transfer wheels with parallel exchanger surfaces. These equations show that both the effectiveness and the pressure drop decrease in a non-linear manner with σ/D_o. These equations assume only that the flow is fully developed and the friction coefficient will vary inversely with Reynolds number of the channel flow. For laminar flow in long narrow channels, these assumptions are valid, while for fully developed turbulent or transition flow with small changes of flow channel Reynolds number, they are nearly valid (Shang and Besant (2004)). The pressure drop ratio can be written as (Shang and Besant (2004)):

$$\frac{\Delta P}{\Delta P_o} = \left[1 + 3\left(\frac{\sigma}{D_o}\right)^2\right]^{-1} \tag{2.17}$$

where, for a given total mass flow rate of air, ΔP is the pressure drop across an energy wheel with random variations in the flow channel hydraulic diameter (Pa), ΔP_o is the pressure drop across the same energy wheel with no variations in the flow channel hydraulic diameter (Pa), σ is the standard

deviation of hydraulic diameters (m) (σ can be measured for fixed air flow channel geometries), and D_o is the mean hydraulic diameter of all pore channels of an energy wheel (m). Figure 2.18 (b) shows that the pressure drop across the exchanger decreases with increasing σ/D_o.

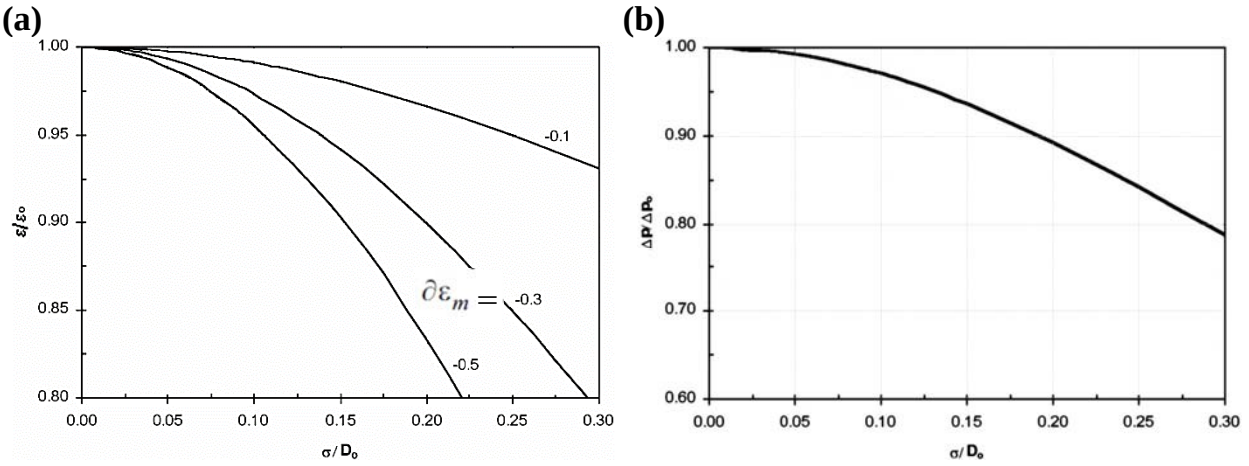

FIGURE 2.18. Effect of variations in the channel width (given by the ratio of the standard deviation of hydraulic diameters to the mean hydraulic diameter) on (a) the ratio of effectiveness of an energy wheel with random variations in channel widths to the effectiveness of the same energy wheel with no variations in channel width (b) the ratio of the pressure drop across an energy wheel with random variations in channel widths to the pressure drop of the same energy wheel with no variations in channel width (Shang and Besant (2004)).

In a similar method of analysis, the ratio of effectiveness with and without random variations in the hydraulic diameter for a parallel-plate exchanger is given as (Shang and Besant (2004)):

$$\frac{\varepsilon}{\varepsilon_o} = 1 + \partial\varepsilon_m \left[\left(\frac{\Delta P}{\Delta P_o}\right)^2 \left[1 + 15\left(\frac{\sigma}{D_o}\right)^2 + 45\left(\frac{\sigma}{D_o}\right)^4 + 15\left(\frac{\sigma}{D_o}\right)^6\right] - \left(\frac{\Delta P}{\Delta P_o}\right)\left[1 + 3\left(\frac{\sigma}{D_o}\right)^2\right]\right] \qquad (2.18)$$

where ε is the effectiveness of an energy wheel with random variations in the hydraulic diameters, ε_o is the effectiveness of the same energy wheel with uniform hydraulic diameters, and $\partial\varepsilon_m$ is a dimensionless ratio coefficient (Shang and Besant (2004)) that is nearly constant for selected typical representative summer and winter operating conditions.

In the current flat-plate LAMEE design study, it is assumed that the above theoretical model for the impact of channel width variations for energy wheels applies to membrane energy exchanger airflow channel spacing variations and $\partial\varepsilon_m = -0.3$ is chosen because it corresponds to the AHRI Standard 1060 (AHRI Standard 1060 (2005)) test conditions for both typical summer and winter conditions (Shang and Besant (2004, 2005)). Unlike energy wheels, direct measurements of membrane deflections within a manufactured membrane energy exchanger are impractical; therefore, deviation between measured data of flat-plate LAMEE effectiveness and numerical simulations for the same flat-plate LAMEE (assuming no spacing variations) are used to indicate magnitude of the change in flat-plate LAMEE effectiveness caused by flow channel spacing variations. Although the uncertainty in this estimate is relatively high, it is an improvement on not including any corrections for the theoretical/numerical performance of flat-plate LAMEEs caused by flow channel width variations.

The dehumidifier studied in this chapter has many air flow channels which each have a length-averaged hydraulic diameter that varies in somewhat random manner from channel to channel, and has a diameter standard deviation of σ. In total they have a mean hydraulic diameter D_o. It is assumed that the theory presented for energy wheels is directly applicable to other types of exchangers. Shang and Besant (2004) were able to measure channel width variations; but for the current design study, where there are several causes for flow channel variations and these variations change with operating conditions; there is a need to define what is meant by the flow channel hydraulic diameter. The literature shows that membrane exchanger theory, where each channel is assumed to have the same flow rate, often overestimates the measured effectiveness values considerably. For example, Hemingson (2010) predicted up to a 29% reduction in effectiveness due to membrane deflections in the prototype of Mahmud at al. (2010), Similarly,

the discrepancy in the effectiveness data measured by Namvar et al. (2012) and analytical model predictions was up to 20% for a flat-plate LAMEE with nominal air channel spacing of 6.35 mm, under air cooling and dehumidifying operating conditions. When greater attention was given to reducing flow channel variations in a flat-plate LAMEE tested under air cooling and dehumidifying operating conditions (Moghaddam et al. (2013a)), the discrepancy between experimental data and simulation was less than 10%.

In the current design study, several values for the air channel width variations (i.e. σ = 1.2, 1.4, 1.6 and 1.8 mm) are selected, while varying the width of air channels from 2 to 6 mm or D_o = 4, 6, 8, 10 and 12 mm. That is, for D_o = 4 mm, σ/D_o = 0.3, 0.35, 0.4 and 0.45 when σ = 1.2, 1.4, 1.6 and 1.8 mm, respectively. Using equation (2.18), the total effectiveness ratios would be $\varepsilon/\varepsilon_o$ = 0.793, 0.732, 0.668 and 0.603 respectively. As well, equation (2.17) would give $\Delta P/\Delta P_o$ = 0.787, 0.731, 0.676 and 0.622 for the same values of σ/D_o.

Using the effectiveness and air pressure drop results, with no channel variations, determined from the numerical simulation as ε_o and ΔP_o respectively, the estimated effectiveness (ε) and air pressure drop (ΔP) with channel variations can be calculated. The results are shown graphically for ε (sensible, latent, and total effectivenesses) and ΔP with different δ_{air} (the nominal air spacing without membrane deflections) values in Figure 2.19. It is clear from Figure 2.19 that the sensible, latent, and total effectivenesses of the dehumidifier decrease with the increase of σ, and these decreases in the effectivenesses increase inversely with δ_{air}. For instance, at δ_{air} = 2 mm, the total effectiveness decreases from 49% to 37% as σ increases from 1.2 mm to 1.8 mm, whereas at δ_{air} = 6 mm, the total effectiveness decreases only from 41% to 39.3% as σ increases from 1.2 mm to 1.8 mm. Therefore, the variations in the air channels width should be kept as small as possible

to achieve high effectivenesses for flat-plate LAMEEs. As well, it is shown in Figure 2.19 that the sensible, latent, and total effectivenesses increase inversely with δ_{air} until a specific value of δ_{air} (i.e. optimum air channel width), where any decrease in δ_{air} beyond this optimum width will cause the effectivenesses to decrease. This optimum width depends on σ, and increases with the increase of σ. Figure 2.19 (d) shows that the air pressure drop across the dehumidifier decreases with the increase of σ, and the decrease in the air pressure drop increases inversely with δ_{air}.

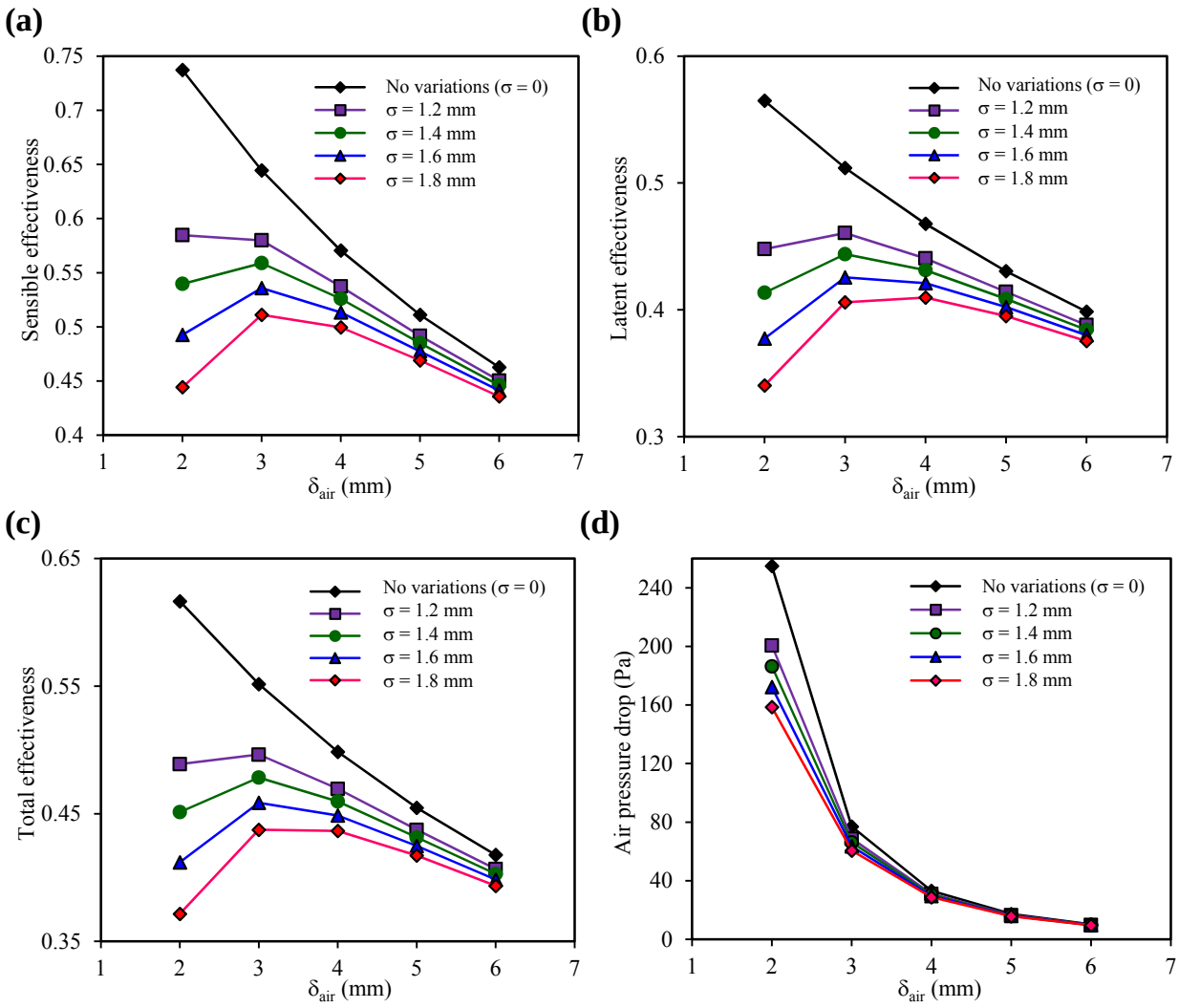

FIGURE 2.19. Variations of (a) sensible effectiveness (b) latent effectiveness (c) total effectiveness (d) air pressure drop of the dehumidifier with δ_{air} (at σ = 0, 1.2, 1.4, 1.6, 1.8 mm and δ_{sol} = 2 mm). Results presented in this figure are obtained based on equations (2.17) and (2.18) developed by Shang and Besant (2004).

The practical implications of these sensitivity results for the design of flat-plate LAMEEs should be considered. First, it is worth mentioning that with pressurized exchanger membranes the mean spacing diameters, with finite liquid pressures in the liquid channels, for the air channel will always be less than the nominal spacing of the membrane with no deflections (e.g. if the deflection resulted in 0.5 mm reduction of membrane air flow space for each membrane, then two adjacent membranes on either side of an air flow channel would cause a 1 mm deduction in the flow channel average spacing). Therefore it would be prudent design to increase the nominal spacing by a similar amount. That is, the prediction of optimum effectiveness as a function of flow channel spacing without deflections should be shifted by 1 mm (i.e. instead of the optimum spacing being between 2 mm and 3 mm one should assume it will likely be between 3 mm and 4 mm spacing). Since the static pressures inside the liquid flow channels of multiple panel flat-plate LAMEEs will change with operating conditions and the static pressure depth of the exchanger, the value of σ/D_o will change for the same exchanger. This implies that the best channel spacing should be further increased, say from 3-4 mm to 4-5 mm. Finally, over long durations of membrane exchanger operations (i.e. 10-20 years of life cycle), the elastic properties of the membrane will change causing some membrane creep or inelastic strain so that the membrane deflections increase slowly over time. This last concern implies that the spacing between membranes should perhaps be further increased to 5-6 mm, provided considerable attention has been given to the design and construction of the membrane exchanger so that variations in the channel widths are as small practical.

2.8.6 Influences of Air and Solution Channel Widths on the Compactness of the Flat-Plate LAMEE

A heat/energy exchanger, with liquid or two-phase flows, is classified to be compact if it has an area density higher than 300 m^2/m^3 (Reay (2002)). Increasing the compactness of a flat-plate

LAMEE results in lower capital, shipping and installation costs. The compactness of the flat-plate LAMEE investigated in the current study is calculated from equation (2.19). For the case of an exchanger with a selected mass flow rate, Figure 2.20 presents the LAMEE's compactness for different air and solution channel widths. It is clear that an area density up to 775 m^2/m^3 can be obtained at δ_{air} = 1 mm and δ_{sol} = 1 mm.

$$Compactness_{\mathrm{LAMEE}} = \frac{N_{\mathrm{mem}} \cdot L_{\mathrm{ex}} \cdot H_{\mathrm{ex}}}{L_{\mathrm{ex}} \cdot H_{\mathrm{ex}} \cdot (N_{\mathrm{air}} \cdot \delta_{\mathrm{air}} + N_{\mathrm{sol}} \cdot \delta_{\mathrm{sol}} + N_{\mathrm{mem}} \cdot \delta_{\mathrm{mem}})} \tag{2.19}$$

where N_{mem} is the number of semi-permeable membranes, L_{ex} is the length of the LAMEE (m), H_{ex} is the height of the LAMEE (m), N_{air} is the number of air channels, N_{sol} is the number of solution channels, and δ_{mem} is the membrane thickness (m).

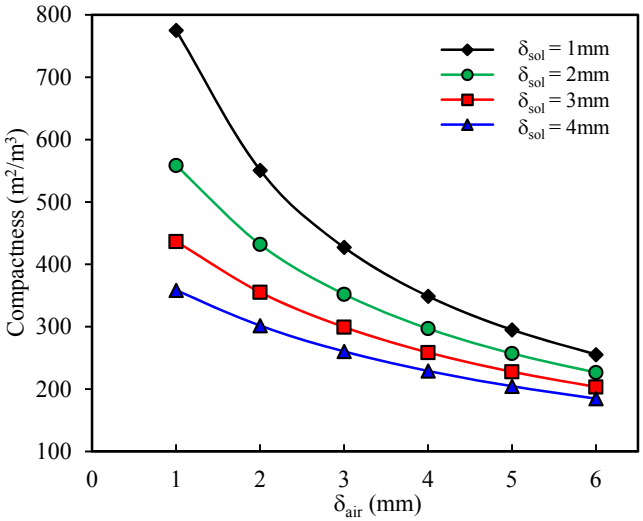

FIGURE 2.20. Influences of air and solution channel widths on the compactness of the studied flat-plate LAMEE.

Although compact heat/energy exchangers have several advantages over conventional ones, increasing the compactness of an exchanger is associated with an increase in the pressure drop and fan and pump power consumption. In addition, increasing the compactness of a flat-plate LAMEE

by decreasing δ_{air} will result in flow maldistribution in the air and solution flows due to membrane deflections, which reduces the effectiveness of the LAMEE. Therefore, a trade-off between the enhancement in the thermal performance (i.e. effectiveness), the pressure drop, and flow maldistribution should be considered in order to develop an optimum design for a flat-plate LAMEE.

2.9 CONCLUSIONS

In this chapter, the influences of the air and solution channel widths on the steady-state effectiveness, moisture removal rate, and airside pressure drop of a flat-plate LAMEE are numerically investigated. Results show that considerable enhancements in the effectivenesses and moisture removal rate of the dehumidifier and the regenerator are possible at narrow air and solution channel widths, provided the variations in the channel widths are small. The results presented in this chapter lead to the following conclusions.

1. The airside is responsible for the majority of the total heat transfer resistance in flat-plate LAMEEs (e.g. 90% of total heat transfer resistance for the recommended practical design), while the vapor diffusion resistance of the membrane accounts for a significant portion (e.g. 31%) of the total moisture transfer resistance.

2. The sensible effectivenesses of the dehumidifier and the regenerator, with no variations in the widths of air and solution channels and no flow maldistribution, increase by up to 40% as the air channels width decreases from 6 mm to 1 mm, whereas the width of solution channels has a negligible influence on the sensible effectiveness of both the dehumidifier and the regenerator.

3. The latent effectiveness of both the dehumidifier and the regenerator, with no variations in the widths of air and solution channels and no flow maldistribution, increases with the decrease of the width of either the air channels or the solution channels. However, for the same reduction in the width of air and/or solution channels, the absolute enhancement in the latent effectiveness of the dehumidifier is greater than the absolute enhancement in the latent effectiveness of the regenerator.

4. Variations in the width of the air channels due to manufacturing tolerances and membrane deflections caused by pressure differences between the air and solution streams, reduce the effectiveness of flat-plate LAMEEs. The reduction in effectiveness become more significant as the standard deviation of hydraulic diameter of the air channels increases or as the nominal width of the air channel decreases. For each specific value of standard deviation of hydraulic diameter of the air channels, there is an optimum nominal air channel width, where further reduction beyond this optimum width results in a reduction in the effectiveness of the flat-plate LAMEE. Considering practical design, construction, and operation of flat-plate LAMEEs, the recommended practical air channel width for flat-plate LAMEEs is 5-6 mm and the practical nominal solution channel width is 1-2 mm.

CHAPTER 3

DESIGN AND TESTING OF A NOVEL 3-FLUID LAMEE

3.1 OVERVIEW OF CHAPTER 3

Based on the design guidelines provided by the numerical studies presented in the previous chapter, a novel 3-fluid LAMEE prototype is designed and fabricated in this chapter. This chapter fulfills part of the second objective of this thesis (i.e. to design and test a 3-fluid LAMEE and compare with a 2-fluid LAMEE). The 3-fluid LAMEE prototype is used to test the rates of heat and moisture transfer in 3-fluid and 2-fluid LAMEEs at several inlet refrigerant temperatures and mass flow rates under air cooling and dehumidifying conditions. The 3-fluid LAMEE prototype is operated as a 2-fluid LAMEE by turning off the refrigerant loop. The design of the 3-fluid LAMEE prototype, the test-facility and the measuring instruments used to test and measure the performances of the 3-fluid and 2-fluid LAMEEs are described in detail in this chapter.

The manuscript presented in this chapter is published in the International Journal of Heat and Mass Transfer.

Design and Testing of a Novel 3-Fluid Liquid-To-Air Membrane Energy Exchanger (3-Fluid LAMEE)

(International Journal of Heat and Mass Transfer, 2016, Volume 92)

Mohamed R. H. Abdel-Salam, Robert W. Besant, Carey J. Simonson

3.2 ABSTRACT

Liquid-to-air membrane energy exchangers (LAMEEs) are constructed with micro-porous semi-permeable membranes and transfer heat and water vapor between two separate fluids (air and liquid desiccant). Over the last decade, research has shown that LAMEEs can significantly reduce the energy consumption of HVAC systems. In this chapter, a novel 3-fluid LAMEE prototype is designed and tested. The main objective of the proposed 3-fluid LAMEE is to enhance the performance (i.e. sensible, latent, and total effectivenesses, moisture removal rate, and sensible cooling capacity) of regular 2-fluid LAMEEs. The major difference between the proposed 3-fluid LAMEE and a 2-fluid flat-plate LAMEE is that refrigeration tubes are placed inside the desiccant solution channels to enhance the cooling capacity and control the temperature of the desiccant solution along the length of the 3-fluid LAMEE. Water is used as the refrigerant in the current work. The main contribution of this chapter is that it shows that the inlet temperature and mass flow rate of the cooling water have significant influences on the steady-state performance of the 3-fluid LAMEE. Compared to a 2-fluid LAMEE with the same design parameters, the sensible, latent, and total effectivenesses, moisture removal rate, and sensible cooling capacity of the 3-fluid LAMEE are improved by up to 69%, 28%, 39%, 54%, and 140% respectively, depending on the inlet temperature and mass flow rate of the cooling water.

3.3 INTRODUCTION

In the past decade, research on liquid-to-air membrane energy exchangers (LAMEEs) has shown the potential for reducing the energy consumption of building HVAC systems (Abdel-Salam et al. (2014c)). A schematic of a flat-plate LAMEE is shown in Figure 1.1. A flat-plate LAMEE is composed of multiple adjacent air and solution channels. The supply air flows in the first channel and is separated from the second channel, where the desiccant solution flows, by a micro-porous semi-permeable membrane. The elastic semi-permeable membrane is permeable to water vapor and impermeable to liquids under small liquid-air pressure differences. The heat and moisture are transferred simultaneously between the supply air and the desiccant solution (or water) streams through the semi-permeable membrane.

A LAMEE can be used in different climates (i.e. cold and dry, cold and humid, hot and dry, hot and humid) which implies different directions of heat and moisture transfer (Moghaddam et al. (2013a)). Also, it can be used as a regenerator for the diluted desiccant solution regeneration (Ge et al. (2014a)). There are several HVAC systems which can benefit from the use of LAMEEs. For instance, LAMEEs can be used for hot-humid air cooling and dehumidifying and diluted desiccant solution regeneration in membrane liquid desiccant air-conditioning systems (Abdel-Salam et al. (2013, 2014a); Abdel-Salam and Simonson (2014b); Zhang and Zhang (2014)) or can be installed in the supply and exhaust airstreams of an HVAC system, and coupled using desiccant solution for passive energy recovery in buildings (Vali et al. (2009); Patel et al. (2014); Hemingson et al. (2011a); Akbari et al. (2012)).

3.4 LITERATURE REVIEW

Comprehensive literature reviews on the development of LAMEEs and their applications have been presented by Abdel-Salam et al. (2014b, 2014c), Huang and Zhang (2013), and Ge et al.

(2013a). Table 3.1 (Moghaddam et al. (2013a, 2013b, 2013c, 2013e); Ge et al. (2014a); Namvar et al. (2012)) summarizes the steady-state sensible and latent effectivenesses of several flat-plate LAMEE prototypes. Based on design parameters and operating conditions, the sensible effectiveness ranged between 29% and 97%, while the latent effectiveness ranged between 37% and 98%. The sensible and latent effectivenesses of flat-plate LAMEEs increases as number of heat transfer units (*NTU*) and number of mass transfer units (NTU_{m}) increase, respectively.

$$NTU = \frac{UA_{\mathrm{mem}}}{C_{\mathrm{min}}} \tag{3.1}$$

$$NTU_{\mathrm{m}} = \frac{U_{\mathrm{m}}A_{\mathrm{mem}}}{\dot{m}_{\mathrm{min}}} \tag{3.2}$$

Large values of *NTU* and NTU_{m} imply large membrane surface areas per unit flow rate of air, which means that high effectivenesses may have high capital costs. Therefore, it is important to modify the current design of the flat-plate LAMEE to enhance its effectiveness without increasing its size or decreasing the air flow rate.

TABLE 3.1. Experimental steady-state sensible and latent effectivenesses for several flat-plate LAMEE prototypes when used for air cooling and dehumidifying.

Reference	*NTU*	NTU_{m}	$\varepsilon_{\mathrm{sen}}$ (%)	$\varepsilon_{\mathrm{lat}}$ (%)
Moghaddam et al. (2013a)	3	1.7	40-86	51-83
Ge et al. (2014a)	5, 6, 7	3.1, 3.7, 4.3	30-94	74-98
Namvar et al. (2012)	6, 8, 10	2.5, 3.4, 4.2	29-88	37-89
Moghaddam et al. (2013e)	2.5, 3.5, 4.5	2.6, 3.3, 3.9	84-90	70-80
Moghaddam et al. (2013b)	4.5, 5.8	-	35-97	48-92
Moghaddam et al. (2013c)	5, 5.5, 6	3, 3.2, 3.6	79-86	79-87

3.5 MOTIVATION OF THE CURRENT STUDY

In LAMEEs, the driving potentials for heat and moisture transfer are the temperature and vapor pressure differences between the supply air and desiccant solution streams. When the desiccant solution absorbs/emits moisture, the heat of phase change is released/absorbed to/from the desiccant solution, which alters the temperature of the desiccant solution. Therefore, as the desiccant solution flows in the channel, the temperature difference between the process air and the desiccant solution decreases, and thus the potential of heat and mass transfer degrades. This decreases the effectiveness of the LAMEE.

For air cooling and dehumidifying process, Figure 3.1 shows the temperature profiles of the working fluids in a counter-flow sensible heat exchanger and a counter-flow LAMEE. As the desiccant solution flows through the exchanger, the increase in the desiccant solution temperature is much higher in the LAMEE than in the sensible heat exchanger because phase change energy is released due to water vapor absorption by the desiccant solution. This shows a need for improvement in the design to improve the effectiveness of the LAMEE.

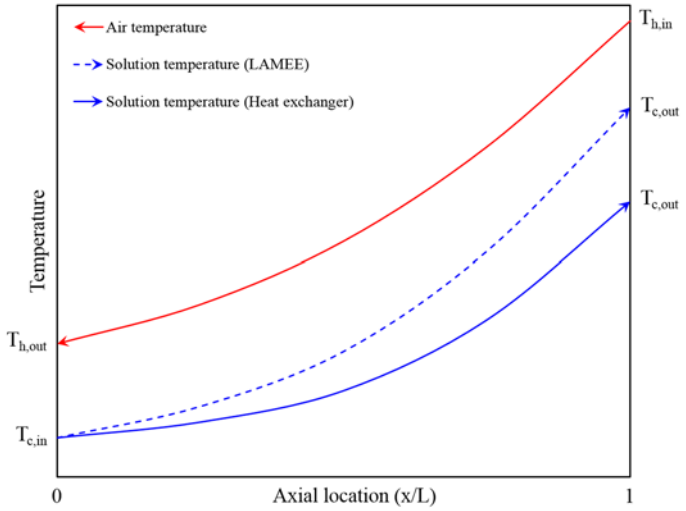

FIGURE 3.1. A schematic representation of the fluid temperatures within a LAMEE and heat exchanger shows that the phase change energy reduces the temperature difference between the air and desiccant solution streams.

To overcome this problem, a new 3-fluid LAMEE was designed, built, and experimentally investigated in this chapter. The new 3-fluid LAMEE is an improved design that is based on the flat-plate LAMEEs that have been designed and tested over the past decade at the University of Saskatchewan (Erb (2009); Mahmud (2009); Beriault (2011); Patel (2012); Namvar (2012); Ge et al. (2013); Moghaddam (2014)). The structure of the 3-fluid LAMEE is similar to the flat-plate LAMEE. The major difference is that in the 3-fluid LAMEE, tubes are installed inside the solution channel and a refrigerant flows inside these tubes to control the temperature of the desiccant solution. The third fluid (i.e. the refrigerant) has been added to control the temperature of the desiccant solution throughout the LAMEE. In this chapter, the design and heat/moisture transfer performance of the novel 3-fluid LAMEE, when used for air cooling and dehumidifying, under different operating conditions will be explored and its effectivenesses (i.e. sensible, latent, and total), moisture removal rate, and sensible cooling capacity (SCC) will be investigated and compared to the conventional 2-fluid flat-plate LAMEE.

3.6 DESIGN OF THE 3-FLUID LAMEE PROTOTYPE

Figures 3.2 (a) and (b) show conceptual schematics of the proposed 3-fluid LAMEE and Figure 3.2 (c) shows a cross-sectional view of the 3-fluid LAMEE. The air and solution channels are separated by a reinforced micro-porous elastic semi-permeable membrane, and refrigeration tubes are accommodated in each solution channel to keep the temperature of the cold desiccant solution constant throughout the LAMEE. Table 3.2 gives the specifications of the 3-fluid LAMEE prototype.

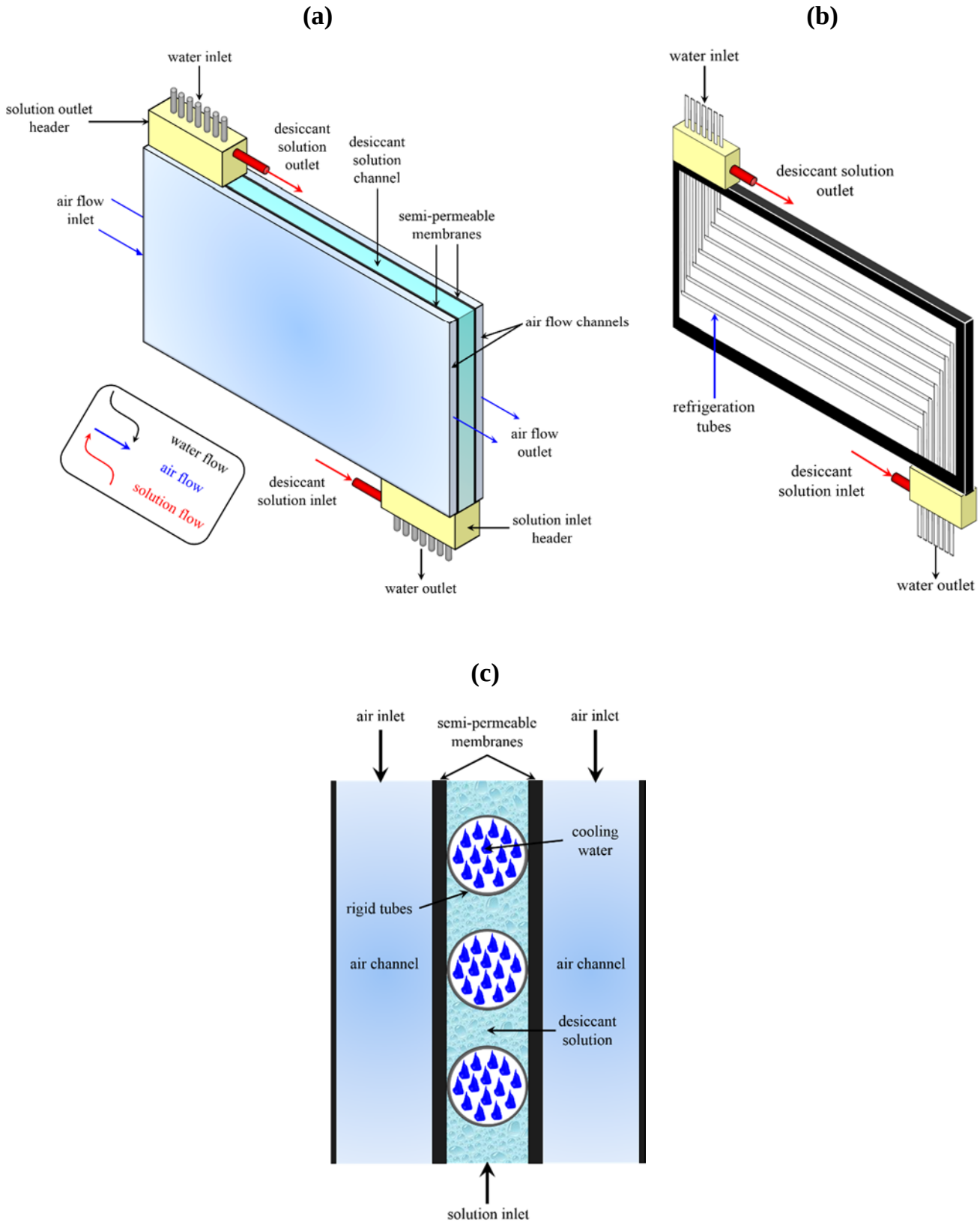

FIGURE 3.2. Conceptual schematics of (a) the 3-fluid LAMEE prototype (b) the solution channel with refrigeration tubes inside (c) a cross-sectional view.

TABLE 3.2. Specifications of the 3-fluid LAMEE prototype.

	Parameter	Value	Unit
Exchanger	flow configuration (solution-air)	counter-cross	-
	flow configuration (solution-refrigerant)	counter	-
	length	470	mm
	height	100	mm
	exchanger solution entrance ratio*	0.11	-
	nominal air channel width (δ_{air})	5	mm
	nominal solution channel width (δ_{sol})	4.2	mm
	number of air channels	2	-
	number of solution channels	1	-
	mass (empty)	1.71	kg
Membrane	thickness	0.3	mm
	mass resistance (R_m)	38	s/m
	liquid penetration pressure	124	kPa
Refrigeration tubes	refrigerant	water	-
	tube material	titanium	-
	number of tubes	7	-
	tube length	660	mm
	inner diameter	2.362	mm
	outer diameter	3.175	mm
	thickness	0.4	mm
	spacing between tubes	9.7	mm
	thermal conductivity	21 (eFunda (2014))	(W/(m·K))

**entrance ratio is defined as the ratio between the length of the inlet/outlet desiccant solution header and the length of the exchanger (Vali (2009)).*

3.6.1 The Prototype

The 3-fluid LAMEE prototype was manufactured at the University of Saskatchewan using a rapid prototype machine. The construction drawings for the 3-fluid LAMEE prototype are presented in Appendix C. The prototype was made of High Temperature Material Objet RGD 525 because of its ability to resist corrosion of liquid desiccants and withstand high temperatures (i.e. up to 63°C).

The prototype is composed of one solution channel and two air channels. This configuration was chosen for three reasons: (1) the smallest available tube diameter is 3.175 mm, (2) the thermal conductivity of the air is lower than that of the desiccant solution, which reduces the heat losses through the LAMEE's walls to the surrounding environment, and (3) to reduce the number of refrigeration tubes which reduces the capital cost.

The prototype walls are made of PVC and each wall has a thickness of 3 mm. The dimensions of the prototype are given in Table 3.2. The width of the air channels is chosen according to the results of the study presented in Chapter 2 (Abdel-Salam et al. (2015)) on the sensitivity of the steady-state performance of flat-plate LAMEEs to the air channels width and flow maldistribution. It was found that effectiveness and moisture removal rate of flat-plate LAMEEs increase inversely with the air channel width. However, the airside pressure drop and the variations in the air channels width due to manufacturing tolerances and membrane deflections (i.e. flow maldistribution), significantly increase for flat-plate LAMEEs with narrow air channel widths. This causes significant reductions in the effectiveness of flat-plate LAMEEs. The study recommended that the optimum nominal air channel width for flat-plate LAMEEs is 5 to 6 mm. Accordingly, the 3-fluid LAMEE prototype is designed with a nominal air spacing of 5 mm.

Under same operating conditions, counter-flow heat/energy exchangers have higher effectivenesses than those with parallel-flow or cross-flow configurations provided that flow maldistribution can be minimized (ASHRAE (2004)). However, designing a flat-plate LAMEE with adjacent inlet/outlet manifolds for the air and solution streams is impractical. Therefore Vali (2009) suggested a counter-cross-flow configuration (see Figure 1.1) where the air and solution streams have a counter-flow configuration along 90% of the LAMEE's length. Figure 3.3 shows a photograph of the solution channel with the refrigeration tubes inside. The tubes are

accommodated inside the solution channel and a high temperature marine glue is used to attach the tubes to the solution header and water header. The membrane is attached to the solution channel using a high temperature marine glue to resist and prevent liquid desiccant leakages through the edges of the solution channel. Figure 3.4 shows a photograph of the solution channel with the membrane glued on it.

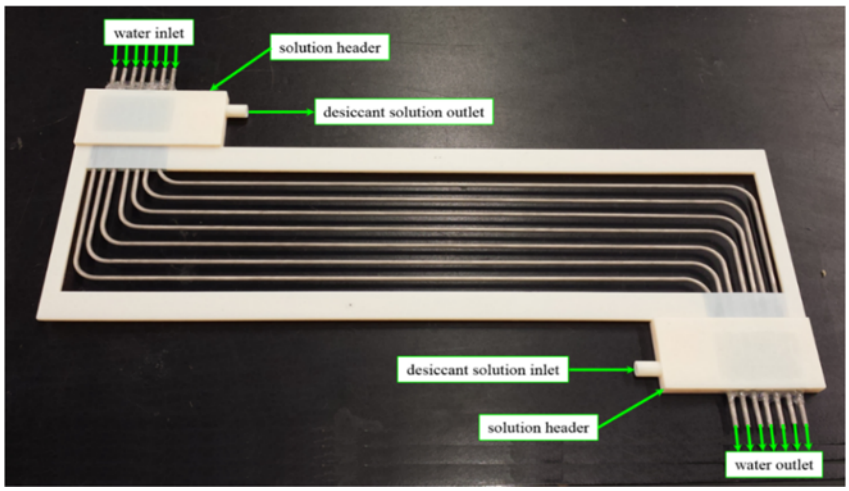

FIGURE 3.3. Photograph of the solution channel with the refrigeration tubes inside.

FIGURE 3.4. Photograph of the solution channel with the membrane glued on it.

Figure 3.5 shows a detailed schematic of a novel solution header which has been designed to allow a counter-cross-flow configuration between the air and the desiccant solution streams, and a

counter-flow configuration between the desiccant solution and the refrigerant streams inside the 3-fluid LAMEE. Leakage of desiccant solution was a major problem during testing previous flat-plate LAMEE prototypes. In these prototypes, the solution header was designed and manufactured as a separate piece and was connected to the solution channel using a glue. A considerable amount of leakage occurred from this connection. Accordingly, the 3-fluid LAMEE is designed with the solution header and the solution channel as a one piece (see Figure 3.5) to prevent desiccant solution leakage from the inlet/outlet solution headers.

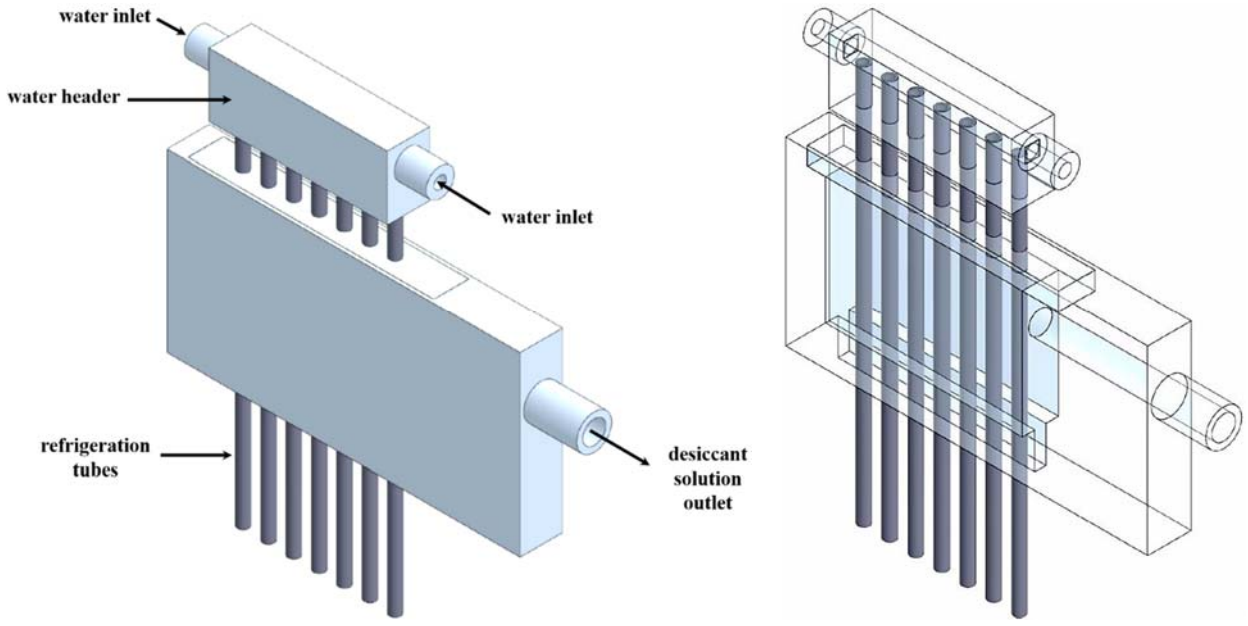

FIGURE 3.5. Conceptual schematics of the novel solution header of the 3-fluid LAMEE prototype.

The desiccant solution may enter the 3-fluid LAMEE either from the top or the bottom header. Mahmud et al. (2010) found that a flat-plate LAMEE with a bottom-to-top flow configuration for the desiccant solution had a higher effectiveness than a flat-plate LAMEE with a top-to-bottom flow configuration. Accordingly, the bottom-to-top flow is chosen for the desiccant solution stream in all experiments presented in the current chapter.

3.6.2 The Refrigeration Tubes

The ideal materials for the refrigeration tubes should have the following thermo-physical properties:

1) The capability to resist the corrosion of liquid desiccant solutions,
2) Ability to withstand high temperatures (i.e. up to 60°C),
3) A high thermal conductivity,
4) A high modulus of elasticity to avoid any deformations in the tubes especially during the regeneration process at high temperatures,
5) Be chemically stable,
6) Low cost.

A market survey was conducted and High-Strength/Lightweight Titanium tubes (McMASTER-CARR (2014)) were chosen. Titanium has a light weight, high resistance to corrosion caused by liquid desiccant solutions, high modulus of elasticity, acceptable thermal conductivity, and can withstand high temperatures up to 315ºC (McMASTER-CARR (2014)). Fernández-Seara et al. (2013) reported that the weight of a heat exchanger can be significantly reduced if titanium is used instead of stainless steel because the specific weight of the titanium is less than that of the stainless steel by 55%.

3.6.3 The Refrigerant

Various types of refrigerants (i.e. water, nanofluids, etc.) could be used to cool/heat the desiccant solution in the 3-fluid LAMEE. Among these refrigerants, water has a high specific heat capacity, high boiling point, low freezing point, low cost, and is non-flammable, non-toxic, non-corrosive, abundant and environmentally friendly. Therefore, water was chosen as the refrigerant in the current research.

3.6.4 The Air Channel Insert

It was found in Chapter 2 (Abdel-Salam et al. (2015)) that the airside resistance is responsible for the majority of the total heat transfer resistance in 2-fluid flat-plate LAMEEs. According to *Chilton-Colburn analogy* (Colburn (1933); Chilton and Colburn (1934)), the convective mass transfer coefficient increases with the increase of the convective heat transfer coefficient, thus enhancing the convective heat transfer coefficient will improve the sensible and latent effectivenesses of LAMEEs.

For laminar air flow in LAMEEs as in this thesis, the heat and mass transfer on the airside can be enhanced by generating secondary air flows which enhance mixing. This can be achieved by installing inserts with specific geometries inside the air channel. For example, installing an insert with cylindrical bars inside the air channels will generate vortices and provide a better mixing on the airside which enhances the rates of heat and moisture transfer in LAMEEs (Kakac et al. (1999)) (see Figure 3.6).

FIGURE 3.6. The effect of cylindrical bars on the airflow (Incropera et al. (2007)).

Oghabi (2014) proposed installing air channel inserts in flat-plate LAMEEs to enhance the convective heat transfer coefficient of the airside. As shown in Figure 3.7, the insert is composed of several horizontal ribs and vertical cylindrical bars. Oghabi (2014) tested several inserts with different vertical spacing between the ribs, different horizontal spacing between the cylindrical bars, and at different Reynolds numbers. He found that increasing Reynolds number or decreasing

either the horizontal or the vertical spacing results in an increase in Nusselt number of the airside, where the influence of the horizontal spacing between the cylindrical bars on the enhancement of convective heat transfer coefficient is more significant than the influence of the vertical spacing between the ribs. On the other hand, he reported that using this insert in the air channels of the flat-plate LAMEEs increases the airside pressure drop.

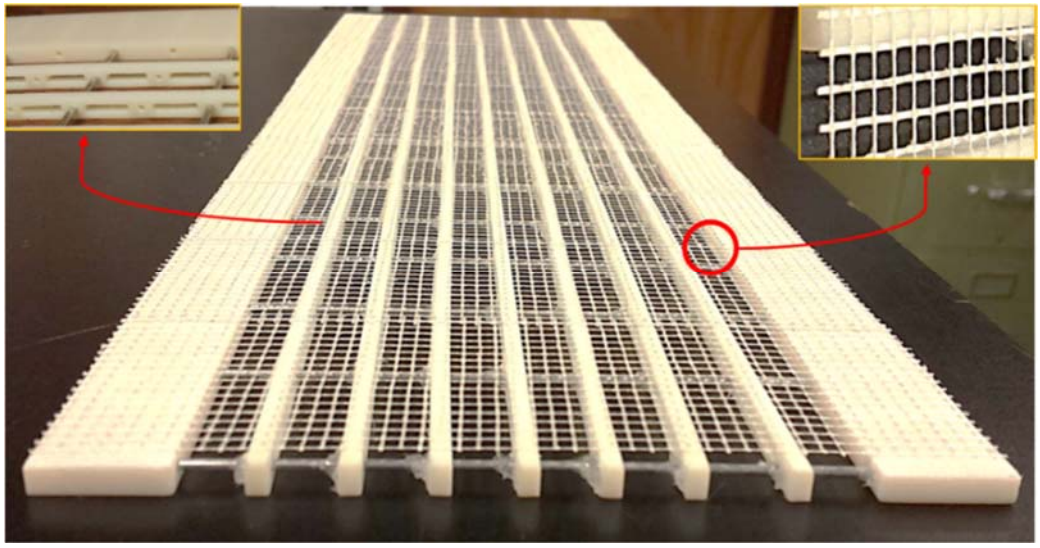

FIGURE 3.7. Photograph of the support grid attached to the air channel insert.

Figure 3.7 shows a photograph of the insert installed in the air channels of the 3-fluid LAMEE prototype. This insert is designed according to the findings of Oghabi (2014). The insert is made of High Temperature Material Objet RGD 525 and has horizontal spacing between the cylindrical bars of 30 mm and vertical spacing between the ribs of 9.8 mm. This vertical spacing was selected to provide an extra support to the refrigeration tubes installed inside the solution channel, where each tube is supported by two ribs from both sides. The enhancement in Nusselt number and the increase in air pressure drop (i.e. increase in the Darcy friction factor) caused by the air channel insert can be calculated from the following empirical correlations (equations (3.3) and (3.4)) which have been developed by Oghabi (2014).

$$Nu = (0.017 \pm 0.001)\left(\frac{\delta_{\text{air}}}{H}\right)^{0.31\pm0.02} Re + (7.1 \pm 0.3)\begin{cases} 900 \le Re \le 2{,}200 \\ Pr = 0.7 \\ 19 \le \dfrac{H}{D} \le 56 \\ \dfrac{\delta_{\text{air}}}{D} = 3.1 \end{cases} \quad (3.3)$$

$$f_D = (0.183 \pm 0.004) \cdot exp\left(\frac{(3801 \pm 205)\left(\frac{\delta_{\text{air}}}{H}\right) + (386 \pm 36)}{Re}\right)\begin{cases} 900 \le Re \le 2{,}200 \\ Pr = 0.7 \\ 19 \le \dfrac{H}{D} \le 56 \\ \dfrac{\delta_{\text{air}}}{D} = 3.1 \end{cases} \quad (3.4)$$

where *Nu* is the average Nusselt number, δ_{air} is the width of the air channel (mm), *H* is the spacing between the cylindrical bars (mm), *Re* is Reynolds number, *Pr* is Prandtl number, *D* is the diameter of the cylindrical bars (mm), and f_D is the Darcy friction factor.

3.6.5 The Semi-Permeable Membrane

The membrane has a significant influence on the LAMEE's performance. The following are the desirable characteristics of the membrane:

1) Low vapor diffusion resistance,
2) High liquid penetration pressure,
3) High modulus of elasticity to reduce membrane deflections,
4) Small tortuosity factor (Khayet (2011)),
5) High selectivity (Zhang et al. (2012c)),
6) High porosity,
7) Ability to withstand high temperatures (i.e. up to 60°C),
8) High durability,
9) Low cost.

Based on our research group's experience, the GE membrane was selected to be used in the 3-fluid LAMEE prototype. A photograph and a scanning electron microscopy (SEM) images of the membrane used in the 3-fluid LAMEE prototype are shown in Figure 3.8. The membrane is composed of two layers; a hydrophobic layer (Teflon layer) which transfers only water vapor, and a hydrophilic layer (support layer) which supports the membrane structure. Vapor diffusion resistance (VDR) of a membrane is the resistance to the diffusion of water vapor molecules through the membrane's pores (Larson (2006)). It was found in Chapter 2 (Abdel-Salam et al. (2015)) that the VDR of a membrane has strong influences on the moisture removal rate and the latent effectiveness of flat-plate LAMEEs, where the moisture removal rate and latent effectiveness increase inversely with the VDR. Therefore, it is necessary to measure the VDR of the membrane used in the 3-fluid LAMEE prototype. A MOCON PERMATRAN-W model 101 K is used to measure the VDR of the semi-permeable membrane used in the 3-fluid LAMEE prototype. The properties (i.e. vapor diffusion resistance, liquid penetration pressure, and thickness) of the membrane used in the 3-fluid LAMEE prototype are given in Table 3.2.

Membranes used in flat-plate LAMEEs are prone to significant deflections due to the pressure differences between the air and solution streams. The results presented in Chapter 2 showed that these deflections create variations in the air and solution channel widths, which cause significant reductions in the performance (i.e. sensible effectiveness, latent effectiveness, total effectiveness, moisture removal rate, and sensible cooling capacity) of flat-plate LAMEEs (Abdel-Salam et al. (2015)). Moreover, these deflections will damage the membrane over long duration of LAMEE operations. Several techniques can be applied to reduce, but not totally eliminate, the membrane deflections in the 3-fluid LAMEE. The most effective technique is to pre-tension the membrane before clamping and gluing it on the solution channel. It is shown in Figure 3.4 that the membrane

of the 3-fluid LAMEE prototype is stretched very well. As well, membrane deflections can be reduced by attaching a support grid to the membrane. Figure 3.7 shows a photograph of the support grid attached to the air channel insert. It is worth mentioning that the support grid reduces the membrane area available for heat and moisture transfer. Therefore, more research is still needed to find effective techniques to minimize the membrane deflections without affecting the rate of heat and moisture transfer across the membrane.

(a)

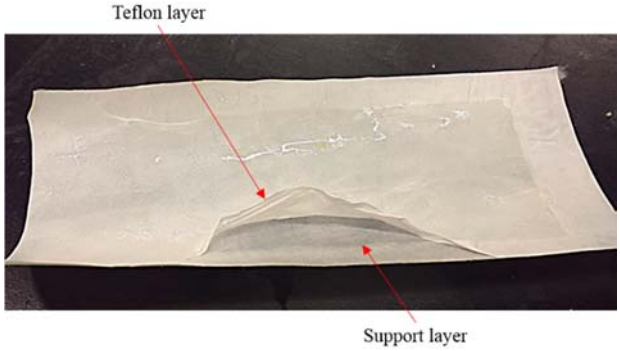

(b)

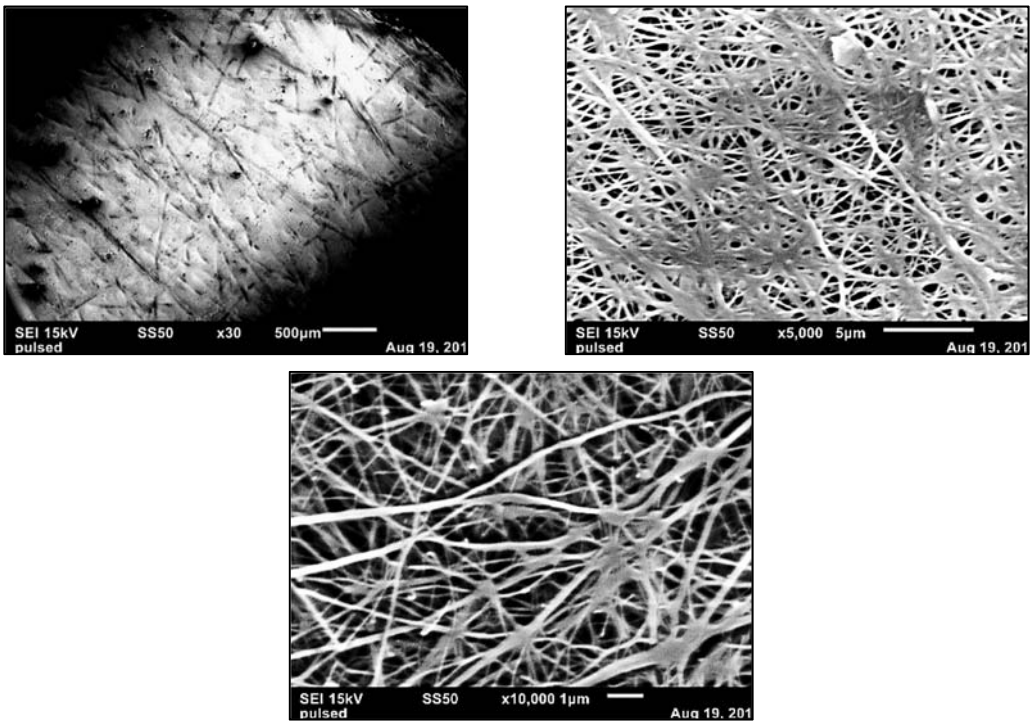

FIGURE 3.8. (a) Photograph (b) scanning electron microscopy (SEM) images of the micro-porous semi-permeable membrane used in the 3-fluid LAMEE prototype.

3.7 PERFORMANCE EVALUATION OF LAMEEs

3.7.1 Effectiveness

As mentioned in Section 2.6.2, for solution-to-air heat capacity ratio (Cr^*) ≥ 1, LAMEE's sensible, latent, and total (Simonson and Besant (1999)) effectivenesses are calculated from equations (3.5) to (3.7).

$$\varepsilon_{\text{sen}} = \frac{T_{\text{air,in}} - T_{\text{air,out}}}{T_{\text{air,in}} - T_{\text{sol,in}}} \tag{3.5}$$

$$\varepsilon_{\text{lat}} = \frac{W_{\text{air,in}} - W_{\text{air,out}}}{W_{\text{air,in}} - W_{\text{sol,in}}} \tag{3.6}$$

$$\varepsilon_{\text{tot}} = \frac{\varepsilon_{sen} + H^* \varepsilon_{\text{lat}}}{1 + H^*} \tag{3.7}$$

where T is the temperature (ºC), W is the humidity ratio (kg_v/kg_{air}), and subscripts *air*, *sol*, *in*, and *out* refer to air, desiccant solution, inlet, and outlet, respectively. H^* is the operating factor which was developed by Simonson and Besant (1999), and is calculated from equation (3.8).

$$H^* = \frac{\Delta H_{\text{lat}}}{\Delta H_{\text{sen}}} \approx 2500 \, \frac{W_{\text{air,in}} - W_{\text{sol,in}}}{T_{\text{air,in}} - T_{\text{sol,in}}} \tag{3.8}$$

3.7.2 Moisture Removal Rate

The rate of water vapor transfer between the air and desiccant solution streams inside a LAMEE.

$$\dot{m}_{\text{rr}} = \dot{m}_{\text{air}} \, (W_{\text{air,in}} - W_{\text{air,out}}) \tag{3.9}$$

where $\dot{m}_{\text{air}}$ is the air mass flow rate (kg/s).

3.7.3 Sensible Cooling Capacity

The rate of heat transfer between the air and desiccant solution streams inside a LAMEE.

$$SCC = \dot{m}_{\text{air}}\ c_{\text{p,air}}\ (T_{\text{air,in}} - T_{\text{air,out}}) \tag{3.10}$$

where $c_{\text{p,air}}$ is the specific heat capacity of the air (J/(kg·K)).

3.7.4 Energy Transfer Rate

$$ETR = \dot{m}_{\text{air}}\ (H_{\text{air,in}} - H_{\text{air,out}}) \tag{3.11}$$

where $H_{\text{air,in}}$ is the inlet air enthalpy (J/kg), and $H_{\text{air,out}}$ is the outlet air enthalpy (J/kg).

The performance (i.e. effectiveness, moisture removal rate, and sensible cooling capacity) of a LAMEE significantly depends on the number of heat transfer units (*NTU*), the number of mass transfer units (NTU_{m}), and the ratio between the heat capacity rates of the desiccant solution and air (Cr^*). *NTU*, NTU_{m}, and Cr^* can be calculated from equations (3.12) to (3.17).

$$NTU = \frac{UA_{\text{mem}}}{C_{\text{min}}} \tag{3.12}$$

$$U = \left[\frac{1}{h_{\text{air}}} + \frac{\delta_{\text{mem}}}{k_{\text{mem}}} + \frac{1}{h_{\text{sol}}}\right]^{-1} \tag{3.13}$$

where U is the overall heat transfer coefficient (W/(m^2·K)), A_{mem} is the membrane surface area (m^2), C_{min} is the minimum heat capacity rate of air and desiccant solution flows (W/K), h_{air} is the convective heat transfer coefficient of the air (W/(m^2·K)), δ_{mem} is the membrane thickness (m), k_{mem} is the membrane thermal conductivity (W/(m·K)), and h_{sol} is the convective heat transfer coefficient of the desiccant solution (W/(m^2·K)).

$$NTU_{\text{m}} = \frac{U_{\text{m}}A_{\text{mem}}}{\dot{m}_{\text{min}}} \tag{3.14}$$

$$U_{\text{m}} = \left[\frac{1}{h_{\text{m,air}}} + \frac{\delta_{\text{mem}}}{k_{\text{m}}} + \frac{1}{h_{\text{m,sol}}}\right]^{-1} \tag{3.15}$$

where U_m is the overall mass transfer coefficient (kg/(m^2·s)), $\dot{m}_{min}$ is the minimum mass flow rate of the air and desiccant solution flows (kg/s), $h_{m,air}$ is the convective mass transfer coefficient of the air (kg/(m^2·s)), k_m is the membrane water vapor permeability (kg/(m·s)), and $h_{m,sol}$ is the convective mass transfer coefficient of the desiccant solution (kg/(m^2·s)).

The convective heat transfer coefficients of the air and desiccant solution streams can be calculated from equation (3.16).

$$h = \frac{Nu\ k}{D_h} \tag{3.16}$$

where h is the convective heat transfer coefficient (W/(m^2·K)), Nu is Nusselt number, k is the coefficient of thermal conductivity (W/(m·K)), and D_h is the hydraulic diameter (m).

$$C_r^* = \frac{C_{sol}}{C_{air}} = \frac{\dot{m}_{sol}\ c_{p,sol}}{\dot{m}_{air}\ c_{p,air}} \tag{3.17}$$

where C_{sol} is the heat capacity rate of the desiccant solution (W/K), C_{air} is the heat capacity rate of the air (W/K), $\dot{m}_{sol}$ is the mass flow rate of the desiccant solution (kg/s), and $c_{p,sol}$ is the specific heat capacity of the desiccant solution (J/(kg·K)).

3.7.5 Desiccant Solution Concentration

Concentration of the liquid desiccant solution is calculated from equation (3.18).

$$C_{sol,in} = \frac{\text{mass of desiccant}}{\text{mass of desiccant} + \text{mass of water}} \tag{3.18}$$

3.7.6 Temperature Ratio

The temperature ratio is developed and presented for the first time in the current chapter. The temperature ratio is a dimensionless parameter that describes the ratio between the temperature

difference between the inlet air and cooling water streams and the temperature difference between the inlet air and desiccant solution streams.

$$T^* = \frac{T_{\text{air,in}} - T_{\text{w,in}}}{T_{\text{air,in}} - T_{\text{sol,in}}} \tag{3.19}$$

The temperature ratio relates between the inlet cooling water temperature and the inlet desiccant solution temperature, where

$T^* < 1$ indicates that $T_{\text{w,in}} > T_{\text{sol,in}}$

$T^* = 1$ indicates that $T_{\text{w,in}} = T_{\text{sol,in}}$

$T^* > 1$ indicates that $T_{\text{w,in}} < T_{\text{sol,in}}$

The proposed 3-fluid LAMEE could be considered as a combination of a liquid-to-air membrane energy exchanger for energy exchange between the air and desiccant solution streams, and a counter-flow liquid-to-liquid heat exchanger for heat exchange between the cooling water and desiccant solution streams. In the next section, the design and operating dimensionless parameters used to design the water-to-desiccant solution heat exchanger are presented.

3.7.7 Design of the Water-to-Desiccant Solution Heat Exchanger

3.7.7.1 Capacity Rate Ratio

The ratio between the minimum and maximum heat capacity rates of the refrigerant and desiccant solution. In the 3-fluid LAMEE, the heat capacity rate of the refrigerant is set to be greater than the heat capacity rate of the desiccant solution to avoid operating the exchanger with high flow rates of solution, and thus reduce the flow maldistribution due to membrane deflections.

$$Cr = \frac{C_{\text{min}}}{C_{\text{max}}} = \frac{C_{\text{sol}}}{C_{\text{ref}}} = \frac{\dot{m}_{\text{sol}}\, c_{\text{p,sol}}}{\dot{m}_{\text{ref}}\, c_{\text{p,ref}}} \tag{3.20}$$

where C_{min} is the minimum heat capacity rate of desiccant solution and refrigerant flows (W/K),

C_{max} is the maximum heat capacity rate of desiccant solution and refrigerant flows (W/K), C_{ref} is the heat capacity rate of the refrigerant (W/K), $\dot{m}_{ref}$ is the mass flow rate of the refrigerant (kg/s), and $c_{p,ref}$ is the specific heat capacity of the refrigerant (J/(kg·K)).

3.7.7.2 Number of Heat Transfer Units between the Desiccant Solution and Refrigerant ($NTU_{ref/sol}$)

A dimensionless number that gives an indication about the amount of heat transfer between the refrigerant and desiccant solution streams.

$$NTU_{ref/sol} = \frac{U_{ref/sol}\, A_{tube}}{C_{min}} \tag{3.21}$$

$$U_{ref/sol} = \left[\frac{1}{h_{ref}} + \frac{Ln\,(\frac{r_o}{r_i})}{2\,\pi\,k_{tube}\,L_{tube}} + \frac{1}{h_{sol}}\right]^{-1} \tag{3.22}$$

where $U_{ref/sol}$ is the overall heat transfer coefficient between the refrigerant and desiccant solution streams (W/(m^2·K)), A_{tube} is the surface area of the refrigeration tubes (m^2), C_{min} is the minimum heat capacity rate of refrigerant and desiccant solution flows (W/K), h_{ref} is the convective heat transfer coefficient of the refrigerant (W/(m^2·K)), r_i is the inner radius of the refrigeration tubes (m), r_o is the outside radius of the refrigeration tubes (m), k_{tube} is the thermal conductivity of the refrigeration tubes (W/(m·K)), L_{tube} is the length of the refrigeration tubes (m), and h_{sol} is the convective heat transfer coefficient of the desiccant solution (W/(m^2·K)).

The convective heat transfer coefficients of the refrigerant and desiccant solution streams can be calculated from equations (3.23) and (3.24).

$$h_{ref} = \frac{Nu\, k_{ref}}{D_h} \tag{3.23}$$

$$h_{\mathrm{sol}} = \frac{Nu\ k_{\mathrm{sol}}}{D_{\mathrm{h}}} \tag{3.24}$$

where k_{ref} is the thermal conductivity of the refrigerant (W/(m·K)), D_{h} is the hydraulic diameter (m), and k_{sol} is the thermal conductivity of the desiccant solution (W/(m^2·K)).

3.7.7.3 Sensible Effectiveness of the Liquid-to-Liquid Heat Exchanger ($\varepsilon_{\mathrm{sen,ref/sol}}$)

The ratio between the actual and maximum sensible heat transfer between two fluid streams inside a heat exchanger. The theoretical sensible effectiveness of the solution-to-water heat exchanger is calculated from equation (3.25) (Kakac et al. (2012)).

$$\varepsilon_{\mathrm{sen,ref/sol}} = \frac{1 - exp\left[-(1 - Cr) * NTU_{\mathrm{ref/sol}}\right]}{1 - Cr * \exp[-(1 - Cr) * NTU_{\mathrm{ref/sol}}]} \tag{3.25}$$

The objective of the current study is to investigate the possible enhancements in the rates of heat and moisture transfer between the air and desiccant solution streams when the desiccant solution is cooled along the length of a 2-fluid flat-plate LAMEE. Therefore, the sensible and latent effectivenesses of the 3-fluid LAMEE will be evaluated based only on the heat and mass transfer performance between the air and desiccant solution streams (i.e. equations (3.5) to (3.7)).

3.8 EXPERIMENTAL SETUP

A schematic diagram and a photograph of the experimental setup used to test the 3-fluid LAMEE are shown in Figures 3.9 and 3.10, respectively. The facility is the same as described in detail by Moghaddam et al. (2013e), except a third loop (i.e. refrigerant loop) has been added to the existing air loop and desiccant solution loop. The description of the experimental setup is as follows.

3.8.1 The Air Loop

The air loop is composed of an air compressor, PVC pipe with inner diameter of 25 mm, bubble

humidifier immersed in a hot water bath, electrical heater, electrical cooler, flow controller, two flow meters, hand operated globe valve, two flow mixers, and two flow straighteners (see Figure 3.9). A dry airstream (i.e. 24ºC and 0.7 g_v/kg_{air}) is supplied by the compressor where the flow controller and the flow meter #1 are used to adjust the air flow rate to a desired value. The flow meter #2 is installed at the inlet of the 3-fluid LAMEE prototype to detect air leakages that may occur along the air loop during the experiments. The bubble humidifier, the electrical cooler, and the electrical heater are used to control the temperature and humidity ratio of the supply airflow to the 3-fluid LAMEE.

3.8.2 The Solution Loop

The solution loop includes a peristaltic pump, two electrical heaters to control the temperature of the desiccant solution, and desiccant solution supply and exhaust tanks. The peristaltic pump (OmegaFlex FPU5-MT-110) has a digital control unit which is capable of controlling and measuring the mass flow rate of the desiccant solution. The desiccant solution is pumped through the 3-fluid LAMEE from bottom-to-top.

An ideal liquid desiccant would be characterized by a low surface vapor pressure, a low risk of crystallization, low corrosivity, a low regeneration temperature, a high density (Mohammad et al. (2013)), a low viscosity (Mohammad et al. (2013)), and cost effective. Lithium chloride (LiCl), Lithium bromide (LiBr), Calcium chloride ($CaCl_2$), Magnesium chloride ($MgCl_2$), and Triethylene glycol are the most popular liquid desiccants. Among these desiccants, LiCl is the most stable candidate, has a low surface vapor pressure (Mei and Dai (2008)) and a low risk of crystallization (Afshin (2010)). Therefore, LiCl was chosen as the liquid desiccant in the current research.

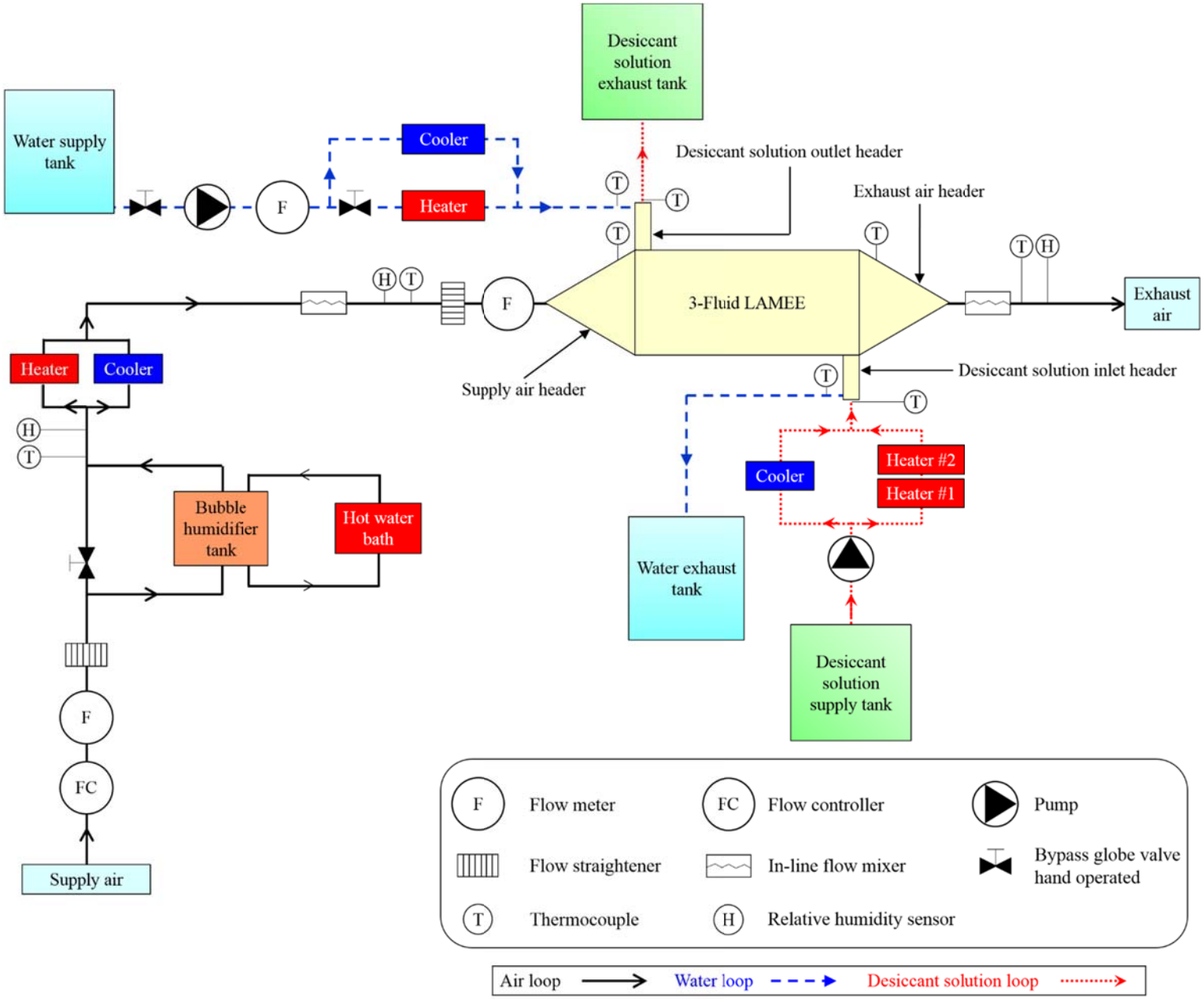

FIGURE 3.9. Schematic diagram of the experimental setup.

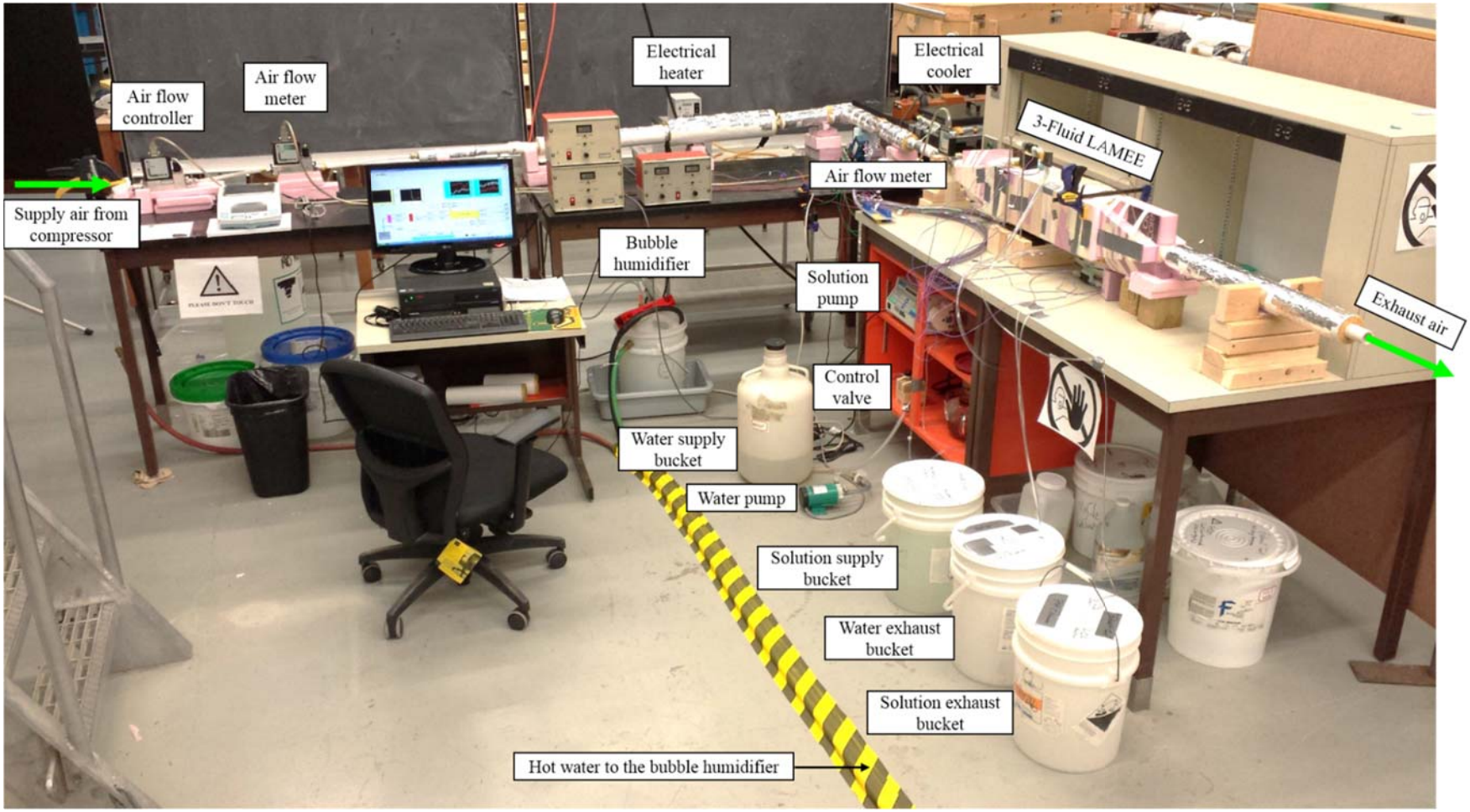

FIGURE 3.10. Photograph of the experimental

3.8.3 The Refrigerant Loop

The refrigerant loop is an open loop and is composed of a centrifugal pump, refrigerated glycol bath cooler, electrical heater, flow meter, two hand operated globe valves, and refrigerant supply and exhaust tanks. The pump has a maximum capacity of 19 L/min and water temperature can be controlled between 2ºC and 70ºC with the cooler and heater.

3.8.4 Instrumentation

Figure 3.9 shows the locations where the temperatures, relative humidities, and mass flow rates of the air, desiccant solution, and water flows are measured, and Table 3.3 provides the overall uncertainty of each instrument which is calculated using equation (3.26) (ASME Performance Test Code 19.1 (1998)). The flow rate of the supply air is controlled by a flow controller (MKS-Type 1559A) has a total uncertainty of 1% of the full-scale, and a flow meter (MKS-Type 0558A) is used to measure the air flow rate. Sixteen T-type thermocouples are used to measure the temperatures of the air, desiccant solution, and water flows at different locations (see Figure 3.9). The relative humidities of the airflow at the inlet and outlet of the 3-fluid LAMEE are measured using five humidity sensors (Honeywell-HIH-4021). Two flow mixers are installed before and after the 3-fluid LAMEE to get an average bulk value for the air temperature and humidity ratio.

$$U_{95\%} = \sqrt{B^2 + (t^* \cdot S)^2} \tag{3.26}$$

where $U_{95\%}$ is the total uncertainty at the 95% confidence level, B is the bias uncertainty, t^* is the student-t distribution constant ($t^* = 2$ for number of readings > 30), and S is the precision uncertainty.

Thermocouples used to measure the air temperature are calibrated using a Hart Scientific Dry-Well Calibrator (Model 9107) has a bias uncertainty of ±0.2ºC, while a circulating water bath (TC-502)

has a bias uncertainty of ±0.5ºC is used to calibrate the thermocouples used to measure the temperatures of the desiccant solution and water flows. A Mini "Two-Pressure" Humidity Generator (Model 1200) with a bias uncertainty of ±0.5% is used to calibrate the humidity sensors in the range of 10-90% at 10, 20, 30, 40 and 49ºC. A density meter device (Anton Paar DMA 4500 M) has a bias uncertainty of ±0.00005 g/cm^3 (Anton Paar (2015)) is used to measure the density of the LiCl solution before and after each experiment. The density of the LiCl solution is used to calculate its concentration based on data reported by Conde (2004). A National Instruments data acquisition system (NI-cDAQ 9174) and a LabVIEW software are used to record temperatures, relative humidities, and mass flow rates of the air, desiccant solution, and water streams.

TABLE 3.3. Specifications of the instruments used to measure temperature, relative humidity, density (concentration), and mass flow rate of fluids.

Parameter	Instrument	Calibration range	Total uncertainty
Air temperature	T-type thermocouples	0-70ºC	±0.15ºC
Solution temperature	T-type thermocouples	2-85ºC	±0.2ºC
Water temperature	T-type thermocouples	2-85ºC	±0.2ºC
Air relative humidity	Honeywell-HIH-4021 sensors	10-90%	±2%
Air flow rate	Flow meter (MKS-Type 0558A)	0-100 L/min	±1%
Solution flow rate	Flow rate sensor	1-2280 mL/min	±3%
Solution density	Density meter device (Anton Paar DMA 4500 M) (Anton Paar (2015))	0-3 g/cm^3	±0.00005 g/cm^3

3.8.5 Energy and Mass Balance

It is necessary to check the energy and mass balance for all experiments to make sure that fluid leakages and heat transfer to the environment are negligible. The energy balance is calculated from equation (3.27) and mass balance is calculated from equation (3.28) (Simonson et al. (1999)).

$$\Delta(\dot{m}H) = \left|\left(\dot{m}_{\text{air,in}} \cdot H_{\text{air,in}} - \dot{m}_{\text{air,out}} \cdot H_{\text{air,out}}\right) + \left(\dot{m}_{\text{sol,in}} \cdot H_{\text{sol,in}} - \dot{m}_{\text{sol,out}} \cdot H_{\text{sol,out}}\right)\right. \quad (3.27)$$
$$\left. + \left(\dot{m}_{\text{w,in}} \cdot H_{\text{w,in}} - \dot{m}_{\text{w,out}} \cdot H_{\text{w,out}}\right)\right| \leq U_{\Delta(\dot{m}H)}$$

$$\Delta(\dot{m}W) = \left|\left(\dot{m}_{\text{air,in}} \cdot W_{\text{air,in}} - \dot{m}_{\text{air,out}} \cdot W_{\text{air,out}}\right) + \left(\dot{m}_{\text{sol,in}} - \dot{m}_{\text{sol,out}}\right)\right| \leq U_{\Delta(\dot{m}W)} \quad (3.28)$$

where $\dot{m}$ is the mass flow rate (kg/hr), H is the enthalpy (W), $U_{\Delta(\dot{m}H)}$ is the uncertainty in the energy balance calculation (W), W is the humidity ratio (kg_v/kg_{air}), $U_{\Delta(\dot{m}W)}$ is the uncertainty in the mass balance calculation (kg/hr), and subscripts *air*, *sol*, *w*, *in*, and *out* refer to air, solution, water, inlet, and outlet, respectively. It is found that the energy and mass balance for all experiments are within the uncertainty limits. Therefore, there are no major fluid (air, desiccant solution or water) leakages, and heat losses to the surrounding environment are small.

3.9 RESULTS AND DISCUSSION

3.9.1 Test Conditions

The objective of the current study is to investigate and compare between the steady-state performances of a 2-fluid flat-plate LAMEE and a 3-fluid LAMEE, when used for air cooling and dehumidifying applications. The 3-fluid LAMEE was operated as a 2-fluid LAMEE by turning off the cooling water loop. All experiments, for both the 2-fluid LAMEE and the 3-fluid LAMEE, were performed under the same test conditions. The outdoor air temperature and humidity ratio were chosen according to AHRI Standard 1060 summer conditions (AHRI Standard 1060 (2005)). Table 3.4 shows the test conditions for the 2-fluid LAMEE and the 3-fluid LAMEE, and Figure 3.11 displays the test conditions on a psychrometric chart. Thermo-physical properties of LiCl solution can be found in Conde (2004).

TABLE 3.4. Test conditions for the 2-fluid LAMEE and the 3-fluid LAMEE.

Parameter	2-Fluid LAMEE		3-Fluid LAMEE	
	Value	Unit	Value	Unit
$T_{air,in}$	35.4	°C	34.9-35.3	°C
$W_{air,in}$	17.9-18	g_v/kg_{air}	17-18.7	g_v/kg_{air}
Re_{air}	730	-	730	-
$T_{sol,in}$	24.3-24.7	°C	24.2-25.3	°C
$W_{sol,in}$	6.5	g/kg	6.5	g/kg
$C_{sol,in}$	32.5	%	32.5	%
Re_{sol}	2	-	2	-
NTU	1.8	-	1.8	-
Cr^*	1.8	-	1.8	-
$T_{w,in}$	-	-	10, 15.1, 20.6, 24.6	°C
Cr	-	-	0.055, 0.11, 0.26, 0.42	-

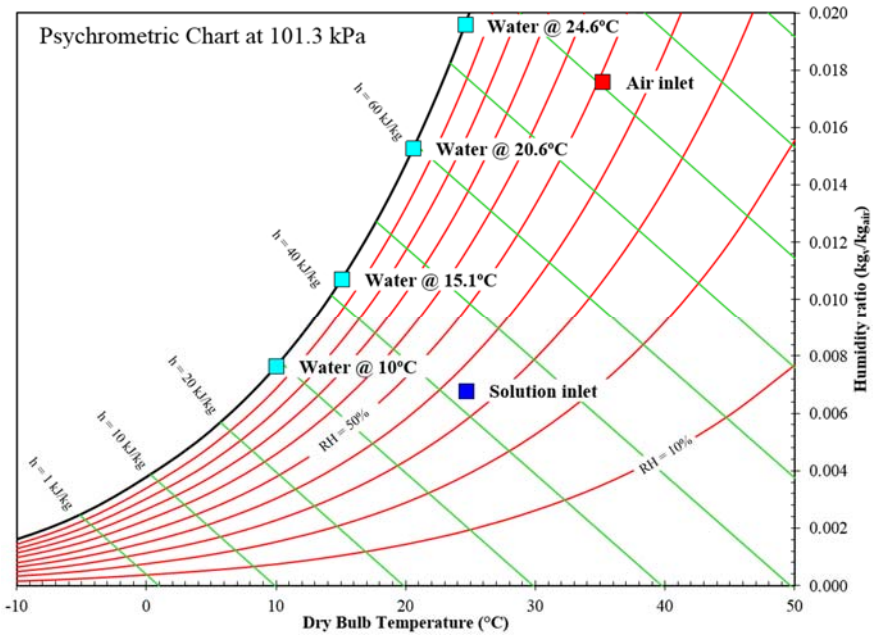

FIGURE 3.11. Inlet conditions of the air, desiccant solution, and water streams on a psychrometric chart.

3.9.2 Effect of Cooling Water Temperature with *Cr* = 0.26

3.9.2.1 Outlet Desiccant Solution Temperature

Figure 3.12 shows the variations of the outlet desiccant solution temperatures and the outlet cooling water temperature of the 2-fluid LAMEE and the 3-fluid LAMEE with the inlet cooling water temperature. It is clear that the temperature of the desiccant solution remains almost constant along the solution channel in the 3-fluid LAMEE at inlet cooling water temperature of 15.1ºC. This implies that the cooling water stream has a temperature of 15.1ºC is able to absorb the heat transferred from the airstream to the desiccant solution and the heat of phase change released to the desiccant solution stream. At inlet cooling water temperature of 10ºC, the outlet desiccant solution temperature is lower than the inlet desiccant solution temperature. It can be concluded that the temperature of the desiccant solution can be maintained constant as it flows along the solution channel of the studied 3-fluid LAMEE at inlet cooling water temperature of 15.1ºC and *Cr* = 0.26.

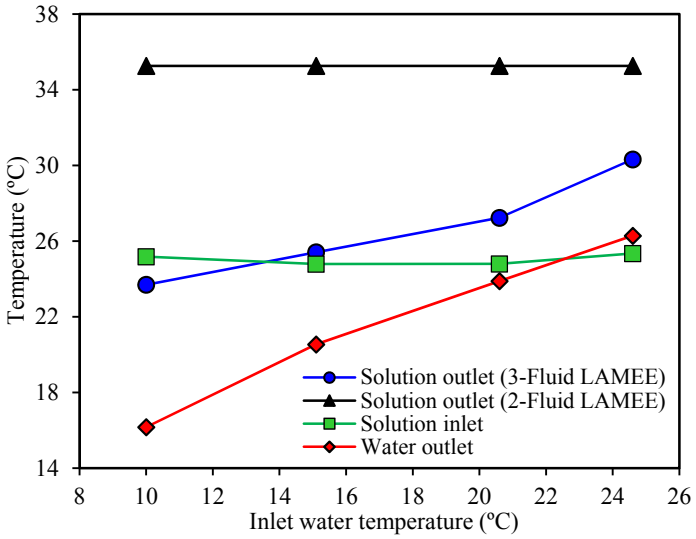

FIGURE 3.12. Variations of outlet desiccant solution temperature and outlet cooling water temperature with the inlet cooling water temperature for the 3-fluid LAMEE. The results for the 2-fluid LAMEE (no cooling water) are presented for comparison (*Cr* = 0.26).

3.9.2.2 Sensible, Latent, and Total Effectivenesses

Figure 3.13 (a) shows a comparison between the sensible effectivenesses of the 2-fluid LAMEE and the 3-fluid LAMEE at several inlet cooling water temperatures. It is clear that the cooling water enhances the sensible effectiveness of the 3-fluid LAMEE compared to the 2-fluid LAMEE, where the enhancement in the sensible effectiveness increases as the inlet cooling water temperature decreases. For instance, compared to the 2-fluid LAMEE, the sensible effectiveness of the 3-fluid LAMEE increases from 44% to 64% and 113% at inlet cooling water temperatures of 24.6ºC and 10ºC, respectively. The enhancement in sensible effectiveness of the 3-fluid LAMEE can be explained as follows. In LAMEEs, the potential for heat transfer is the difference between the temperatures of the air and the desiccant solution streams. In the 2-fluid LAMEE, the heat transferred from the airstream to the desiccant solution and the heat of phase change released to the desiccant solution increase the temperature of the desiccant solution stream as it flows along the exchanger, which reduces the potential for heat transfer between the air and the desiccant solution streams. In the 3-fluid LAMEE, the cooling water continuously cools the desiccant solution as it flows along the exchanger, which keeps a high difference between the temperatures (i.e. high potential for heat transfer) of the air and the desiccant solution streams. It can be concluded from Figures 3.12 and 3.13 (a) that the sensible effectiveness of the studied 2-fluid LAMEE increases from 44% to 94% when the temperature of the desiccant solution is maintained constant along the exchanger and $Cr = 0.26$.

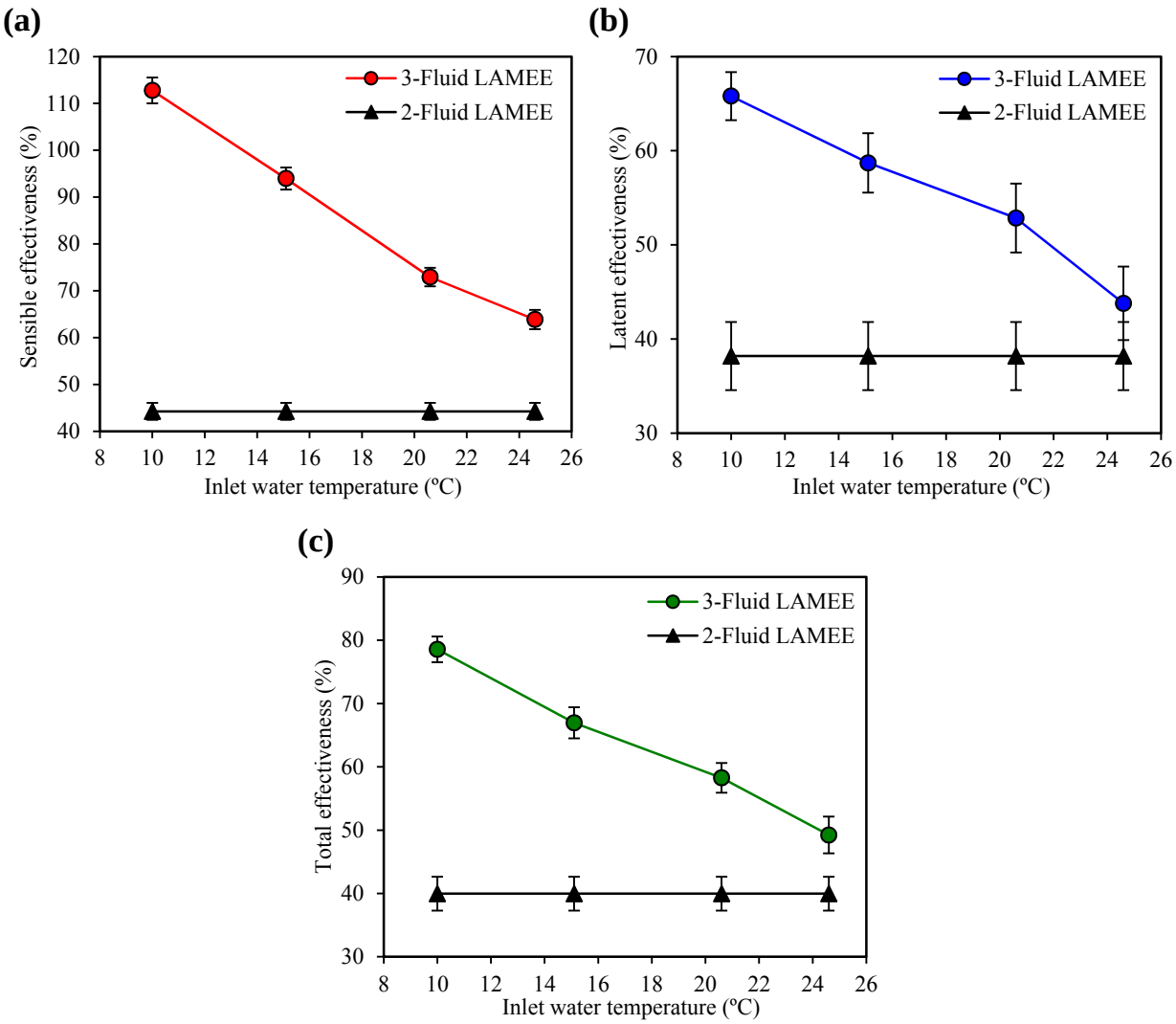

FIGURE 3.13. Variations of (a) sensible effectivenesses (b) latent effectivenesses (c) total effectivenesses of the 2-fluid LAMEE and the 3-fluid LAMEE with the inlet cooling water temperature (Cr = 0.26).

Figure 3.13 (b) displays the latent effectivenesses of the 2-fluid LAMEE and the 3-fluid LAMEE at several inlet cooling water temperatures. It is clear that the latent effectiveness of the 3-fluid LAMEE increases as the inlet cooling water temperature decreases. Compared to the 2-fluid LAMEE, the latent effectiveness of the 3-fluid LAMEE increases from 38% to 44% and 66% at inlet cooling water temperatures of 24.6ºC and 10ºC, respectively. The enhancement in the latent effectiveness as inlet cooling water temperature decreases can be explained as follows. In

LAMEEs, the potential for moisture transfer is the difference between the vapor pressures of the air and desiccant solution streams. The heat transferred from the airstream to the desiccant solution and the heat of phase change released to the desiccant solution increase the temperature of the desiccant solution as it flows along the exchanger. The vapor pressure of the desiccant solution increases with the increase of its temperature, which decreases the potential for moisture transfer in the exchanger. In the 3-fluid LAMEE, the cooling water continuously cools the desiccant solution as it flows along the exchanger, which maintains a high difference between the vapor pressures (i.e. high potential for moisture transfer) of the air and the desiccant solution streams. It can be concluded from Figures 3.12 and 3.13 (b) that the latent effectiveness of the studied 2-fluid LAMEE increases from 38% to 59% when the temperature of the desiccant solution is maintained constant along the exchanger and $Cr = 0.26$.

Figure 3.13 (c) shows the total effectivenesses of the 2-fluid LAMEE and the 3-fluid LAMEE at several inlet cooling water temperatures. The total effectiveness of the 3-fluid LAMEE increases as the inlet cooling water temperature decreases. Compared to the total effectiveness of the 2-fluid LAMEE, the total effectiveness of the 3-fluid LAMEE increases from 40% to 49% and 79% at inlet cooling water temperatures of 24.6ºC and 10ºC, respectively. It is clear from equation (3.7) that the total effectiveness of LAMEEs depends on their sensible and latent effectivenesses, therefore the enhancements in the sensible and latent effectivenesses with the decrease of the inlet cooling water temperature improve the total effectiveness. It can be concluded from Figures 3.12 and 3.13 (c) that the total effectiveness of the studied 2-fluid LAMEE increases from 40% to 67% when the desiccant solution temperature is maintained constant along the exchanger and $Cr = 0.26$.

3.9.2.3 Moisture Removal Rate

A comparison between the moisture removal rates of the 2-fluid LAMEE and the 3-fluid LAMEE

at several inlet cooling water temperatures is illustrated in Figure 3.14. It is clear that the moisture removal rate of the 3-fluid LAMEE is higher than the 2-fluid LAMEE over the entire range of inlet cooling water temperature studied. The moisture removal rate of the 3-fluid LAMEE increases inversely with the inlet cooling water temperature, where the improvement in the moisture removal rate decreases as the inlet cooling water temperature decreases. For example, the moisture removal rate increases by 23%, 14%, and 5% as the inlet cooling water temperature decreases from 24.6ºC, 20.6ºC, and 15.1ºC to 20.6ºC, 15.1ºC, and 10ºC, respectively. Moreover, at inlet cooling water temperature of 24.6ºC, the improvement in the moisture removal rate of the 3-fluid LAMEE compared to 2-fluid LAMEE is only 6%. This can be explained as follows. The difference between the inlet cooling water temperature and the inlet desiccant solution temperature is very small (i.e. ~ 0.2ºC), and thus the potential for heat transfer between the water and desiccant solution streams is very low. As well, it is clear from Figure 3.12 that at inlet cooling water temperature of 24.6ºC, the outlet cooling water temperature is higher than the inlet desiccant solution temperature, thus the water heats the desiccant solution stream at some part near the exchanger outlet.

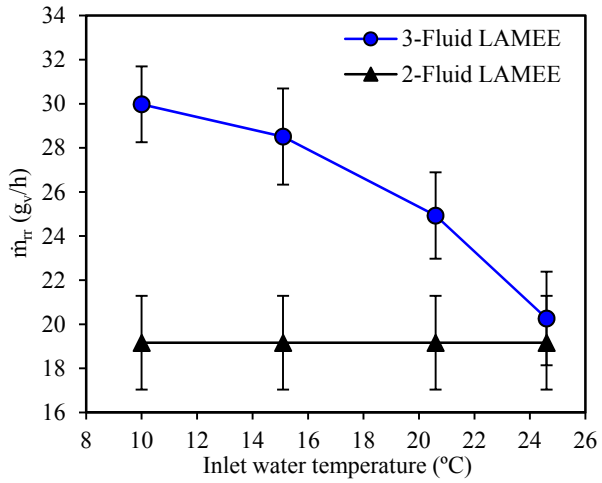

FIGURE 3.14. Comparison between moisture removal rates of the 2-fluid LAMEE and the 3-fluid LAMEE at several inlet cooling water temperatures (Cr = 0.26).

3.9.2.4 Influences of Temperature Ratio (T^*) on the Performance of the 3-Fluid LAMEE

The dimensionless temperature ratio describes the ratio between the difference in the inlet temperatures of the air and cooling water streams and the difference in the inlet temperatures of the air and desiccant solution streams. Figure 3.15 (a) displays the variations of the sensible, latent, and total effectivenesses of the 3-fluid LAMEE with T^*, and Figure 3.15 (b) displays the variations of the moisture removal rate and the sensible cooling capacity of the 3-fluid LAMEE with T^*. It is clear that the sensible, latent, and total effectivenesses, moisture removal rate, and sensible cooling capacity of the 3-fluid LAMEE increase as T^* increases. This is because higher T^* values implies lower inlet cooling water temperatures. $T^* = 2$ implies that the difference between the inlet temperatures of the air and cooling water streams is double the difference between the inlet temperatures of the air and desiccant solution streams. At $T^* = 2$, the sensible effectiveness increases to around 100%. As well, increasing T^* has a greater influence on the sensible effectiveness than the latent effectiveness. It can be concluded that the performance of the 3-fluid LAMEE improves as T^* increases.

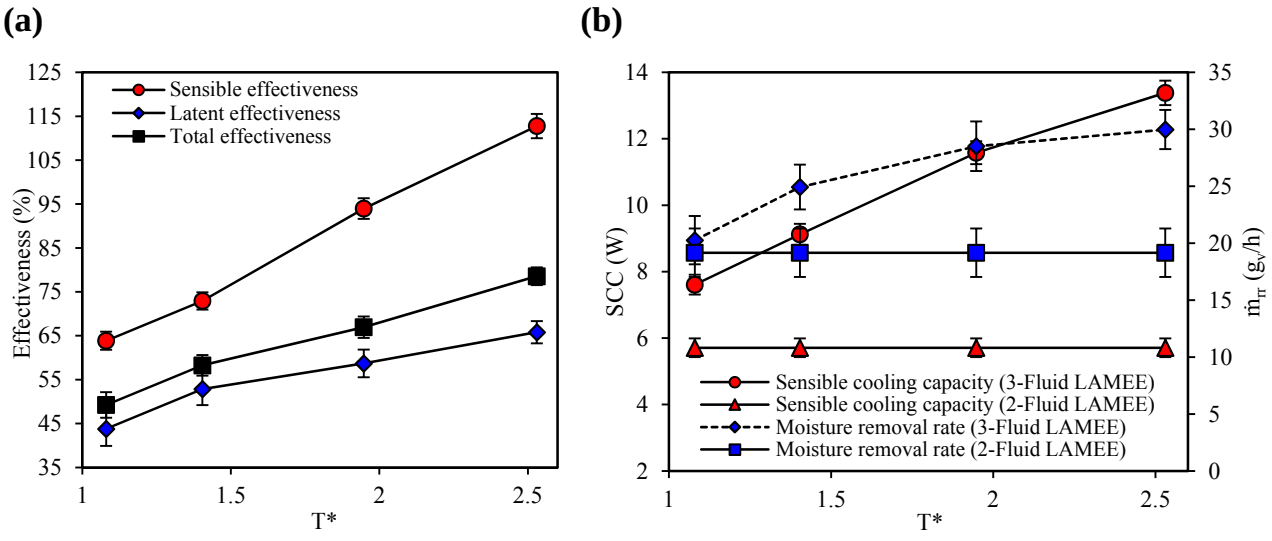

FIGURE 3.15. Variations of (a) sensible, latent, and total effectivenesses (b) moisture removal rate and sensible cooling capacity of the 3-fluid LAMEE with T^* ($Cr = 0.26$).

3.9.3 Effect of Cooling Water Flow Rate

In this section, the performance of the 3-fluid LAMEE is tested at several cooling water flow rates (i.e. Cr = 0.055, 0.11, 0.26 and 0.42) and a constant inlet cooling water temperature (i.e. $T_{w,in}$ = 20.6ºC).

3.9.3.1 Outlet Desiccant Solution Temperature

Figure 3.16 displays the outlet desiccant solution temperatures and the outlet cooling water temperatures for the 2-fluid LAMEE and the 3-fluid LAMEE at several Cr values. The outlet desiccant solution temperature of the 3-fluid LAMEE is less than the 2-fluid LAMEE over the entire range of Cr studied. At Cr = 0.11, the temperature of the desiccant solution remains constant as it flows along the 3-fluid LAMEE, which implies that the cooling water stream is able to remove the heat transferred from the airstream to the desiccant solution and the heat of phase change released to the desiccant solution.

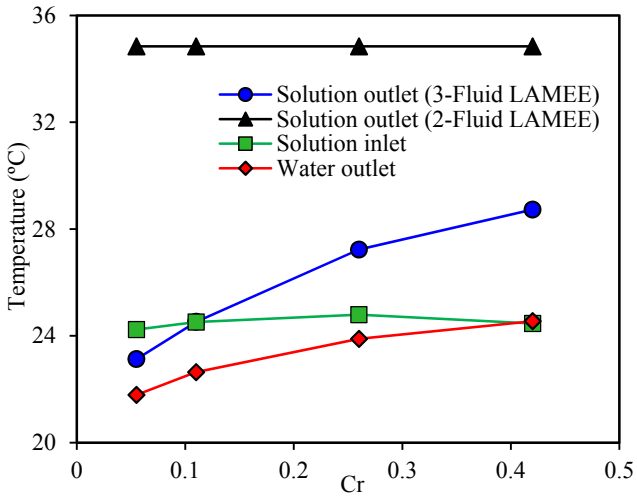

FIGURE 3.16. Variations of the outlet desiccant solution temperatures and outlet cooling water temperature for the 2-fluid LAMEE and the 3-fluid LAMEE with Cr.

3.9.3.2 Sensible, Latent, and Total Effectivenesses

Figure 3.17 (a) shows a comparison between the sensible effectivenesses of the 2-fluid LAMEE

and the 3-fluid LAMEE at several *Cr* values. It is clear that the sensible effectiveness of the 3-fluid LAMEE is higher than the sensible effectiveness of the 2-fluid LAMEE over the entire range of *Cr* studied. The sensible effectiveness of the 3-fluid LAMEE increases as the cooling water flow rate increases (i.e. *Cr* decreases). For example, compared to the 2-fluid LAMEE, the sensible effectiveness of the 3-fluid LAMEE increases from 44% to 63% and 88% at *Cr* = 0.42 and 0.055, respectively.

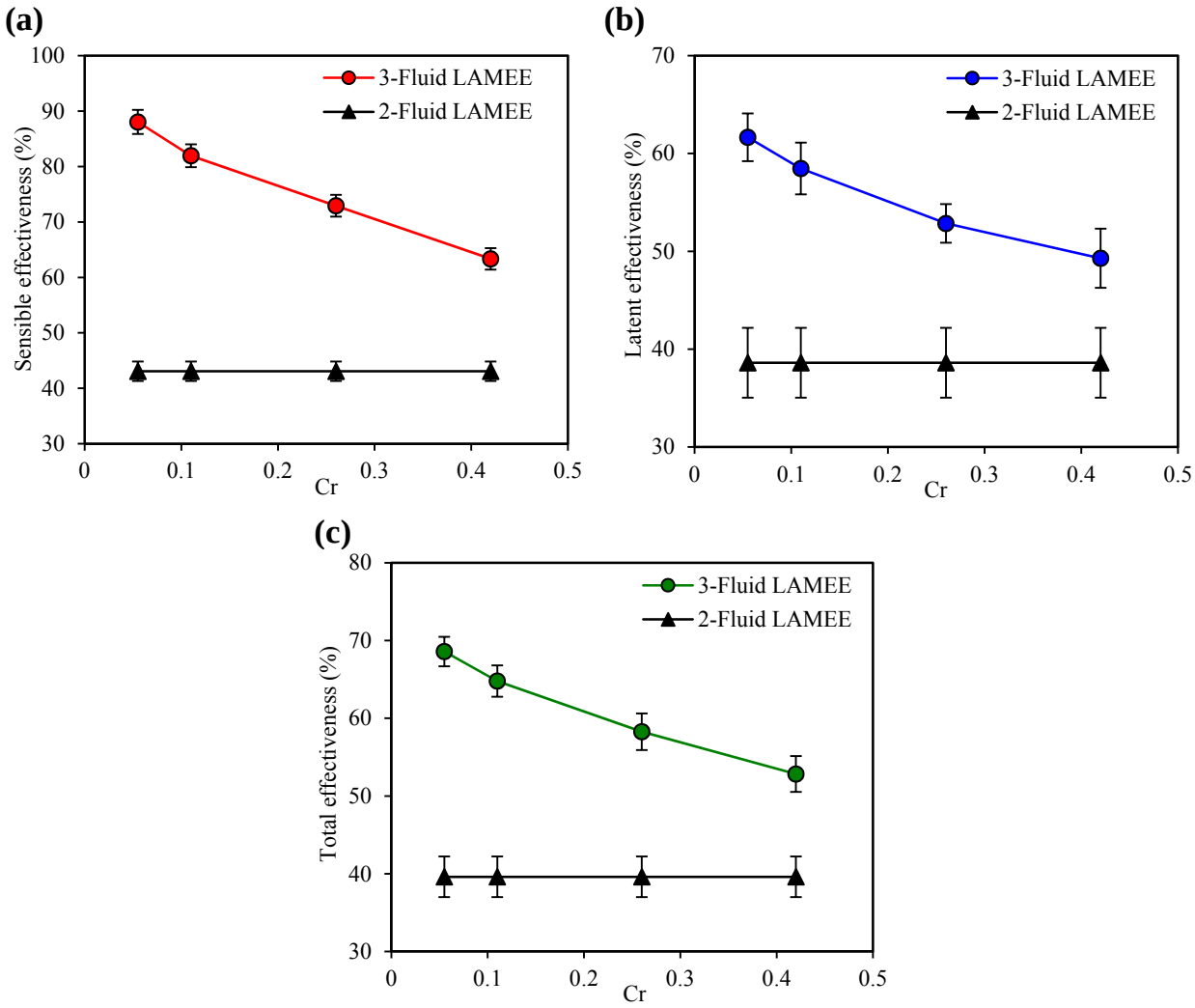

FIGURE 3.17. Variations of (a) sensible effectivenesses (b) latent effectivenesses (c) total effectivenesses of the 2-fluid LAMEE and the 3-fluid LAMEE with *Cr*.

Figure 3.17 (b) displays the variations of the latent effectivenesses of the 2-fluid LAMEE and the 3-fluid LAMEE with the cooling water flow rate (*Cr*). The latent effectiveness of the 3-fluid LAMEE is higher than the latent effectiveness of the 2-fluid LAMEE over the entire range of *Cr* studied. Compared to the latent effectiveness of the 2-fluid LAMEE, the latent effectiveness of the 3-fluid LAMEE improves by up to 28% at $Cr = 0.055$. As well, the latent effectiveness of the 3-fluid LAMEE increases as the mass flow rate of the cooling water increases (i.e. *Cr* decreases). It can be concluded that the mass flow rate of the cooling water has a more significant effect on the enhancement of the sensible effectiveness than the enhancement of the latent effectiveness.

Figure 3.17 (c) displays the total effectivenesses of the 2-fluid LAMEE and the 3-fluid LAMEE at several *Cr* values. It is clear that the total effectiveness of the 3-fluid LAMEE is higher than the total effectiveness of the 2-fluid LAMEE over the entire range of *Cr* studied. Compared to the total effectiveness of the 2-fluid LAMEE, the total effectiveness of the 3-fluid LAMEE improves by up to 29% at $Cr = 0.055$. As well, the total effectiveness of the 3-fluid LAMEE increases as the cooling water flow rate increases (i.e. *Cr* decreases).

3.9.3.3 Moisture Removal Rate

Figure 3.18 shows a comparison between the moisture removal rates of the 2-fluid LAMEE and the 3-fluid LAMEE at several *Cr* values. The moisture removal rate of the 3-fluid LAMEE is higher than the moisture removal rate of the 2-fluid LAMEE over the entire range of *Cr* studied. Compared to the 2-fluid LAMEE, the moisture removal rate of the 3-fluid LAMEE increases by up to 52% at $Cr = 0.055$. As well, the moisture removal rate of the 3-fluid LAMEE increases inversely with *Cr*.

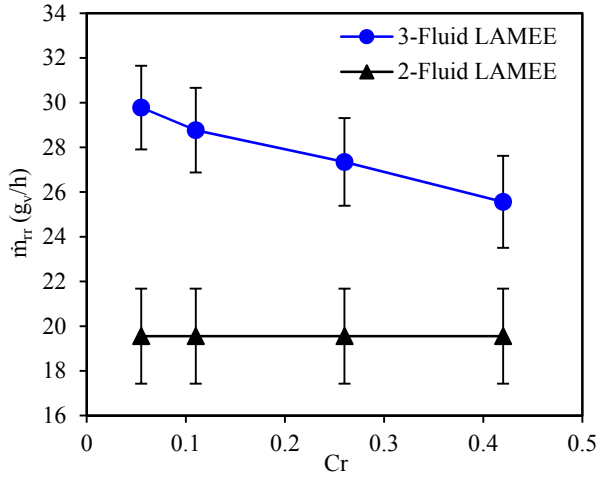

FIGURE 3.18. Comparison between moisture removal rates of the 2-fluid LAMEE and the 3-fluid LAMEE at several *Cr* values.

3.10 SUMMARY OF INFLUENCES OF INLET TEMPERATURE AND FLOW RATE OF COOLING WATER ON THE PERFORMANCE OF THE 3-FLUID LAMEE

It has been noticed that under the same operating conditions, the desiccant solution temperature is maintained almost constant along the 3-fluid LAMEE either at low inlet cooling water temperature test conditions (i.e. $T_{w,in}$ = 15ºC and Cr = 0.26) or high cooling water flow rate test conditions (i.e. $T_{w,in}$ = 20.6ºC and Cr = 0.11) (see Figures 3.12 and 3.16). Although the temperature of the desiccant solution is maintained constant in both test conditions, the sensible effectiveness of the 3-fluid LAMEE at low inlet cooling water temperature test conditions is higher (i.e. 94%) than at high cooling water flow rate (i.e. 82%) test conditions. This is because the refrigeration tubes are in direct contact with the membrane. Therefore, at low inlet cooling water temperature test conditions, the cooling water flowing inside the refrigeration tubes cools the membrane which cools the airstream (see Figures 3.12, 3.13 (a), 3.16, and 3.17 (a)).

Figure 3.19 (a) displays the outlet air conditions on a psychrometric chart for the 2-fluid and 3-fluid LAMEEs at several inlet cooling water temperatures. It is clear that the inlet cooling water

temperature has significant influences on the outlet air temperature and humidity ratio, where the outlet air temperature and humidity ratio decrease as the inlet cooling water decreases. At cooling water temperature of 10ºC, the 3-fluid LAMEE is able to cool and dehumidify the supply hot-humid air to 23.9ºC and 53.8% RH.

Figure 3.19 (b) shows the outlet air conditions on a psychrometric chart for the 2-fluid and 3-fluid LAMEEs at several *Cr* values. It is clear that the outlet air temperature and humidity ratio decrease as the mass flow rate of the cooling water increases (i.e. *Cr* decreases). At $Cr = 0.055$ (i.e. high cooling water flow rates), the 3-fluid LAMEE is able to cool and dehumidify the supply hot-humid air to 25.5ºC and 55% RH.

In conclusion, the mass flow rate and the inlet temperature of the cooling water have significant influences on the steady-state performance of the 3-fluid LAMEE, where the performance of the 3-fluid LAMEE improves as the inlet cooling water temperature decreases or the cooling water flow rate increases. However, increasing the cooling water mass flow rate is economically more feasible than decreasing the inlet cooling water temperature.

(a)

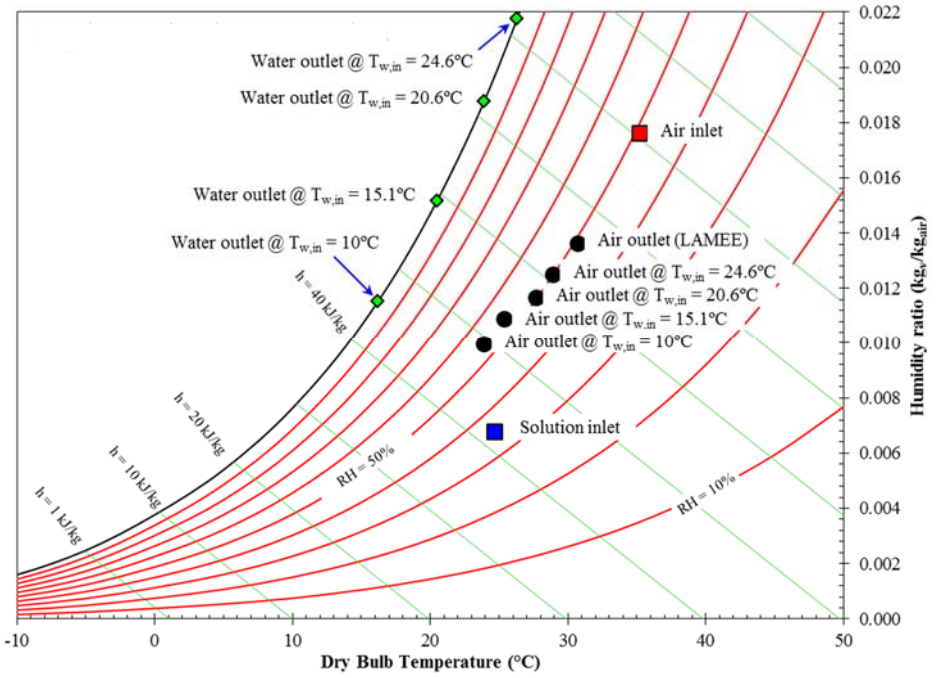

(b)

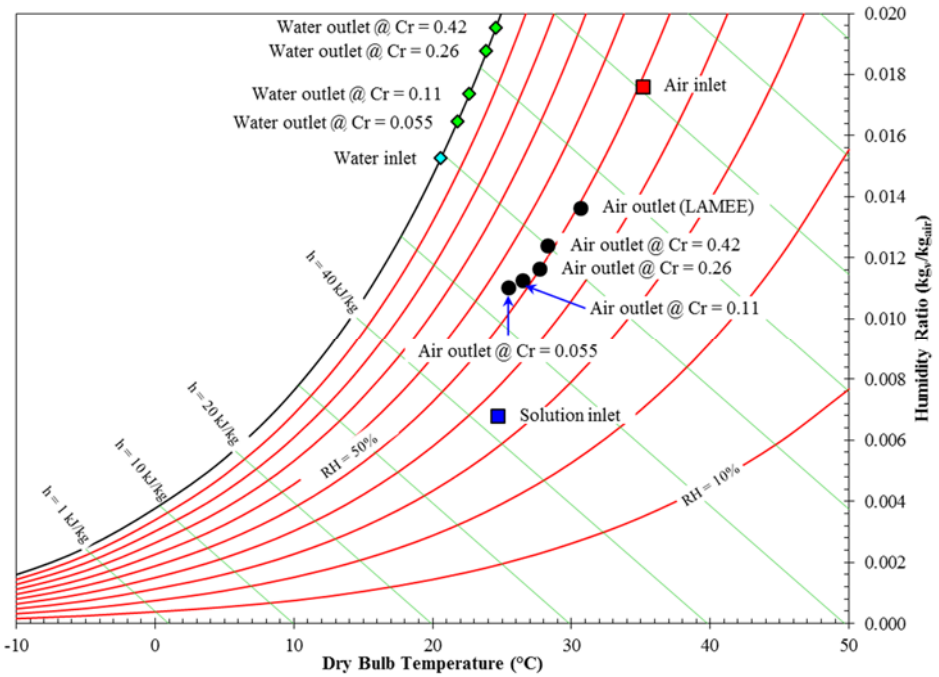

FIGURE 3.19. Inlet air, inlet desiccant solution, outlet air, outlet cooling water conditions on a psychrometric chart for the 2-fluid LAMEE and the 3-fluid LAMEE at (a) several inlet cooling water temperatures and Cr = 0.26 (b) several Cr values and $T_{w,in}$ = 20.6ºC.

3.11 CONCLUSIONS

The main contribution of this chapter is that it presents experimental data for a new 3-fluid LAMEE which uses cooling water to cool the desiccant solution. The data presented in this chapter show that the performance of the 3-fluid LAMEE is better than the performance of a 2-fluid LAMEE with the same design and operating parameters, which proves that the main hypothesis of this thesis (i.e. adding a third fluid to control the desiccant solution temperature inside the 3-fluid LAMEE may improve the rates of heat and moisture transfer between the air and desiccant solution compared to 2-fluid LAMEEs) is true under air cooling and dehumidifying conditions. The sensible effectiveness, latent effectiveness, total effectiveness, moisture removal rate, and sensible cooling capacity of the 2-fluid LAMEE increase by 39% (43%-82%), 20% (39%-59%), 25% (40%-65%), 53% (19-29 g_v/h), and 84% (6W-11W), respectively when the temperature of desiccant solution stream is maintained constant along the exchanger by the cooling water. The steady-state performance (i.e. sensible effectiveness, latent effectiveness, total effectiveness, moisture removal rate, and sensible cooling capacity) of the 3-fluid LAMEE increases as the inlet cooling water temperature decreases and/or the cooling water flow rate increases.

CHAPTER 4

PERFORMANCE TESTING OF 2-FLUID AND 3-FLUID LAMEES DURING AIR COOLING AND DEHUMIDIFICATION

4.1 OVERVIEW OF CHAPTER 4

The results presented in the previous chapter proved that the hypothesis of this thesis (i.e. adding a third fluid to control the desiccant solution temperature inside the 3-fluid LAMEE may improve the rates of heat and moisture transfer between the air and desiccant solution compared to 2-fluid LAMEEs) is true under air cooling and dehumidifying conditions. In this chapter, the effect of the phase change energy on the temperature of the desiccant solution and air during air cooling and dehumidifying will be quantified, and the effects of key operating parameters on the performance of the 3-fluid LAMEE will be tested under air cooling and dehumidifying conditions. Results presented in this chapter fulfill part of the second objective of this thesis (i.e. to design and test a 3-fluid LAMEE and compare with a 2-fluid LAMEE).

The purpose of the refrigerant is to minimize the variations of the desiccant solution temperature inside LAMEEs. There are two sources for variations of the desiccant solution temperature inside LAMEEs; the sensible heat transferred between the air and desiccant solution, and the phase change energy associated with the moisture transfer process. To the best of my knowledge, no other work in the literature has quantified the impact of phase change energy on the temperature of the desiccant solution and air in LAMEEs. In this chapter, the effects of phase change energy on the solution and air temperatures inside the 3-fluid and 2-fluid LAMEEs are tested and compared under air cooling and dehumidifying conditions.

In the previous chapter, the performances of the 3-fluid and 2-fluid LAMEEs were tested and

compared at several inlet refrigerant temperatures and mass flow rates under air cooling and dehumidifying conditions. However, the effect of other key operating parameters on the performance of the 3-fluid LAMEE should be determined to develop a full performance map of the 3-fluid LAMEE. In this chapter, the performances of the 3-fluid and 2-fluid LAMEEs are tested and compared at several inlet air humidity ratios and desiccant solution mass flow rates under air cooling and dehumidifying conditions.

The work presented in this chapter was presented at the 2016 ASHRAE Winter Conference in Orlando, Florida, USA. The manuscript presented in this chapter is published in *ASHRAE Transactions*. The manuscript presented in this chapter is different from the published paper in the following sections: the description of the test facility, the schematics of the 2-fluid and 3-fluid LAMEEs, and the equations used to evaluate the LAMEE performance presented in the published paper are removed since they were presented in Chapters 2 and 3.

Dr. Gaoming Ge and my Ph.D. supervisors (Professors Besant and Simonson) are co-authors of the manuscript presented in this chapter. Dr. Ge is a Postdoctoral fellow in the Department of Mechanical Engineering at the University of Saskatchewan. Dr. Ge contributed to this manuscript by critically reviewing the manuscript and giving comments and advice which enhanced the quality of the manuscript. My contributions to this manuscript are: (a) testing the 3-fluid and 2-fluid LAMEEs, (b) analyzing the experimental data, (c) writing the paper, and (d) responding to the reviewer comments.

Experimental Study of Effects of Phase-Change Energy and Operating Parameters on Performances of Two-Fluid and Three-Fluid Liquid-To-Air Membrane Energy Exchangers

(ASHRAE Transactions, 2016, Volume 122, Part 1)

Mohamed R. H. Abdel-Salam, Gaoming Ge, Robert W. Besant, Carey J. Simonson

4.2 ABSTRACT

Liquid-to-air membrane energy exchangers (LAMEEs) are used to transfer heat and moisture between air and desiccant solution streams. LAMEEs use semi-permeable membranes to prevent the penetration of desiccant droplets to the airstream. When a LAMEE is used for air cooling and dehumidifying, the energy of phase change is released as the desiccant solution absorbs moisture from the humid airstream. Consequently, the temperature of the desiccant solution increases as it flows along the exchanger which decreases the LAMEE's performance. A 3-fluid LAMEE is a novel type of LAMEE which includes a refrigerant circuit to cool/heat the desiccant solution along the exchanger. The main contribution of this chapter is that it shows for the first time the effects of the energy of phase change released in liquid desiccant energy exchangers on the temperatures of the air and desiccant solution streams under air cooling and dehumidifying operating conditions. The effects of phase change energy on the performances of a 2-fluid LAMEE and a 3-fluid LAMEE are experimentally investigated and compared under air cooling and dehumidifying operating conditions. Also tested are the effects of inlet air humidity ratio and desiccant solution flow rate on the performances of the 2-fluid LAMEE and 3-fluid LAMEE.

4.3 INTRODUCTION

Over the past few decades, research has shown that liquid desiccant air-conditioning systems can achieve significant energy savings compared to conventional vapor compression air-conditioning systems (Abdel-Salam et al. (2014c)). There are two types of liquid desiccant energy exchangers; direct-contact energy exchangers (i.e. packed beds or towers) and membrane energy exchangers. In direct-contact energy exchangers, supply air directly contacts desiccant solution where heat and moisture are transferred between the two streams. These exchangers suffer from the carryover of liquid desiccant droplets into the airstream, which reduces the indoor air quality and causes corrosion problems along the duct system. In liquid-to-air membrane energy exchangers (LAMEEs) (Abdel-Salam et al. (2014b)), the heat and moisture are transferred between air and desiccant solution streams through micro-porous semi-permeable membranes, which prevent the carryover problem. Figure 1.1 shows a schematic of a 2-fluid flat-plate LAMEE. A 2-fluid flat-plate LAMEE is composed of several parallel air and desiccant solution channels, where each adjacent air and solution channels are seperated by a semi-permeable membrane.

When a LAMEE is used for air cooling and dehumidifying, heat and moisture are transferred from a hot-humid airstream to a cool concentrated desiccant solution stream. The process of moisture transfer is accompanied with the release of phase change energy to the desiccant solution stream. The sensible heat transferred from the hot-humid airstream and the energy of phase change increase the temperature of the desiccant solution as it flows along the exchanger, which decreases the driving forces for heat and moisture transfer between the air and desiccant solution streams along the exchanger. The amount of phase change energy released to the desiccant solution stream depends on the operating parameters of both the air and desiccant solution streams, such as temperature and humidity ratio of the airstream, temperature and concentration of the desiccant

stream, and the type of desiccant (see Figure 4.1) (Koronaki et al. (2013)).

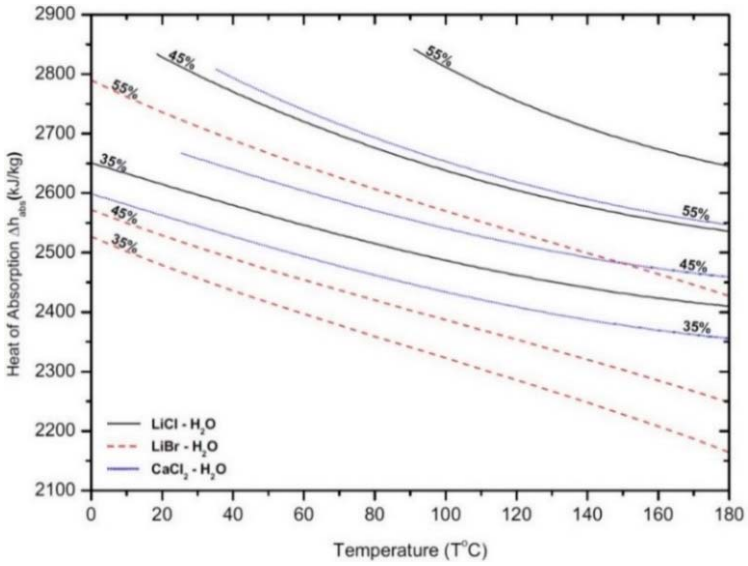

FIGURE 4.1. Variation of heat of phase change with the type, temperature, and concentration of the desiccant solution (Koronaki et al. (2013)).

In direct-contact liquid desiccant systems, internally cooled dehumidifiers have been proposed and studied by several researchers (Bansal et al. (2011); Gao et al. (2013); Ren et al. (2007); Yin et al. (2008)). Bansal et al. (2011) who found that, at the same design parameters and operating conditions, the effectiveness of an internally cooled direct-contact dehumidifier is enhanced compared to an adiabatic dehumidifier. Gao et al. (2013) reported that the effectiveness and moisture removal rate of internally cooled dehumidifiers increase as the cooling water temperature decreases.

In the proposed 3-fluid LAMEE, a third fluid (water or refrigerant) is added to keep the temperature of the desiccant solution nearly constant along the exchanger. Figure 3.2 shows a schematic of the 3-fluid LAMEE prototype, and its specifications are given in Table 3.2. The nominal design widths of the air and desiccant solution channels were selected according to design guidelines given in Chapter 2 (Abdel-Salam et al. (2015)). The desiccant solution and air channels

are seperated by semi-permeable membranes. Refrigeration tubes are placed inside the desiccant solution channels to control the temperature of the desiccant solution along the exchanger. Figure 4.2 (a) shows a photograph of the desiccant solution channel and the refrigeration tubes. The air and desiccant solution streams have a counter-cross flow configuration, while the desiccant solution and water streams have a counter-flow configuration. Figure 4.2 (b) shows a photograph of an insert installed in the air channels to support the membrane against the pressure from the solution side and to increase the rate of heat transfer between the air and desiccant solution streams.

(a)

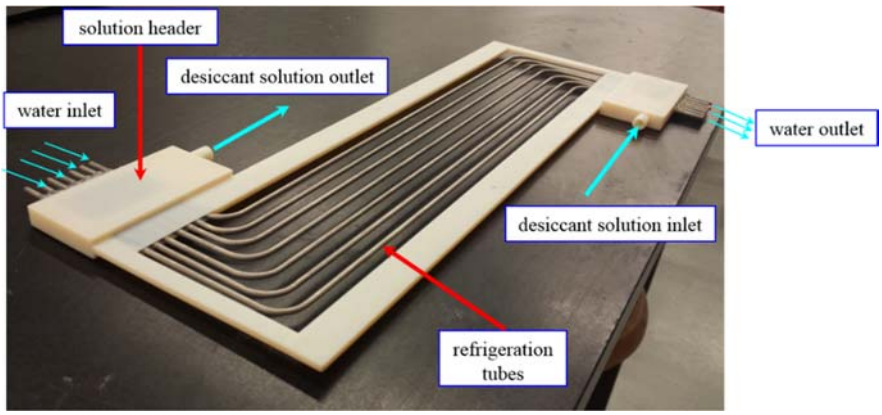

(b)

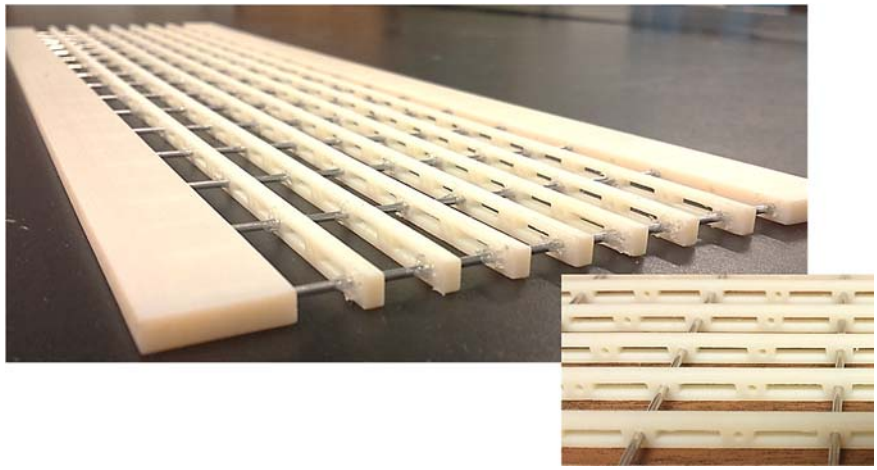

FIGURE 4.2. (a) Photograph of the desiccant solution channel with the refrigeration tubes before attaching the membrane (b) Photograph of the insert used to enhance the heat transfer between the air and desiccant solution streams inside the 3-fluid LAMEE prototype.

The performance of the 3-fluid LAMEE was tested in Chapter 3 (Abdel-Salam et al. (2016a)), where some minor desiccant solution leakages were observed. Consequently, a 3M Scotch ATG969 double layer adhesive tape was used to attach the membrane on the frame of the desiccant solution channel and no desiccant solution leakage was observed.

In Chapter 3 (Abdel-Salam et al. (2016a)) the performance of a 3-fluid LAMEE was tested and compared with the performance of a 2-fluid LAMEE at several inlet cooling water temperatures and flow rates under air cooling and dehumidifying operating conditions. Results showed that rates of heat and moisture transfer between the air and desiccant solution streams in the 3-fluid LAMEE were higher than the 2-fluid LAMEE under the entire range of inlet cooling water temperatures and flow rates studied. The objectives of the current chapter are: (1) to determine the effect of phase change energy released to the desiccant solution stream on the temperatures of the air and desiccant solution streams, (2) to investigate the effects of inlet air humidity ratio on rates of heat and moisture transfer between the air and desiccant solution inside the 2-fluid and 3-fluid LAMEEs, and (3) investigate the effects of the desiccant solution flow rate on rates of heat and moisture transfer between the air and desiccant solution inside the 2-fluid and 3-fluid LAMEEs.

4.4 RESULTS AND DISCUSSION

In this section, results of testing the 2-fluid LAMEE and the 3-fluid LAMEE are presented and discussed. The 3-fluid LAMEE was used to test the performance of the 2-fluid LAMEE by turning off the cooling water circuit. Therefore, the 2-fluid and 3-fluid LAMEEs have the same design parameters. The effectivenesses of heat and moisture transfer between the air and desiccant solution streams inside the 2-fluid LAMEE and the 3-fluid LAMEE are calculated using equations (3.5) to (3.7).

4.4.1 Effect of Inlet Air Humidity Ratio on LAMEE's Performance

When a LAMEE is used for air cooling and dehumidifying, the temperature of the desiccant solution increases as it flows along the exchanger due to the phase change energy released into the desiccant solution, and the heat transfer from the hot-humid airstream. In this section, the effects of phase change energy on the temperatures of the desiccant solution and air streams are investigated at several inlet air humidity ratios. As well, the effects of the inlet air humidity ratio on the amount of phase change energy released, latent effectiveness, and moisture removal rate are investigated.

The design (NTU = 2) and operating (Cr^* and inlet conditions) parameters are the same for both the 2-fluid and 3-fluid LAMEEs (Table 4.1). The inlet air and inlet desiccant solution temperatures are kept equal which means that there would be no heat transfer between the air and desiccant solution streams if there was no phase change energy released due to moisture transfer. The inlet air humidity ratio is varied between 9 and 15.2 g_v/kg_{air}. Thermo-physical properties of LiCl solution are given in Conde (2004).

4.4.1.1 Outlet Desiccant Solution and Air Temperatures

Figure 4.3 (a) displays the difference between the inlet and outlet desiccant solution temperatures at several inlet air humidity ratios for the 2-fluid and 3-fluid LAMEEs. It is clear that the outlet desiccant solution temperatures of the 2-fluid and 3-fluid LAMEEs increase as the inlet air humidity ratio increases under the entire range of inlet air humidity ratio studied. This implies that the amount of phase change energy released to the desiccant solution stream increases as the inlet air humidity ratio increases. It is worth mentioning that the increase in the desiccant solution temperature is attributed to the released phase change energy because the inlet air and inlet desiccant solution temperatures are equal. The heat generated due to phase change energy

increases the temperature of the desiccant solution across the 2-fluid LAMEE by up to 3ºC, which is much higher than the 3-fluid LAMEE.

TABLE 4.1. Test conditions for the 2-fluid and 3-fluid LAMEEs at several inlet air humidity ratios.

Parameter	2-Fluid LAMEE		3-Fluid LAMEE	
	Value	Unit	Value	Unit
$T_{air,in}$	23-23.4	°C	23-23.4	°C
$W_{air,in}$	9, 11.8, 15.2	g_v/kg_{air}	9, 11.8, 15.2	g_v/kg_{air}
$T_{sol,in}$	23-23.4	°C	23-23.4	°C
$W_{sol,in}$	5.7	g/kg	5.7	g/kg
$C_{sol,in}$	30.8	%	30.8	%
NTU	2	-	2	-
*Cr**	2.5	-	2.5	-
$T_{w,in}$	-	-	22.6	°C
*T**	-	-	1	-
Cr	-	-	0.1	-

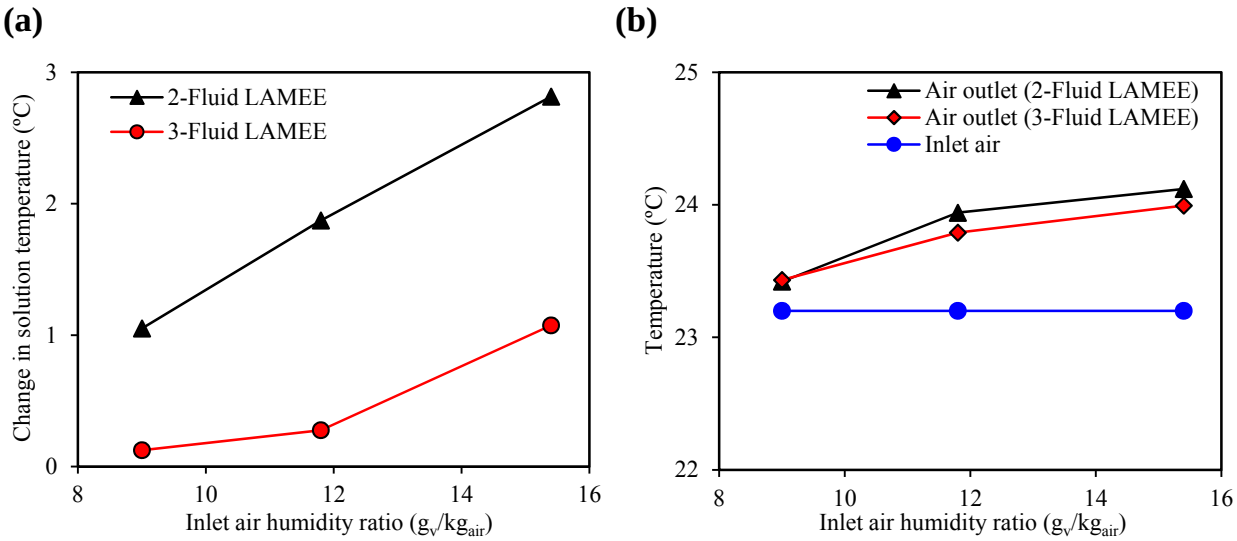

FIGURE 4.3. Variations of (a) difference between inlet and outlet desiccant solution temperatures (b) outlet air temperature with inlet air humidity ratio for the 2-fluid LAMEE and the 3-fluid LAMEE.

Figure 4.3 (b) shows that part of the heat accompanied with the phase change energy is transferred to the airstream across the membrane which increases the temperature of the airstream. However, the effect of phase change energy on the desiccant solution temperature is stronger than its effect on the airstream temperature. It can be concluded that under air cooling and dehumidifying operating conditions, the phase change energy has a considerable contribution in raising the temperatures of the desiccant solution and air streams along liquid desiccant energy exchangers, and the amount of phase change energy released increases as the inlet air humidity ratio increases.

4.4.1.2 Latent Effectiveness

Figure 4.4 displays the variations of the latent effectivenesses of the 2-fluid and 3-fluid LAMEEs with inlet air humidity ratio. It is clear that the latent effectivenesses of the 2-fluid and 3-fluid LAMEEs increase as the inlet air humidity ratio increases. This can be explained as follows. The actual rate of moisture transfer in LAMEEs increases as the inlet air humidity ratio increases. As well, the maximum potential of moisture transfer in LAMEEs increases as the difference between the humidity ratios of the inlet air and inlet desiccant solution increases. However, the enhancement in the actual moisture transfer rate is higher than the enhancement in the maximum potential of moisture transfer. Figure 4.4 shows that the latent effectiveness of the 3-fluid LAMEE is higher than the latent effectiveness of the 2-fluid LAMEE under the entire range of inlet air humidity ratio studied. However, the improvement in the latent effectiveness of the 3-fluid LAMEE compared with the 2-fluid LAMEE decreases as the inlet air humidity ratio increases.

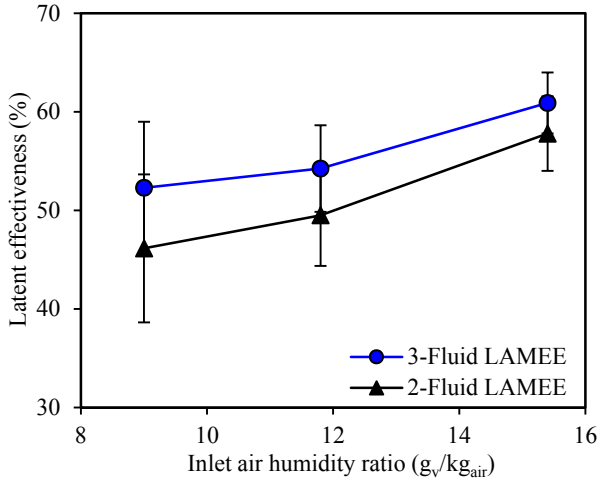

FIGURE 4.4. Variations of latent effectivenesses of the 2-fluid LAMEE and the 3-fluid LAMEE with inlet air humidity ratio.

4.4.1.3 Moisture Removal Rate

Figure 4.5 illustrates the variations of the moisture removal rates of the 2-fluid and 3-fluid LAMEEs with the inlet air humidity ratio. It is clear that inlet air humidity ratio has strong influences on the moisture removal rates (mass transfer) of the 2-fluid LAMEE and the 3-fluid LAMEE. The moisture removal rates of the 2-fluid and 3-fluid LAMEEs increase as inlet air humidity ratio increases. It shown in Figure 4.5 that the moisture removal rate of the 3-fluid LAMEE is slightly higher than the moisture removal rate of the 2-fluid LAMEE under the entire range of inlet air humidity ratio studied, because the average temperature of the desiccant solution is lower in the 3-fluid LAMEE which enhances the actual moisture transfer rate. In addition, the inlet air humidity ratio has negligible effect on the difference between the moisture removal rates of the 2-fluid and 3-fluid LAMEEs.

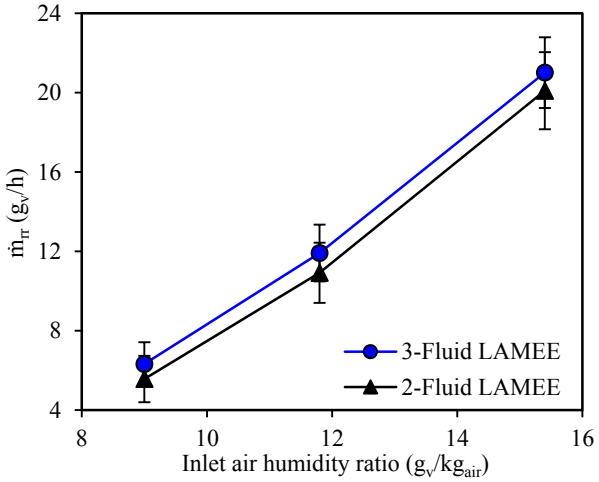

FIGURE 4.5. Variations of moisture removal rates of the 2-fluid LAMEE and the 3-fluid LAMEE with inlet air humidity ratio.

4.4.2 Effects of *Cr** on the Performances of the 2-Fluid and 3-Fluid LAMEEs

In this section, the effects of the desiccant solution flow rate (*Cr**) on the performances of the 2-fluid and 3-fluid LAMEEs are investigated. Also investigated is the influence of *Cr** on the enhancement of the performance of the 3-fluid LAMEE compared with the 2-fluid LAMEE. The design and operating parameters are the same for both the 2-fluid and 3-fluid LAMEEs (Table 4.2). The inlet air conditions were selected according to AHRI summer operating conditions (AHRI Standard 1060 (2005)). The *Cr** is varied between 1.3 and 4.8.

4.4.2.1 Outlet Desiccant Solution and Air Temperatures

Figure 4.6 (a) displays the variations of the outlet desiccant solution temperature with *Cr** for the 2-fluid and 3-fluid LAMEEs. It is clear that the outlet desiccant solution temperature of the 3-fluid LAMEE is lower than the 2-fluid LAMEE under the entire range of *Cr** studied, since a part of the phase change heat released in the desiccant solution stream is transferred to the water flow in the 3-fluid LAMEE. The outlet desiccant solution temperature of the 2-fluid LAMEE decreases as *Cr** increases, while *Cr** has a negligible influence on the outlet desiccant solution temperature of the 3-fluid LAMEE.

TABLE 4.2. Test conditions for the 2-fluid and 3-fluid LAMEEs at several desiccant solution mass flow rates (*Cr**).

Parameter	2-Fluid LAMEE		3-Fluid LAMEE	
	Value	Unit	Value	Unit
$T_{air,in}$	35.4-35.6	°C	35.4-35.7	°C
$W_{air,in}$	16.7-17.1	g_v/kg_{air}	16.7-17.2	g_v/kg_{air}
Re_{air}	610	-	610	-
$T_{sol,in}$	22.7-23.2	°C	22.8-23.2	°C
$W_{sol,in}$	5.65	g/kg	5.65	g/kg
$C_{sol,in}$	31	%	31	%
Re_{sol}	4.3	-	4.3	-
NTU	2	-	2	-
*Cr**	1.3, 2.2, 3.4, 4.8	-	1.3, 2.2, 3.4, 4.8	-
*H**	2.2	-	2.2	-
$T_{w,in}$	-	-	22.6-23.3	°C
$\dot{m}_{w,in}$	-	-	20	kg/hr

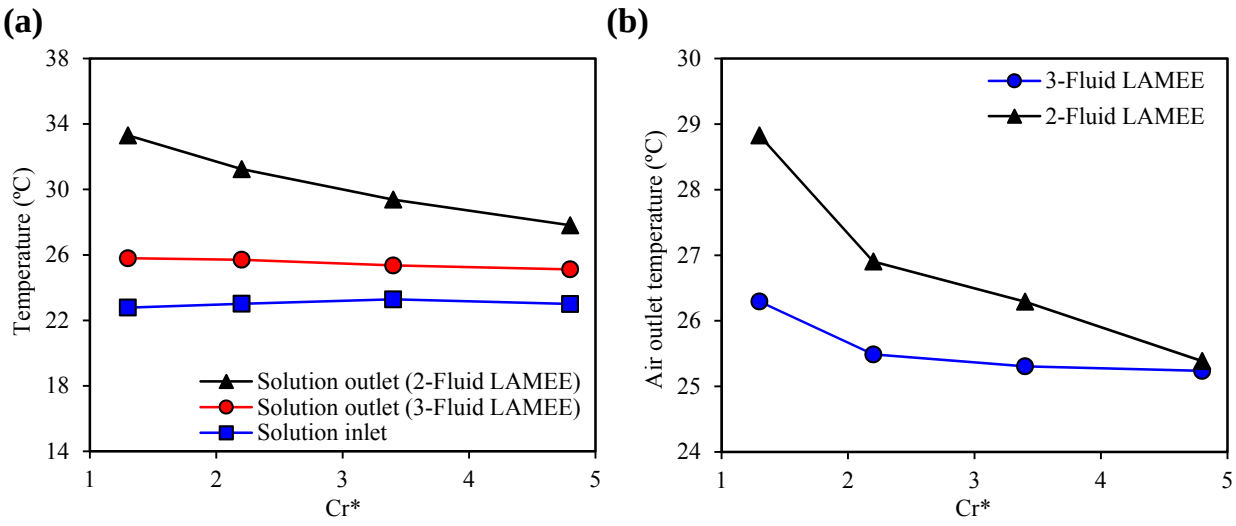

FIGURE 4.6. Variations of (a) outlet desiccant solution temperatures (b) outlet air temperatures of the 2-fluid LAMEE and 3-fluid LAMEE with *Cr**.

Figure 4.6 (b) shows the variations of the outlet air temperature with *Cr** for the 2-fluid and 3-fluid LAMEEs. The outlet air temperature decreases as *Cr** increases in the 2-fluid and 3-fluid LAMEEs, where *Cr** has a stronger effect on the outlet air temperature of the 2-fluid LAMEE. As well, the outlet air temperature of the 3-fluid LAMEE is lower than the outlet air temperature of the 2-fluid LAMEE under the entire range of *Cr** studied because the cooling water decreases the temperature of the desiccant solution along the 3-fluid LAMEE.

4.4.2.2 Sensible, Latent, and Total Effectivenesses

Figure 4.7 (a) displays the variations of the sensible effectivenesses of the 2-fluid and 3-fluid LAMEEs with *Cr** and Figure 4.7 (b) shows the variations of the latent effectivenesses of the 2-fluid and 3-fluid LAMEEs with *Cr**. It is clear that the sensible and latent effectivenesses of the 2-fluid LAMEE increase as *Cr** increases under the entire range of *Cr** studied, while the sensible and latent effectivenesses of the 3-fluid LAMEE increase as *Cr** increases until a certain point, and thereafter no considerable enhancement occurs. The effects of *Cr** on the sensible and latent effectivenesses of the 2-fluid LAMEE are stronger than its effects on the sensible and latent effectivenesses of the 3-fluid LAMEE. For example, as *Cr** increases from 1.3 to 4.8, the sensible effectivenesses of the 2-fluid and 3-fluid LAMEEs increase from 52% to 81% and from 72% to 82%, respectively, and the latent effectivenesses of the 2-fluid and 3-fluid LAMEEs increase by 19% and 4%, respectively.

Figure 4.7 (a) shows that the sensible effectiveness of the 3-fluid LAMEE is higher than the sensible effectiveness of the 2-fluid LAMEE under the entire range of *Cr** studied. However, the difference between the sensible effectivenesses of the 3-fluid and 2-fluid LAMEEs decreases as *Cr** increases. For instance, the absolute enhancements in the sensible effectiveness of the 3-fluid LAMEE compared with the 2-fluid LAMEE are 20% and 1% at *Cr** = 1.3 and 4.8, respectively.

Similar results are obtained for the comparison of the latent and total effectivenesses, as shown in Figures 4.7 (b) and (c). The absolute enhancements in the latent effectiveness of the 3-fluid LAMEE compared with the 2-fluid LAMEE are 16% and 1% at $Cr^* = 1.3$ and 4.8, respectively. It is concluded that the design of the 3-fluid LAMEE is more superior to improve the sensible and latent effectivenesses at low Cr^* operating conditions compared with the 2-fluid LAMEE.

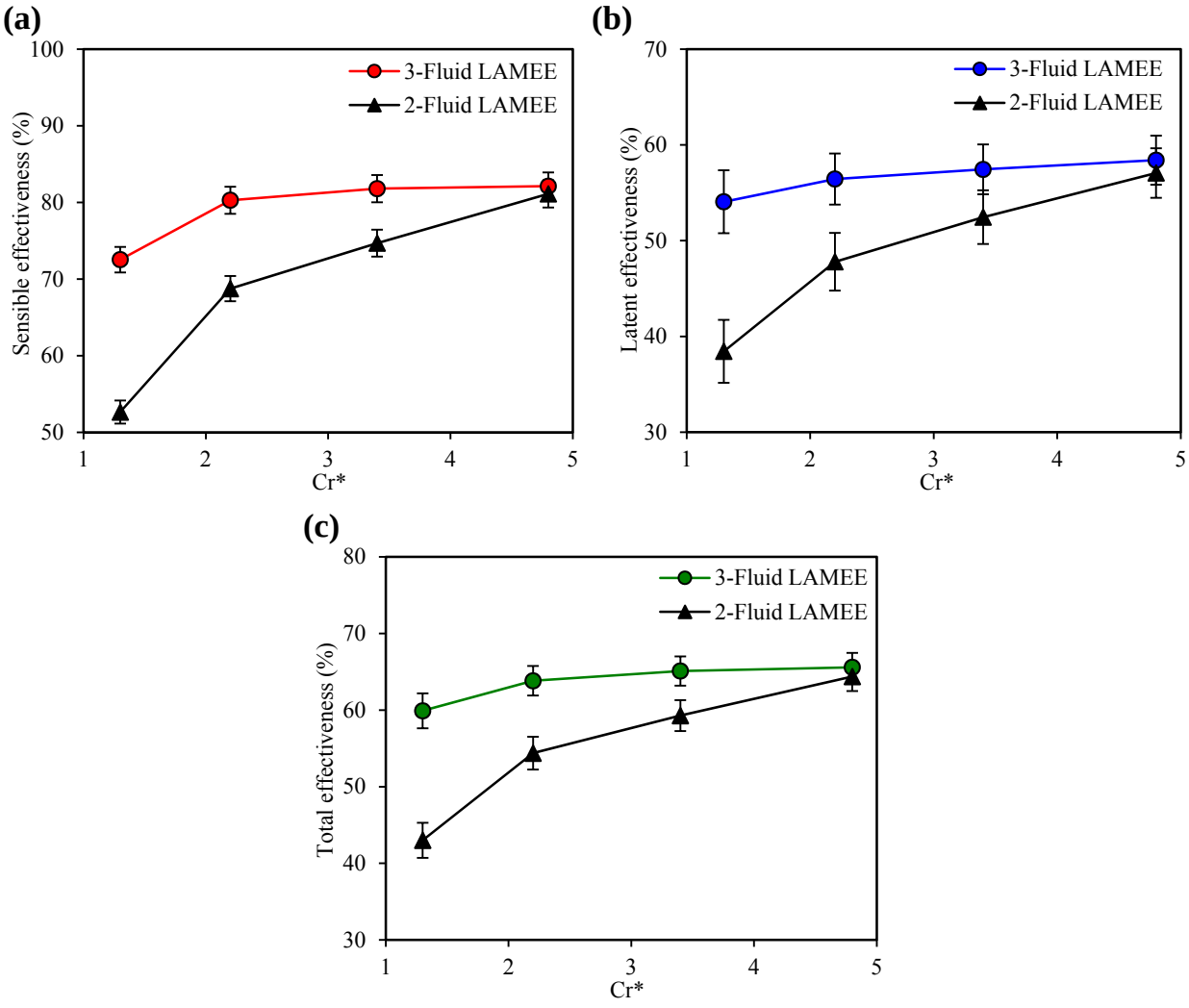

FIGURE 4.7. Variations of (a) sensible effectivenesses (b) latent effectivenesses (c) total effectivenesses of the 2-fluid LAMEE and 3-fluid LAMEE with Cr^*.

4.4.2.3 Moisture Removal Rate

Figure 4.8 displays the variations of moisture removal rates of the 2-fluid and 3-fluid LAMEEs with *Cr**. The moisture removal rates of both the 2-fluid LAMEE and the 3-fluid LAMEE increase as *Cr** increases. However, the effect of *Cr** on the moisture removal rate of the 2-fluid LAMEE is stronger than that of the 3-fluid LAMEE. The moisture removal rate of the 3-fluid LAMEE is higher than the moisture removal rate of the 2-fluid LAMEE under the entire range of *Cr** studied. However, the enhancement become smaller as *Cr** increases. For example, the moisture removal rate of the 3-fluid LAMEE is higher than that of the 2-fluid LAMEE by 41% and 3% at *Cr** = 1.3 and 4.8, respectively. It is concluded that higher enhancements in the moisture removal rate of a 3-fluid LAMEE compared with the 2-fluid LAMEE can be achieved at low *Cr** values.

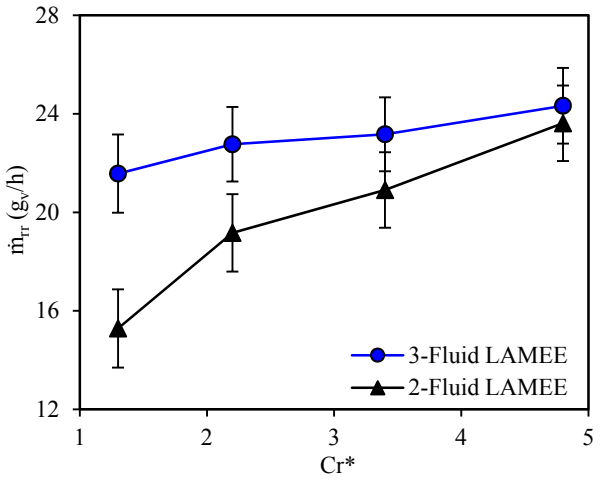

FIGURE 4.8. Variations of moisture removal rates of the 2-fluid LAMEE and the 3-fluid LAMEE with *Cr**.

4.5 CONCLUSIONS

The results presented in the previous chapter proved the research hypothesis of this thesis (i.e. adding a third fluid to control the desiccant solution temperature inside the 3-fluid LAMEE may improve the rates of heat and moisture transfer between the air and desiccant solution compared

to 2-fluid LAMEEs) to be true at several inlet refrigerant temperatures and flow rates under air cooling and dehumidifying conditions. In this chapter, the effects of the phase change energy on the temperatures of air and desiccant solution inside 3-fluid and 2-fluid LAMEEs are quantified, and the effects of inlet air humidity ratio and desiccant solution mass flow rate (Cr^*) on the performances of 3-fluid and 2-fluid LAMEEs are experimentally investigated under air cooling and dehumidifying conditions. The main conclusions are summarized as listed below.

1. Phase change energy has a considerable effect on the temperature of the desiccant solution stream in 2-fluid LAMEEs, and the amount of phase change energy released to the desiccant solution increases as the inlet air humidity ratio increases.
2. The latent effectivenesses and moisture removal rates of the 2-fluid and 3-fluid LAMEEs increase as the inlet air humidity ratio increases, and the latent effectiveness and moisture removal rate of the 3-fluid LAMEE are higher than the 2-fluid LAMEE under the entire range of the inlet air humidity ratio studied.
3. The enhancement in the latent effectiveness of the 3-fluid LAMEE compared with the latent effectiveness of the 2-fluid LAMEE decreases as the inlet air humidity ratio increases.
4. The performances (sensible, latent, and total effectivenesses, and moisture removal rate) of 2-fluid and 3-fluid LAMEEs increase as Cr^* increases, where the effect of Cr^* on the performance of the 2-fluid LAMEE is stronger than its effect on the performance of the 3-fluid LAMEE.
5. Enhancement of the performance of the 3-fluid LAMEE compared with the 2-fluid LAMEE decreases as Cr^* increases.

CHAPTER 5

PERFORMANCE TESTING OF 2-FLUID AND 3-FLUID LAMEES DURING SOLUTION REGENERATION

5.1 OVERVIEW OF CHAPTER 5

The experimental data presented in Chapters 3 and 4 have proved that the hypothesis of this thesis (i.e. adding a third fluid to control the desiccant solution temperature inside the 3-fluid LAMEE may improve the rates of heat and moisture transfer between the air and desiccant solution compared to 2-fluid LAMEEs) is true under air cooling and dehumidifying conditions. This chapter will test the thesis hypothesis under desiccant solution regeneration conditions. Results presented in this chapter fulfill part of the second objective of this thesis (i.e. to design and test a 3-fluid LAMEE and compare with a 2-fluid LAMEE). In this chapter, the rates of heat and moisture transfer in 3-fluid and 2-fluid LAMEEs are tested and compared at several inlet refrigerant temperatures, refrigerant mass flow rates, and desiccant solution mass flow rates under desiccant solution regeneration conditions. To further investigate the effect of the operating conditions on the improvement in the 3-fluid LAMEE performance compared with 2-fluid LAMEEs, the results presented in this chapter are compared with the air cooling and dehumidifying results presented in Chapter 3.

The driving forces for heat and moisture transfer in LAMEEs increase as the difference between the air and desiccant solution temperature increases. However, it was found in a previous Ph.D. study (Moghaddam et al. (2013d)) that during solution regeneration, the latent effectiveness of 2-fluid LAMEEs increases as the inlet desiccant solution temperature increases until a specific point, and thereafter the latent effectiveness decreases as the inlet solution temperature increases.

To further understand this trend, the effect of the inlet solution temperature on the effectiveness of 2-fluid LAMEEs is tested under solution regeneration conditions and is presented in this chapter.

The manuscript presented in this chapter is published in the International Journal of Heat and Mass Transfer. The manuscript presented in this chapter is different from the published paper in the following sections: (a) the description of the test facility, the schematics of the 2-fluid and 3-fluid LAMEEs, and the equations used to evaluate the LAMEE performance presented in the published paper are removed since they were presented in Chapters 2 and 3, and (b) Section 5.8 presented in this chapter was not included in the published paper.

Performance Testing of a Novel 3-Fluid Liquid-To-Air Membrane Energy Exchanger (3-Fluid LAMEE) under Desiccant Solution Regeneration Operating Conditions

(International Journal of Heat and Mass Transfer, 2016, Volume 95)

Mohamed R. H. Abdel-Salam, Robert W. Besant, Carey J. Simonson

5.2 ABSTRACT

Liquid-to-air membrane energy exchangers (LAMEEs) use semi-permeable membranes to transfer heat and moisture between air and a desiccant solution, and prevent the transfer of desiccant droplets to the airside. A 2-fluid flat-plate LAMEE is composed of several adjacent air and desiccant solution channels each separated by a semi-permeable membrane. A 3-fluid LAMEE is the new generation of LAMEEs which has a structure similar to a 2-fluid flat-plate LAMEE. The novelty of the 3-fluid LAMEE is that it includes titanium tubes inside the desiccant solution channels to control the temperature of the desiccant solution along the exchanger. In this chapter, the performances of a 2-fluid LAMEE and 3-fluid LAMEE are tested and compared under diluted desiccant solution regeneration operating conditions. Also studied are the effects of operating conditions (inlet heating water temperature, heating water mass flow rate, desiccant solution mass flow rate, and inlet desiccant solution temperature) on the performances of the 2-fluid and 3-fluid LAMEEs. For the chosen test conditions, results show that effectiveness and moisture removal rate of the 3-fluid LAMEE are higher than the 2-fluid LAMEE under the entire range of inlet heating water temperature, heating water flow rate, and desiccant solution flow rate studied. The effectiveness and moisture removal rate of the 3-fluid LAMEE increase as the inlet heating water temperature and/or flow rate increases. The sensible, latent, and total effectivenesses, and moisture removal rate of the LAMEE increase by 38%, 40%, 39%, and 6 times when the temperature of desiccant solution is maintained constant along the exchanger. Compared with the 2-fluid

LAMEE, the sensible, latent, and total effectivenesses, and moisture removal rate of the 3-fluid LAMEE are improved by up to 104%, 141%, 128%, and 17 times, respectively.

5.3 INTRODUCTION

Heating, ventilation, and air-conditioning (HVAC) systems are responsible for significant amounts of global energy consumption and greenhouse gas emissions. For instance, HVAC systems account for 34% of the total energy consumed in the industrialized countries (Zhang (2008)). Liquid-to-air membrane energy exchangers (LAMEEs) use micro-porous semi-permeable membranes to transfer heat and water vapor between air and desiccant solution streams. Figure 1.1 shows a schematic of a 2-fluid flat-plate LAMEE. 2-fluid LAMEEs have achieved considerable energy savings when integrated with liquid-desiccant air-conditioning systems (Abdel-Salam et al. (2014a, 2014c); Bergero and Chiari (2011); Abdel-Salam and Simonson (2014a); Zhang and Zhang (2014)). LAMEEs are used for diluted desiccant solution regeneration in liquid desiccant membrane air-conditioning (LDMAC) systems (Abdel-Salam et al. (2014a, 2014c); Bergero and Chiari (2011); Abdel-Salam and Simonson (2014a); Zhang and Zhang (2014)) and in run-around membrane energy exchangers (RAMEEs) (Ge et al. (2013a); Vali et al. (2009); Patel et al. (2014)).

5.4 STATE-OF-THE-ART

A review of the literature (Abdel-Salam et al. (2014b)) revealed that only four studies (Abdel-Salam et al. (2015); Ge et al. (2014a); Moghaddam et al. (2013d, 2014)) were conducted on the performance of LAMEEs when used for diluted desiccant solution regeneration. Chapter 2 (Abdel-Salam et al. (2015)) shows a numerical study on the effects of air and desiccant solution channel widths on the performance of a 2-fluid flat-plate LAMEE when operated as a diluted desiccant solution regenerator. The results showed that the regenerator's performance increases as the width of air and/or solution channels decreases. Based on the widths of the air and solution

channels, the regenerator's sensible, latent, and total effectivenesses varied between 48%-87%, 28%-52%, and 35%-65%, respectively. Ge et al. (2014a) tested the performance of a 2-fluid flat-plate LAMEE when operated as a desiccant solution regenerator and reported that the sensible and latent effectivenesses varied between 55%-84% and 36%-62%, respectively. Moghaddam et al. (2013d) tested a 2-fluid flat-plate LAMEE under desiccant solution regeneration operating conditions and found that the latent effectiveness varied between 48%-60%. Moghaddam et al. (2014) found that the sensible, latent, and total effectivenesses of a 2-fluid flat-plate LAMEE when used for diluted desiccant solution regeneration varied between 55%-82%, 25%-54%, and 33%-59%, respectively. This shows that 2-fluid LAMEEs have low effectiveness under diluted desiccant solution regeneration operating conditions and there is a need to modify the current design of flat-plate LAMEEs to improve their performances for diluted desiccant solution regeneration applications.

For desiccant solution regeneration process, Figure 5.1 shows the variations of the regeneration air and diluted desiccant solution temperatures along a counter-flow heat exchanger and a counter-flow LAMEE. It is clear that as the diluted desiccant solution flows along the solution channel, the decrease in the solution temperature is much higher in the LAMEE than in the sensible heat exchanger. The decrease in the desiccant solution temperature in the LAMEE is attributed to the absorbed phase change energy of the released moisture. The decrease of the desiccant solution temperature reduces the difference between the air and desiccant solution temperatures, which reduces the driving forces for heat and moisture transfer between the air and desiccant solution streams, and the effectiveness of the regenerator.

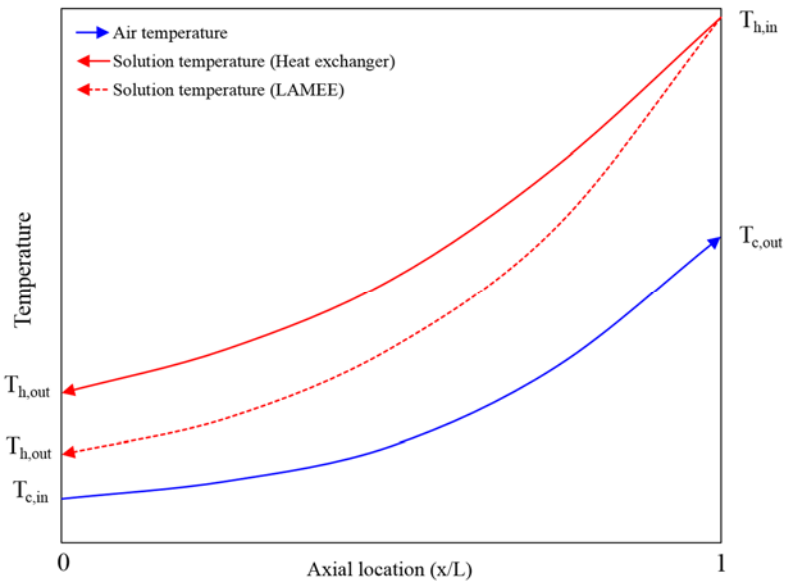

FIGURE 5.1. A schematic diagram of the air and desiccant solution temperatures along a 2-fluid LAMEE and heat exchanger shows that the phase change energy reduces the temperature difference between the air and desiccant solution streams under diluted desiccant solution regeneration operating conditions.

5.5 THE 3-FLUID LAMEE

The performance of the 3-fluid LAMEE under air cooling and dehumidifying operating conditions was tested in Chapters 3 and 4 (Abdel-Salam et al. (2016a, 2016b)). In Chapter 3 (Abdel-Salam et al. (2016a)), the results showed that heat and moisture transfer between the air and desiccant solution streams inside the 3-fluid LAMEE were higher than a 2-fluid LAMEE, and the performance of the 3-fluid LAMEE is enhanced as inlet cooling water temperature decreases or cooling water flow rate increases. The results presented in Chapter 4 (Abdel-Salam et al. (2016b)) showed that the phase change energy (i.e. enthalpy of condensation) increases the temperatures of the desiccant solution and air streams inside LAMEEs under air cooling and dehumidifying operating conditions. Moreover, the enhancement in the performance of the 3-fluid LAMEE compared with a 2-fluid LAMEE decreases as the ratio between heat capacities of desiccant solution and air (Cr^*) increases (Abdel-Salam et al. (2016b)).

5.6 OBJECTIVES OF THE CURRENT STUDY

(1) Test and compare the performances of the novel 3-fluid LAMEE and a 2-fluid LAMEE when used for diluted desiccant solution regeneration under several operating conditions.

(2) Test the effects of operating parameters (inlet heating water temperature, heating water flow rate, desiccant solution flow rate, and inlet desiccant solution temperature) on the performance of the 2-fluid and 3-fluid LAMEEs under diluted desiccant solution regeneration operating conditions.

5.7 RESULTS AND DISCUSSION

Table 5.1 shows the test conditions for the 2-fluid and 3-fluid LAMEEs.

TABLE 5.1. Test conditions for the 2-fluid LAMEE and the 3-fluid LAMEE.

Parameter	2-Fluid LAMEE		3-Fluid LAMEE	
	Value	Unit	Value	Unit
$T_{air,in}$	29.4-30	°C	29.6-30.2	°C
$W_{air,in}$	13-14.8	g_v/kg_{air}	12.4-15	g_v/kg_{air}
Re_{air}	610	-	610	-
$T_{sol,in}$	40.1-40.3	°C	39.9-40.5	°C
$W_{sol,in}$	20.4-20.6	g/kg	20.4-20.9	g/kg
$C_{sol,in}$	30	%	30	%
Re_{sol}	4.3	-	4.3	-
NTU	2	-	2	-
Cr^*	2, 3.4, 4.8	-	2, 3.4, 4.8	-
$T_{w,in}$	-	-	42.3, 49.9, 57.1, 65.7	°C
Cr	-	-	0.039, 0.135, 0.265	-

5.7.1 Effect of Inlet Heating Water Temperature

In this section, the performances of the 2-fluid LAMEE and the 3-fluid LAMEE at several inlet heating water temperatures are presented and discussed. The 3-fluid LAMEE was operated at

several inlet heating water temperatures (42.3°C, 49.9°C, 57.1°C, and 65.7°C), nearly constant heating water flow rate (Cr = 0.24-0.28), and constant desiccant solution flow rate (Cr^* = 2).

5.7.1.1 Outlet Desiccant Solution Temperature

Figure 5.2 displays the outlet desiccant solution temperatures of the 2-fluid LAMEE and the 3-fluid LAMEE at several inlet heating water temperatures ($T_{w,in}$). It is clear that the outlet solution temperature of the 3-fluid LAMEE is higher than the 2-fluid LAMEE under the entire range of $T_{w,in}$ studied, and increases as $T_{w,in}$ increases. As well, the difference between the outlet solution temperatures of the 2-fluid and 3-fluid LAMEEs increases as $T_{w,in}$ increases. The desiccant solution temperature is maintained almost constant along the 3-fluid LAMEE at $T_{w,in}$ = 50ºC, which implies that the hot water stream is able to compensate the decrease in the desiccant solution temperature caused by the sensible heat transfer to the regeneration air and the phase change energy accompanied with the moisture transfer from the diluted desiccant solution to the regeneration airstream.

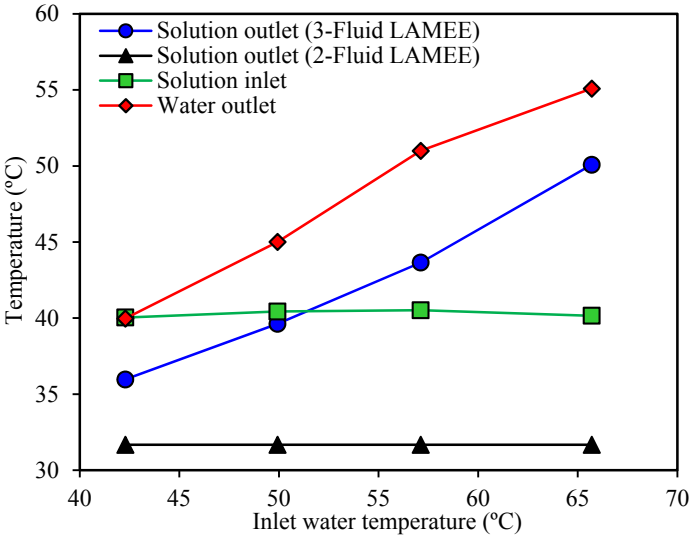

FIGURE 5.2. Variations of the outlet desiccant solution temperature and outlet heating water temperature with the inlet heating water temperature for the 2-fluid LAMEE and the 3-fluid LAMEE.

5.7.1.2 Sensible, Latent, and Total Effectivenesses

The main objective of the 3-fluid LAMEE is to enhance the rates of heat and moisture transfer between the air and desiccant solution streams. In this work, the sensible, latent, and total effectivenesses of the 3-fluid LAMEE are calculated based on rates of heat and moisture transfer between the regeneration air and diluted desiccant solution streams. The traditional effectiveness equations (equations (3.5) to (3.7)) are used to calculate the sensible, latent, and total effectivenesses of the 2-fluid LAMEE and 3-fluid LAMEE. This implies that the hot water stream is excluded from effectiveness calculations for the 3-fluid LAMEE. Therefore, it is predicted that the effectiveness of the 3-fluid LAMEE will exceed 100% under specific operating conditions (i.e. high temperatures and flow rates of heating water stream). New equations for calculating the effectiveness of 3-fluid energy exchangers will be developed in Chapter 7.

Figure 5.3 (a) shows the sensible effectivenesses of the 2-fluid and 3-fluid LAMEEs at several inlet heating water temperatures ($T_{w,in}$). The sensible effectiveness of the 3-fluid LAMEE is higher than the 2-fluid LAMEE under the entire range of $T_{w,in}$ studied, and the difference between the sensible effectivenesses of the 2-fluid and 3-fluid LAMEEs increases as $T_{w,in}$ increases. Based on $T_{w,in}$, the sensible effectiveness of the 3-fluid LAMEE is enhanced by up to 79% compared with the 2-fluid LAMEE. The $T_{w,in}$ has a significant effect on the sensible effectiveness of the 3-fluid LAMEE. For instance, the sensible effectiveness of the 3-fluid LAMEE increases from 44% to 107% as $T_{w,in}$ increases from 42ºC to 66ºC. It is concluded that the sensible effectiveness of the LAMEE increases from 28% to 66% when the desiccant solution temperature is maintained constant along the exchanger.

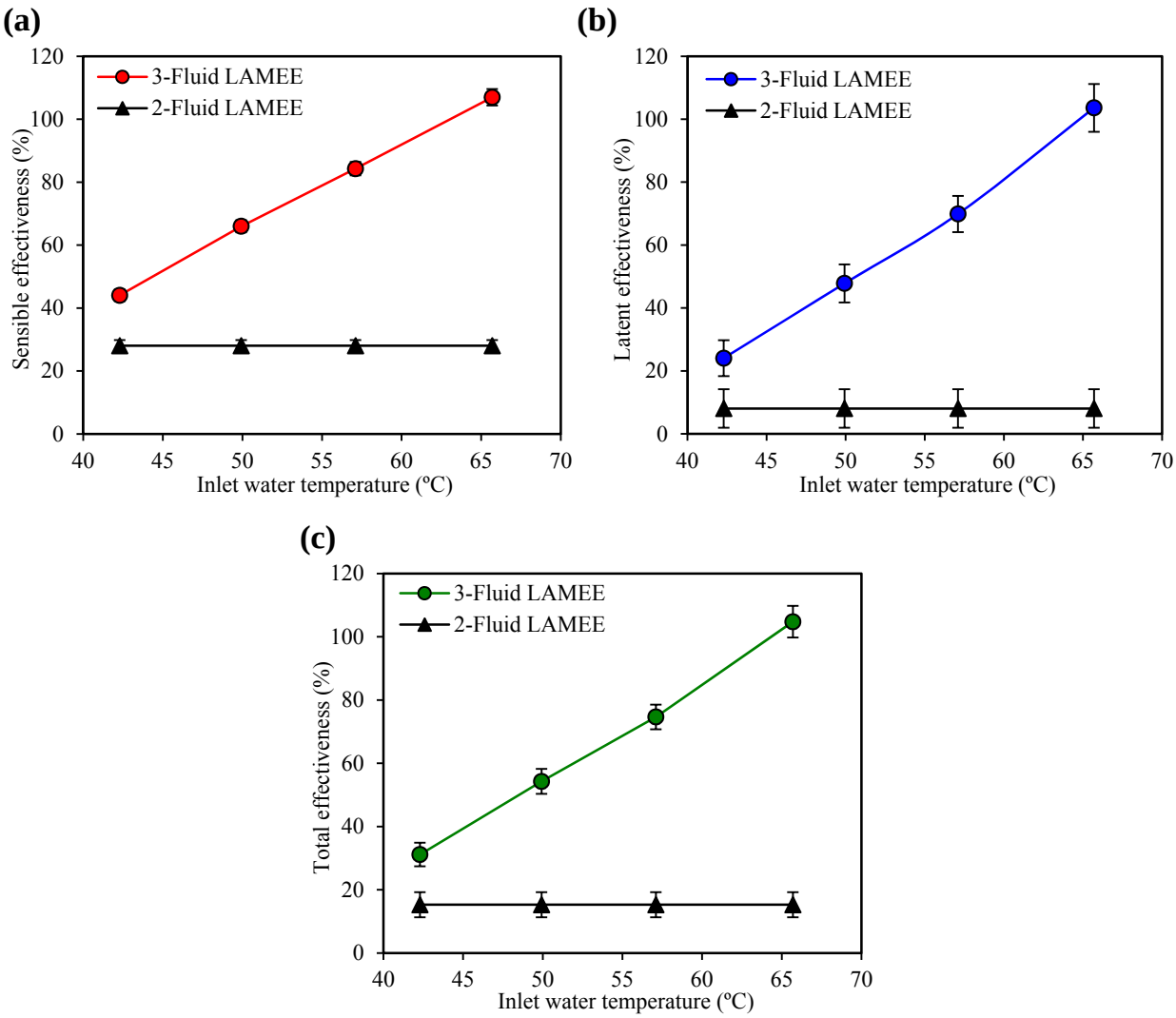

FIGURE 5.3. Variations of (a) sensible effectivenesses (b) latent effectivenesses (c) total effectivenesses of the 2-fluid LAMEE and the 3-fluid LAMEE with the inlet heating water temperature.

Figure 5.3 (b) shows the variations of the latent effectivenesses of the 2-fluid and 3-fluid LAMEEs with $T_{w,in}$. It is clear that the latent effectiveness of the 2-fluid LAMEE is very low (8%) under the current test conditions. The latent effectiveness of the 3-fluid LAMEE is higher than the 2-fluid LAMEE under the entire range of $T_{w,in}$ studied. At $T_{w,in}$ = 66ºC, the absolute enhancement in latent effectiveness of the 3-fluid LAMEE compared with the 2-fluid LAMEE is 95%. This can be explained as follow. The temperature and equivalent humidity ratio of the desiccant solution

increase as $T_{w,in}$ increases. Thus the driving force for moisture transfer (difference between humidity ratios of regeneration air and desiccant solution streams) increases as $T_{w,in}$ increases. The $T_{w,in}$ has a strong effect on the latent effectiveness of the 3-fluid LAMEE. For example, the latent effectiveness of the 3-fluid LAMEE increases from 24% to 103% as $T_{w,in}$ increases from 42ºC to 66ºC. The latent effectiveness of the LAMEE is enhanced from 8% to 48% when the desiccant solution temperature is maintained constant along the exchanger. It can be concluded that the influence of $T_{w,in}$ on the latent effectiveness is stronger than the sensible effectiveness. For instance, the absolute enhancements of the sensible effectiveness and latent effectiveness of the LAMEE are 79% and 95%, respectively, at $T_{w,in}$ = 66ºC.

Figure 5.3 (c) shows the variations of the total effectiveness with $T_{w,in}$ for the 2-fluid and 3-fluid LAMEEs. It is clear that the total effectiveness of the 3-fluid LAMEE is higher than the 2-fluid LAMEE under the entire range of $T_{w,in}$ studied. Equation (3.7) shows that the total effectiveness of a LAMEE depends on its sensible and latent effectivenesses. Therefore, the total effectiveness of the 3-fluid LAMEE is enhanced as $T_{w,in}$ increases due to the enhancements in the sensible and latent effectivenesses. The total effectiveness of the LAMEE increases from 15% to 54% when the desiccant solution temperature is maintained constant along the exchanger.

5.7.1.3 Moisture Removal Rate

Figure 5.4 displays the variations of the moisture removal rates of the 2-fluid and 3-fluid LAMEEs with $T_{w,in}$. The moisture removal rate of the 3-fluid LAMEE is higher than the 2-fluid LAMEE under the entire range of $T_{w,in}$ studied, and the difference between the moisture removal rates of the 2-fluid and 3-fluid LAMEEs increases as $T_{w,in}$ increases. Compared with the 2-fluid LAMEE, the moisture removal rate of the 3-fluid LAMEE is enhanced by 12 times at $T_{w,in}$ = 66ºC. The $T_{w,in}$ has a strong effect on the moisture removal rate of the 3-fluid LAMEE. For instance, the moisture

removal rate of the 3-fluid LAMEE increases by 316% as $T_{w,in}$ increases from 42ºC to 66ºC. In conclusion, the moisture removal rate of the LAMEE is enhanced by 6 times when the desiccant solution temperature is maintained constant along the exchanger.

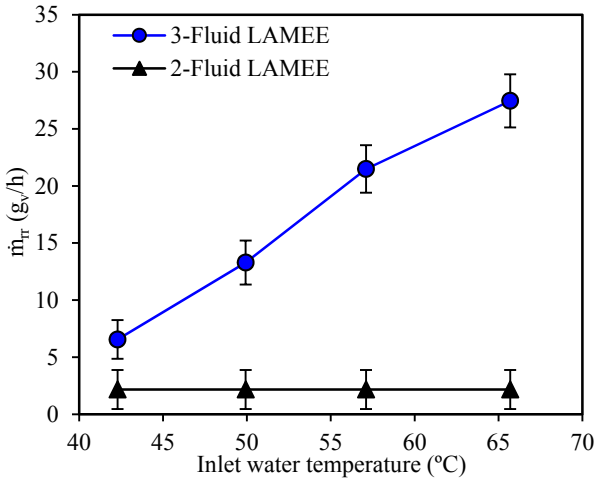

FIGURE 5.4. Variations of moisture removal rates of the 2-fluid LAMEE and the 3-fluid LAMEE with inlet heating water temperature.

5.7.1.4 Effect of Temperature Ratio (T^*) on Performance of the 3-Fluid LAMEE

Temperature ratio is the ratio between the difference between inlet temperatures of the regeneration air and hot water streams and the difference between inlet temperatures of the regeneration air and diluted desiccant solution streams (Abdel-Salam et al. (2016a)). T^* is calculated from equation (5.1) (Abdel-Salam et al. (2016a)).

$$T^* = \frac{T_{\text{air,in}} - T_{\text{w,in}}}{T_{\text{air,in}} - T_{\text{sol,in}}} \tag{5.1}$$

where $T_{w,in}$ is the inlet heating water temperature (ºC).

For desiccant solution regeneration operating conditions; where $T_{air,in} < T_{sol,in}$ and $T_{air,in} < T_{w,in}$:

$T^* < 1$ implies that $T_{w,in} < T_{sol,in}$

$T^* = 1$ implies that $T_{w,in} = T_{sol,in}$

$T^* > 1$ implies that $T_{w,in} > T_{sol,in}$

Figure 5.5 (a) shows the variations of the sensible, latent, and total effectivenesses of the 3-fluid LAMEE with T^*. It is clear that the sensible, latent, and total effectivenesses increase as T^* increases. At $T^* < 3$, the sensible effectiveness is higher than latent effectiveness, while the sensible and latent effectivenesses have almost the same value at $T^* = 3.5$. This implies that the effect of T^* on the enhancement of the latent effectiveness is stronger than the sensible effectiveness.

Figure 5.5 (b) displays the variation of moisture removal rate of the 3-fluid LAMEE with T^*. It is clear that the moisture removal rate increases as T^* increases. This can be explained as follows. Higher T^* implies higher inlet heating water temperatures, thus higher equilibrium desiccant solution humidity ratios. Increasing the equilibrium desiccant solution humidity ratio increases the difference between the humidity ratios of the regeneration air and diluted desiccant solution streams, which increases the driving force for moisture transfer inside the LAMEE. Consequently, moisture removal rate increases as T^* increases.

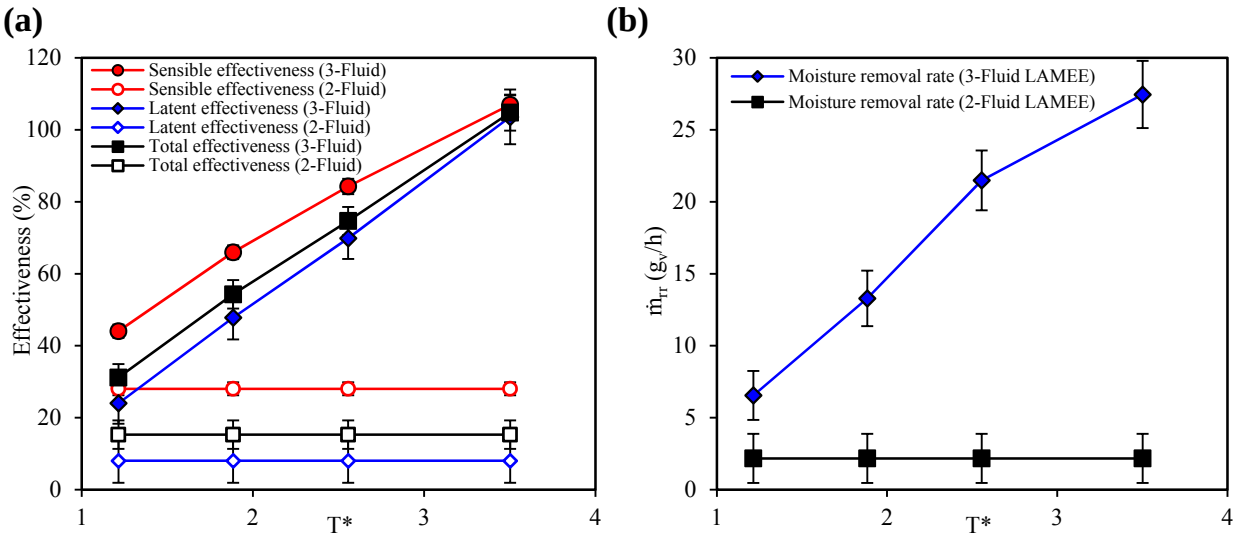

FIGURE 5.5. Variations of (a) sensible, latent, and total effectivenesses (b) moisture removal rate of the 2-fluid and 3-fluid LAMEEs with T^*.

5.7.2 Effect of Heating Water Flow Rate (*Cr*)

In this section, the performances of the 2-fluid LAMEE and the 3-fluid LAMEE at several inlet heating water mass flow rates are presented and discussed. The 3-fluid LAMEE was operated at several heating water flow rates (*Cr* = 0.039, 0.135, and 0.265), nearly constant inlet heating water temperature (55.3-58.4°C), and constant desiccant solution flow rate (*Cr** = 2).

5.7.2.1 Outlet Desiccant Solution Temperature

A comparison between the variations of the outlet desiccant solution temperature with the heating water flow rate (*Cr*) for the 2-fluid and 3-fluid LAMEEs is shown in Figure 5.6. The outlet desiccant solution temperature of the 3-fluid LAMEE is higher than the 2-fluid LAMEE under the entire range of *Cr* studied, and increases as *Cr* decreases. It should be noted that the outlet desiccant solution temperature at *Cr* = 0.039 should be higher than the outlet desiccant solution temperature at *Cr* = 0.135, however, the outlet desiccant solution at *Cr* = 0.135 is higher than at *Cr* = 0.039 in Figure 5.6. This is because the inlet heating water temperature at *Cr* = 0.039 is lower than at *Cr* = 0.135.

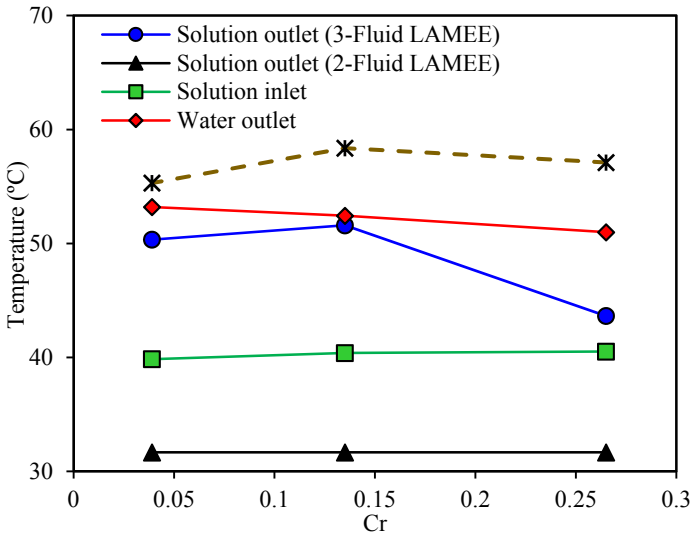

FIGURE 5.6. Variations of the outlet desiccant solution temperature and outlet heating water temperature for the 2-fluid LAMEE and the 3-fluid LAMEE with *Cr*.

5.7.2.2 Sensible, Latent, and Total Effectivenesses

A comparison between the variations of sensible effectiveness with *Cr* for the 2-fluid and 3-fluid LAMEEs is shown in Figure 5.7 (a). The sensible effectiveness of the 3-fluid LAMEE is higher than the 2-fluid LAMEE under the entire range of *Cr* studied, and the difference between the sensible effectivenesses of the 2-fluid and 3-fluid LAMEEs increases as *Cr* decreases. Compared with the 2-fluid LAMEE, the sensible effectiveness of the 3-fluid LAMEE is enhanced by up to 104% at $Cr = 0.039$. This can be explained as follow. Sensible effectiveness of heat transfer between the desiccant solution and heating water streams increases as heating water flow rate increases (*Cr* decreases), thus, the desiccant solution temperature increases as *Cr* decreases. Increasing the desiccant solution temperature increases the driving forces for heat transfer between the desiccant solution and regeneration air streams. It is clear that *Cr* has a strong effect on the sensible effectiveness of the 3-fluid LAMEE. For example, the sensible effectiveness of the 3-fluid LAMEE increases from 84% to 132% as *Cr* decreases from 0.265 to 0.039.

Figure 5.7 (b) displays the variations of the latent effectivenesses of the 2-fluid and 3-fluid LAMEEs with *Cr*. The latent effectiveness of the 3-fluid LAMEE is higher than the 2-fluid LAMEE under the entire range of *Cr* studied. The absolute enhancement in the latent effectiveness of the 3-fluid LAMEE compared with the 2-fluid LAMEE is 141% at $Cr = 0.039$. It is clear that *Cr* has a strong effect on the latent effectiveness of the 3-fluid LAMEE, where latent effectiveness increases from 70% to 149% as *Cr* decreases from 0.265 to 0.039.

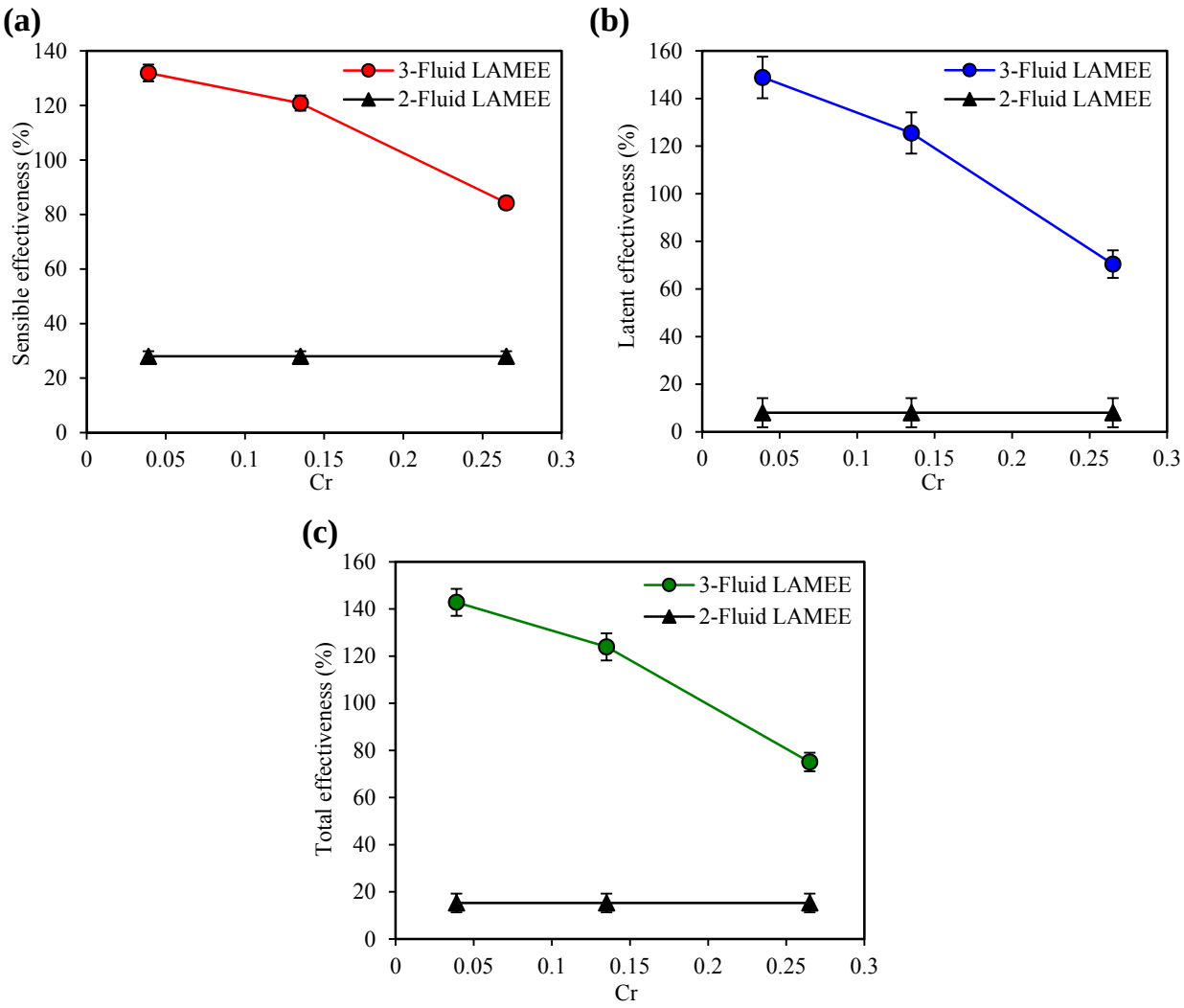

FIGURE 5.7. Variations of (a) sensible effectivenesses (b) latent effectivenesses (c) total effectivenesses of the 2-fluid LAMEE and the 3-fluid LAMEE with *Cr*.

Figure 5.7 (c) displays the variations of the total effectivenesses of the 2-fluid and 3-fluid LAMEEs with *Cr*. As it was mentioned before, the total effectiveness of a LAMEE depends on its sensible and latent effectivenesses. Therefore, the total effectiveness of the 3-fluid LAMEE increases as *Cr* decreases due to the enhancements in the sensible and latent effectivenesses.

5.7.2.3 Moisture Removal Rate

A comparison between the variations of the moisture removal rates of the 2-fluid and 3-fluid LAMEEs with *Cr* is shown in Figure 5.8. It is clear that the moisture removal rate of the 3-fluid

LAMEE increases as *Cr* decreases. As well, *Cr* has a strong effect on the moisture removal rate of the 3-fluid LAMEE. For example, the moisture removal rate of the 3-fluid LAMEE increases by 78% as *Cr* decreases from 0.265 to 0.039. The moisture removal rate of the 3-fluid LAMEE is much higher than the 2-fluid LAMEE under the entire range of *Cr* studied. At *Cr* = 0.039, the moisture removal rate of the 3-fluid LAMEE is higher than the moisture removal rate of the 2-fluid LAMEE by 17 times.

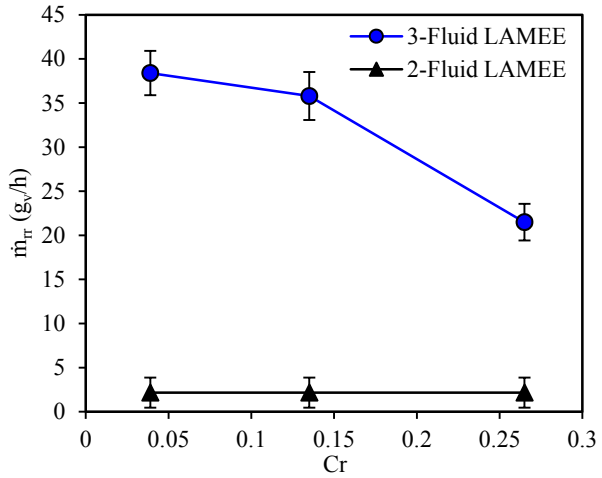

FIGURE 5.8. Variations of moisture removal rates of the 2-fluid LAMEE and the 3-fluid LAMEE with *Cr*.

5.7.3 Effect of Desiccant Solution Flow Rate (*Cr**)

In this section, the effects of desiccant solution flow rate (*Cr**) on performances of the 2-fluid LAMEE and the 3-fluid LAMEE are presented and discussed. The performances of the 2-fluid and 3-fluid LAMEEs were tested at several desiccant solution flow rates (*Cr** = 2, 3.4, and 4.8), constant inlet heating water temperature (40-40.3°C), and constant heating water flow rate ($\dot{m}_w$ = 115-130 g/min).

5.7.3.1 Outlet Desiccant Solution Temperature

Figure 5.9 displays the variations of the outlet desiccant solution temperature and outlet heating

water temperature with the desiccant solution flow rate (Cr^*) for the 2-fluid and 3-fluid LAMEEs. It is clear that the outlet desiccant solution temperature of the 3-fluid LAMEE is higher than the 2-fluid LAMEE under the entire range of Cr^* studied, and the difference between the outlet solution temperatures of the 2-fluid and 3-fluid LAMEEs decreases as Cr^* increases. The outlet solution temperatures of the 2-fluid and 3-fluid LAMEEs increase as Cr^* increases, where the effect of Cr^* on the outlet solution temperature of the 2-fluid LAMEE is stronger than the 3-fluid LAMEE. The outlet heating water temperature of the 3-fluid LAMEE increases as Cr^* increases.

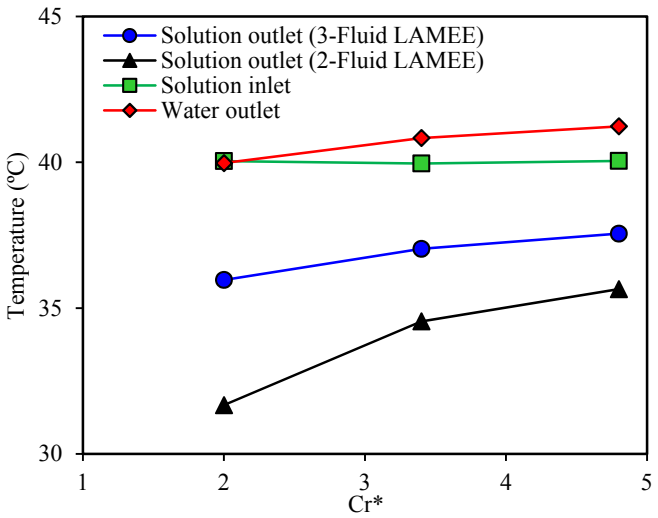

FIGURE 5.9. Variations of the outlet desiccant solution temperature and outlet heating water temperature for the 2-fluid LAMEE and the 3-fluid LAMEE with Cr^*.

5.7.3.2 Sensible, Latent, and Total Effectivenesses

Variations of the sensible, latent, and total effectivenesses of the 2-fluid LAMEE and the 3-fluid LAMEE with Cr^* are displayed in Figure 5.10. The sensible, latent, and total effectivenesses of the 3-fluid LAMEE are higher than the 2-fluid LAMEE under the entire range of Cr^* studied, where the enhancements in the effectivenesses of the 3-fluid LAMEE compared with the 2-fluid LAMEE decrease as Cr^* increases. The sensible, latent, and total effectivenesses of the 2-fluid and 3-fluid LAMEEs increase as Cr^* increases, where the effect of Cr^* on the enhancement of the

effectivenesses of the 2-fluid LAMEE is more significant than the 3-fluid LAMEE.

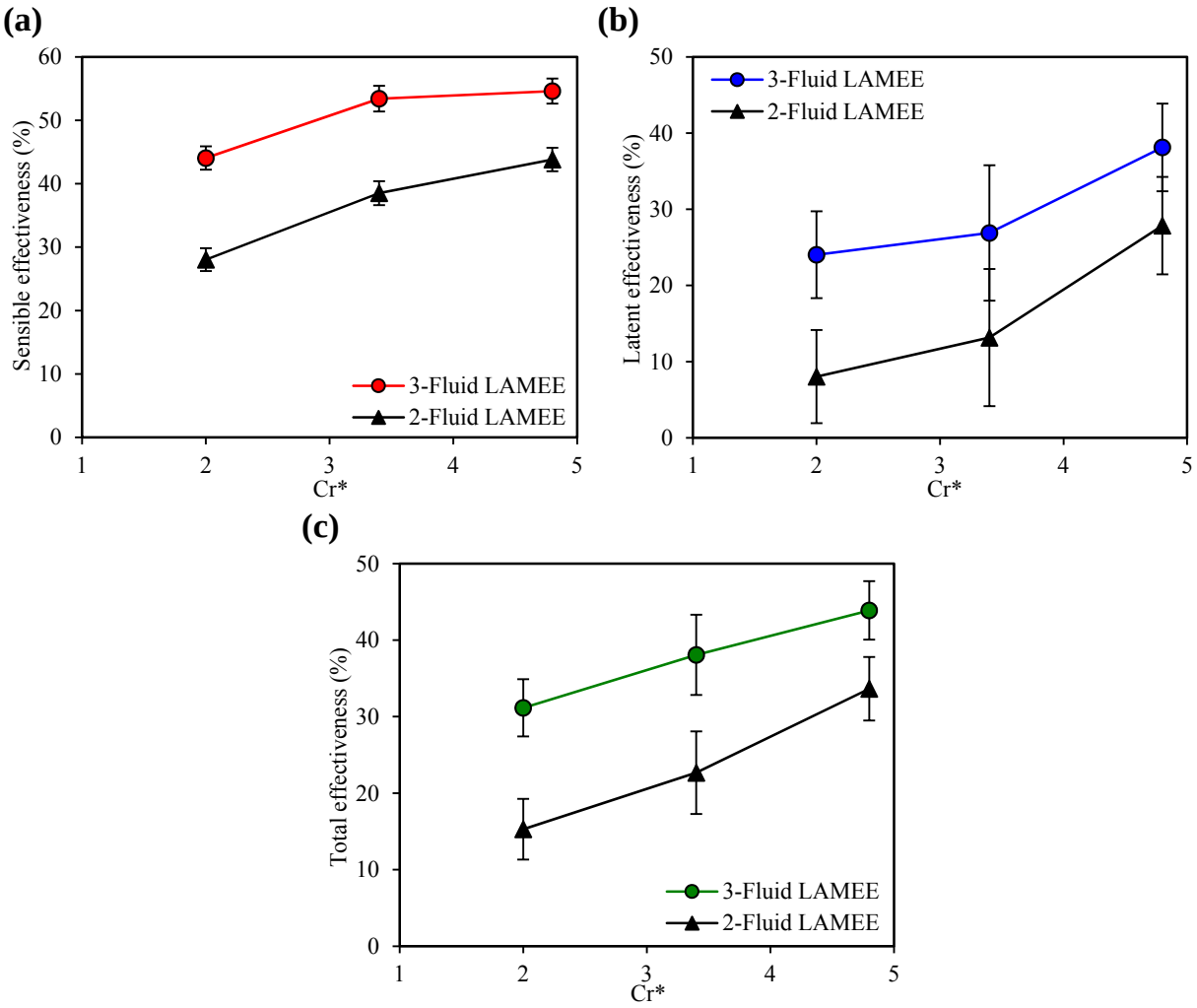

FIGURE 5.10. Variations of (a) sensible effectivenesses (b) latent effectivenesses (c) total effectivenesses of the 2-fluid LAMEE and the 3-fluid LAMEE with *Cr**.

5.7.3.3 Moisture Removal Rate

Figure 5.11 shows the variations of the moisture removal rates of the 2-fluid and 3-fluid LAMEEs with *Cr**. It is clear that the moisture removal rates of the 2-fluid and 3-fluid LAMEEs increase as *Cr** increases, where the moisture removal rate of the 3-fluid LAMEE is higher than the 2-fluid LAMEE under the entire range of *Cr** studied. However, the difference between the moisture removal rates of the 2-fluid and 3-fluid LAMEEs decreases as *Cr** increases. Compared with the

2-fluid LAMEE, the moisture removal rate of the 3-fluid LAMEE is enhanced by 200% and 38% at Cr^* = 2 and 4.8, respectively. As well, the effect of Cr^* on the enhancement of the moisture removal rate of the 2-fluid LAMEE is stronger than the 3-fluid LAMEE.

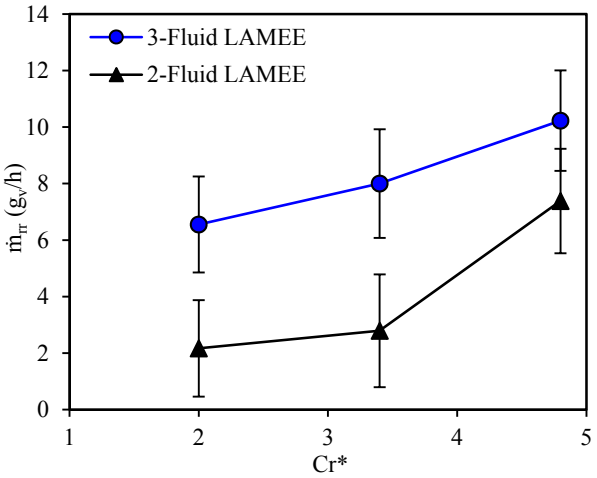

FIGURE 5.11. Variations of moisture removal rates of the 2-fluid LAMEE and the 3-fluid LAMEE with Cr^*.

5.7.4 Effect of Inlet Desiccant Solution Temperature on the Performance of 2-Fluid LAMEEs

The effect of inlet desiccant solution temperature on the performance of the 2-fluid LAMEE is tested and presented in this section. The test conditions are shown in Table 5.2.

TABLE 5.2. Test conditions for the 2-fluid LAMEE under diluted desiccant solution regeneration operating conditions.

Parameter	Value	Unit
$T_{air,in}$	29.4-29.7	°C
$W_{air,in}$	12-13	g_v/kg_{air}
$T_{sol,in}$	40.1, 50.7, 62.8	°C
$W_{sol,in}$	20.5-71.2	g/kg
$C_{sol,in}$	30	%
NTU	2	-
Cr^*	2	-

5.7.4.1 Sensible, Latent, and Total Effectivenesses

Figure 5.12 (a) displays the effect of the inlet desiccant solution temperature ($T_{sol,in}$) on the sensible effectiveness of the 2-fluid LAMEE. It is clear that the sensible effectiveness slightly deceases as $T_{sol,in}$ increases. This can be explained as follows. Increasing $T_{sol,in}$ increases the difference between the air and solution temperatures which increases the driving force for heat transfer. However, the desiccant solution absorbs phase change energy as moisture transfers to the airstream which decreases the desiccant solution temperature. Figure 5.12 (b) shows the variation of the latent effectiveness with $T_{sol,in}$. The latent effectiveness increases as $T_{sol,in}$ increases until $T_{sol,in}$ reaches 51ºC, afterwards the latent effectiveness decreases as $T_{sol,in}$ increases. The decrease of latent effectiveness at $T_{sol,in} > 51$ºC may be attributed to the desiccant solution crystallization, where desiccant crystals are accumulated on the membrane and block its pores. Figure 5.12 (c) shows that the trend of the total effectiveness variation with $T_{sol,in}$ is similar to the latent effectiveness.

Moghaddam et al. (2013d) tested the effects of $T_{sol,in}$ on sensible, latent, and total effectivenesses and moisture removal rate of a 2-fluid flat-plate LAMEE when used for diluted desiccant solution regeneration. The results of the current study are compared with the experimental results reported by Moghaddam et al. (2013d) (see Figure 5.12). It is clear that the trend of the effect of $T_{sol,in}$ on the sensible effectiveness is different from the trend reported by Moghaddam et al. (2013d). This can be attributed to the differences in the design parameters (channel width, channel height, surface area available for heat/moisture transfer (membrane surface area), and thermo-physical properties of membrane) and operating conditions (air flow rate, inlet air temperature, inlet air humidity ratio, solution flow rate, inlet solution concentration, and inlet solution humidity ratio). Values of dimensionless parameters (*NTU* and *Cr**) in this study are different from Moghaddam et al. (2013d). The values of *NTU* and *Cr** are 2 and 2 in this study, and 5 and 4 in

Moghaddam et al. (2013d). Inlet solution temperature may has a stronger effect on sensible effectiveness at high *NTU* values and/or high *Cr** values.

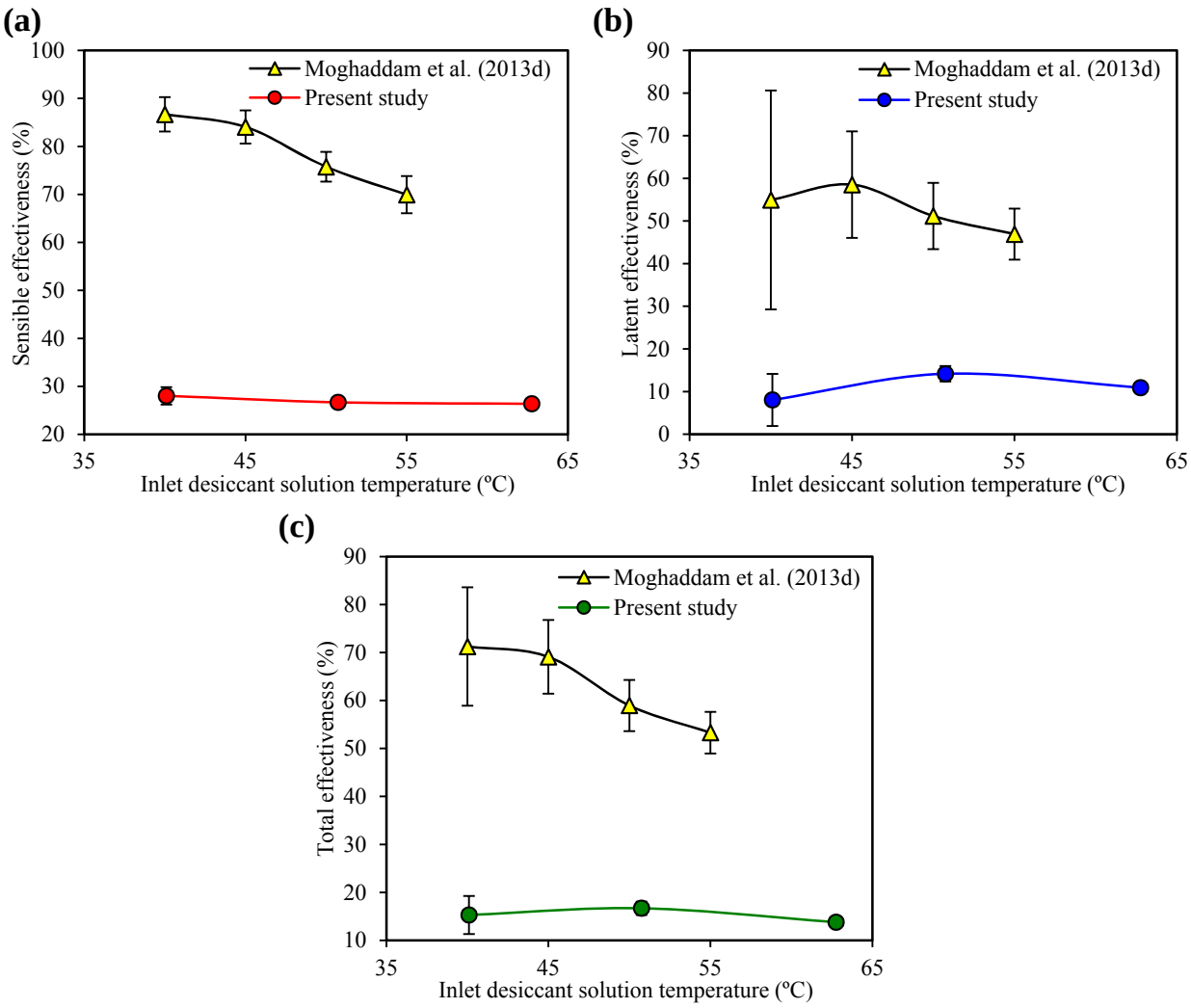

FIGURE 5.12. Variations of (a) sensible effectiveness (b) latent effectiveness (c) total effectiveness of the 2-fluid LAMEE with inlet desiccant solution temperature.

5.7.4.2 Moisture Removal Rate

Figure 5.13 displays the variation of the moisture removal rate of the 2-fluid LAMEE with $T_{sol,in}$. It is clear that the moisture removal rate increases as $T_{sol,in}$ increases under the entire range of $T_{sol,in}$ studied. As well, $T_{sol,in}$ has a strong effect on the moisture removal rate. For example, the moisture removal rate increases by nearly 10 times as $T_{sol,in}$ increases from 40ºC to 63ºC. This can be

explained as follows. The inlet equilibrium desiccant solution humidity ratio increases as $T_{sol,in}$ increases thus the difference between the inlet humidity ratios of the regeneration air and diluted solution increases, which increases the driving force for moisture transfer between the regeneration air and solution streams. The results of the current study are compared with the experimental results reported by Moghaddam et al. (2013d). Results reported by Moghaddam et al. (2013d) shows that $T_{sol,in}$ has a stronger effect on the moisture removal rate. As mentioned previously, this can be attributed to the differences in the design parameters and operating conditions.

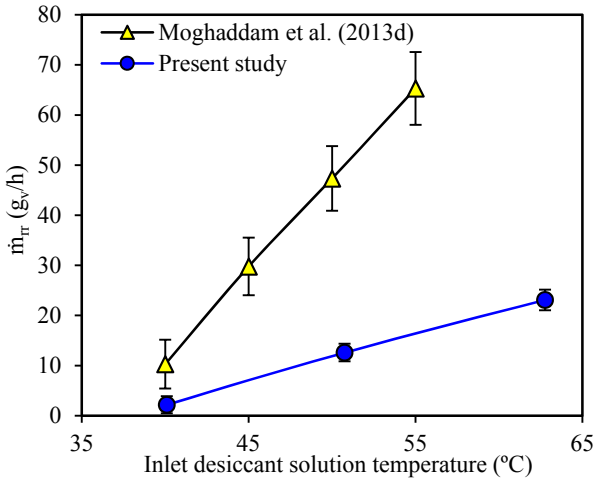

FIGURE 5.13. Variation of moisture removal rate of the 2-fluid LAMEE with inlet desiccant solution temperature.

5.8 COMPARISON BETWEEN AIR COOLING AND DEHUMIDIFYING CONDITIONS AND SOLUTION REGENERATION CONDITIONS

Figures 5.14 and 5.15 show the improvement in sensible and latent effectivenesses between the air and desiccant solution in the 3-fluid LAMEE compared to the 2-fluid LAMEE at different inlet refrigerant temperatures and mass flow rates (*Cr*) under air cooling and dehumidifying conditions (Chapter 3, Abdel-Salam et al. (2016a)) and desiccant solution regeneration conditions (Chapter 5, Abdel-Salam et al. (2016c)). It is clear that the improvement in the sensible effectiveness under air cooling and dehumidifying conditions is similar to solution regeneration conditions. On the

other hand, the improvement in the latent effectiveness under solution regeneration conditions is much higher than air cooling and dehumidifying conditions. One reason for this may be the low latent effectiveness of the 2-fluid LAMEE under solution regeneration conditions (8%) compared to air cooling and dehumidifying conditions (38%).

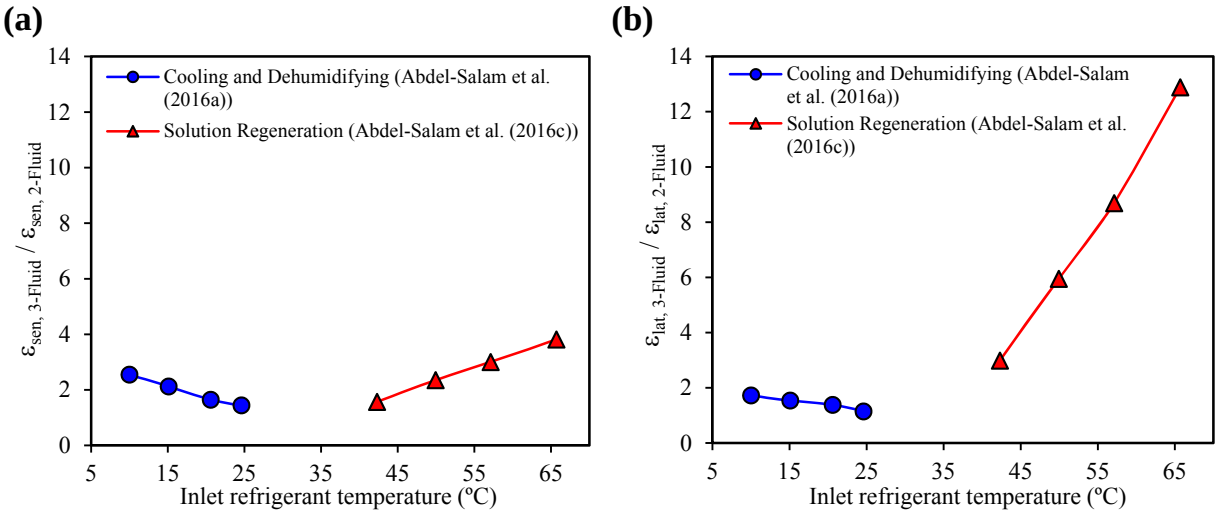

FIGURE 5.14. Ratio between the 3-fluid and 2-fluid LAMEEs effectivenesses for (a) sensible and (b) latent at different inlet refrigerant temperatures under air cooling and dehumidifying conditions and solution regeneration conditions (cooling and dehumidifying: $NTU = 1.8$, $Cr^* = 1.8$, $Cr = 0.26$; regeneration: $NTU = 2$, $Cr^* = 2$, $Cr = 0.26$).

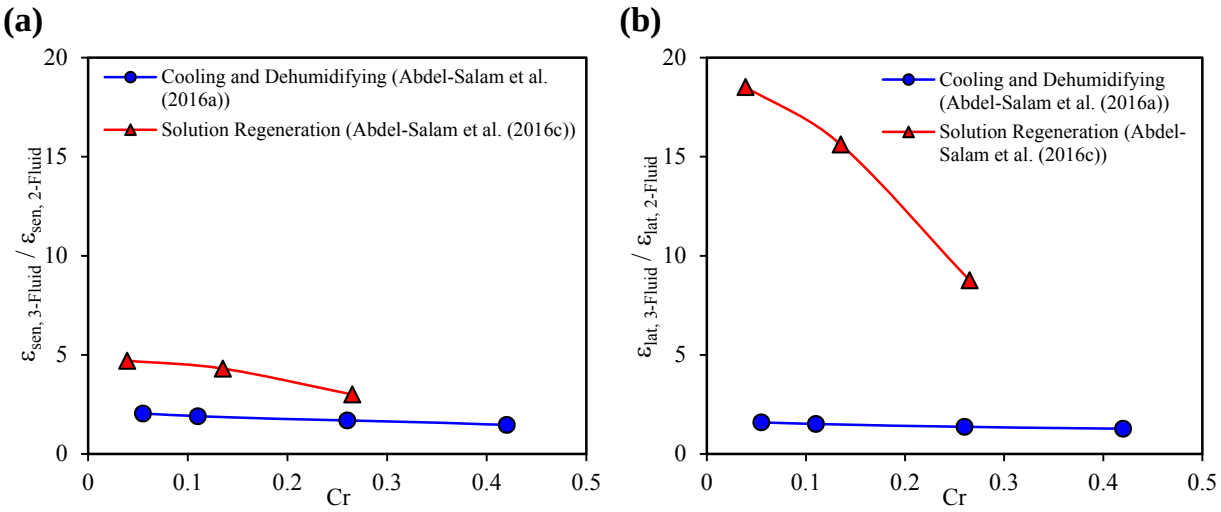

FIGURE 5.15. Ratio between the 3-fluid and 2-fluid LAMEEs effectivenesses for (a) sensible and (b) latent at different refrigerant mass flow rates (Cr) under air cooling and dehumidifying conditions and solution regeneration conditions (cooling and dehumidifying: $NTU = 1.8$, $Cr^* = 1.8$, $T_{ref,in} = 20.6$ºC; regeneration: $NTU = 2$, $Cr^* = 2$, $T_{ref,in} = 57$ºC).

The most likely reason for the low latent effectiveness of the 2-fluid LAMEE under solution regeneration conditions is related to desiccant solution crystallization. Afshin et al. (2010) reported that there is a high risk of desiccant solution crystallization in 2-fluid LAMEEs during solution regeneration. During solution regeneration in 2-fluid LAMEEs, the concentration of the desiccant solution increases while its temperature decreases rapidly especially at the interface between the membrane and the desiccant solution. Mei et al. (2008) reported that the risk of desiccant solution crystallization increases at low desiccant solution temperatures and high concentrations. On the other hand, the temperature of the desiccant solution remains high along the entire length of the 3-fluid LAMEE which decreases the risk of desiccant solution crystallization in the 3-fluid LAMEE under solution regeneration conditions. As mentioned in Section 5.7.4.1, the occurrence of desiccant solution crystallization may block some membrane pores which reduces the moisture transfer rate between the air and solution (i.e. latent effectiveness) in 2-fluid LAMEEs under solution regeneration conditions.

Another reason for the low latent effectiveness of the 2-fluid LAMEE under solution regeneration conditions may be the potential for moisture transfer between the air and desiccant solution (i.e. the difference between air and solution inlet humidity ratios) under solution regeneration conditions is lower than under air cooling and dehumidifying conditions by 35%.

5.9 CONCLUSIONS

The main contribution of this chapter is that it shows that the performance of LAMEEs when operated under desiccant solution regeneration conditions can be significantly enhanced by using a hot water stream inside the desiccant solution channel to heat the desiccant solution along the exchanger, which proves the research hypothesis of this thesis (i.e. adding a third fluid to control the desiccant solution temperature inside the 3-fluid LAMEE may improve the rates of heat and

moisture transfer between the air and desiccant solution compared to 2-fluid LAMEEs) to be true under solution regeneration conditions. Compared with the 2-fluid LAMEE, the sensible, latent, and total effectivenesses, and moisture removal rate of the 3-fluid LAMEE are improved by up to 104%, 141%, 128%, and 17 times, respectively. Following are the most important conclusions drawn from this chapter.

1- The sensible, latent, and total effectivenesses and moisture removal rate of the 3-fluid LAMEE are higher than the 2-fluid LAMEE under the entire range of inlet heating water temperature and heating water flow rate studied.

2- The sensible, latent, and total effectivenesses and moisture removal rate of the 3-fluid LAMEE significantly increase as the inlet heating water temperature or mass flow rate increases.

3- The sensible, latent, and total effectivenesses, and moisture removal rate of the LAMEE increase by 38%, 40%, 39%, and 6 times when a third fluid maintains the desiccant solution temperature constant along the exchanger.

4- The sensible, latent, and total effectivenesses, and moisture removal rate of the 3-fluid LAMEE are higher than the 2-fluid LAMEE under the entire range of desiccant solution flow rate (Cr^*) studied, where the differences between the effectivenesses and moisture removal rates of the 2-fluid and 3-fluid LAMEEs decrease as Cr^* increases.

5- The sensible, latent, and total effectivenesses, and moisture removal rate of the 2-fluid and 3-fluid LAMEEs increase as Cr^* increases, where the effect of Cr^* on the 2-fluid LAMEE is stronger than the 3-fluid LAMEE.

6- The inlet desiccant solution temperature ($T_{sol,in}$) has a negligible effect on the sensible effectiveness of 2-fluid LAMEEs, whereas the latent effectiveness increases as $T_{sol,in}$ increases

until a certain point, and thereafter the latent effectiveness decreases as $T_{sol,in}$ increases.

7- The moisture removal rate of 2-fluid LAMEEs significantly increases as $T_{sol,in}$ increases under the entire range of $T_{sol,in}$ studied (40ºC-63ºC).

In conclusion, results presented in Chapters 3, 4, and 5 show that the proposed 3-fluid LAMEE can achieve the same effectiveness as a 2-fluid LAMEE at lower values of *NTU* and *Cr** under air cooling and dehumidifying conditions and solution regeneration conditions.

CHAPTER 6

PERFORMANCE TESTING OF 2-FLUID AND 3-FLUID LAMEES DURING AIR HEATING AND HUMIDIFICATION

6.1 OVERVIEW OF CHAPTER 6

The results presented in the previous chapters proved that the main hypothesis of this thesis (i.e. adding a third fluid to control the desiccant solution temperature inside the 3-fluid LAMEE may improve the rates of heat and moisture transfer between the air and desiccant solution compared to 2-fluid LAMEEs) is true under air cooling and dehumidifying conditions and desiccant solution regeneration conditions. However, the experimental data presented in Chapters 3 and 5 showed that the improvement in the latent effectiveness of the 3-fluid LAMEE compared to the 2-fluid LAMEE under desiccant solution regeneration conditions is much higher than air cooling and dehumidifying conditions. This implies that the improvement in the 3-fluid LAMEE performance compared to 2-fluid LAMEEs depends on the operating conditions. Therefore, in this chapter, the performances of the 3-fluid and 2-fluid LAMEEs are tested and compared under air heating and humidifying conditions. Also tested are the effects of the phase change energy on the temperature of the desiccant solution in 2-fluid and 3-fluid LAMEEs under air heating and humidifying conditions.

The effect of flow maldistribution, caused by membrane deflections, on the performance of flat-plate LAMEEs was numerically studied and estimated at several membrane deflections in Chapter 2. However, the actual membrane deflections in flat-plate LAMEEs are unknown. To the best of my knowledge, there is no published study that has experimentally studied flow maldistribution in flat-plate LAMEEs. For the first time, this chapter will present an experimental

study of the feasibility of applying pre-tension to the membrane to reduce flow maldistribution caused by membrane deflections in flat-plate LAMEEs. The membrane deflections in the 3-fluid LAMEE prototype are investigated with and without membrane pre-tension. The numerical results presented in Chapter 2 and the measured membrane deflections are used to estimate the degradation of the 3-fluid LAMEE performance due to membrane deflections.

The results presented in this chapter fulfill part of the first objective (i.e. to develop design recommendations for flat-plate LAMEEs) and part of the second objective (i.e. to design and test a 3-fluid LAMEE and compare with a 2-fluid LAMEE) of this thesis.

The manuscript presented in this chapter was submitted to International Journal of Heat and Mass Transfer. The manuscript presented in this chapter is different from the submitted paper in the following sections: the description of the test facility, the schematics of the 2-fluid and 3-fluid LAMEEs, and the equations used to evaluate the LAMEE performance presented in the submitted paper are removed since they were presented in Chapters 2 and 3.

Performance Testing of 2-Fluid and 3-Fluid Liquid-To-Air Membrane Energy Exchangers for HVAC Applications in Cold-Dry Climates

(Submitted to *International Journal of Heat and Mass Transfer*)

Mohamed R. H. Abdel-Salam, Robert W. Besant, Carey J. Simonson

6.2 ABSTRACT

Liquid-to-air membrane energy exchangers (LAMEEs) can avoid the problem of desiccant droplets carryover by using semi-permeable membranes to separate the air and desiccant solution streams. The aim of this study is to test and compare the heat and moisture transfer performances between the air and desiccant solution inside a novel 3-fluid LAMEE and a 2-fluid LAMEE under air heating and humidifying operating conditions. The effect of flow maldistribution on the deterioration of the 3-fluid LAMEE's performance is estimated, and an experimental study of the feasibility of membrane pre-tension to reduce flow maldistribution caused by membrane deflections in flat-plate LAMEEs is presented. Unlike heat exchangers where the lowest possible outlet hot fluid temperature is equal to the inlet cold fluid temperature, experimental data show that the outlet desiccant solution (hot fluid) temperature of the 2-fluid LAMEE may be lower than the inlet air (cold fluid) temperature. This is attributed to the effect of the phase change energy associated with the air humidification process.

6.3 INTRODUCTION

In dry and cold climates, building heating, ventilation, and air-conditioning (HVAC) systems consume considerable amounts of energy. Liquid desiccants have the ability to humidify/dehumidify air streams and can be regenerated using solar energy. A liquid desiccant membrane HVAC system uses semi-permeable membranes to prevent the transfer of desiccant droplets to the airstream during humidification or dehumidification. Liquid desiccant membrane HVAC systems could be used for air dehumidification/humidification in residential/commercial buildings, the food and beverage industry, and the pharmaceutical industry. Over the past decade, research has indicated that installing liquid desiccant membrane HVAC systems in buildings can significantly reduce the total energy consumption and improve the indoor air quality (Abdel-Salam and Simonson (2014a); Abdel-Salam et al. (2014c); Bergero and Chiari (2011); Ge et al. (2013a); Zhang and Zhang (2014)).

Figure 6.1 shows a schematic of a possible solar liquid desiccant membrane HVAC system under air heating and humidifying operation mode. The system is composed of two liquid desiccant membrane energy exchangers, one operating as an air humidifier and the other operating as a desiccant solution regenerator. In the humidifier, heat and moisture are transferred from a hot diluted desiccant solution to the outdoor cool-dry airstream, where the temperature of the desiccant solution decreases and its concentration increases. Afterwards, the air is supplied to the conditioned space and the cool concentrated desiccant solution is circulated through the regenerator. In the regenerator, heat and moisture are transferred from a hot-humid regeneration airstream to the cool concentrated desiccant solution. Solar energy is used to heat and humidify the regeneration air, and a portion of the hot diluted desiccant solution is stored in a storage tank to be used during the nighttime which allows for 24-hour operation of the HVAC system.

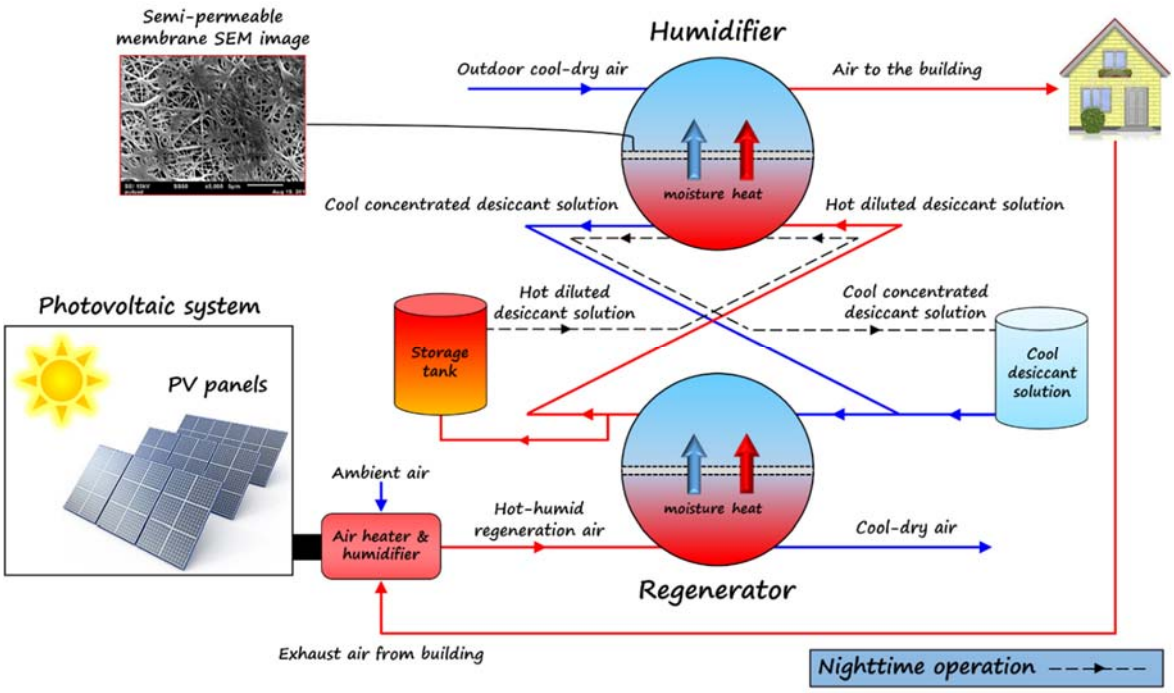

FIGURE 6.1. Schematic of a solar liquid desiccant membrane HVAC system under air heating and humidifying operation mode.

The solar liquid desiccant membrane HVAC system has several advantages over conventional vapor compression HVAC systems, such as (1) a high ability to remove contaminants (germs, bacteria, airborne microorganisms, CO_2, toluene, formaldehyde, etc.) from the supply airstream (Welty; Advantix Systems (2010); Chung et al. (1993, 1995)) which improves the indoor air quality, (2) avoiding frosting problems which reduce the performance of conventional heat/energy recovery ventilators in cold climates (Nasr et al. (2014)), and (3) operating by solar energy where a portion of the desiccant solution heated during the daytime is stored to be used during the nighttime. This implies low operating costs and net zero greenhouse gas emissions.

6.4 LIQUID-TO-AIR MEMBRANE ENERGY EXCHANGERS (LAMEEs)

The conventional design of flat-plate LAMEEs (see Figure 1.1) is similar to a parallel-plate sensible heat exchanger, but the hot and cold fluids (i.e. air and desiccant solution) are separated

by a semi-permeable membrane which allows simultaneous heat and moisture transfer between the air and desiccant solution but prevents the transfer of desiccant droplets to the airstream.

In liquid desiccant heat and moisture exchangers, the driving forces for heat and moisture transfer between the air and desiccant solution are the differences between the air and desiccant solution temperatures and vapor pressures inside the exchanger. The conjugate heat and moisture transfer between the air and desiccant solution is accompanied with the release/absorption of phase change energy, which changes the average desiccant solution temperature along the exchanger. In the air cooling and dehumidifying process, the effect of phase change energy increases the temperature of the desiccant solution as it flows along the exchanger, while in air heating and humidifying/diluted desiccant solution regeneration processes, the effect of phase change energy decreases the temperature of the desiccant solution as it flows along the exchanger. The change in the average desiccant solution temperature reduces the differences between the air and desiccant solution temperatures and vapor pressures, which reduces the driving forces and rates of heat and moisture transfer between the air and desiccant solution inside the exchanger. In Chapter 4 (Abdel-Salam et al. (2016b)), the influences of the phase change energy on the temperatures of air and desiccant solution inside a 2-fluid flat-plate LAMEE were tested under air cooling and dehumidifying operating conditions. Results showed that the desiccant solution and air temperatures increased across the exchanger by up to 3ºC and 1ºC, respectively, due to the effect of phase change energy.

Experimental data presented in Chapters 3, 4, and 5 (Abdel-Salam et al. (2016a, 2016b, 2016c)) have shown that maintaining the desiccant solution temperature almost constant along the entire length of LAMEEs resulted in considerable improvement in rates of heat and moisture transfer

between the air and desiccant solution under air cooling and dehumidifying operating conditions and diluted desiccant solution regeneration operating conditions.

The objectives of the current chapter are (1) to test and compare the heat and moisture transfer performances between the air and desiccant solution inside the 3-fluid and 2-fluid LAMEEs under air heating and humidifying operating conditions, (2) to test the effect of phase change energy, associated with the air humidification process, on the desiccant solution temperature at different desiccant solution mass flow rates, (3) to estimate the effect of flow maldistribution on the deterioration of the 3-fluid LAMEE's performance, and (4) experimentally investigate the feasibility of membrane pre-tension to reduce flow maldistribution caused by membrane deflections in flat-plate LAMEEs.

6.5 RESULTS AND DISCUSSION

6.5.1 Test Conditions

In this section, the heat and moisture transfer performances between the air and desiccant solution inside the 3-fluid LAMEE and a 2-fluid LAMEE are compared at several desiccant solution mass flow rates (Cr^*) under air heating and humidifying operating conditions. The value of Cr^* is changed by changing the desiccant solution mass flow rate. The 3-fluid LAMEE prototype (see Figure 3.2) was tested as a 2-fluid LAMEE by turning off the refrigerant loop. Table 6.1 shows the test conditions for the 2-fluid and 3-fluid LAMEEs which simulate cool and dry climate conditions. Figure 6.2 shows the inlet conditions of the air, desiccant solution, and water flows on the psychrometric chart.

TABLE 6.1. Test conditions for the 2-fluid LAMEE and the 3-fluid LAMEE under air heating and humidifying conditions.

Parameter	2-Fluid LAMEE		3-Fluid LAMEE	
	Value	Unit	Value	Unit
$T_{air,in}$	17.2-17.5	°C	17.3-17.5	°C
$W_{air,in}$	0.8-0.9	g_v/kg_{air}	0.8-0.9	g_v/kg_{air}
Re_{air}	560	-	560	-
$T_{sol,in}$	24.5-24.9	°C	24.6-25	°C
$W_{sol,in}$	6.75-6.9	g/kg	6.8-6.9	g/kg
Re_{sol}	4.4	-	4.4	-
$C_{sol,in}$	32.485	%	32.485	%
NTU	2.1	-	2.1	-
Cr^*	1.15, 3.2, 5.35	-	1.15, 3.2, 5.35	-
$T_{w,in}$	-	-	25.3	°C
$\dot{m}_w$	-	-	80-93	g/min

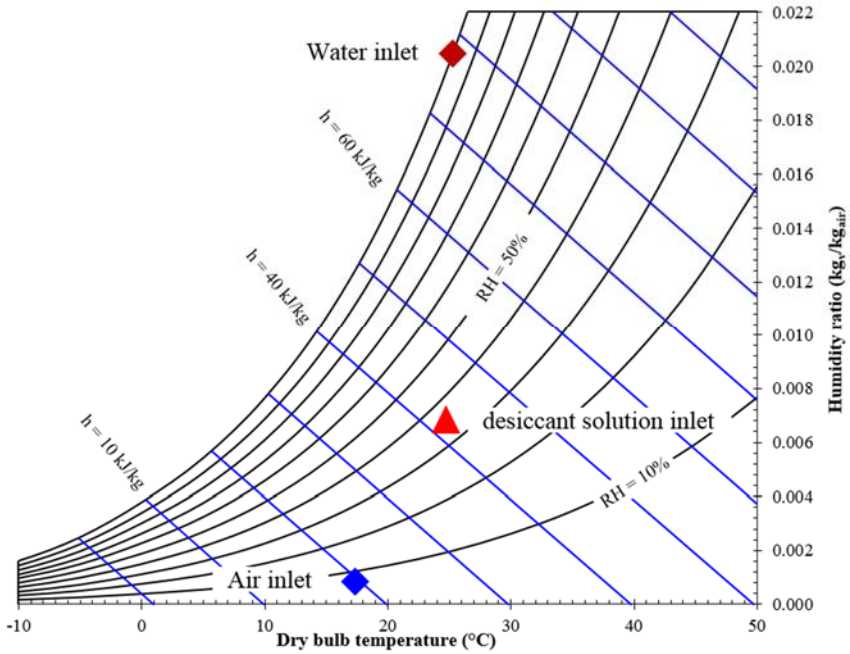

FIGURE 6.2. Inlet conditions of the air, desiccant solution, and water flows on a psychrometric chart.

6.5.2 Temperature Data

In sensible heat exchangers, the lowest possible outlet hot fluid temperature is equal to the inlet cold fluid temperature. Figure 6.3 displays the inlet and outlet temperatures of the air and desiccant solution in the 2-fluid LAMEE at several *Cr** values. It is clear that the outlet desiccant solution temperature (hot fluid) in the 2-fluid LAMEE is lower than the inlet air temperature (cold fluid) at *Cr** = 1.15. This is attributed to the energy required to evaporate the liquid water (i.e. phase change energy) at the interface of the membrane and desiccant solution. This phase change energy comes from the desiccant solution and cools the desiccant solution below the temperature of the air. At higher *Cr** values, the effect of phase change energy on the desiccant solution temperature in the 2-fluid LAMEE decreases because the heat capacity of the desiccant solution increases as *Cr** increases. Figure 6.3 also shows that the trend of air and desiccant solution temperatures variations across the 2-fluid LAMEE at *Cr** = 3.2 is very close to a counter-flow heat exchanger with hot and cold fluids with equal heat capacity rates (i.e. *Cr* = 1).

A comparison between the variations of inlet and outlet temperatures of the air and desiccant solution with *Cr** for the 2-fluid and 3-fluid LAMEEs is presented in Figure 6.3. The outlet desiccant solution temperature in the 2-fluid LAMEE is lower than the 3-fluid LAMEE under the entire range of *Cr** tested. However, the difference between the outlet desiccant solution temperatures of the 2-fluid and 3-fluid LAMEEs decreases as *Cr** increases. Also, the outlet desiccant solution temperatures of the 2-fluid and 3-fluid LAMEEs increase as *Cr** increases, however the influence of *Cr** on the outlet desiccant solution temperature of the 2-fluid LAMEE is stronger than the 3-fluid LAMEE. For example, the outlet desiccant solution temperatures of the 2-fluid LAMEE and the 3-fluid LAMEE increase by 5.4ºC and 0.9ºC as *Cr** increases from 1.15 to 5.35, respectively. This is attributed to the refrigerant which increases the heat capacity of the

desiccant solution inside the 3-fluid LAMEE, and thus the variations of the desiccant solution temperature along the exchanger decrease.

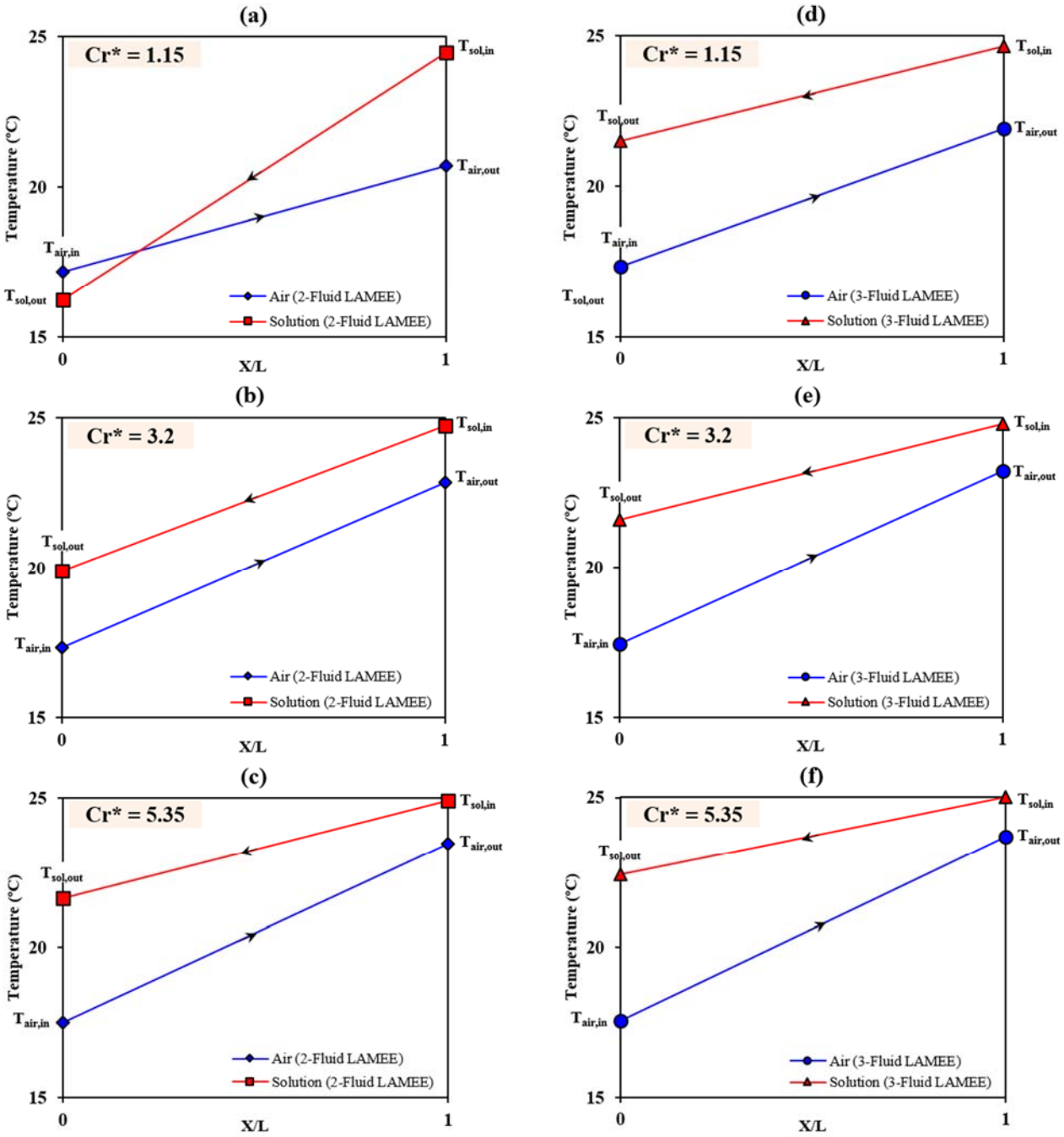

FIGURE 6.3. Inlet and outlet temperatures of the air and desiccant solution at several *Cr** values for the 2-fluid LAMEE ((a), (b) and (c)) and the 3-fluid LAMEE ((d), (e) and (f)) under air heating and humidifying conditions.

6.5.3 Effectiveness Data

Figure 6.4 shows the sensible, latent, and total effectivenesses between the air and desiccant solution at several *Cr** values for the 2-fluid and 3-fluid LAMEEs. It is clear that the effectivenesses of the 2-fluid and 3-fluid LAMEEs increase as *Cr** increases under the entire range of *Cr** tested, however the effect of *Cr** on the improvement in the effectivenesses of the 2-fluid and 3-fluid LAMEEs decreases as *Cr** increases. Also, the effect of *Cr** on the improvement in the sensible and latent effectivenesses of the 2-fluid LAMEE is stronger than the 3-fluid LAMEE. For example, the sensible effectiveness of the 2-fluid LAMEE and 3-fluid LAMEE increases by 26% and 16%, respectively, as *Cr** increases from 1.15 to 3.2 and by 7% and 4%, respectively, as *Cr** increases from 3.2 to 5.35, and the latent effectiveness of the 2-fluid LAMEE and the 3-fluid LAMEE increases by 15% and 10%, respectively, as *Cr** increases from 1.15 to 3.2 and by 4% and 2%, respectively, as *Cr** increases from 3.2 to 5.35. This can be explained as follows. The desiccant solution has a higher heat capacity at higher *Cr** values, which reduces the drop of the desiccant solution temperature along the exchanger and guarantees high differences between the air and desiccant solution temperatures and vapor pressures along the entire length of the exchanger.

The sensible, latent, and total effectivenesses of the 3-fluid LAMEE are higher than the 2-fluid LAMEE under the entire range of *Cr** tested. However, the differences between the effectivenesses of the 3-fluid LAMEE and the 2-fluid LAMEE decrease as *Cr** increases. For example, the absolute improvement in the sensible and latent effectivenesses of the 3-fluid LAMEE compared with the 2-fluid LAMEE are 14% and 8% at *Cr** = 1.15 and 2% and 1% at *Cr** = 5.35, respectively. The improvement in the sensible and latent effectivenesses is attributed to the effect of the refrigerant (water) which keeps the temperature of the desiccant solution almost

constant inside the exchanger, and maintains high differences between the temperature and vapor pressure of the air and desiccant solution along the entire length of the exchanger. The low sensible and latent effectivenesses of the 2-fluid LAMEE at $Cr^* = 1.15$ is attributed to the effect of phase change energy on the desiccant solution temperature, where the desiccant solution temperature decreases below the air temperature near the exchanger inlet (see Figure 6.3 (a)).

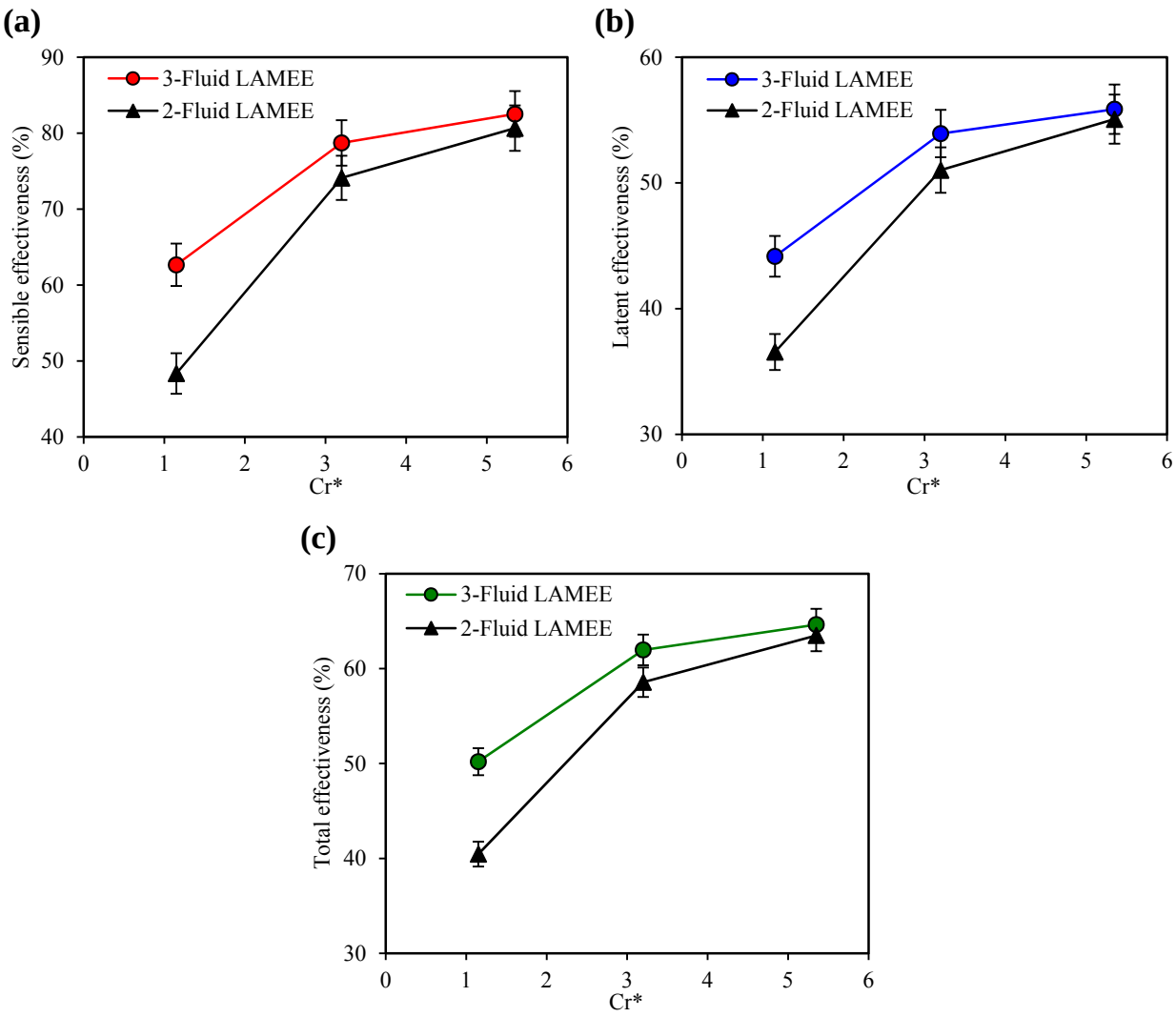

FIGURE 6.4. Comparison between (a) sensible effectivenesses (b) latent effectivenesses (c) total effectivenesses of the 2-fluid LAMEE and the 3-fluid LAMEE at several Cr^* values under air heating and humidifying conditions.

The results presented in Figure 6.4 show that the effectivenesses of the 2-fluid and 3-fluid LAMEEs are almost equal at $Cr^* = 5.3$. These effectiveness trends are similar to the air cooling and dehumidifying conditions presented in Chapter 4 (Abdel-Salam et al. (2016b)). On the other hand, at the same design parameters, number of heat transfer units (*NTU*), and difference between refrigerant and solution temperatures, the results presented in Chapter 5 (Abdel-Salam et al. (2016c)) show that the sensible and latent effectivenesses of the 3-fluid LAMEE are much higher than the 2-fluid LAMEE at $Cr^* = 4.8$ under solution regeneration conditions. This implies that further improvements in the LAMEEs effectiveness are possible at higher Cr^* values (i.e. $Cr^* > 5$) under solution regeneration conditions. This may be due to reduced desiccant crystallization in the 3-fluid LAMEE.

It should be noted that greater improvements in the effectivenesses of the 3-fluid LAMEE can be achieved at higher refrigerant (water) temperatures and mass flow rates under air heating and humidifying operating conditions. However, higher refrigerant temperatures and mass flow rates are accompanied with higher operating costs. Therefore, a techno-economic study of the overall performance of the liquid desiccant membrane HVAC system is necessary to determine the feasibility of installing 3-fluid LAMEEs as the humidifier and regenerator.

6.6 FLOW MALDISTRIBUTION

Since there is no other work in the literature that has experimentally studied flow maldistribution in flat-plate LAMEEs, this section presents an experimental study of the feasibility of pre-tensioning the membrane to reduce flow maldistribution in flat-plate LAMEEs. As mentioned in Chapter 2 (Abdel-Salam et al. (2015)) and Abdel-Salam et al. (2014b), a majority of flow maldistribution in flat-plate LAMEEs may be caused by the deflection of the membrane due to the

high pressure differences between the air and desiccant solution flows. Membrane deflections can be measured before attaching the membrane onto the solution channel frame by applying a pressure difference across the membrane and measuring the membrane deflection. Figure 6.5 shows a device known as the bulge test apparatus that was used to measure the membrane deflections by Larson (2006), Larson et al. (2007) and Beriault (2011). The bulge test apparatus creates a pressure difference across a clamped membrane and measures the membrane deflection with a linear variable displacement transducer (Larson (2006)). Figure 6.5 (b) shows the membrane deflection inside the test cell where the deflection in square membranes can be calculated from equation (6.1) (Larson (2006)).

$$\frac{P}{E} = c_1 \frac{\left(\frac{t}{a}\right)\left(\frac{h}{a}\right)^3}{1-\nu} + c_2 \left(\frac{\sigma_o}{E}\right)\left(\frac{t}{a}\right)\left(\frac{h}{a}\right) \tag{6.1}$$

where P is the applied pressure (Pa), E is the membrane modulus of elasticity (Pa), t is the membrane thickness (m), a is the radius of the bulge test cell (m), h is the membrane deflection (m), ν is Poisson's ratio, σ_o is the pre-stress (Pa), $c_1 = 0.8 + 0.062\,\nu$, and c_2 = 3.393 (Xiang et al. (2005)).

The most accurate technique that can be used to measure the membrane deflection during actual operation of a LAMEE would be to build a LAMEE with transparent walls to be able to visualize the membrane deflections during the LAMEE operation and use laser technology to measure the membrane deflections under different operating conditions.

(a)

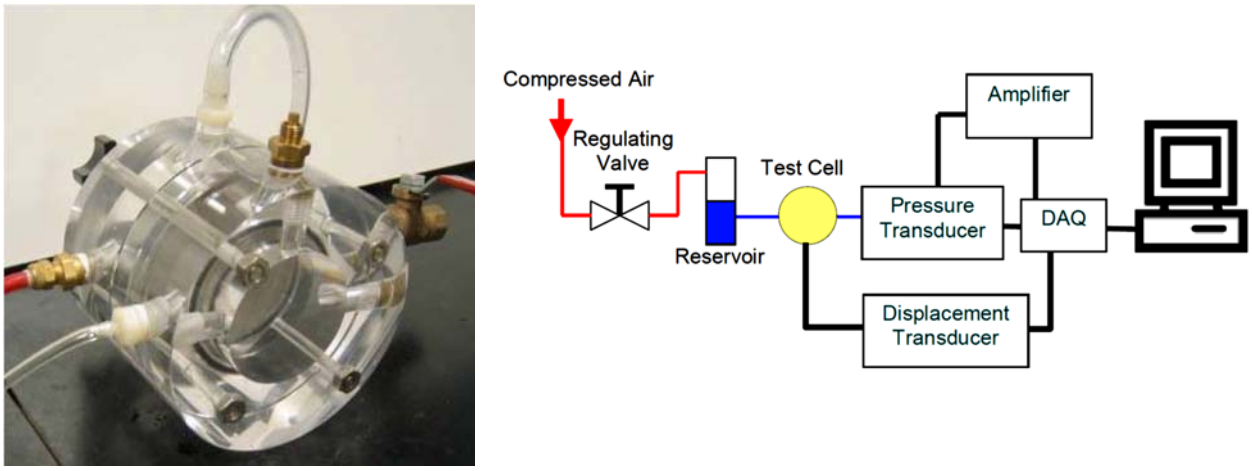

(b)

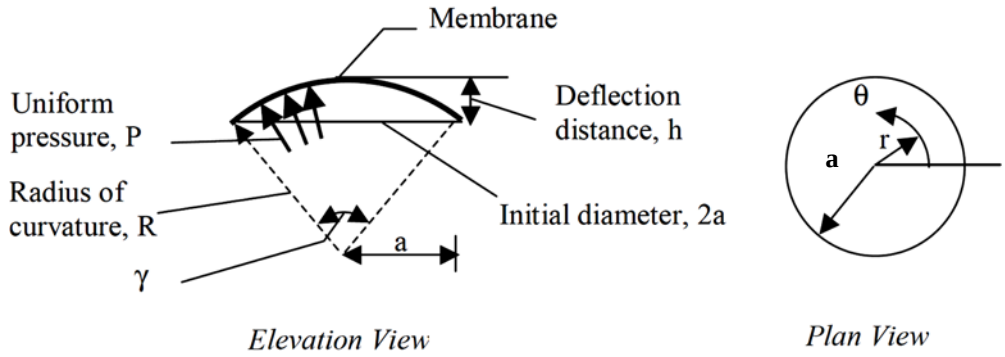

FIGURE 6.5. (a) Photograph of the bulge test apparatus (b) schematic of the membrane deflection in the test cell (Larson (2006)).

The following techniques can be applied to minimize flow maldistribution caused by membrane deflections in LAMEEs.

1. Select a membrane with a high modulus of elasticity.
2. The nominal air and solution channel widths should be ≥ 5 mm and ≤ 2 mm, respectively (Chapter 2; Abdel-Salam et al. (2015)),
3. Install a supporting insert inside the air channels (see Figure 3.6),
4. Attach support grids on both sides of the membrane (see Figure 3.6),
5. Pre-tension the membrane before attaching it onto the solution channel frame. Larson (2006)

reported that membrane deflections could be reduced if pre-tension is applied to the membrane,

6. Operate the LAMEE with low pressure differences across the membrane.

Among the membrane thermo-physical properties, the membrane modulus of elasticity has a strong influence on the membrane deflections where membranes with low modulus of elasticity are vulnerable to large deflections during operation. Therefore, the membrane deflections can be reduced if membranes with high modulus of elasticity are used in LAMEEs. Table 6.2 shows the modulus of elasticity of several commercial membranes measured by Beriault (2011).

TABLE 6.2. Modulus of elasticity of several commercial membranes (Beriault (2011)).

Membrane	Modulus of elasticity (MPa)
Porex® PM3V	12
Porex® PM6M	16
Propore™	17
Tredegar #2	45
Japanese Tyvek®	382
AY Tech ePTFE Laminate	387

6.6.1 Liquid Marine Glue (No Pre-tension)

Techniques 1 to 4 were applied during the fabrication of the 3-fluid LAMEE prototype used to perform the experimental work presented in Chapter 3 (Abdel-Salam et al. (2016a)). The membrane was attached onto the solution channel frame using a liquid marine glue. During the drying of the liquid glue, the pre-tension in the membrane was significantly diminished, therefore only techniques 1 to 3 were effective in this set of tests. The exchanger was tested under air cooling and dehumidifying conditions (maximum air/solution temperature was 36ºC and low pressure difference across the membrane ($Cr^* < 2$)) for 70 hours over five consecutive days. Thereafter,

the 3-fluid LAMEE was disassembled and the membrane was visually inspected (see the picture in Figure 6.6 (a)).

(a)

(b)

FIGURE 6.6. Photographs of the semi-permeable membrane of the 3-fluid LAMEE at the end of testing for the case where the membrane was pre-tensioned but tension was significantly diminished during the drying of the liquid glue used to attach the membrane onto the solution channel frame (a) and the membrane was pre-tensioned and was attached onto the solution channel frame using a double-sided tape to maintain the membrane pre-tension (b).

It is clear from Figure 6.6 (a) that there is bulging over the entire surface area of the membrane. This implies that there is likely even more bulging during operation of the exchanger when the desiccant solution is pressurized. Measuring the effect of flow maldistribution on the performance of flat-plate LAMEEs is a complex challenge due to the nature of the membrane deflection which depends on multiple parameters (i.e. the exchanger design parameters, ratio between desiccant solution and air mass flow rates, type and properties of the membrane, age of the membrane,

process of gluing the membrane onto the solution channel frame, etc.). Shang and Besant (2004) developed equations to calculate the deterioration in the effectiveness of energy wheels due to flow maldistribution, and these equations were used to investigate the effects of flow maldistribution on the performance of flat-plate LAMEEs in Chapter 2 (Abdel-Salam et al. (2015)). It was found in Section 2.8.5 that the effectiveness of flat-plate LAMEEs decreases as the magnitude of flow maldistribution due to bulging increases.

Based on membrane deflections observed in the disassembled exchanger (see the picture in Figure 6.6 (a)), the standard deviation of the hydraulic diameters of air channels of the 3-fluid LAMEE is estimated to be 1.6 mm. It should be noted that depending on the operating parameters, larger standard deviations may have occurred during the LAMEE operation.

The 3-fluid LAMEE tested in Chapter 3 (Abdel-Salam et al. (2016a)) is a small-scale prototype with only two air channels and one solution channel. This implies that the membrane deflections caused by the pressure difference between the air and solution flows decreased the width of the air channels during the LAMEE operation which increased the airside convective heat transfer coefficient. Therefore, the higher airside convective heat transfer coefficient would have increased the effectiveness of the small-scale 3-fluid LAMEE tested in Chapter 3 (Abdel-Salam et al. (2016a)) compared to an exchanger without membrane deflections. Based on the membrane deflections observed in the disassembled exchanger, it is estimated that the air channel width was reduced during the 3-fluid LAMEE operation from 5 mm to approximately 4 mm due to membrane deflections. According to the numerical study presented in Chapter 2 (Abdel-Salam et al. (2015)), the increase in the effectiveness of the small-scale 3-fluid LAMEE due to reduced air channel width caused by membrane deflections is estimated to be 5%.

Unlike the small-scale 3-fluid LAMEE which has only two air channels and one solution channel, LAMEEs used in practical HVAC applications are full-scale exchangers with multiple air and solution channels. In full-scale 3-fluid LAMEEs, membrane deflections will result in variations in the solution channels width and thus uneven distribution of the solution inside the exchanger where some solution channels will have a higher solution flow rate than the design value while other solution channels will have a less solution flow rate than the design value. This will result in variations in the air channels width where some air channels will have larger widths and thus lower convective heat transfer coefficients and higher mass flow rates than the design value. Equation (2.7) shows that decreasing the airside convective heat transfer coefficient while maintaining the membrane surface area and mass flow rate constant will decrease the *NTU* (number of heat transfer units). Therefore, membrane deflections may reduce the effectiveness of full-scale 3-fluid LAMEEs. Assuming that the effectiveness of the full-scale 3-fluid LAMEE will be the same as the small-scale 3-fluid LAMEE tested in Chapter 3 (Abdel-Salam et al. (2016a)), and based on the membrane deflections observed in the disassembled exchanger, and the studies presented by Shang and Besant (2004) and in Chapter 2 (Abdel-Salam et al. (2015)), Figure 6.7 (a) shows that the effectiveness of a full-scale 3-fluid LAMEE with mean air channels width of 5 mm and $\sigma/D_o = 0.16$ can be reduced by up to 5% due to flow maldistribution caused by membrane deflections.

Another assumption is that during the operation of the full-scale 3-fluid LAMEE, the pressure on the solution side will be always higher than on the airside. Therefore, the membrane deflections will decrease all air channel widths and thus the mean hydraulic diameter of the air channels will be smaller than the design value (i.e. the thickness of the air channel insert). Assuming that the mean hydraulic diameter will be 4 mm (as assumed for the small-scale prototype based on

Figure 6.6 (a)), then the standard deviation of the air channels hydraulic diameter of 1.6 mm will result in $\sigma/D_o = 0.2$. Figure 6.7 (b) shows that the flow maldistribution caused by variations in air channel widths can degrade the effectiveness of a full-scale 3-fluid LAMEE with mean air channel hydraulic diameter of 4 mm and $\sigma/D_o = 0.2$ by up to 7%.

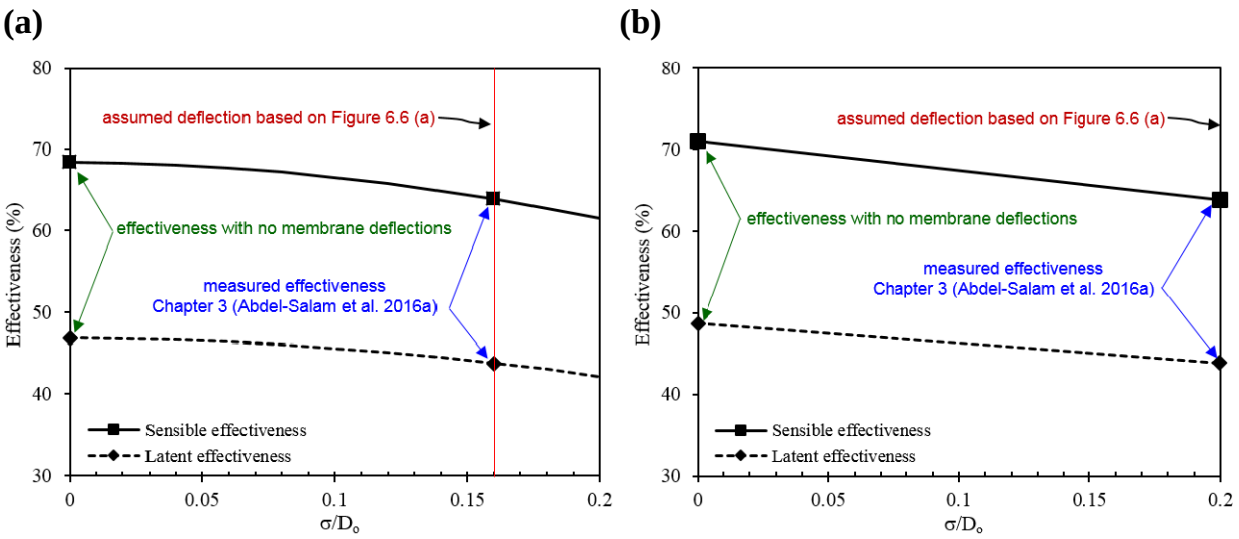

FIGURE 6.7. Effect of membrane deflections (σ/D_o) on sensible and latent effectivenesses of a full-scale 3-fluid LAMEE with mean air channel hydraulic diameter of (a) 5 mm (b) 4 mm.

6.6.2 Double-Sided Adhesive Tape (Pre-tension)

As mentioned in Section 6.6.1, the 3-fluid LAMEE without membrane pre-tension was disassembled at the end of the testing. Thereafter, the membrane was replaced with a new membrane and the exchanger was reassembled and was used to perform the experiments presented in Chapters 4, 5, and 6. The membrane was attached onto the solution channel frame using a double-sided adhesive tape to maintain the membrane pre-tension. This implies techniques 1 to 4 were effective in this exchanger. The exchanger was tested under air cooling and dehumidifying conditions (Chapter 4), diluted desiccant solution regeneration conditions (Chapter 5), and air

heating and humidifying conditions (Chapter 6). This resulted in approximately 165 hours of testing over eight consecutive months and maximum air/solution temperatures of 63ºC and high pressure difference across the membrane (Cr^* up to 5.3). Compared to the exchanger with no membrane pre-tension (Section 6.6.1), the picture in Figure 6.6 (b) shows that despite the longer testing period, the higher desiccant solution temperatures, and the higher pressure differences across the membrane, there is almost no bulging over the entire surface area of the membrane. This indicates that pre-tensioning the membrane while gluing it onto the solution channel frame has significantly reduced the membrane deflections and flow maldistribution during the LAMEE operation.

6.7 CONCLUSIONS

This chapter presents an experimental study and comparison between the performances of the 3-fluid and 2-fluid LAMEEs at several desiccant solution mass flow rates under air heating and humidifying conditions. Results show that both the sensible and latent effectivenesses of the 3-fluid LAMEE are higher than the 2-fluid LAMEE especially at low Cr^* values, which proves that the research hypothesis of this thesis (i.e. adding a third fluid to control the desiccant solution temperature inside the 3-fluid LAMEE may improve the rates of heat and moisture transfer between the air and desiccant solution compared to 2-fluid LAMEEs) is true under air heating and humidifying conditions. The trends of the 3-fluid and 2-fluid LAMEEs effectivenesses variations with Cr^* are almost similar to the air cooling and dehumidifying conditions presented in Chapter 4 (Abdel-Salam et al. (2016b)), where the effectivenesses improve as Cr^* increases, especially over the low range of Cr^* values, until the effectivenesses of the 3-fluid and 2-fluid LAMEEs are nearly equal at $Cr^* = 5.3$. This trend is different from solution regeneration conditions, where the results presented in Chapter 5 (Abdel-Salam et al. (2016c)) show that further improvements in the sensible

and latent effectivenesses of the solution regenerator can be achieved at higher Cr^* values (i.e. $Cr^* > 5$).

Unlike sensible heat exchangers, results show that at low Cr^* values, the outlet desiccant solution (hot fluid) temperature in 2-fluid LAMEEs can go below the inlet air (cold fluid) temperature due to the effect of the phase change energy accompanied with the air humidification. The feasibility of applying pre-tension to the membrane to reduce the flow maldistribution caused by membrane deflections in flat-plate LAMEEs is experimentally investigated. It is found that pre-tensioning the membrane during the exchanger manufacturing can significantly reduce the membrane deflections in flat-plate LAMEEs provided that the pre-tension in the membrane is maintained while the membrane is attached onto the solution channel frame. Moreover, the numerical results presented in Chapter 2 are used to estimate the effect of flow maldistribution caused by membrane deflections on the degradation of the effectiveness of a full-scale 3-fluid LAMEE. Results show that membrane deflections may reduce the effectiveness of full-scale 3-fluid LAMEEs for the design parameters and operating conditions in this chapter by up to 7%.

CHAPTER 7

PERFORMANCE DEFINITIONS FOR 3-FLUID LAMEES

7.1 OVERVIEW OF CHAPTER 7

In the previous chapters, the performance of heat and moisture transfer between the air and desiccant solution in the 3-fluid LAMEE was tested and measured under several operating conditions. In this chapter, performance definitions for 3-fluid LAMEEs will be presented. The definitions include the heat transfer between the refrigerant and desiccant solution, and are less dependent on the inlet refrigerant temperature than the traditional energy exchanger effectiveness equations. Thus, the overall heat and moisture transfer performances of 3-fluid LAMEEs can be calculated using these definitions. The experimental data presented in Chapter 3 are used to determine and compare the sensible and latent effectivenesses of the 3-fluid LAMEE studied in this thesis when calculated using the traditional energy exchanger effectiveness equations and the definitions presented in this chapter.

This chapter fulfills the third objective (i.e. to present performance definitions for 3-fluid LAMEEs) of this thesis.

The manuscript presented in this chapter was submitted to Transactions of the ASME: Journal of Heat Transfer. The manuscript presented in this chapter is different from the submitted paper in the following sections: the description and schematics of the 3-fluid LAMEE presented in the submitted paper are removed since they were presented in Chapter 3.

Performance Definitions for 3-Fluid Heat and Moisture Exchangers

(Submitted to *Transactions of the ASME: Journal of Heat Transfer*)

Mohamed R. H. Abdel-Salam, Robert W. Besant, Carey J. Simonson

7.2 ABSTRACT

This chapter presents performance definitions for calculating the overall effectiveness of 3-fluid heat and moisture exchangers. The 3-fluid heat and moisture exchanger considered in this chapter is a combination of a liquid-to-liquid heat exchanger for heat transfer between a desiccant solution and a refrigerant and an energy exchanger for heat and moisture transfer between desiccant solution and air streams. The performance definitions presented in this chapter are used to calculate the overall sensible and latent effectivenesses of the 3-fluid LAMEE using the experimental data presented in Chapter 3 (Abdel-Salam et al. (2016a)). The effectiveness of the 3-fluid LAMEE is compared when calculated using the traditional energy exchanger effectiveness equations and the overall performance definitions. Results show that the overall performance definitions provide effectiveness values that are less sensitive to changes in the inlet refrigerant temperature and therefore are more generally applicable for energy exchanger design than the traditional effectiveness equations used in the literature.

7.3 INTRODUCTION

Over the last decade, research has shown that liquid desiccant heat and moisture exchangers (energy exchangers) may achieve considerable energy savings when integrated with heating, ventilation, and air-conditioning (HVAC) systems (Abdel-Salam et al. (2014c); Abdel-Salam and Simonson (2014a); Ge et al. (2013a); Bergero and Chiari (2011)). A liquid desiccant energy exchanger can be used either for air dehumidification or diluted desiccant solution regeneration applications. In liquid desiccant energy exchangers, heat and moisture are transferred between air

and desiccant solution streams. Liquid desiccant energy exchangers can be classified according to the heat and moisture transfer process as direct-contact energy exchangers and indirect-contact (membrane) energy exchangers. The main concern in direct-contact liquid desiccant energy exchangers is the carryover of desiccant droplets within the air stream which decreases the life time of the exchanger and other equipment due to corrosion and may cause adverse impacts on the occupants' health. The novelty of liquid desiccant membrane energy exchangers is that the air and desiccant solution streams are separated by a semi-permeable membrane which prevents the transfer of the liquid desiccant into the airstream.

Over the last decade, numerous theoretical and experimental studies have been performed to enhance the effectiveness of liquid desiccant energy exchangers by determining the optimum design and operating parameters (Abdel-Salam and Simonson (2016); Abdel-Salam et al. (2014b, 2015); Huang and Zhang (2013)). Recently, the design of liquid desiccant energy exchangers has been modified by adding a third fluid (refrigerant) inside the solution channels to cool/heat the desiccant solution within the exchanger. The new design is referred to as a 3-fluid energy exchanger. It was found in Chapters 3 and 5 (Abdel-Salam et al. (2016a, 2016c)) that under the same design and operating parameters, the rates of heat and moisture transfer between the air and desiccant solution in a 3-fluid energy exchanger are higher than 2-fluid energy exchangers. The main objectives of this chapter are:

(1) To present equations which include the third fluid (i.e. the refrigerant) to calculate the overall sensible and latent effectivenesses of 3-fluid energy exchangers.
(2) To use experimental data from a specific 3-fluid energy exchanger to verify the overall effectiveness equations for 3-fluid energy exchangers.

7.4 PERFORMANCE EVALUATION OF 3-FLUID ENERGY EXCHANGERS

Effectiveness is the most widely used dimensionless parameter to quantify the performance of heat and moisture exchangers. It is especially useful in the design of heat exchangers because the effectiveness is nearly constant over a wide range of operating temperatures. The traditional equations used to calculate the sensible and latent effectivenesses (equations (7.1) and (7.2)) of the 2-fluid heat and moisture exchangers can be used to evaluate the performance of heat and mass transfer between the air and desiccant solution streams in 3-fluid energy exchangers.

$$\varepsilon_{\text{sen}} = \frac{\text{actual heat transfer rate}}{\text{maximum possible heat transfer rate}} = \frac{T_{\text{air,in}} - T_{\text{air,out}}}{T_{\text{air,in}} - T_{\text{sol,in}}} \tag{7.1}$$

$$\varepsilon_{\text{lat}} = \frac{\text{actual moisture transfer rate}}{\text{maximum possible moisture transfer rate}} = \frac{W_{\text{air,in}} - W_{\text{air,out}}}{W_{\text{air,in}} - W_{\text{sol,in}}} \tag{7.2}$$

where $T_{\text{air,in}}$ is the inlet air temperature (ºC), $T_{\text{air,out}}$ is the outlet air temperature (ºC), $T_{\text{sol,in}}$ is the inlet solution temperature (ºC), $W_{\text{air,in}}$ is the inlet air humidity ratio (g_v/kg_{air}), $W_{\text{air,out}}$ is the outlet air humidity ratio (g_v/kg_{air}), and $W_{\text{sol,in}}$ is the inlet solution humidity ratio (g/kg).

The physical meaning of sensible/latent effectiveness of an energy exchanger is the ratio between the actual heat/moisture transfer rate and the maximum possible heat/moisture transfer rate between the working fluids inside the exchanger. This implies that sensible/latent effectiveness of an energy exchanger should be ≤ 1. However, using equations (7.1) and (7.2) to calculate the effectivenesses of heat and moisture transfer between the air and desiccant solution in 3-fluid LAMEEs give effectiveness values ≥ 1 under specific operating conditions (see Figures 3.12, 5.3, and 5.7) (Abdel-Salam et al. (2016a, 2016c)), which contradicts the physical definition of the energy exchangers effectiveness equations. This implies that equations (7.1) and (7.2) do not give an accurate indication of the overall performance of 3-fluid energy exchangers because the

denominator (maximum possible heat/moisture transfer) does not consider the refrigerant (i.e. the third fluid). Therefore, there is a need to modify these equations to be used to calculate the overall sensible and latent effectivenesses of 3-fluid energy exchangers.

Furthermore, the experimental results presented in Chapter 3 (Abdel-Salam et al. (2016a)) show that the effectiveness values calculated using equations (7.1) and (7.2) are strongly dependent on the temperature of the refrigerant which reduces the benefit of effectiveness as a universal dimensionless parameter. Therefore, there is a desire to modify the effectiveness equations (equations (7.1) and (7.2)) to provide a dimensionless parameter that is constant for a range of operating temperatures. Such relations would be more valuable for energy exchanger design and application of 3-fluid energy exchangers. These relations would also reduce the number of tests required to quantify the performance of 3-fluid energy exchangers because the effectiveness at one operating condition could be applied for a broader range of operating conditions.

7.4.1 Sensible Effectiveness of 3-Fluid Heat Exchangers

A 3-fluid heat exchanger is used to transfer heat between three fluid streams: a cold fluid (c), an intermediate fluid (i), and a hot fluid (h). Shrivastava and Ameel (2004) reported that the sensible effectiveness of a 3-fluid heat exchanger can be calculated based on its operational objective (i.e. cooling a hot fluid, heating a cold fluid, cooling an intermediate fluid, or heating an intermediate fluid). When a 3-fluid heat exchanger is used to cool a hot fluid (air cooling and humidifying/dehumidifying) where the hot fluid stream has a counter-flow configuration with the other two fluid streams, if the heat capacity of the hot fluid is lower than the heat capacities of the other two fluids, the sensible effectiveness of this 3-fluid heat exchanger can be calculated from equation (7.3) (Shrivastava and Ameel (2004)), whereas the sensible effectiveness of this 3-fluid heat exchanger is calculated from equation (7.4) if the heat capacity of the hot fluid is greater than

the heat capacities of the other two fluids (Shrivastava and Ameel (2004)).

$$\varepsilon_{\text{sen}} = \frac{T_{\text{h,in}} - T_{\text{h,out}}}{T_{\text{h,in}} - T_{\text{c,in}}} \tag{7.3}$$

$$\varepsilon_{\text{sen}} = \frac{C_{\text{h}} \left(T_{\text{h,in}} - T_{\text{h,out}}\right)}{C_{\text{i}} \left(T_{\text{h,in}} - T_{\text{i,in}}\right) + C_{\text{c}} \left(T_{\text{h,in}} - T_{\text{c,in}}\right)} \tag{7.4}$$

where $T_{\text{h,in}}$ is the inlet hot fluid temperature (ºC), $T_{\text{h,out}}$ is the outlet hot fluid temperature (ºC), $T_{\text{c,in}}$ is the inlet cold fluid temperature (ºC), $T_{\text{i,in}}$ is the inlet intermediate fluid temperature (ºC), C_{h} is the heat capacity of the hot fluid (W/K), C_{i} is the heat capacity of the intermediate fluid (W/K), and C_{c} is the heat capacity of the cold fluid (W/K).

When a 3-fluid heat exchanger is used to heat a cold fluid (air heating and humidifying/dehumidifying or desiccant solution regeneration) where the cold fluid stream has a counter-flow configuration with the other two fluid streams, if the heat capacity of the cold fluid is lower than the heat capacities of the other two fluids, the sensible effectiveness of this 3-fluid heat exchanger can be calculated from equation (7.5) (Shrivastava and Ameel (2004)), whereas the sensible effectiveness of this 3-fluid heat exchanger is calculated from equation (7.6) if the heat capacity of the cold fluid is greater than the heat capacities of the other two fluids (Shrivastava and Ameel (2004)).

$$\varepsilon_{\text{sen}} = \frac{T_{\text{c,out}} - T_{\text{c,in}}}{T_{\text{h,in}} - T_{\text{c,in}}} \tag{7.5}$$

$$\varepsilon_{\text{sen}} = \frac{C_{\text{c}} \left(T_{\text{c,out}} - T_{\text{c,in}}\right)}{C_{\text{i}} \left(T_{\text{i,in}} - T_{\text{c,in}}\right) + C_{\text{h}} \left(T_{\text{h,in}} - T_{\text{c,in}}\right)} \tag{7.6}$$

where $T_{\text{c,out}}$ is the outlet cold fluid temperature (ºC).

The results presented in Chapters 3 and 4 (Abdel-Salam et al. (2016a, 2016b)) showed that in order

to attain acceptable performance (effectiveness and moisture removal rate) of 3-fluid energy exchangers when used for air cooling and dehumidifying applications, the following criteria should be maintained: (1) the desiccant solution temperature should be lower than the air temperature, (2) the refrigerant temperature should be lower than the desiccant solution and air temperatures, (3) the desiccant solution heat capacity rate should be greater than the air heat capacity rate ($Cr^* > 1$), and (4) the refrigerant heat capacity rate should be greater than the desiccant solution heat capacity rate ($Cr < 1$). Therefore, equation (7.3) can be used to calculate the sensible effectiveness of 3-fluid energy exchangers when used for air cooling and dehumidifying applications.

The results presented in Chapters 5 and 6 (Abdel-Salam et al. (2016c, 2016d)) showed that in order to achieve acceptable performance of 3-fluid energy exchangers when used for air heating and humidifying/diluted desiccant solution regeneration applications, the following criteria should be maintained: (1) the desiccant solution temperature should be higher than the air temperature, (2) the refrigerant temperature should be higher than the desiccant solution and air temperatures, (3) the desiccant solution heat capacity rate should be greater than the air heat capacity rate ($Cr^* > 1$), and (4) the refrigerant heat capacity rate should be greater than the desiccant solution heat capacity rate ($Cr < 1$). Therefore, equation (7.5) can be used to calculate the sensible effectiveness of 3-fluid energy exchangers when used for air heating and humidifying/diluted desiccant solution regeneration applications.

It is worth mentioning that 3-fluid energy exchangers are used to improve the heat and moisture transfer between the air and desiccant solution streams by controlling the desiccant solution temperature and eliminating the effect of phase change energy. In air cooling and humidifying/air heating and dehumidifying processes, the phase change energy reduces/raises the desiccant solution temperature which enhances the rates of heat and moisture transfer and thus the

exchanger's performance (effectiveness and moisture transfer rate) is enhanced. Therefore, it will be difficult to apply 3-fluid energy exchangers for air cooling and humidifying/air heating and dehumidifying applications. 3-fluid energy exchangers are not likely to be recommended in these applications where the heat and moisture transfer are in opposite directions.

7.4.2 Sensible Effectiveness of 3-Fluid Energy Exchangers

Applying equation (7.3) to 3-fluid energy exchangers when used to cool and dehumidify a hot-humid airstream for typical case of HVAC applications (i.e. the heat capacity rate of the air is lower than the heat capacity rates of the other two fluids (desiccant solution and refrigerant), and the inlet refrigerant temperature is lower than the inlet desiccant solution temperature), the sensible effectiveness of a 3-fluid energy exchanger can be calculated from equation (7.7).

$$\varepsilon_{\text{sen}} = \frac{T_{\text{air,in}} - T_{\text{air,out}}}{T_{\text{air,in}} - T_{\text{ref,in}}} \tag{7.7}$$

where $T_{\text{air,in}}$ is the inlet air temperature (ºC), $T_{\text{air,out}}$ is the outlet air temperature (ºC), and $T_{\text{ref,in}}$ is the inlet refrigerant temperature (ºC).

Applying equation (7.5) to 3-fluid energy exchangers when used for air heating and humidifying/desiccant solution regeneration for typical case of HVAC applications (i.e. the heat capacity rate of the air is lower than the heat capacity rates of the desiccant solution and refrigerant, and the inlet refrigerant temperature is higher than the inlet desiccant solution temperature), the sensible effectiveness of a 3-fluid energy exchanger can be calculated from equation (7.8).

$$\varepsilon_{\text{sen}} = \frac{T_{\text{air,out}} - T_{\text{air,in}}}{T_{\text{ref,in}} - T_{\text{air,in}}} \tag{7.8}$$

Figure 7.1 shows a comparison between the maximum possible heat transfer rates in 2-fluid and 3-fluid energy exchangers under air cooling and dehumidifying operating conditions. It is clear

that adding a third fluid (i.e. refrigerant) within the solution channels in 3-fluid energy exchangers increases the maximum possible heat transfer between the air and desiccant solution. In 3-fluid energy exchangers, the refrigerant is cooler than the desiccant solution under air cooling and dehumidifying operating conditions, where the temperature of the desiccant solution can become equal to the inlet refrigerant temperature inside the exchanger if the sensible effectiveness of heat transfer between the desiccant solution and refrigerant is 1.0. Therefore, the maximum possible heat transfer in 3-fluid energy exchangers is the difference between the inlet air and refrigerant temperatures, which is greater than 2-fluid energy exchangers.

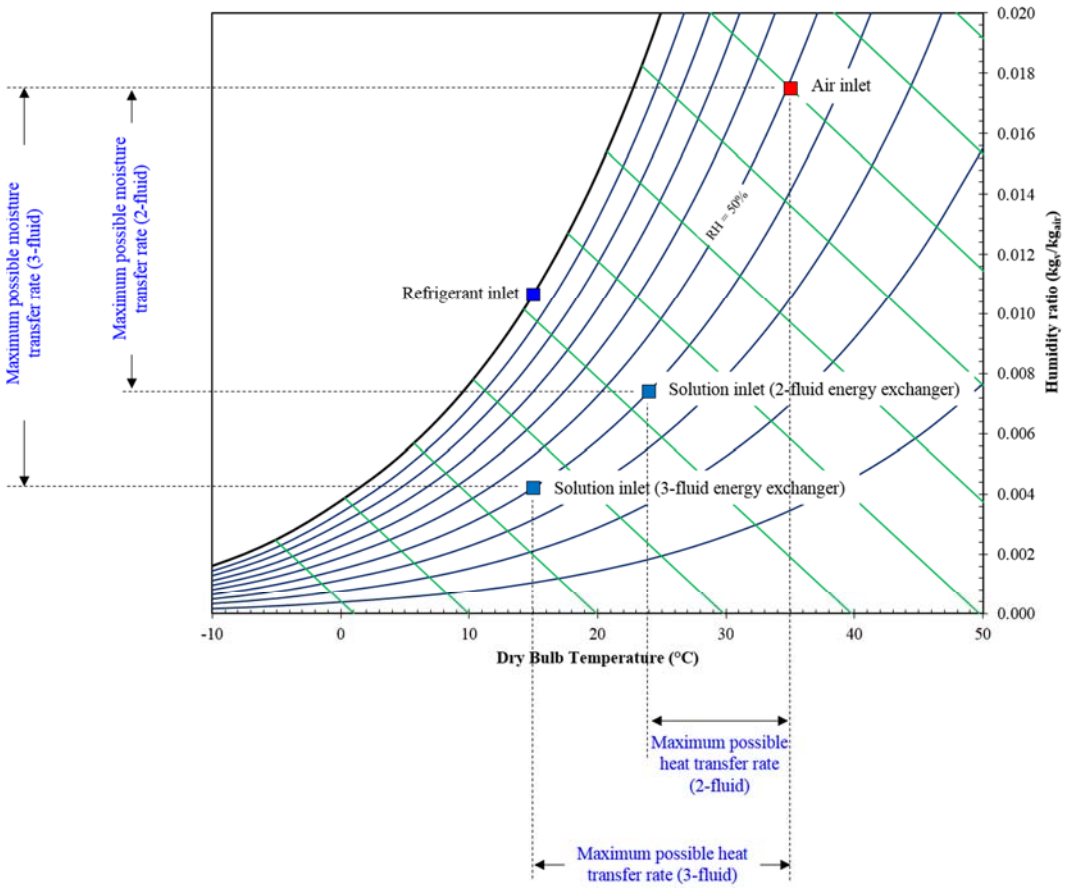

FIGURE 7.1. Comparison between maximum possible heat and moisture transfer rates in the 2-fluid and 3-fluid energy exchangers under air cooling and dehumidifying operating conditions.

7.4.3 Latent Effectiveness of 3-Fluid Energy Exchangers

In 3-fluid energy exchangers, the actual moisture transfer rate depends on the difference between the inlet and outlet air humidity ratios, while the maximum possible rate of moisture transfer depends on the difference between the inlet air humidity ratio and the equivalent humidity ratio of the desiccant solution calculated at the inlet refrigerant temperature and inlet desiccant solution concentration. For air cooling and dehumidifying process (i.e. $T_{ref,in} \leq T_{sol,in}$) and air heating and humidifying/desiccant solution regeneration processes (i.e. $T_{ref,in} \geq T_{sol,in}$), the latent effectiveness of a 3-fluid energy exchanger can be calculated from equation (7.9).

$$\varepsilon_{lat} = \left| \frac{W_{air,in} - W_{air,out}}{W_{air,in} - W_{sol,in\ @C_{sol,in}\ \&\ T_{ref,in}}} \right| \tag{7.9}$$

where $W_{air,in}$ is the inlet air humidity ratio (g_v/kg_{air}), $W_{air,out}$ is the outlet air humidity ratio (g_v/kg_{air}), and $W_{sol,in\ @C_{sol,in}\ \&\ T_{ref,in}}$ is the equivalent inlet desiccant solution humidity ratio calculated at inlet desiccant solution concentration and inlet refrigerant temperature (g/kg).

Figure 7.1 shows that compared to 2-fluid energy exchangers, adding a third fluid (i.e. refrigerant) within the solution channels in 3-fluid energy exchangers increases the maximum possible moisture transfer between the air and desiccant solution. The inlet refrigerant temperature in 3-fluid energy exchangers is lower than the inlet desiccant solution temperature under air cooling and dehumidifying operating conditions, where the temperature of the desiccant solution can become equal to the inlet refrigerant temperature inside the exchanger if the sensible effectiveness of heat transfer between the refrigerant and desiccant solution is 1.0. Cooling the desiccant solution while keeping its concentration nearly constant results in a decrease in its equivalent humidity ratio. Therefore the maximum possible moisture transfer in 3-fluid energy exchangers is the difference between the inlet air humidity ratio and the equivalent desiccant solution humidity ratio

calculated at inlet desiccant solution concentration and inlet refrigerant temperature.

7.5 RESULTS AND DISCUSSION

The rates of heat and moisture transfer between the air and desiccant solution in the 3-fluid LAMEE studied in this thesis were tested and calculated under different operating conditions in Chapters 3, 4, 5 and 6. In this section, the experimental data presented in Chapter 3 (Abdel-Salam et al. (2016a)) are used to calculate the sensible and latent effectivenesses of the 3-fluid LAMEE using the traditional effectiveness equations (equations (7.1) and (7.2)) and the overall effectiveness equations which include the refrigerant loop (equations (7.7) and (7.9)).

7.5.1 Sensible and Latent Effectivenesses at Several Inlet Refrigerant Temperatures

In this section, the sensible and latent effectivenesses of the 3-fluid LAMEE are presented at several inlet cooling water temperatures and constant cooling water mass flow rate (Cr = 0.26) in Figure 7.2.

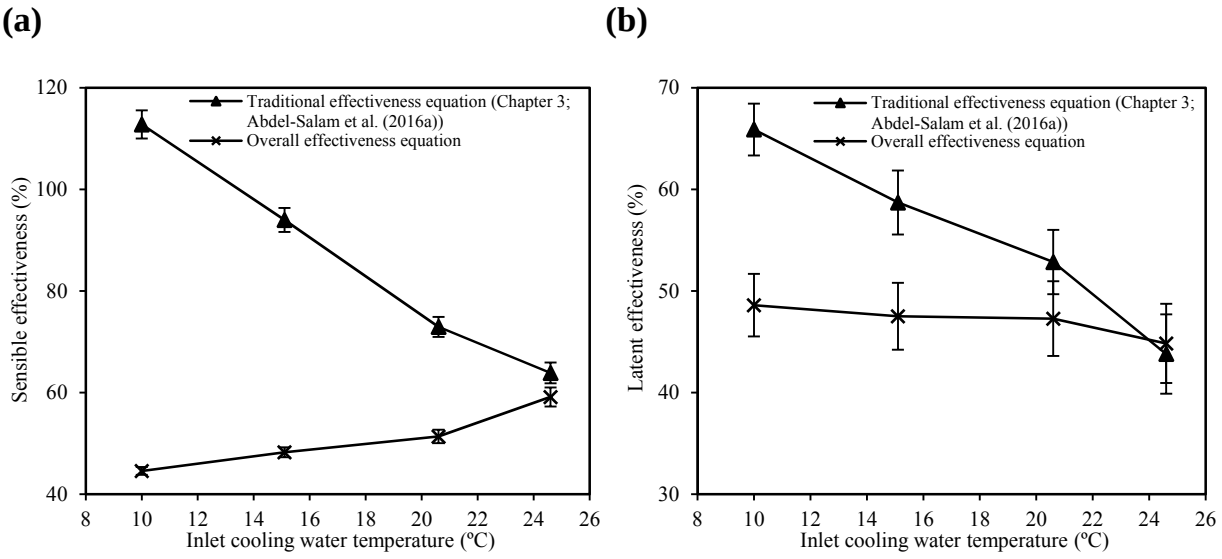

FIGURE 7.2. Comparison between (a) sensible effectivenesses (b) latent effectivenesses of the 3-fluid LAMEE calculated using the traditional and overall effectiveness equations at several inlet cooling water temperatures.

From Figure 7.2 (a) it is clear that the traditional effectiveness equation predicts a higher sensible effectiveness than the overall effectiveness equation, especially at low inlet cooling water temperatures. The overall effectiveness equation (equation (7.7)) results in sensible effectiveness values that are less dependent on the inlet cooling water temperature. Unfortunately, the overall effectiveness values are also dependent on the inlet refrigerant temperature because of the conjugate heat and moisture transfer between the air and desiccant solution, where the amount of phase change energy released during moisture absorption by the desiccant solution increases as inlet cooling water temperature decreases. The phase change energy released during moisture absorption by the desiccant solution is not considered in the overall effectiveness equation (equation (7.7)), and therefore the sensible effectiveness is not totally constant with inlet cooling water temperature.

The slight decrease in sensible effectiveness, calculated using the overall effectiveness equation, with inlet cooling water temperature can be explained as follow. Decreasing the inlet cooling water temperature results in a decrease in the desiccant solution temperature which decreases the outlet air temperature. However, the amount of phase change energy released during moisture absorption by the desiccant solution increases as the inlet cooing water temperature decreases, which reduces the decrease in the outlet air temperature. On the other hand, decreasing the inlet cooling water temperature increases the maximum possible amount of heat transfer inside the exchanger. The sensible effectiveness of the 3-fluid LAMEE decreases as the inlet cooling water temperature decreases because the enhancement in the actual sensible heat transfer rate is less than the increase in the maximum possible heat transfer rate in the exchanger (see equation (7.7)). The actual sensible heat transfer rate in 3-fluid energy exchangers depends on the amount of phase change energy released during moisture transfer and the effectiveness of heat transfer between the cooling

water and desiccant solution, which depends on several design and operating parameters (i.e. number of heat transfer units (*NTU*) and heat capacity ratio between the solution and cooling water flows (*Cr*)). Therefore, increasing the *NTU* or *Cr* between the solution and cooling water will improve the actual rate of heat transfer between the air and solution.

Figure 7.2 (b) shows the latent effectiveness of the 3-fluid LAMEE calculated using the traditional and overall effectiveness equations at several inlet cooling water temperatures. Similar to the sensible effectiveness, the traditional effectiveness equation provides a higher latent effectiveness value that is much more dependent on the inlet cooling water temperature. Compared to the traditional equation, Figure 7.2 (b) shows that the inlet cooling water temperature has a negligible effect on the latent effectiveness calculated using the overall effectiveness equation. The constant value of the latent effectiveness at several inlet cooling water temperatures means that the overall effectiveness equation is more universal and can be used for design and application over a range of refrigerant temperatures. The constant value of the latent effectiveness at several inlet cooling water temperatures can be explained as follows. Decreasing the inlet cooling water temperature results in lower outlet air temperature and humidity ratio and lower inlet solution equivalent humidity ratio (see equation (7.9)). The negligible effect of the inlet cooling water temperature on the latent effectiveness as inlet cooling water temperature decreases implies that the enhancement in the actual moisture transfer rate (i.e. the decrease in the outlet air humidity ratio) is almost equal to the enhancement in the maximum possible moisture transfer rate (i.e. the decrease in the inlet solution equivalent humidity ratio).

7.5.2 Sensible and Latent Effectivenesses at Several Refrigerant Mass Flow Rates

In this section, the sensible and latent effectivenesses of the 3-fluid LAMEE are presented at several cooling water mass flow rates (*Cr*) and constant inlet cooling water temperature

($T_{w,in}$ = 20.6ºC). It is worth mentioning that value of *Cr* is changed by changing the mass flow rate of the cooling water, while the mass flow rate of the desiccant solution is maintained constant for all values of *Cr* in order to maintain the value of *Cr** constant.

Figure 7.3 shows the sensible and latent effectivenesses of the 3-fluid LAMEE calculated using the traditional and overall effectiveness equations at several cooling water mass flow rates. The traditional equations predict higher sensible and latent effectivenesses values. The sensible and latent effectivenesses increase as *Cr* increases for both effectiveness definitions. This is expected from the ε-NTU heat exchanger theory where decreasing *Cr* (i.e. increasing the cooling water flow rate) results in an increase in the sensible effectiveness between the cooling water and desiccant solution, thus the average temperature and equivalent humidity ratio of the desiccant solution inside the exchanger decrease which results in lower outlet air temperature and humidity ratio. On the other hand, decreasing *Cr* (i.e. increasing the cooling water flow rate) has no effect on the maximum possible rates of heat and moisture transfer inside the exchanger. Equation (7.7) shows that decreasing the outlet air temperature, while keeping the inlet air and inlet cooling water temperatures constant, results in an increase in the sensible effectiveness of 3-fluid energy exchangers. As well, equation (7.9) shows that latent effectiveness of 3-fluid energy exchangers increases by decreasing the outlet air humidity ratio while keeping the inlet air humidity ratio and inlet desiccant solution equivalent humidity ratio constant.

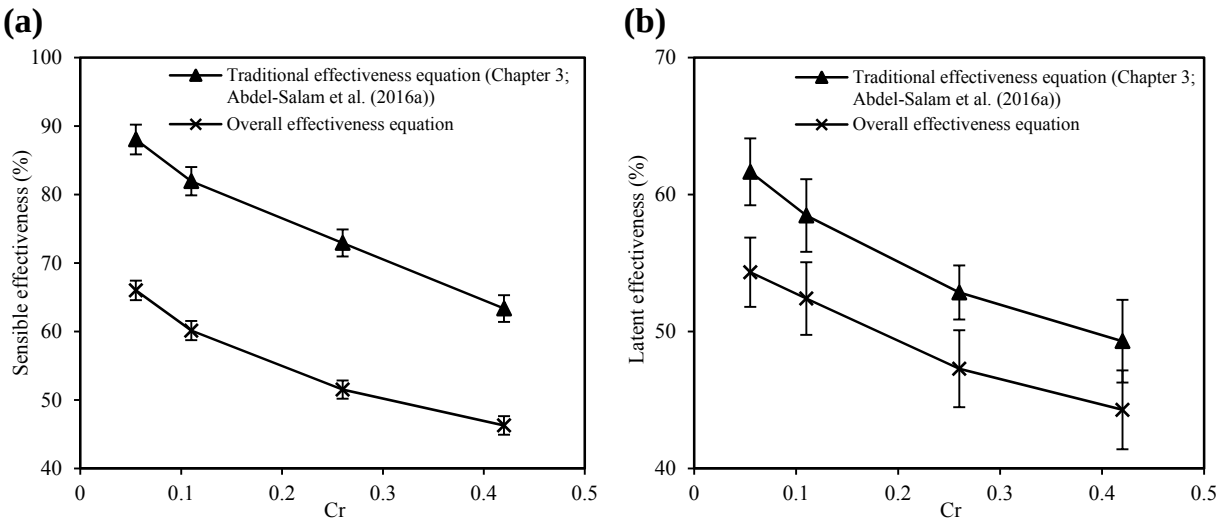

FIGURE 7.3. Comparison between (a) sensible effectivenesses (b) latent effectivenesses of the 3-fluid LAMEE calculated using the traditional and overall effectiveness equations at several cooling water mass flow rates.

7.6 CONCLUSIONS

The main contribution of this chapter is that it presents equations to calculate the overall effectiveness of 3-fluid energy exchangers. The sensible and latent effectivenesses of the 3-fluid LAMEE developed in this thesis have been calculated using the traditional energy exchanger effectiveness equations and the overall effectiveness equations. Traditional equations evaluate the effectiveness of 3-fluid LAMEEs based only on the performance of heat and moisture transfer process between the air and desiccant solution and excludes the refrigerant loop. On the other hand, the overall effectiveness equations evaluate the effectiveness of 3-fluid LAMEEs based on heat and moisture transfer process between the air and desiccant solution and the heat transfer process between the refrigerant and desiccant solution. Results show that the overall effectiveness equations are less dependent on the refrigerant temperature than the traditional effectiveness equations, and the traditional equations predict higher values of sensible and latent effectivenesses of 3-fluid energy exchangers. It is concluded that the overall effectiveness equations are more universal for calculating sensible and latent effectivenesses of 3-fluid energy exchangers.

CHAPTER 8

SUMMARY, CONCLUSIONS, CONTRIBUTIONS AND FUTURE WORK

The main goal of the thesis research was to develop a novel 3-fluid LAMEE that has higher rates of heat and moisture transfer between the air and desiccant solution than conventional 2-fluid LAMEEs. Three main objectives were set to meet the main goal of this thesis: (1) develop design recommendations for flat-plate LAMEEs, (2) design, build and test a novel 3-fluid LAMEE prototype and compare its performance with a 2-fluid LAMEE under a wide range of operating conditions, and (3) present performance definitions for 3-fluid LAMEEs. The important conclusions and contributions of this thesis and suggested topics for future research are summarized in this chapter.

8.1 SUMMARY

8.1.1 Objective 1: Develop Design Recommendations for Flat-Plate LAMEEs

This Ph.D. thesis focuses on improving the rates of heat and moisture transfer between the air and desiccant solution in LAMEEs. The first objective of the thesis research was addressed in Chapters 2 and 6. In Chapter 2, a numerical study was performed to determine the practical air and solution channel widths for flat-plate LAMEEs. The effects of the air and solution channel widths on the rates of heat and moisture transfer between the air and desiccant solution were studied under air cooling and dehumidifying conditions and solution regeneration conditions. Results showed that the rates of heat and moisture transfer increased as air and/or solution channel width decreased. However, in flat-plate LAMEEs, pressure difference across the membranes may cause membrane deflections and flow maldistribution. This implies that LAMEEs designed with narrow air channels may experience partial or complete blockage of the air channels due to membrane

deflections. Therefore, another numerical study was performed to determine the effects of the flow maldistribution, caused by membrane deflections, on LAMEEs performance at different air channel widths. It was found that flat-plate LAMEEs may experience large membrane deflections which create flow maldistribution and reduce the LAMEE's performance by up to 24%. Based on the results of the two numerical studies, it was concluded that the recommended air and solution channel widths for flat-plate LAMEEs are 5-6 mm and 1-2 mm, respectively.

In Chapter 6, the feasibility of applying pre-tension to the membrane to reduce flow maldistribution caused by membrane deflections was experimentally investigated and the degradation in the LAMEEs performance due to membrane deflections was estimated. It was found that flow maldistribution caused by membrane deflections in flat-plate LAMEEs can be reduced to a great extent by pre-tensioning the membrane provided that the pre-tension in the membrane is maintained during the LAMEE manufacturing. Furthermore, results showed that flow maldistribution caused by membrane deflections may reduce the effectiveness of a full-scale 3-fluid LAMEE that has a similar design as the 3-fluid LAMEE tested in this thesis by up to 7%.

8.1.2 Objective 2: Design, Build and Test a Novel 3-Fluid LAMEE Prototype and Compare its Performance with a 2-Fluid LAMEE under a Wide Range of Operating Conditions

In Chapter 3, a novel 3-fluid LAMEE prototype was designed and fabricated according to the design recommendations for channel width developed in Chapter 2 and previous designs of flat-plate LAMEEs. The 3-fluid LAMEE prototype was used to fulfill the second objective of this thesis in Chapters 3, 4, 5 and 6. The rates of heat and moisture transfer between the air and desiccant solution in 3-fluid and 2-fluid LAMEEs were tested and compared under: (a) air cooling and dehumidifying conditions in Chapters 3 and 4, (b) solution regeneration conditions in

Chapter 5, and (c) air heating and humidifying conditions in Chapter 6. The effects of key operating parameters on the rates of heat and moisture transfer in 3-fluid and 2-fluid LAMEEs were tested and compared under these different operating conditions in Chapters 3, 4, 5 and 6. Results showed that the rates of heat and moisture transfer between the air and desiccant solution in the 3-fluid LAMEE were higher than the 2-fluid LAMEE under the entire range of operating parameters tested. The improvement in the rates of heat and moisture transfer between the air and desiccant solution in 3-fluid LAMEEs compared to 2-fluid LAMEEs was strongly dependent on the operating parameters (the inlet refrigerant temperature, refrigerant mass flow rate, desiccant solution mass flow rate, and inlet air humidity ratio). The sensible effectiveness, latent effectiveness and moisture transfer rate between the air and desiccant solution in the 3-fluid LAMEE compared to 2-fluid LAMEEs were improved by up to 69%, 28%, and 54%, respectively, under air cooling and dehumidifying conditions, and by up to 104%, 141%, and 17 times, respectively, under diluted desiccant solution regeneration conditions. Furthermore, it was found that the improvement in the rate of heat transfer between the air and desiccant solution in the 3-fluid LAMEE compared to 2-fluid LAMEEs was almost the same under air cooling and dehumidifying conditions and solution regeneration conditions, while the improvement in the rate of moisture transfer under solution regeneration conditions was much higher than under air cooling and dehumidifying conditions. This may be attributed to the reduced desiccant solution crystallization in the 3-fluid LAMEE compared to the 2-fluid LAMEE under solution regeneration conditions.

The effects of the phase change energy associated with the moisture transfer on the temperatures of the desiccant solution and air in 3-fluid and 2-fluid LAMEEs were experimentally quantified and compared under air cooling and dehumidifying conditions in Chapter 4 and under air heating

and humidifying conditions in Chapter 6. It was found that the phase change energy had a considerable effect on the temperature of the desiccant solution in LAMEEs. Results showed that the phase change energy increased the temperatures of the desiccant solution and air in a 2-fluid LAMEE by up to 3°C and 1°C, respectively, under air cooling and dehumidifying conditions. Under specific design and operating parameters, the outlet desiccant solution (hot fluid) temperature in a 2-fluid LAMEE was cooled below the inlet air (cold fluid) temperature due to the phase change energy.

8.1.3 Objective 3: Present Performance Definitions for 3-Fluid LAMEEs

The third objective of this thesis was addressed in Chapter 7, where performance definitions for calculating the overall effectiveness of 3-fluid LAMEEs were presented and tested using the experimental data presented in Chapter 3. The sensible and latent effectivenesses of the 3-fluid LAMEEs were compared when calculated using the traditional effectiveness equations and the overall effectiveness equations. It was found that the overall effectiveness equations were less dependent on the inlet refrigerant temperature than the traditional effectiveness equations. For example, when the inlet refrigerant temperature decreased from 25ºC to 10ºC, the sensible and latent effectivenesses of the 3-fluid LAMEE increased by 49% and 22%, respectively, when calculated using the traditional effectiveness equations and by 15% and 4% respectively, when calculated using the overall effectiveness equations. Therefore, the overall performance definitions can be used for designing 3-fluid LAMEEs over a wide range of operating conditions.

8.2 CONCLUSIONS

The following list contains the principal conclusions obtained from this thesis.

- Using a refrigerant to control the temperature of the desiccant solution inside 3-fluid LAMEEs results in considerable improvements in the rates of heat and moisture transfer between the air and desiccant solution.

- The operating parameters (the inlet refrigerant temperature and refrigerant mass flow rate) have a strong effect on the improvement in the rates of heat and moisture transfer between the air and desiccant solution in 3-fluid LAMEEs.

- The sensible effectiveness, latent effectiveness and moisture transfer rate of the 2-fluid LAMEE can be improved by up to 39%, 20%, and 53%, respectively, under air cooling and dehumidifying conditions, and by up to 38%, 40%, and 6 times, respectively, under diluted desiccant solution regeneration conditions, if the temperature of the desiccant solution is kept nearly constant along the entire length of the exchanger.

- The improvement in the rate of heat transfer between the air and desiccant solution in 2-fluid LAMEEs resulted from using a third fluid (refrigerant) to control the temperature of the desiccant solution is almost the same under air cooling and dehumidifying conditions and solution regeneration conditions, whereas the improvement in the rate of moisture transfer under solution regeneration conditions is higher than under air cooling and dehumidifying conditions. One reason for this may be that desiccant solution crystallization is reduced in the 3-fluid LAMEE under solution regeneration conditions.

- The phase change energy associated with the moisture transfer has a strong effect on the temperature of the desiccant solution in 2-fluid LAMEEs, where under specific operating

conditions, the outlet temperature of the desiccant solution (hot fluid) can be cooled below the inlet temperature of the air (cold fluid) due to the phase change energy.

- The traditional effectiveness equations overestimate the sensible and latent effectivenesses of 3-fluid LAMEEs and are more dependent on the refrigerant temperature than the overall effectiveness equations.
- The recommended practical air and solution channel widths for flat-plate LAMEEs are 5-6 mm and 1-2 mm, respectively. Decreasing the air channel width may decrease the LAMEE's effectiveness due to flow maldistribution caused by membrane deflections.
- Pre-tensioning the membrane during manufacturing of flat-plate LAMEEs is an effective technique to reduce flow maldistribution caused by membrane deflections.

8.3 CONTRIBUTIONS

The contributions of this Ph.D. research are summarized as follows.

- During this Ph.D. research, a novel 3-fluid LAMEE was designed and manufactured which can achieve higher heat and moisture transfer rates between the air and desiccant solution than conventional 2-fluid LAMEEs.
- The effects of key operating parameters on the performance of 3-fluid LAMEEs were determined from experimental data under air cooling and dehumidifying, air heating and humidifying, and diluted desiccant solution regeneration operating conditions.
- Performance definitions for 3-fluid LAMEEs were presented and tested.
- The importance of phase change energy on the desiccant solution and air temperatures in 2-fluid and 3-fluid LAMEEs under different operating conditions was quantified.

- Design recommendations were developed for flat-plate LAMEEs.
- The effects of flow maldistribution on the performance of 2-fluid and 3-fluid LAMEEs were estimated.
- Membrane deflections in the 3-fluid LAMEE were estimated.
- The feasibility of pre-tensioning the membrane to reduce membrane deflections and flow maldistribution in flat-plate LAMEEs was experimentally investigated.

8.4 FUTURE WORK

The 3-fluid LAMEE proposed and studied in this thesis is a new generation of liquid desiccant membrane energy exchangers. The results obtained in this thesis show that the 3-fluid LAMEE can overcome several technical problems associated with conventional LAMEEs that limit the development of liquid desiccant HVAC technology as a reliable substitute for conventional HVAC systems. Therefore, the following topics are suggested for future research.

- Develop a numerical model for 3-fluid LAMEEs.
- Perform techno-economic studies of liquid desiccant membrane HVAC systems and RAMEE systems when a 3-fluid LAMEE is used as the air dehumidifier/humidifier and the desiccant solution regenerator.
- Determine the feasibility of using the same amount of energy consumed to cool/heat the refrigerant to directly cool/heat the desiccant solution before flowing through a 2-fluid LAMEE.

- Test and compare the performances of 2-fluid and 3-fluid LAMEEs at different *NTU* values (number of heat transfer units) under air cooling and dehumidifying, air heating and humidifying, and desiccant solution regeneration operating conditions.
- Test and compare the transient performances of 3-fluid and 2-fluid LAMEEs under air cooling and dehumidifying, air heating and humidifying, and desiccant solution regeneration operating conditions.
- Test other 3-fluid LAMEE configurations (i.e. an exchanger composed of multiple parallel air, solution, and refrigerant channels) and compare with the 3-fluid LAMEE studied in this thesis.
- Test the performance of 3-fluid LAMEEs using various refrigerants.
- Study the effects of design and operating parameters on the flow maldistribution caused by membrane deflections in LAMEEs.
- Study the desiccant solution crystallization phenomena which may occur in LAMEEs at specific operating conditions during the desiccant solution regeneration process.

REFERENCES

Abdel-Salam A.H., Ge G., Simonson C.J., 2013. Performance analysis of a membrane liquid desiccant air-conditioning system. *Energy and Buildings*, **62**, 559-569.

Abdel-Salam A.H., Simonson C.J., 2014a. Annual evaluation of energy, environmental and economic performances of a membrane liquid desiccant air conditioning system with/without ERV. *Applied Energy*, **116**, 134-148.

Abdel-Salam A.H., Simonson C.J., 2014b. Capacity matching in heat-pump membrane liquid desiccant air conditioning systems. *International Journal of Refrigeration*, **48**, 166-177.

Abdel-Salam A.H., Simonson C.J., 2016. State-of-the-art in liquid desiccant air conditioning equipment and systems. *Renewable and Sustainable Energy Reviews*, **58**, 1152-1183.

Abdel-Salam A.H., Ge G., Simonson C.J., 2014a. Thermo-economic performance of a solar membrane liquid desiccant air conditioning system. *Solar Energy*, **102**, 56-73.

Abdel-Salam M.R.H., Ge G., Fauchoux M., Besant R.W., Simonson C.J., 2014b. State-of-the- art in liquid-to-air membrane energy exchangers (LAMEEs): a comprehensive review. *Renewable and Sustainable Energy Reviews*, **39**, 700-728.

Abdel-Salam M.R.H., Fauchoux M., Ge G., Besant R.W., Simonson C.J., 2014c. Expected energy and economic benefits, and environmental impacts for liquid-to-air membrane energy exchangers (LAMEEs) in HVAC systems: a review. *Applied Energy*, **127**, 202-218.

Abdel-Salam M.R.H., Besant R.W., Simonson C.J., 2015. Sensitivity of the performance of a flat-plate liquid-to-air membrane energy exchanger (LAMEE) to the air and solution channel widths and flow maldistribution. *International Journal of Heat and Mass Transfer*, **84**, 1082-1100.

Abdel-Salam M.R.H., Besant R.W., Simonson C.J., 2016a. Design and testing of a novel 3-fluid liquid-to-air membrane energy exchanger (3-fluid LAMEE). *International Journal of Heat and Mass Transfer*, **92**, 312-329.

Abdel-Salam M.R.H., Ge G., Besant R., Simonson C., 2016b. Experimental study of effects of phase-change energy and operating parameters on performances of two-fluid and three-fluid liquid-to-air membrane energy exchangers. *ASHRAE Transactions,* **122(1)**, 134-145.

Abdel-Salam M.R.H., Besant R.W., Simonson C.J., 2016c. Performance testing of a novel 3-fluid liquid-to-air membrane energy exchanger (3-fluid LAMEE) under desiccant solution regeneration operating conditions. *International Journal of Heat and Mass Transfer*, **95**, 773-786.

Abdel-Salam M.R.H., Besant R.W., Simonson C.J., 2016d. Performance testing of 2-fluid and 3-fluid liquid-to-air membrane energy exchangers for HVAC applications in cold-dry climates. *International Journal of Heat and Mass Transfer*, Submitted.

Advantix Systems, 2010. Liquid desiccant technology delivers energy cost reductions and indoor air quality improvements. White Paper (www.cmhsolutionsinc.com/downloads/GreenLEEDUpdate2011-12-DEC/AdvantixEnergySavings.pdf) (accessed on January 2016).

Afshin M., 2010. Selection of the liquid desiccant in a run-around membrane energy exchanger. M.Sc. Thesis, Department of Mechanical Engineering, College of Engineering, University of Saskatchewan, Canada.

Afshin M., Simonson C., Besant R., 2010. Crystallization limits of LiCl-water and $MgCl_2$-water salt solutions as operating liquid desiccant in the RAMEE system. *ASHRAE Transactions*, **116 (2)**, 494-506.

AHRI, ANSI/ARI Standard 1060, 2005. Standard for rating air-to-air exchangers for energy recovery ventilation equipment. Air-Conditioning & Refrigeration Institute, Arlington, VA.

Akbari S., Hemingson H.B., Beriault D., Simonson C.J., Besant R.W., 2012. Application of neural networks to predict the steady state performance of a run-around membrane energy exchanger. *International Journal of Heat and Mass Transfer*, **55**, 1628-1641.

ANSI/ASHRAE Standard 84-2008. Method of test for air-to-air heat/energy exchangers. American Society of Heating, Refrigerating, and Air-Conditioning Engineers, Atlanta, GA.

Anton Paar (www.anton-paar.com/ca-en/products/details/density-meters-dma-generation-m/) (accessed on January 23, 2015).

ASHRAE Handbook 2004. HVAC Systems and Equipment. American Society of Heating, Refrigerating and Air-Conditioning Engineers, Atlanta, GA.

ASME Performance Test Code 19.1-1998. Test uncertainty: instruments and apparatus. American Society of Mechanical Engineers, New York.

Awbi H.B., 1998. Chapter 7-Ventilation. *Renewable and Sustainable Energy Reviews*, **2**, 157-188.

Bansal P., Jain S., and Moon C., 2011. Performance comparison of an adiabatic and an internally cooled structured packed-bed dehumidifier, *Applied Thermal Engineering,* **31**, 14-19.

Bergero S., Chiari A., 2004. Passive hygrometric control of confined environments by means of membrane contactors and hygroscopic solutions. 5th International Congress on Energy, Environment and Technological Innovation (EETI) 2004, Riocentro, Rio de Janeiro, Brazil, 4-7 October, 9 Pages.

Bergero S., Chiari A., 2010. Performance analysis of a liquid desiccant and membrane contactor hybrid air-conditioning system. *Energy and Buildings*, **42**, 1976-1986.

Bergero S., Chiari A., 2011. On the performances of a hybrid air-conditioning system in different climatic conditions. *Energy*, **36**, 5261-5273.

Beriault D.A., 2011. Run-around membrane energy exchanger prototype 4 design and laboratory testing. M.Sc. Thesis, Department of Mechanical Engineering, College of Engineering, University of Saskatchewan, Canada.

British petroleum statistical review of world energy, June 2009, (bp.com/statisticalreview) (accessed on June 5, 2013).

British petroleum statistical review of world energy, June 2012, (bp.com/statisticalreview) (accessed on May 22, 2013).

Budaiwi I., Abdou A., 2013. HVAC system operational strategies for reduced energy consumption in buildings with intermittent occupancy: the case of mosques. *Energy Conversion and Management*, **73**, 37-50.

Çengel Y.A., 2006. *Heat and mass transfer: a practical approach*. 3rd Edition, McGraw-Hill, New York.

Chilton T.H., Colburn A.P., 1934. Mass transfer (absorption) coefficients prediction from data on heat transfer and fluid friction. *Industrial & Engineering Chemistry,* **26**, 1183-1187.

Chua K.J., Chou S.K., Yang W.M., Yan J., 2013. Achieving better energy-efficient air conditioning - a review of technologies and strategies. *Applied Energy*, **104**, 87-104.

Chung T.W., Ghosh T.K., Hines A.L., Novosel D., 1995. Dehumidification of moist air with simultaneous removal of selected indoor pollutants by triethylene glycol solutions in a packed-bed absorber. *Separation Science and Technology*, **30**, 1807-1832.

Colburn A.P., 1933. A method of correlating forced convection heat transfer data and a comparison with fluid friction. *AIChE Journal*, **29**, 174-210.

Conde M.R., 2004. Properties of aqueous solutions of lithium and calcium chlorides: formulations for use in air conditioning equipment design. *International Journal of Thermal Sciences*, **43**, 367-382.

Conde-Petit M., Weber R., November 2006. Open absorption system for cooling and air conditioning using membrane contactors. 2006 Annual Report, M. Conde Engineering, Zurich, Switzerland.

Daou K., Wang R.Z., Xia Z.Z., 2006. Desiccant cooling air conditioning: a review. *Renewable and Sustainable Energy Reviews*, **10**, 55-77.

eFunda (www.efunda.com/materials/elements/TC_Table.cfm?Element_ID=Ti) (accessed on June 8, 2014).

El-Dessouky H., Ettouney H., Al-Zeefari A., 2004. Performance analysis of two-stage evaporative coolers. *Chemical Engineering Journal*, **102**, 255-266.

Elsayed M.M., Gari H.N., Radhwan A.M., 1993. Effectiveness of heat and mass transfer in packed beds of liquid desiccant system. *Renewable Energy*, **3**, 661-668.

Enteria N., Yoshino H., Mochida A., 2013. Review of the advances in open-cycle absorption air-conditioning systems. *Renewable and Sustainable Energy Reviews*, **28**, 265-289.

Erb B., 2009. Run-around membrane energy exchanger performance and operational control strategies. M.Sc. Thesis, Department of Mechanical Engineering, College of Engineering, University of Saskatchewan, Canada.

Erb B., Ahmadi M.S., Simonson C.J., Besant R.W., 2009. Experimental measurements of a run-around membrane energy exchanger (RAMEE) with comparison to a numerical model. *ASHRAE Transactions*, **115**, 689-705.

Fan H., 2005. Modeling a run-around heat and moisture recovery system. M.Sc. Thesis, Department of Mechanical Engineering, College of Engineering, University of Saskatchewan, Canada.

Fan H., Simonson C.J., Besant R.W., Shang W., 2005. Run-around heat recovery system using cross-flow flat-plate heat exchangers with aqueous ethylene glycol as the coupling fluid. *ASHRAE Transactions*, **111(1)**, 901-910.

Fan H., Simonson C.J., Besant R.W., Shang W., 2006. Performance of a run-around system for HVAC heat and moisture transfer applications using cross-flow plate exchangers coupled with aqueous lithium bromide. *HVAC&R Research*, **12:2**, 313-336.

Fernández-Seara J., Diz R., Uhía F.J., 2013. Pressure drop and heat transfer characteristics of a titanium brazed plate-fin heat exchanger with offset strip fins. *Applied Thermal Engineering*, **51**, 502-511.

Gao W.Z., Shi Y.R., Cheng Y.P., and Sun W.Z., 2013. Experimental study on partially internally cooled dehumidification in liquid desiccant air conditioning system, *Energy and Buildings,* **61**, 202-209.

Ge G., Abdel-Salam M.R.H., Besant R.W., Simonson C.J., 2013a. Research and applications of liquid-to-air membrane energy exchangers in building HVAC systems at University of Saskatchewan: a review. *Renewable and Sustainable Energy Reviews*, **26**, 464-479.

Ge G., Moghaddam D.G., Namvar R., Simonson C.J., Besant R.W., 2013b. Analytical model based performance evaluation, sizing and coupling flow optimization of liquid desiccant run-around membrane energy exchanger systems. *Energy and Buildings*, **62**, 248-257.

Ge G., Moghaddam D.G., Abdel-Salam A.H., Besant R.W., Simonson C.J., 2014a. Comparison of experimental data and a model for heat and mass transfer performance of a liquid-to-air membrane energy exchanger (LAMEE) when used for air dehumidification and salt solution regeneration. *International Journal of Heat and Mass Transfer,* **68**, 119-131.

Ge G., Mahmood G.I., Moghaddam D.G., Simonson C.J., Besant R.W., Hanson S., Erb B., Gibson P.W., 2014b. Material properties and measurements for semi-permeable membranes used in energy exchangers. *Journal of Membrane Science*, **453**, 328-336.

Haniff M.F., Selamat H., Yusof R., Buyamin S., Ismail F.S., 2013. Review of HVAC scheduling techniques for buildings towards energy-efficient and cost-effective operations. *Renewable and Sustainable Energy Reviews*, **27**, 94-103.

Hemingson H., 2010. The impacts of outdoor air conditions and non-uniform exchanger channels on a run-around membrane energy exchanger. M.Sc. Thesis, Department of Mechanical Engineering, College of Engineering, University of Saskatchewan, Canada.

Hemingson H.B., Simonson C.J., Besant R.W., 2011a. Steady-state performance of a run-around membrane energy exchanger (RAMEE) for a range of outdoor air conditions. *International Journal of Heat and Mass Transfer*, **54**, 1814-1824.

Hemingson H.B., Simonson C.J., Besant R.W., 2011b. Effects of non-uniform channels on the performance of a run-around membrane energy exchanger (RAMEE). The 12th International Conference on Air Distribution in Rooms, ROOMVENT 2011, 19-22 June, Trondheim, Norway, 8 Pages.

Huang S.M., Zhang L.Z., 2013. Researches and trends in membrane-based liquid desiccant air dehumidification. *Renewable and Sustainable Energy Reviews*, **28**, 425-440.

Incropera F.P., Dewitt D.P., 2002. *Fundamentals of heat and mass transfer*. John Wiley & Sons, New York.

Incropera F.P., DeWitt D.P., Bergman T.L., Lavine A.S., 2007. *Fundamentals of Heat and Mass Transfer*, Vol. 6. New York: John Wiley & Sons.

Isetti C., Nannei E., Magrini A., 1997. On the application of a membrane air-liquid contactor for air dehumidification. *Energy and Buildings*, **25**, 185-193.

Kakac S., Bergles A.E., Mayinger F., Yuncu H., 1999. *Heat Transfer Enhancement of Heat Exchangers.* Vol. 355, Springer Netherlands.

Kakac S., Liu H., Pramuanjaroenkij A., 2012. *Heat exchangers: selection, rating, and thermal design*. 3rd edition, Taylor & Francis Group, New York.

Kamali H., 2014. Non-contact membrane deflection measurement using laser. Internal Report, Department of Mechanical Engineering, University of Saskatchewan.

Kamali H., Ge G., Besant R.W., Simonson C.J., 2016. Extension of the concepts of heat capacity rate ratio and effectiveness-number of transfer units model to the coupled heat and moisture exchange in liquid-to-air membrane energy exchangers. *Transactions of the ASME: Journal of Heat Transfer*, **138(9)**, 1-12.

Kays W.M., Crawford M.E., 1990. *Convective heat and mass transfer*. 3rd Edition, McGraw-Hill, New York.

Khan T.S., Khan M.S., Chyu M.C., Ayub Z.H., 2012. Experimental investigation of evaporation heat transfer and pressure drop of ammonia in a 60º chevron plate heat exchanger. *International Journal of Refrigeration*, **35**, 336-348.

Khayet M., 2011. Membranes and theoretical modeling of membrane distillation: a review. *Advances in Colloid and Interface Science*, **164**, 56-88.

Kolokotsa D., Rovas D., Kosmatopoulos E., Kalaitzakis K., 2011. A roadmap towards intelligent net zero and positive-energy buildings. *Solar Energy*, **85**, 3067-3084.

Koronaki I.P., Christodoulaki R.I., Papaefthimiou V.D., Rogdakis E.D., 2013. Thermodynamic analysis of a counter flow adiabatic dehumidifier with different liquid desiccant materials, *Applied Thermal Engineering,* **50**, 361-373.

Kusiak A., Li M., Tang F., 2010. Modeling and optimization of HVAC energy consumption. *Applied Energy*, **87**, 3092-3102.

Larson M.D., 2006. The performance of membranes in a newly proposed runaround heat and moisture exchanger. M.Sc. Thesis, Department of Mechanical Engineering, College of Engineering, University of Saskatchewan, Canada.

Larson M.D., Simonson C.J., Besant R.W., Gibson P.W., 2007. The elastic and moisture transfer properties of polyethylene and polypropylene membranes for use in liquid-to-air energy exchangers. *International Journal of Membrane Science*, **302**, 136-149.

Liu X.H., Jiang Y., Chang X.M., Yi X.Q., 2007. Experimental investigation of the heat and mass transfer between air and liquid desiccant in a cross-flow regenerator. *Renewable Energy*, **32**, 1623-1636.

Luo X., Roetzel W., 1998. Theoretical investigation on cross-flow heat exchangers with axial dispersion in one fluid. *Revue générale de thermique*, **37**, 223-233.

Mahmud K., 2009. Design and performance testing of counter-cross-flow run-around membrane energy exchanger system. M.Sc. Thesis, Department of Mechanical Engineering, College of Engineering, University of Saskatchewan, Canada.

Mahmud K., Mahmood G.I., Simonson C.J., Besant R.W., 2010. Performance testing of a counter-cross-flow run-around membrane energy exchanger (RAMEE) system for HVAC applications. *Energy and Buildings,* **42**, 1139-1147.

Martin V., Goswami D.Y., 2000. Effectiveness of heat and mass transfer processes in a packed bed liquid desiccant dehumidifier/regenerator. *HVAC&R Research*, **6:1**, 21-39.

McMASTER-CARR (www.mcmaster.com/#standard-metal-tubing/=s5epmz) (accessed on June 1, 2014).

Mehendale S.S., Shah R.K., Jacobi A.M., 2000. Fluid flow and heat transfer at micro-and meso-scales with application to heat exchanger design. *Applied Mechanics Reviews*, **53(7)**, 175-193.

Mei L., Dai Y.J., 2008. A technical review on use of liquid-desiccant dehumidification for air-conditioning application. *Renewable and Sustainable Energy Reviews*, **12**, 662-689.

Mohammad A.T., Mat S.B., Sulaiman M.Y., Sopian K., Al-abidi A.A., 2013. Survey of hybrid liquid desiccant air conditioning systems. *Renewable and Sustainable Energy Reviews*, **20**, 186-200.

Moghaddam D.G., 2014. Testing small-scale and full-scale liquid-to-air membrane energy exchangers (LAMEEs). M.Sc. Thesis, Department of Mechanical Engineering, College of Engineering, University of Saskatchewan, Canada.

Moghaddam D.G., LePoudre P., Besant R.W., Simonson C.J., 2013a. Steady-state performance of a small-scale liquid-to-air membrane energy exchanger for different heat and mass transfer directions, and liquid desiccant types and concentrations: experimental and numerical data. *Transactions of the ASME: Journal of Heat Transfer*, **135**, 1-13.

Moghaddam D.G., LePoudre P., Besant R.W., Simonson C.J., 2013b. Evaluating the steady-state performance of a small-scale single-panel liquid-to-air membrane energy exchanger (LAMEE) under summer AHRI test conditions. CLIMA 2013, 11th REHVA World Congress & 8th International Conference on IAQVEC, 16-19 June, Prague, Czech Republic, 10 Pages.

Moghaddam D.G., Mahmood G., Ge G., Bolster J., Besant R.W., Simonson C.J., 2013c. Steady-state performance of a prototype (200 CFM) liquid-to-air membrane energy exchanger (LAMEE) under summer and winter test conditions. Proceedings of the ASME 2013 Summer Heat Transfer Conference, 14-19 July, 2013, Minneapolis, MN, USA, 7 Pages.

Moghaddam D.G., Ge G., Abdel-Salam A.H., Besant R.W., Simonson C.J., 2013d. Effects of solution inlet temperature on the effectiveness and moisture removal rate of a liquid-to-air membrane energy exchanger (LAMEE) during regenerator operating conditions. Proceedings of the 24th CANCAM, 2-6 June, Saskatoon, Saskatchewan, Canada, 5 Pages.

Moghaddam D.G., LePoudre P., Ge G., Besant R.W., Simonson C.J., 2013e. Small-scale single-panel liquid-to-air membrane energy exchanger (LAMEE) test facility development, commissioning and evaluating the steady-state performance. *Energy and Buildings*, **66**, 424-436.

Moghaddam D.G., Besant R.W., Simonson C.J., 2014. Solution-side effectiveness for a liquid-to-air membrane energy exchanger used as a dehumidifier/regenerator. *Applied Energy*, **113**, 872-882.

Namvar R., 2012. Transient and steady-state performance of a liquid-to-air membrane energy exchanger (LAMEE). M.Sc. Thesis, Department of Mechanical Engineering, College of Engineering, University of Saskatchewan, Canada.

Namvar R., Pyra D., Ge G., Simonson C.J., Besant R.W., 2012. Transient characteristics of a liquid-to-air membrane energy exchanger (LAMEE) experimental data with correlations. *International Journal of Heat and Mass Transfer*, **55**, 6682-6694.

Nasr M.R., Fauchoux M., Besant R.W., Simonson C.J., 2014. A review of frosting in air-to-air energy exchangers. *Renewable and Sustainable Energy Reviews*, **30**, 538-554.

Nellis G., Klein S., 2009. *Heat transfer*. Cambridge University Press, New York, USA.

Nielsen K.K., Engelbrecht K., Bahl C.R.H., 2013. The influence of flow maldistribution on the performance of inhomogeneous parallel plate heat exchangers. *International Journal of Heat and Mass Transfer*, **60**, 432-439.

NRCan (http://oee.nrcan.gc.ca/corporate/statistics/neud/dpa/showTable.cfm?type=HB&sector=aaa&juris=ca&rn=2&page=6&CFID=30286177&CFTOKEN=1e4962d1f111b44cAA3B7047-9276-078E-875007B660714222) (accessed on July 7, 2014).

Oghabi A., 2014. Measurement of heat transfer enhancement and pressure drop for turbulence enhancing inserts in liquid-to-air membrane energy exchangers (LAMEEs). M.Sc. Thesis, Department of Mechanical Engineering, College of Engineering, University of Saskatchewan, Canada.

Omer A.M., 2008. Energy, environment and sustainable development. *Renewable and Sustainable Energy Reviews*, **12**, 2265-2300.

Patel H., 2012. Contaminant transfer in a run-around membrane energy exchanger. M.Sc. Thesis, Department of Mechanical Engineering, College of Engineering, University of Saskatchewan, Canada.

Patel H., Ge G., Abdel-Salam M.R.H., Abdel-Salam A.H., Besant R.W., Simonson C.J., 2014. Contaminant transfer in run-around membrane energy exchangers. *Energy and Buildings*, **70**, 94-105.

Radhwan A.M., Gari H.N., Elsayed M.M., 1993. Parametric study of a packed bed dehumidifier/regenerator using $CaCl_2$ liquid desiccant. *Renewable Energy*, **3**, 49-60.

Rasouli M., Akbari S., Simonson C.J., Besant R.W., 2014. Energetic, economic and environmental analysis of a health-care facility HVAC system equipped with a run-around membrane energy exchanger. *Energy and Buildings*, **69**, 112-121.

Reay D.A., 2002. Compact heat exchangers, enhancement and heat pumps. *International Journal of Refrigeration*, **25**, 460-470.

Ren C.Q., Tu M., Wang H.H., 2007. An analytical model for heat and mass transfer processes in internally cooled or heated liquid desiccant–air contact units, *International Journal of Heat and Mass Transfer,* **50**, 3545-3555.

Schulze T., Eicker U., 2013. Controlled natural ventilation for energy efficient buildings. *Energy and Buildings*, **56**, 221-232.

Seyed-Ahmadi M., 2008. Modeling the transient behavior of a run-around heat and moisture exchanger system. M.Sc. Thesis, Department of Mechanical Engineering, College of Engineering, University of Saskatchewan, Canada.

Seyed-Ahmadi M., Erb B., Simonson C.J., Besant R.W., 2009. Transient behavior of run-around heat and moisture exchanger system: part I: model formulation and verification. *International Journal of Heat and Mass Transfer*, **52**, 6000-6011.

Shang W., Besant R.W., 2004. Measurement of pore size variation and its effect on energy wheel performance. *ASHRAE Transactions*, **110**, 410-421.

Shang W., Besant R.W., 2005. Effects of pore size variations on regenerative wheel performance. *Journal of Engineering for Gas Turbines and Power*, **127**, 121-135.

Shrivastava D., Ameel T.A., 2004. Three-fluid heat exchangers with three thermal communications. Part B: effectiveness evaluation. *International Journal of Heat and Mass Transfer*, **47**, 3867-3875.

Simonson C.J., Besant R.W., 1999. Energy wheel effectiveness: part I-development of dimensionless groups. *International Journal of Heat and Mass Transfer*, **42**, 2161-2170.

Simonson C.J., Ciepliski D.L., Besant R.W., 1999. Determining the performance of energy wheels: Part I Experimental and numerical method. *ASHRAE Transactions*, **105(1)**, 174-187.

Spengler J.D., Sexton K., July 1983. Indoor air pollution: a public health perspective. *Science*, **221**, 4605, 9-17.

Vali A., 2009. Modeling a run-around heat and moisture exchanger using two counter/cross flow exchangers. M.Sc. Thesis, Department of Mechanical Engineering, College of Engineering, University of Saskatchewan, Canada.

Vali A., Simonson C.J., Besant R.W., Mahmood G., 2009. Numerical model and effectiveness correlations for a run-around heat recovery system with combined counter and cross flow exchangers. *International Journal of Heat and Mass Transfer*, **52**, 5827-5840.

Vestrelli F., 2006. Study on membrane contactors: performances analysis, system simulations and fields of application. PhD thesis "Doctorate of Philosophy in Technical Physics", Faculty of Engineering, University of Genoa, Genoa, Italy.

Wang L., Greenberg S., Fiegel J., Rubalcava A., Earni S., Pang X., Yin R., Woodworth S., Hernandez-Maldonado J., 2013. Monitoring-based HVAC commissioning of an existing office building for energy efficiency. *Applied Energy*, **102**, 1382-1390.

Wang X., Cai W., Lu J., Sun Y., Ding X., 2013. A hybrid dehumidifier model for real-time performance monitoring, control and optimization in liquid desiccant dehumidification system. *Applied Energy*, **111**, 449-455.

Welty J.R., Wicks C.E., Wilson R.E., Rorrer G., 2001. *Fundamentals of momentum, heat and mass transfer*. John Wiley & Sons Inc., New York.

Welty S., Liquid desiccant air conditioning: the revolutionary deep drying dehumidification system delivering energy efficiency and healthier indoor air. (www.intelligentpowerandair.com/documents/newsroom/Advantix%20Supporting%20Documents/LDAC_White_Paper%20for%20Healthcare.pdf) (accessed on April 12, 2016).

White F.M., 1998. *Fluid Mechanics*. 4th edition, McGraw-Hill Ryerson, Canada.

Wyon D.P., 2004. The effects of indoor air quality on performance and productivity. *Indoor Air*, **14**, 92-101.

Xiang Y., Chen X., Vlassak J.J., 2005. Plane-strain bulge test for thin films. *Journal of Materials Research*, **20**, 2360-2370.

Yin Y., Zhang X., Wang G., Luo L., 2008. Experimental study on a new internally cooled/heated dehumidifier/regenerator of liquid desiccant systems, *International Journal of Refrigeration,* **31**, 857-866.

Zhang L.Z., 2008. *Total heat recovery: heat and moisture recovery from ventilation air*. Nova Science Publishing Co., New York.

Zhang L.Z., 2011. An analytical solution to heat and mass transfer in hollow fiber membrane contactors for liquid desiccant air dehumidification. *Transactions of the ASME: Journal of Heat Transfer*, **133 (9)**, 1-8.

Zhang L.Z., Huang S.M., 2011. Coupled heat and mass transfer in a counter flow hollow fiber membrane module for air humidification. *International Journal of Heat and Mass Transfer*, **54**, 1055-1063.

Zhang L.Z., Huang S.M., Pei L.X., 2012a. Conjugate heat and mass transfer in a cross-flow hollow fiber membrane contactor for liquid desiccant air dehumidification. *International Journal of Heat and Mass Transfer*, **55**, 8061-8072.

Zhang L.Z., Huang S.M., Chi J.H., Pei L.X., 2012b. Conjugate heat and mass transfer in a hollow fiber membrane module for liquid desiccant air dehumidification: a free surface model approach. *International Journal of Heat and Mass Transfer*, **55**, 3789-3799.

Zhang L.Z., Zhang X.R., Miao Q.Z., Pei L.X., 2012c. Selective permeation of moisture and VOCs through polymer membranes used in total heat exchangers for indoor air ventilation. *Indoor Air*, **22**, 321-330.

Zhang L.Z., Zhang N., 2014. A heat pump driven and hollow fiber membrane-based liquid desiccant air dehumidification system: modeling and experimental validation. *Energy*, **65**, 441-451.

APPENDIX A

COPYRIGHT PERMISSIONS

This appendix includes the copyright permissions for the published and co-authored manuscripts presented in this thesis. For manuscripts that form part of a thesis, the College of Graduate Studies and Research (CGSR) requires a written request from:

- the publisher (copyright holder) for previously published manuscripts, and
- the co-author(s) for unpublished manuscripts.

The permissions for using the published manuscripts in this thesis are presented in Sections A.1 and A.2, and the permissions for using the unpublished manuscripts are presented in Sections A.3 and A.4.

A.1 Permission for manuscripts used in Chapters 1, 2, 3 and 5

The manuscripts used in Chapters 1, 2, 3 and 5 are published by Elsevier. For manuscripts published by Elsevier, the authors can use their publication as a part of their theses without obtaining a written permission from Elsevier. The following snapshot is copied from Elsevier website.

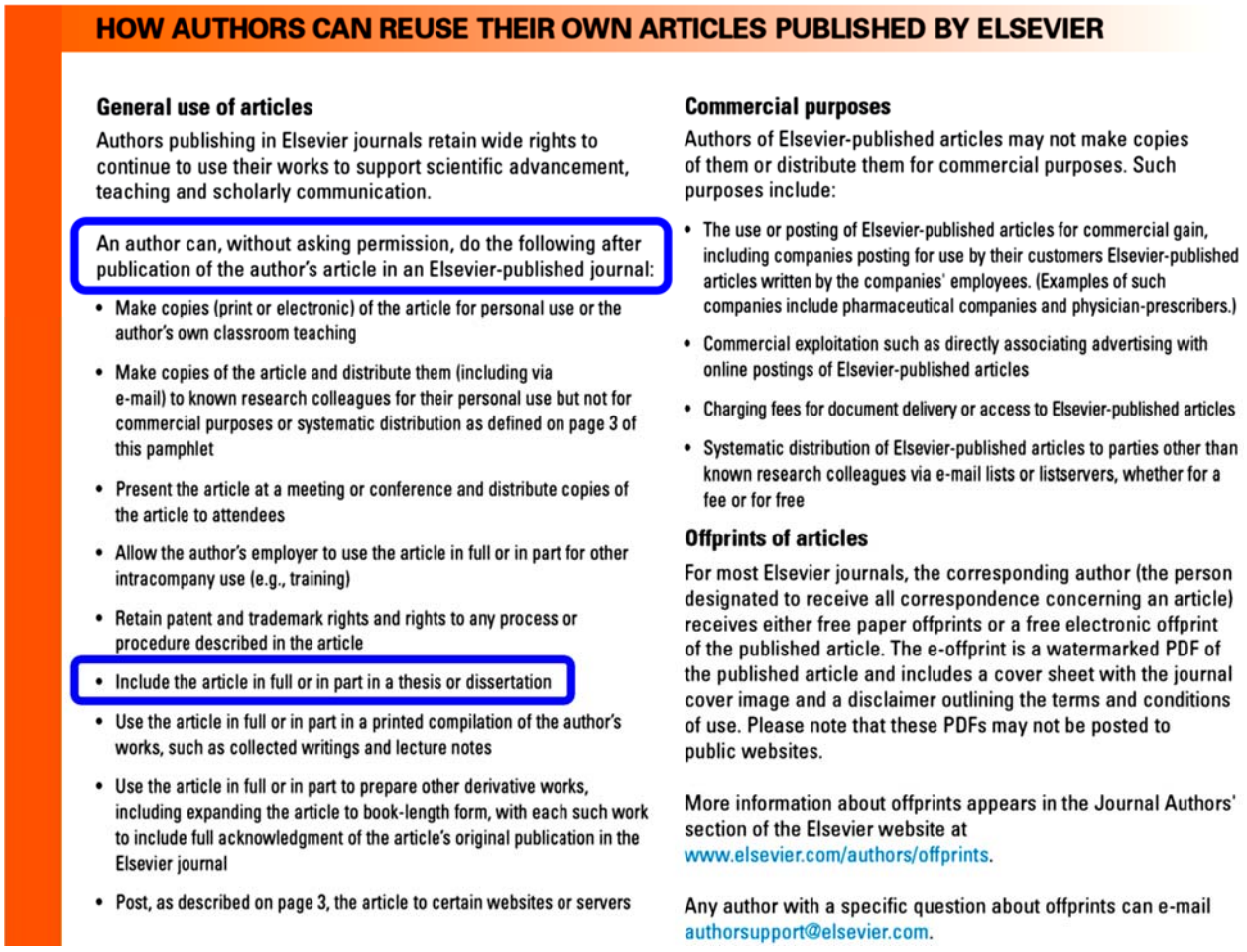

HOW AUTHORS CAN REUSE THEIR OWN ARTICLES PUBLISHED BY ELSEVIER

General use of articles

Authors publishing in Elsevier journals retain wide rights to continue to use their works to support scientific advancement, teaching and scholarly communication.

An author can, without asking permission, do the following after publication of the author's article in an Elsevier-published journal:

- Make copies (print or electronic) of the article for personal use or the author's own classroom teaching
- Make copies of the article and distribute them (including via e-mail) to known research colleagues for their personal use but not for commercial purposes or systematic distribution as defined on page 3 of this pamphlet
- Present the article at a meeting or conference and distribute copies of the article to attendees
- Allow the author's employer to use the article in full or in part for other intracompany use (e.g., training)
- Retain patent and trademark rights and rights to any process or procedure described in the article
- Include the article in full or in part in a thesis or dissertation
- Use the article in full or in part in a printed compilation of the author's works, such as collected writings and lecture notes
- Use the article in full or in part to prepare other derivative works, including expanding the article to book-length form, with each such work to include full acknowledgment of the article's original publication in the Elsevier journal
- Post, as described on page 3, the article to certain websites or servers

Commercial purposes

Authors of Elsevier-published articles may not make copies of them or distribute them for commercial purposes. Such purposes include:

- The use or posting of Elsevier-published articles for commercial gain, including companies posting for use by their customers Elsevier-published articles written by the companies' employees. (Examples of such companies include pharmaceutical companies and physician-prescribers.)
- Commercial exploitation such as directly associating advertising with online postings of Elsevier-published articles
- Charging fees for document delivery or access to Elsevier-published articles
- Systematic distribution of Elsevier-published articles to parties other than known research colleagues via e-mail lists or listservers, whether for a fee or for free

Offprints of articles

For most Elsevier journals, the corresponding author (the person designated to receive all correspondence concerning an article) receives either free paper offprints or a free electronic offprint of the published article. The e-offprint is a watermarked PDF of the published article and includes a cover sheet with the journal cover image and a disclaimer outlining the terms and conditions of use. Please note that these PDFs may not be posted to public websites.

More information about offprints appears in the Journal Authors' section of the Elsevier website at www.elsevier.com/authors/offprints.

Any author with a specific question about offprints can e-mail authorsupport@elsevier.com.

Source: http://libraryconnect.elsevier.com/sites/default/files/lcp0404.pdf (accessed in March 2016)

A.2 Permission for manuscript used in Chapter 4

The manuscript used in Chapter 4 is published in ASHRAE Transactions. The following is a written permission to include this manuscript in my Ph.D. thesis.

Abdel Salam, Mohamed Rani Abdel-Salam

From: Phillips, Michshell <mphillips@ashrae.org>
Sent: Thursday, October 01, 2015 6:11 AM
To: Abdel-Salam, Mohamed Rani Abdel-Salam
Subject: RE: TRNS-00117-2015.R1

Hi Mohamed,

As an ASHRAE author, you have ASHRAE's permission to use your entire paper (as published in ASHRAE Transactions) in your PhD thesis. But, you must use the final published version and the paper must acknowledge the following ASHRAE copyright:

"Copyright 2016 ASHRAE, www.ashrae.org. Published in ASHRAE Transactions, Volume 122, Part 1. This article may not be copied and/or distributed electronically or in paper form without permission of ASHRAE."

The Orlando papers are expected to be published around April or May 2016.

Michshell

ASHRAE
Shaping Tomorrow's Built Environment Today

Michshell Phillips
Editorial Coordinator for Special Publications
ASHRAE
1791 Tullie Circle NE
Atlanta, GA 30329
Tel: 678-539-1191
mphillips@ashrae.org
www.ASHRAE.org

A.3 Permission for manuscript used in Chapter 6

The College of Graduate Studies and Research requires a written permission from the co-authors for unpublished manuscripts. The manuscript used in Chapter 6 is unpublished, therefore copyright permissions are obtained from the co-authors as follows.

Copyright Permission Request Form

I am preparing the publication of a manuscript titled "*Perofrmance testing of 2-fluid and 3-fluid liquid-to-air membrane energy exchangers for HVAC applications in cold-dry climates*" to be published as the sixth chapter of my Ph.D. thesis, and to be submitted to the Department of Mechanical Engineering at the University of Saskatchewan. The authors contributing in the completion of this manuscript are

Mohamed R.H. Abdel-Salam, Robert W. Besant, and Carey J. Simonson

I am requesting permission to use the materials described in aforementioned mansucript in my Ph.D. thesis and all subsequent editions that may be prepared at the University of Saskachewan. Please indicate agreeemnt by signing below.

Sincerely,

Mohamed Abdel-Salam

May 28, 2016

Permission granted by: Carey J. Simonson Signature: Date:

Permission granted by: Robert W. Besant Signature: Date:

A.4 Permission for manuscript used in Chapter 7

The College of Graduate Studies and Research requires a written permission from the co-authors for unpublished manuscripts. The manuscript used in Chapter 7 is unpublished, therefore copyright permissions are obtained from the co-authors as follows.

Copyright Permission Request Form

I am preparing the publication of a manuscript titled "*Performance definitions for 3-fluid heat and moisture exchangers*" to be published as the seventh chapter of my Ph.D. thesis, and to be submitted to the Department of Mechanical Engineering at the University of Saskatchewan. The authors contributing in the completion of this manuscript are

Mohamed R.H. Abdel-Salam, Robert W. Besant, and Carey J. Simonson

I am requesting permission to use the materials described in aforementioned mansucript in my Ph.D. thesis and all subsequent editions that may be prepared at the University of Saskachewan. Please indicate agreeemnt by signing below.

Sincerely,

Mohamed Abdel-Salam

May 28, 2016

Permission granted by: Carey J. Simonson Signature: Date:

Permission granted by: Robert W. Besant Signature: Date:

APPENDIX B

Heat and Moisture Transfer Governing Equations

This appendix presents the heat and moisture transfer governing equations used to develop the numerical model used in Chapter 2 (Fan (2005); Fan et al. (2006); Seyed (2008); Seyed et al. (2009); Vali (2009); Vali et al. (2009); Hemingson (2010)).

$$\rho_{\mathrm{air}} \cdot \delta_{\mathrm{air}} \cdot \frac{\partial W_{\mathrm{air}}}{\partial t} = -2 \cdot U_{\mathrm{m}} \cdot (W_{\mathrm{air}} - W_{\mathrm{sol}}) - J_{\mathrm{air}} \cdot \nabla W_{\mathrm{air}} \cdot \delta_{\mathrm{air}} \tag{B.1}$$

$$\rho_{\mathrm{s}} \cdot \delta_{\mathrm{sol}} \cdot \frac{\partial X}{\partial t} = 2 \cdot U_{\mathrm{m}} \cdot (W_{\mathrm{air}} - W_{\mathrm{sol}}) - J_{\mathrm{s}} \cdot \nabla X \cdot \delta_{\mathrm{sol}} \tag{B.2}$$

$$\rho_{\mathrm{air}} \cdot c_{\mathrm{p,air}} \cdot \delta_{\mathrm{air}} \cdot \frac{\partial T_{\mathrm{air}}}{\partial t} = 2 \cdot [-U \cdot (T_{\mathrm{air}} - T_{\mathrm{sol}}) + U_{\mathrm{m}} \cdot (W_{\mathrm{air}} - W_{\mathrm{sol}}) \cdot h_{\mathrm{fg}} \cdot (1 - \eta)] - J_{\mathrm{air}} \cdot \nabla T_{\mathrm{air}} \cdot c_{\mathrm{p,air}} \cdot \delta_{\mathrm{air}} \tag{B.3}$$

$$\rho_{\mathrm{sol}} \cdot c_{\mathrm{p,sol}} \cdot \delta_{\mathrm{sol}} \cdot \frac{\partial T_{\mathrm{sol}}}{\partial t} = 2 \cdot [U \cdot (T_{\mathrm{air}} - T_{\mathrm{sol}}) + U_{\mathrm{m}} \cdot (W_{\mathrm{air}} - W_{\mathrm{sol}}) \cdot h_{\mathrm{fg}} \cdot \eta] - J_{\mathrm{sol}} \cdot \nabla T_{\mathrm{sol}} \cdot c_{\mathrm{p,sol}} \cdot \delta_{\mathrm{sol}} \tag{B.4}$$

where ρ is the density (kg/m^3), δ is the channel width (m), W is the humidity ratio (g/kg), U_{m} is the overall mass transfer coefficient (kg/(m^2·s)), J is the mass flux (kg/(m^2·s)), X is the ratio between the mass of water and mass of desiccant salt in the desiccant solution (kg/kg), c_{p} is the specific heat capacity (kJ/(kg·K)), T is the temperature (ºC), h_{fg} is the enthalpy of vaporization (kJ/kg), η is the fraction of the energy of phase change absorbed/emitted by the desiccant solution, and subscripts *air*, *sol* and *s* refer to air, desiccant solution, and desiccant salt, respectively.

APPENDIX C

3-FLUID LAMEE PROTOTYPE CONSTRUCTION DRAWINGS

This appendix presents the construction drawings of the 3-fluid LAMEE prototype developed in this thesis.

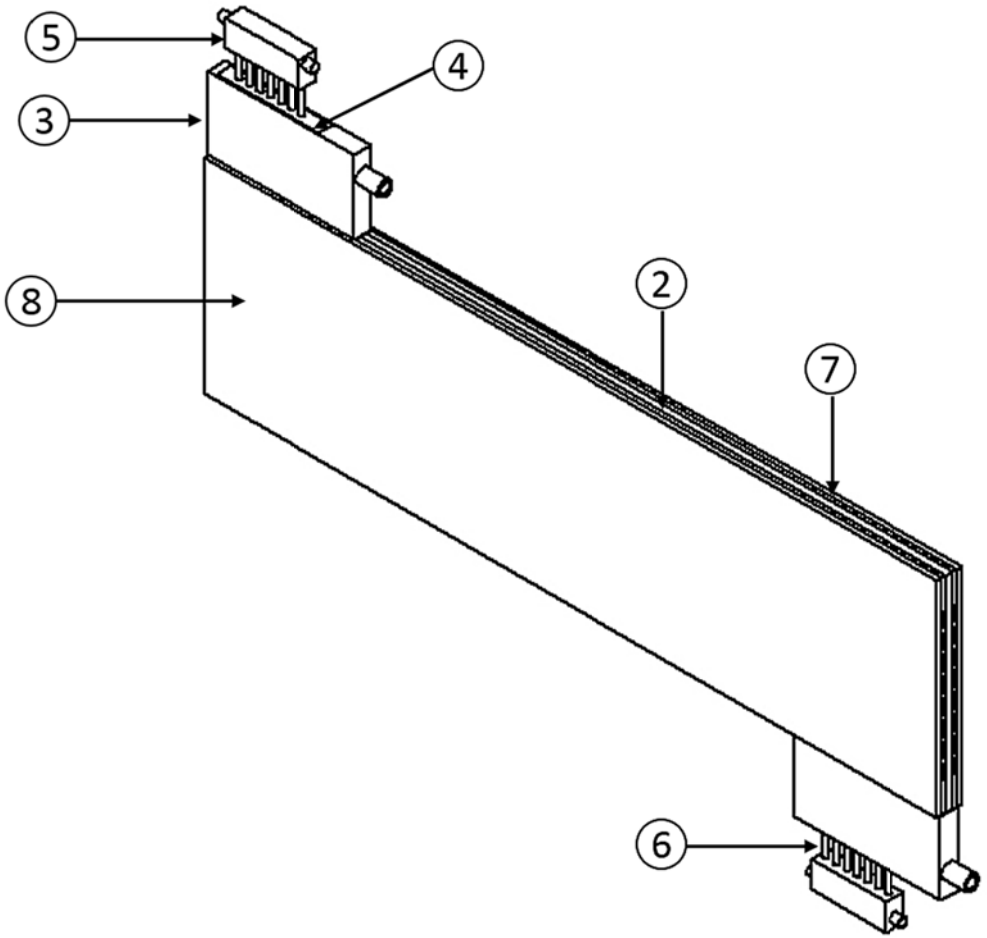

UNLESS OTHERWISE SPECIFIED: DIMENSIONS ARE IN MILLIMETERS SURFACE FINISH: TOLERANCES: LINEAR: ANGULAR:			FINISH:		DO NOT SCALE DRAWING / REVISION
	NAME	SIGNATURE	DATE		TITLE: 3-Fluid LAMEE Prototype
DRAWN	M.R.H.A.		2/9/2013		
CHK'D					
APPV'D					
MFG					
Q.A				MATERIAL: N/A	DWG NO. 1 / A4
				WEIGHT:	SCALE: 1:4 / SHEET 1 OF 1

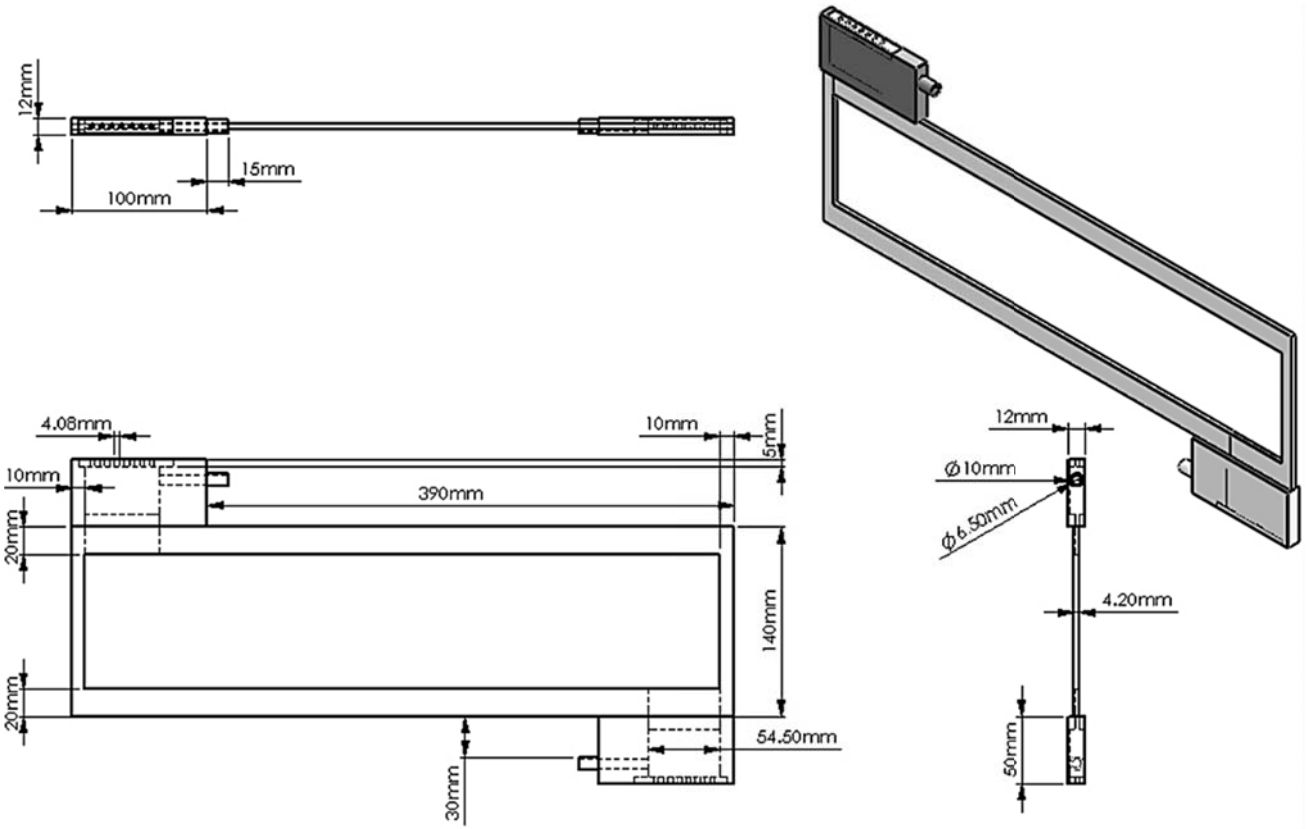

UNLESS OTHERWISE SPECIFIED: DIMENSIONS ARE IN MILLIMETERS SURFACE FINISH: TOLERANCES: LINEAR: ANGULAR:		FINISH:		DO NOT SCALE DRAWING	REVISION
	NAME	SIGNATURE	DATE		TITLE:
DRAWN	M.R.H.A.		2/9/2013		Solution Channel
CHK'D					
APPV'D					
MFG					
Q.A				MATERIAL: Objet RGD525	DWG NO. 2 / A4
				WEIGHT:	SCALE: 1:3.5 / SHEET 1 OF 1

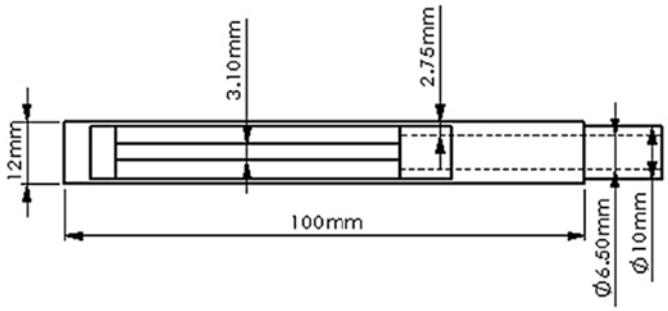

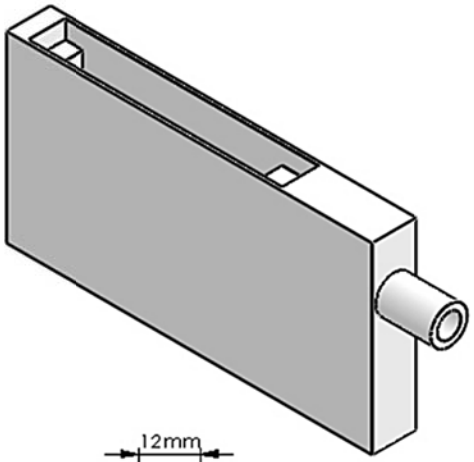

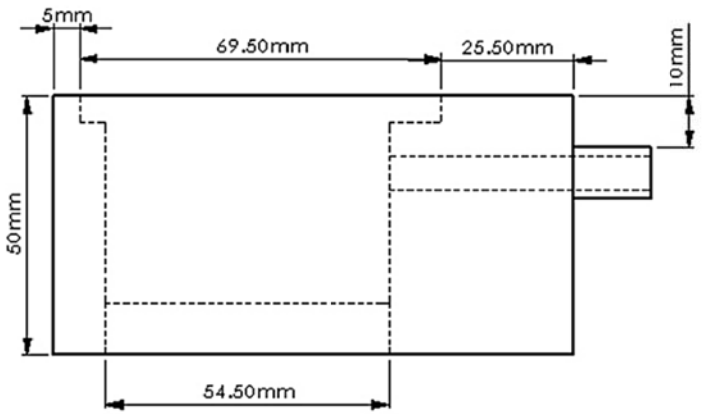

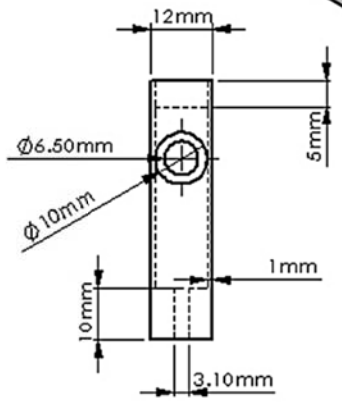

UNLESS OTHERWISE SPECIFIED: DIMENSIONS ARE IN MILLIMETERS SURFACE FINISH: TOLERANCES: LINEAR: ANGULAR:			FINISH:		DO NOT SCALE DRAWING / REVISION
	NAME	SIGNATURE	DATE		TITLE: Solution Header
DRAWN	M.R.H.A.		2/9/2013		
CHK'D					
APPV'D					
MFG					
Q.A				MATERIAL: Objet RGD525	DWG NO. 3 / A4
				WEIGHT:	SCALE: 1:1 / SHEET 1 OF 1

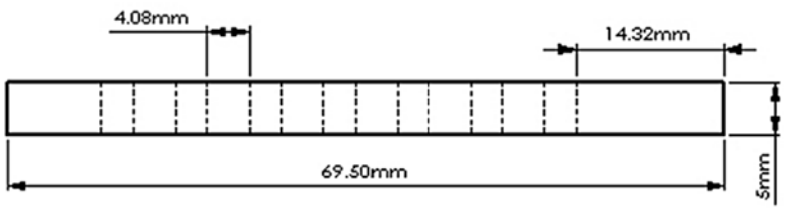

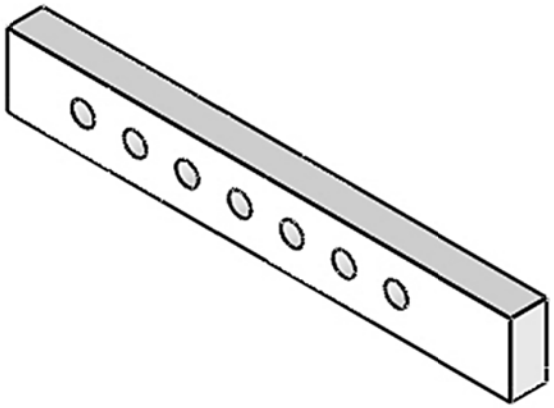

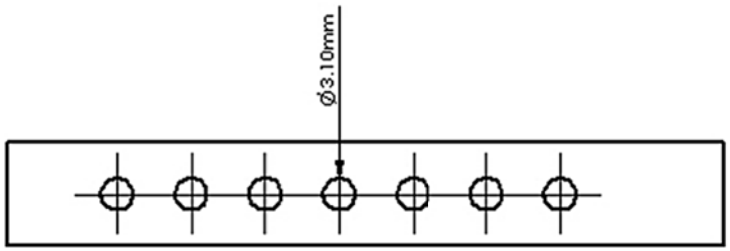

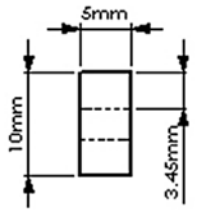

UNLESS OTHERWISE SPECIFIED: DIMENSIONS ARE IN MILLIMETERS SURFACE FINISH: TOLERANCES: LINEAR: ANGULAR:			FINISH:	DO NOT SCALE DRAWING	REVISION
	NAME	SIGNATURE	DATE	TITLE:	
DRAWN	M.R.H.A.		2/9/2013	Solution Header Cover	
CHK'D					
APPV'D					
MFG					
Q.A				MATERIAL: Objet RGD525	DWG NO. 4 A4
				WEIGHT:	SCALE: 2:1 SHEET 1 OF 1

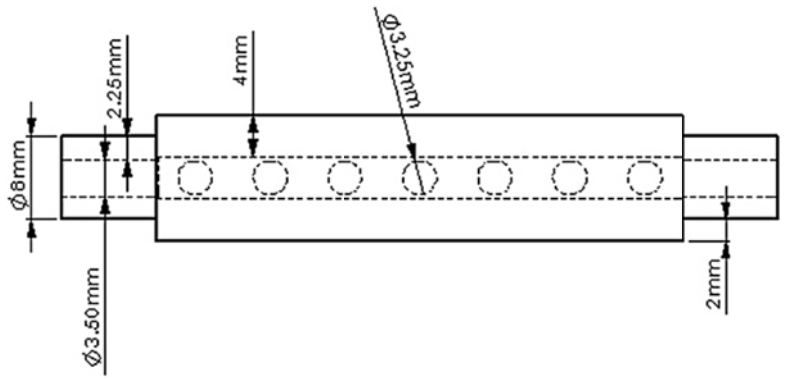

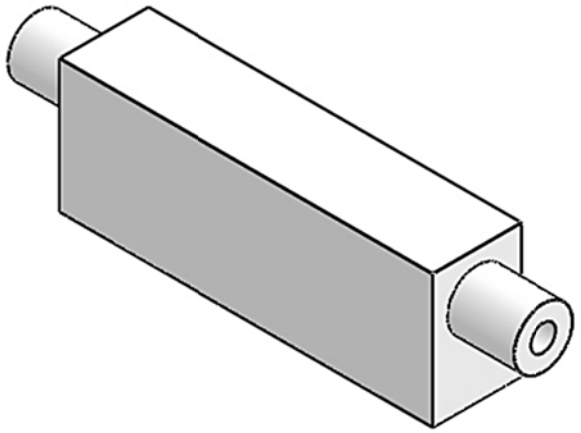

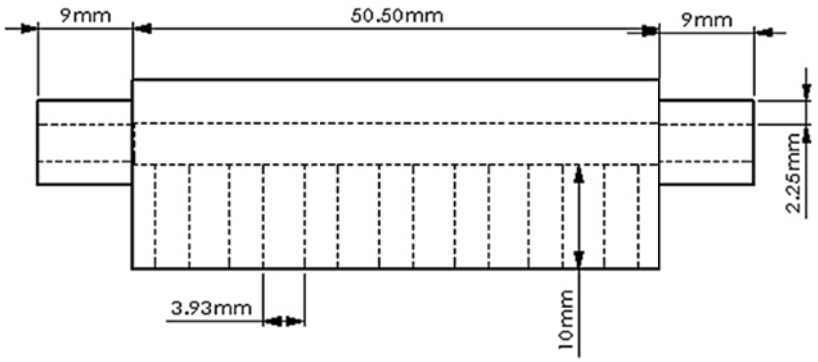

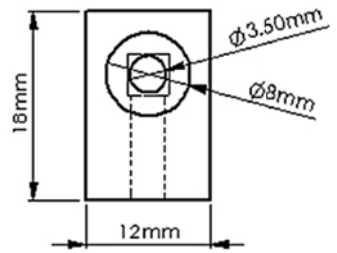

UNLESS OTHERWISE SPECIFIED: DIMENSIONS ARE IN MILLIMETERS SURFACE FINISH: TOLERANCES: LINEAR: ANGULAR:		FINISH:		DO NOT SCALE DRAWING	REVISION
	NAME	SIGNATURE	DATE		TITLE: Water Header
DRAWN	M.R.H.A.		2/9/2013		
CHK'D					
APPV'D					
MFG					
Q.A				MATERIAL: Objet RGD525	DWG NO. 5 / A4
				WEIGHT:	SCALE: 2:1 / SHEET 1 OF 1

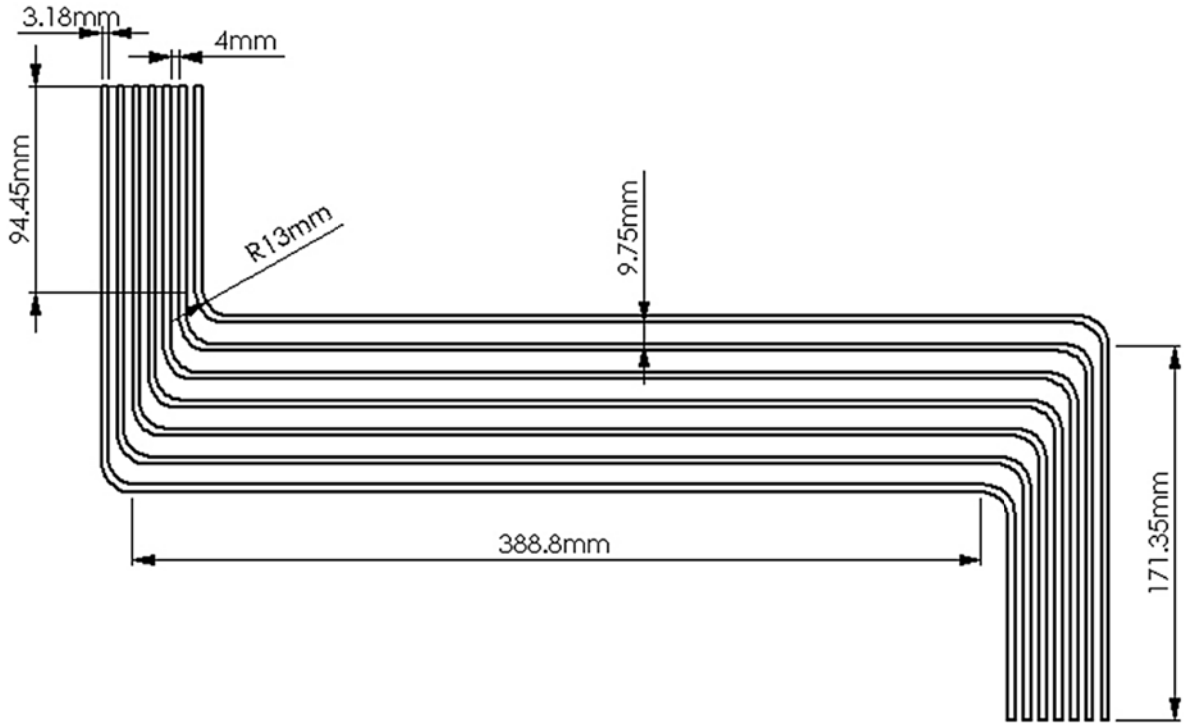

UNLESS OTHERWISE SPECIFIED: DIMENSIONS ARE IN MILLIMETERS SURFACE FINISH: TOLERANCES: LINEAR: ANGULAR:				FINISH:	DO NOT SCALE DRAWING / REVISION
	NAME	SIGNATURE	DATE		TITLE: Refrigerant Tubes
DRAWN	M.R.H.A.		2/9/2013		
CHK'D					
APPV'D					
MFG					
QA				MATERIAL: Titanium	DWG NO. 6 / A4
				WEIGHT:	SCALE: 1:3 / SHEET 1 OF 1

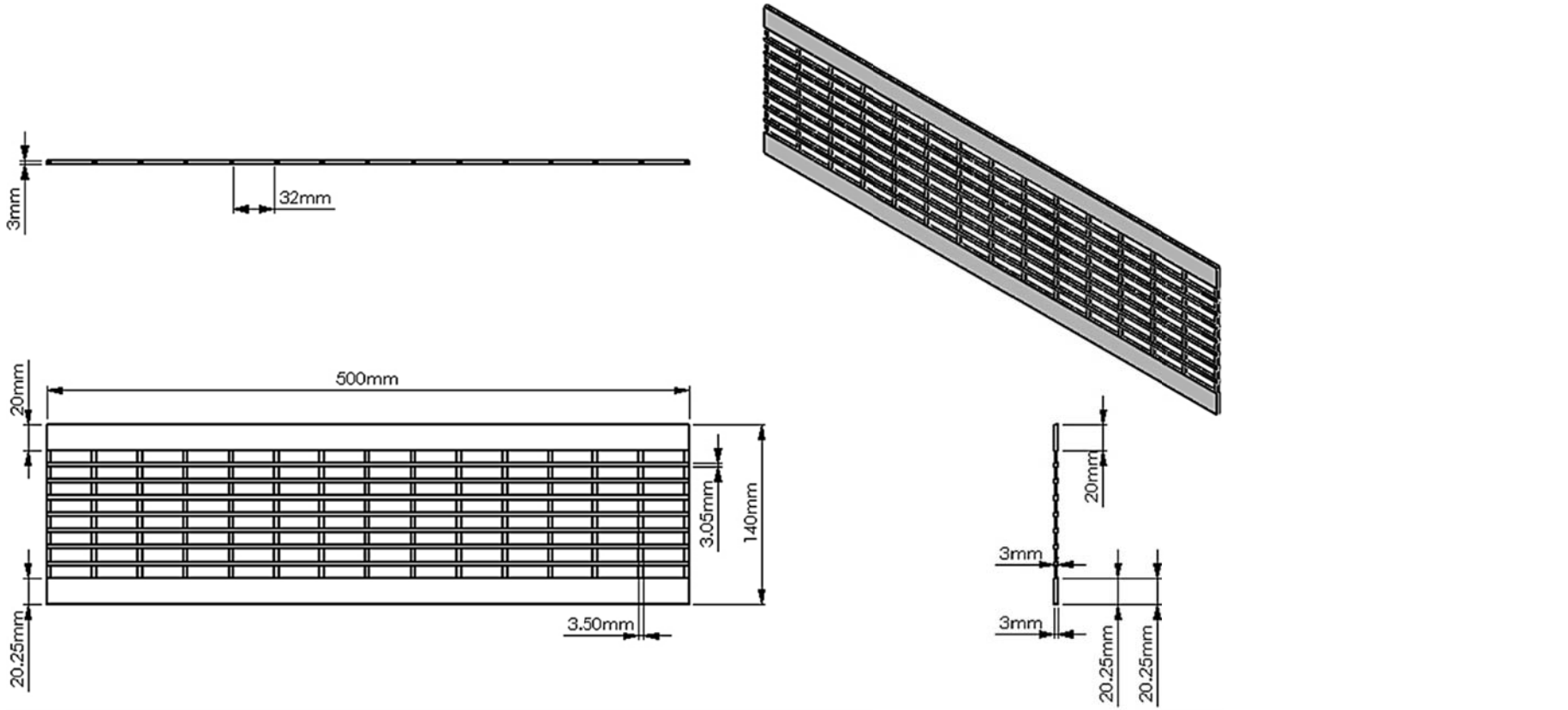

UNLESS OTHERWISE SPECIFIED: DIMENSIONS ARE IN MILLIMETERS SURFACE FINISH: TOLERANCES: LINEAR: ANGULAR:			FINISH:		DO NOT SCALE DRAWING / REVISION
	NAME	SIGNATURE	DATE		TITLE: Air Insert
DRAWN	M.R.H.A.		2/9/2013		
CHK'D					
APPV'D					
MFG					
Q.A				MATERIAL: Objet RGD525	DWG NO. 7 / A4
				WEIGHT:	SCALE: 1:3.5 / SHEET 1 OF 1

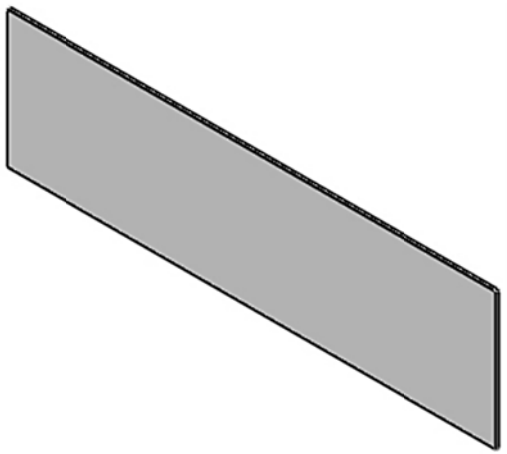

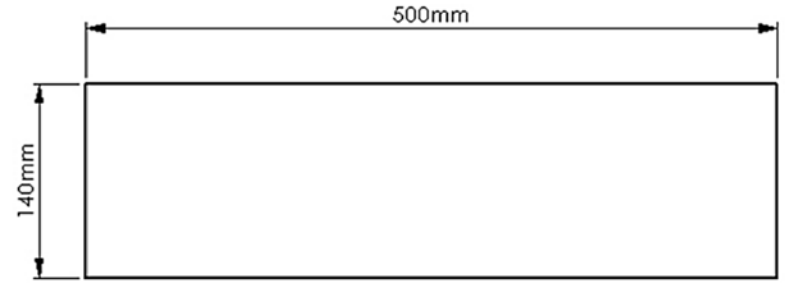

UNLESS OTHERWISE SPECIFIED: DIMENSIONS ARE IN MILLIMETERS SURFACE FINISH: TOLERANCES: LINEAR: ANGULAR:			FINISH:		DO NOT SCALE DRAWING / REVISION
	NAME	SIGNATURE	DATE		TITLE: Exchanger Wall
DRAWN	M.R.H.A.		2/9/2013		
CHK'D					
APPV'D					
MFG					
Q.A				MATERIAL: PVC	DWG NO. 8 / A4
				WEIGHT:	SCALE: 1:4 / SHEET 1 OF 1